THE CB2 CANNABINOID SYSTEM: A NEW STRATEGY IN NEURODEGENERATIVE DISORDER AND NEUROINFLAMMATION

EDITED BY: Marialessandra Contino, Elena Capparelli, Nicola A. Colabufo and Ashley I. Bush

PUBLISHED IN: Frontiers in Neuroscience

frontiers Research Topics

Frontiers Copyright Statement

© Copyright 2007-2017 Frontiers Media SA. All rights reserved.

All content included on this site, such as text, graphics, logos, button icons, images, video/audio clips, downloads, data compilations and software, is the property of or is licensed to Frontiers Media SA ("Frontiers") or its licensees and/or subcontractors. The copyright in the text of individual articles is the property of their respective authors, subject to a license granted to Frontiers.

The compilation of articles constituting this e-book, wherever published, as well as the compilation of all other content on this site, is the exclusive property of Frontiers. For the conditions for downloading and copying of e-books from Frontiers' website, please see the Terms for Website Use. If purchasing Frontiers e-books from other websites or sources, the conditions of the website concerned apply.

Images and graphics not forming part of user-contributed materials may not be downloaded or copied without permission.

Individual articles may be downloaded and reproduced in accordance with the principles of the CC-BY licence subject to any copyright or other notices. They may not be re-sold as an e-book.

As author or other contributor you grant a CC-BY licence to others to reproduce your articles, including any graphics and third-party materials supplied by you, in accordance with the Conditions for Website Use and subject to any copyright notices which you include in connection with your articles and materials.

All copyright, and all rights therein, are protected by national and international copyright laws.

The above represents a summary only. For the full conditions see the Conditions for Authors and the Conditions for Website Use.

ISSN 1664-8714
ISBN 978-2-88945-223-1
DOI 10.3389/978-2-88945-223-1

About Frontiers

Frontiers is more than just an open-access publisher of scholarly articles: it is a pioneering approach to the world of academia, radically improving the way scholarly research is managed. The grand vision of Frontiers is a world where all people have an equal opportunity to seek, share and generate knowledge. Frontiers provides immediate and permanent online open access to all its publications, but this alone is not enough to realize our grand goals.

Frontiers Journal Series

The Frontiers Journal Series is a multi-tier and interdisciplinary set of open-access, online journals, promising a paradigm shift from the current review, selection and dissemination processes in academic publishing. All Frontiers journals are driven by researchers for researchers; therefore, they constitute a service to the scholarly community. At the same time, the Frontiers Journal Series operates on a revolutionary invention, the tiered publishing system, initially addressing specific communities of scholars, and gradually climbing up to broader public understanding, thus serving the interests of the lay society, too.

Dedication to Quality

Each Frontiers article is a landmark of the highest quality, thanks to genuinely collaborative interactions between authors and review editors, who include some of the world's best academicians. Research must be certified by peers before entering a stream of knowledge that may eventually reach the public - and shape society; therefore, Frontiers only applies the most rigorous and unbiased reviews.
Frontiers revolutionizes research publishing by freely delivering the most outstanding research, evaluated with no bias from both the academic and social point of view.
By applying the most advanced information technologies, Frontiers is catapulting scholarly publishing into a new generation.

What are Frontiers Research Topics?

Frontiers Research Topics are very popular trademarks of the Frontiers Journals Series: they are collections of at least ten articles, all centered on a particular subject. With their unique mix of varied contributions from Original Research to Review Articles, Frontiers Research Topics unify the most influential researchers, the latest key findings and historical advances in a hot research area! Find out more on how to host your own Frontiers Research Topic or contribute to one as an author by contacting the Frontiers Editorial Office: **researchtopics@frontiersin.org**

THE CB2 CANNABINOID SYSTEM: A NEW STRATEGY IN NEURODEGENERATIVE DISORDER AND NEUROINFLAMMATION

Topic Editors:
Marialessandra Contino, Università degli Studi di Bari Aldo Moro, Italy
Elena Capparelli, Catholic University "Our Lady of Good Counsel", Albania
Nicola A. Colabufo, Università degli Studi di Bari Aldo Moro, Italy
Ashley I. Bush, University of Melbourne, Australia

The neurodegenerative disorders such as Parkinson's disease (PD) or Alzheimer's disease (AD) are the most common forms of dementia and no pharmacological treatments are to date available for these diseases. Indeed, the only used drugs are symptomatic and no useful to block the progression of the diseases. The lack of a therapeutic approach is also due to a lack of an early diagnosis.

This Research Topic describes a new target that is involved in the firs step of these disorders and that can be useful for the treatment and the diagnosis of such pathologies: the cannabinoid receptor subtype 2 or CB2R.

Indeed, CB2R is overexpressed in reactive microglia and activated astrocytes during neuroinflammation and thus their detection by PET probes can be an easily strategy for an early diagnosis of neurodegeneration.

Moreover, CB2 agonists and inverse agonists displayed neuroprotective effects and they so can be candidated as new therapeutich drugs for the treatment of these pathologies.

Therefore, the aim of this Research Topic is to show the great potential of CB2R ligands for the development of new tools/drugs for both the therapy and the diagnosis of neurodegeneration.

Citation: Contino, M., Capparelli, E., Colabufo, N. A., Bush, A. I., eds. (2017). The CB2 Cannabinoid System: A New Strategy in Neurodegenerative Disorder and Neuroinflammation. Lausanne: Frontiers Media. doi: 10.3389/978-2-88945-223-1

Table of Contents

frontiers in Neuroscience

EDITORIAL
published: 06 April 2017
doi: 10.3389/fnins.2017.00196

Editorial: The CB2 Cannabinoid System: A New Strategy in Neurodegenerative Disorder and Neuroinflammation

*Marialessandra Contino *, Elena Capparelli, Nicola A. Colabufo and Ashley I. Bush*

Dipartimento di Farmacia-Scienze del Farmaco, Università degli Studi di Bari Aldo Moro, Bari, Italy

Keywords: CB2R, CB2R ligands, microglial activation, neurodegenerative diseases, inflammation

Editorial on the Research Topic

The CB2 Cannabinoid System: A New Strategy in Neurodegenerative Disorder and Neuroinflammation

OPEN ACCESS

Edited by:
Sadayuki Hashioka, Shimane University, Japan

Reviewed by:
Sadayuki Hashioka, Shimane University, Japan
Raffaella Gozzelino, Universidade NOVA De Lisboa, Portugal
Ruoyu Zhang, Zhejiang University, China

****Correspondence:***
Marialessandra Contino
marialessandra.contino@uniba.it

Specialty section:
This article was submitted to Neurodegeneration, a section of the journal Frontiers in Neuroscience

Received: *10 February 2017*
Accepted: *23 March 2017*
Published: *06 April 2017*

Citation:
Contino M, Capparelli E, Colabufo NA and Bush AI (2017) Editorial: The CB2 Cannabinoid System: A New Strategy in Neurodegenerative Disorder and Neuroinflammation. Front. Neurosci. 11:196. doi: 10.3389/fnins.2017.00196

The cannabinoid receptors subtype 2 (CB2R) are emerging as novel targets for the development of new therapeutic approaches and PET probes useful to early diagnose neuroinflammation as first step in several neurodegenerative disorders such as Alzheimer's disease (AD) and Parkinson disease (PD). Differently from the CB1 subtype (CB1R) present in the CNS where it modulates several functions (memory, cognition, emotion, and pain control), CB2R is mainly localized in the immune system (macrophages) and are overexpressed in microglia in response to neuroinflammation. Two microglial activation states, M1 and M2, are widely reported. The M1 state (neurotoxic state) is characterized by the release of pro-inflammatory factors (such as IL-1B, IL-18, and IL-6 and inducible nitric oxide synthase) while the M2 state (neuroprotective state) is associated to the release of anti-inflammatory factors (IL-10, IL-4, and NGF). CB2R plays a pivotal role in microglial-derived neuroinflammation, since modulates cell proliferation, migration, and differentiation into M1 or M2 phenotypes (Mecha et al., 2015).

This Research Topic is mainly focused on the involvment of CB2R in neurodegenerative disorders and on the usefulness of CB2R ligands in the therapy and early diagnosis of neuroinflammation as onset of neurodegeneration.

In the reviews of Aso and Ferrer and Cassano et al. an interesting and exaustive overview of the endogenous cannabinoid signaling and its role in neuroinflammation and neurogenesis is reported. The potential of CB2R as therapeutic target in AD is argued by several evidences derived by robust experimental models and the effects modulated by CB2R agonists on different pathways involved in the pathogenesis of AD are discussed; indeed, these ligands are able to reduce inflammation, Aβ production and deposition, tau protein hyper-phosphorylation and oxidative stress damage caused by Aβ peptides. CB2R agonists are also able to induce Aβ clearance leading to cognitive improvement in AD models.

Javed et al. focused their study on the neuroprotective effect of β-caryophyllene (BCP), a natural CB2R agonist, in a rotenone (ROT)-induced animal model of PD. In their paper, the authors reported the beneficial neuroprotective effect due to BCP activity against ROT-induced neurodegeneration; the observed beneficial effects has been linked to CB2R activation since the administration of the CB2R antagonist AM630 was able to decrease the neuroprotective effects of BCP.

Navarro-Dorado et al. in their research article deepened the beneficial effects of CBR ligands in AD-type pathology studying the effects of the CB1/CB2 mixed agonist WIN 55,212-2 and the CB2

selective agonist JWH-133 on the vessel density in amyloid precursor protein (APP) transgenic mice, line 2,576, observing an improvment of the vascular responses.

Navarro et al. considered the localization of the CB2R subtype in specific cell types (activated astrocytes, reactive microglia, perivascular microglia, oligodendrocytes, and neural progenitor cells) and structures (blood-brain barrier) pivotal for the maintenance of the CNS integrity; moreover, they underlined the challenges faced in the CB2R-based drug design for the development of CB2R PET probes and for an innovative therapeutic strategy for neurodegeneration. Therefore, the authors reported an overview of the CB2R ligands planned as therapeutic and diagnostic agents in CNS diseases. In the diagnostic field, starting from the first PET radiotracer developed to image CB2R aspect, [11C]-NE40, the structural optimization performed with the aim to improve the brain penetration and to decrease the non-specific binding of these CB2R probes has been reported. The authors identified a 18F-triazine scaffold as a promising PET tracer candidate for the *in vivo* evaluation of inflammation. In the therapeutic field, the authors showed the findings reported by CB2R agonists in *in vitro* (BV-2 microglial cell line and in primary culture of microglia) and *in vivo* models (murine model) of neurodegeneration establishing a direct link between CB2R-targeting and neuroprotecion. Despite the increasing number of CB2R ligands developed, few synthetic CB2R agonists have reached clinical trials; the CB2R agonists GW842166X, CP55940, S-777469, and JTE-907 completed phase II for the pain therapy but none of them has been used in neurodegenerative diseases. However, the *in vitro* and *in vivo* studies performed led to several scaffolds useful to the development of CB2R ligands able to exert neuroprotection and neurorestoration.

Bu et al. shed light on a new scenario in neurodegenerative diseases since suggests a new therapeutic approach by the use of CB2R inverse agonists. Indeed, in their research article the authors deepened their previous work focused on the pivotal role of the CB2R inverse agonist, SMM-189, on neuroprotection, demonstrating the ability of SMM-189 to act on brain microglia converting it to the beneficial M2 state leading to neurons rescue in cortex, striatum, and amygdala. Therefore, not only CB2R agonists but also CB2R inverse agonists could be an useful strategy to face neuroinflammation in neurodegeneration; the difference between the two CB2R profiles (agonist and inverse agonist) is that the treatment with a CB2R agonist decreases M1 activation but do not induce M2 activation state.

Ahamed et al. and Haider et al. reported the development of PET-imaging agents to target CB2R: [11C]MA2 and [18F]MA3 and [11C]AAT-015 and [11C]AAT-778.

The first two probes are 11C- and 18F- radiolabelled analogs of the highly potent arylamide oxadiazole CB2 agonist. Both the analogs displayed a good affinity toward the desired target (CB2R), good radiochemical yield, high radiochemical purity, and high specific activity. Both probes displayed good results *in vivo* since displayed an efficient blood clearance and high brain uptake. By contrast, the thiophene-based radiotracers [11C]AAT-778 and [11 C]AAT-015 developed by Haider et al. failed *in vivo* because of the lack of specificity for CB2R-positive spleen tissue and thus the two tracers were not further evaluated in neuroinflammatory animal models. However, the high CB2R affinity and selectivity makes this class of compounds the starting point for structural optimization to improve physicochemical and pharmacological properties.

In conclusion, considering that neuroinflammation has been widely reported as indicator and modulator of neurodegeneration (Wyss-Coray and Mucke, 2002), the reduction of the neuroinflammatory responses could be considered as a new therapeutic strategy in these diseases. Moreover, the selective CB2R overexpression on the activated-microglial cells provides also a highly specialized target useful to an early diagnosis of the neurodegenerative diseases.

AUTHOR CONTRIBUTIONS

MC managed the topic and wrote the manuscript. EC, NC, and AB helped to the manage step of the topic and to the realization of the Editorial.

REFERENCES

Mecha, M., Feliú, A., Carrillo-Salinas, F. J., Rueda-Zubiaurre, A., Ortega-Gutiérrez, S., de Sola, R. G., et al. (2015). Endocannabinoids drive the acquisition of an alternative phenotype in microglia. *Brain Behav. Immun.* 49, 233–245. doi: 10.1016/j.bbi.2015.06.002

Wyss-Coray, T., and Mucke, L. (2002). Inflammation in neurodegenerative disease - a double edge sword. *Neuron* 35, 419. doi: 10.1016/S0896-6273(02)00794-8

Conflict of Interest Statement: The authors declare that the research was conducted in the absence of any commercial or financial relationships that could be construed as a potential conflict of interest.

Copyright © 2017 Contino, Capparelli, Colabufo and Bush. This is an open-access article distributed under the terms of the Creative Commons Attribution License (CC BY). The use, distribution or reproduction in other forums is permitted, provided the original author(s) or licensor are credited and that the original publication in this journal is cited, in accordance with accepted academic practice. No use, distribution or reproduction is permitted which does not comply with these terms.

frontiers in Neuroscience

MINI REVIEW
published: 02 February 2017
doi: 10.3389/fnins.2017.00030

Cannabinoid Receptor 2 Signaling in Neurodegenerative Disorders: From Pathogenesis to a Promising Therapeutic Target

Tommaso Cassano[1], Silvio Calcagnini[2], Lorenzo Pace[1], Federico De Marco[3], Adele Romano[2] and Silvana Gaetani[2]*

[1] Department of Clinical and Experimental Medicine, University of Foggia, Foggia, Italy, [2] Department of Physiology and Pharmacology, Sapienza University of Rome, Rome, Italy, [3] Laboratory of Virology, The Regina Elena National Cancer Institute, IRCCS, Rome, Italy

As a consequence of an increasingly aging population, the number of people affected by neurodegenerative disorders, such as Alzheimer's disease, Parkinson's disease and Huntington's disease, is rapidly increasing. Although the etiology of these diseases has not been completely defined, common molecular mechanisms including neuroinflammation, excitotoxicity and mitochondrial dysfunction have been confirmed and can be targeted therapeutically. Moreover, recent studies have shown that endogenous cannabinoid signaling plays a number of modulatory roles throughout the central nervous system (CNS), including the neuroinflammation and neurogenesis. In particular, the up-regulation of type-2 cannabinoid (CB2) receptors has been found in a number of neurodegenerative disorders. Thus, the modulation of CB2 receptor signaling may represent a promising therapeutic target with minimal psychotropic effects that can be used to modulate endocannabinoid-based therapeutic approaches and to reduce neuronal degeneration. For these reasons this review will focus on the CB2 receptor as a promising pharmacological target in a number of neurodegenerative diseases.

Keywords: Alzheimer's disease, Parkinson's disease, neuroprotection, neuroinflammation, microglia, astrocytes

OPEN ACCESS

Edited by:
Marialessandra Contino, University of Bari Aldo Moro, Italy

Reviewed by:
Luigi Bubacco, University of Padua, Italy
Kevin Donald Broad, UCL Institute for Women's Health, UK

****Correspondence:***
Tommaso Cassano
tommaso.cassano@unifg.it

Specialty section:
This article was submitted to Neurodegeneration, a section of the journal Frontiers in Neuroscience

Received: *16 November 2016*
Accepted: *16 January 2017*
Published: *02 February 2017*

Citation:
Cassano T, Calcagnini S, Pace L, De Marco F, Romano A and Gaetani S (2017) Cannabinoid Receptor 2 Signaling in Neurodegenerative Disorders: From Pathogenesis to a Promising Therapeutic Target. Front. Neurosci. 11:30. doi: 10.3389/fnins.2017.00030

INTRODUCTION

The field of cannabinoid (CB) research has flourished over the past decade and has brought to light diverse functions of the CB system in normal and pathological conditions (D'Addario et al., 2014; Bonnet and Marchalant, 2015). In fact, several studies have demonstrated that endocannabinoid (eCB) system plays significant roles in many biological processes, including neurogenesis, synaptic plasticity, emotional regulation and stress responsiveness (Lu and Mackie, 2015).

The eCB system consists of eCBs, cannabinoid receptors and enzymes involved in the synthesis and degradation of endogenous ligands (Lu and Mackie, 2015).

The eCBs are endogenous lipids that engage CB receptors, affecting behavior in a fashion that at least partially recapitulates the effects produced by the psychoactive components of cannabis, most notably (2)-trans-Δ9-tetrahydrocannabinol (THC) (Mechoulam and Gaoni, 1965; Mechoulam, 1970). The two best-characterized eCBs are N-arachidonoylethanolamide (anandamide, AEA) (Devane et al., 1992) and 2-arachidonoylglycerol (2-AG) (Mechoulam et al., 1995; Sugiura et al., 1995). Both eCBs are synthetized at the post-synaptic terminal from membrane lipid precursors

in response to high intracellular calcium concentration (Howlett et al., 2002). Thus, eCBs act as retrograde messengers to depress transmitter release from presynaptic terminals (Freund et al., 2003; Fagan and Campbell, 2014).

AEA and 2-AG possess specific pharmacological properties, are engaged in different forms of synaptic plasticity and modulate different behavioral functions (Mechoulam and Parker, 2013).

The CB type 1 (CB1) and type 2 (CB2) receptors are coupled to G-protein, and their signal transduction is mediated by the inhibition of adenylyl cyclases and voltage-gated calcium channels (e.g., N-type, P/Q-type and L-type calcium currents), and by the activation of mitogen-activated protein kinases (MAPK) and inwardly rectifying potassium channels (Howlett et al., 2002; Lu and Mackie, 2015). AEA is a high affinity, CB1-selective partial agonist, whereas 2-AG is a moderate affinity, CB1/CB2 full agonist (Sugiura et al., 2000). AEA activates also peroxisome proliferator-activated receptors-alpha and transient receptor potential vannilloid-1 channels (Maccarrone et al., 2010). In humans, CB1 is localized preferentially in the terminals of central and peripheral neurons and glial cells, where it regulates neurotransmitter release and psychoactivity (Egertová et al., 2003; Sánchez and García-Merino, 2012). As far as peripheral tissues, CB1 is also expressed in heart, uterus, testis, liver and small intestine, as well as in immune cells (Maccarrone et al., 2001; Nong et al., 2001; Klein et al., 2003) and adipose tissue (Spoto et al., 2006).

CB2 was dubbed the "peripheral cannabinoid receptor" as a result of *in situ* hybridization study that showed high CB2 mRNA expression in spleen, whereas no expression was observed in the brain (Shire et al., 1996; Griffin et al., 2000; Brown et al., 2002). Besides the cells of the immune and hematopoietic systems (e.g., leukocytes, spleen and tonsils), CB2 receptors were found also in other peripheral organs, such as muscle, liver, intestine and testis (Liu et al., 2009). However, CB2 receptor can be also detected in the central nervous system (CNS) (albeit at a lower expression level than CB1receptors) (Núñez et al., 2004; Van Sickle et al., 2005), where its expression is significantly increased following a number of stressful conditions (Viscomi et al., 2009). In particular, CB2 receptor expression is found in neurons within the brainstem, microglia and astrocytes only after specific insults (e.g., neuroinflammation), whereas it cannot be detected in resting microglia (Van Sickle et al., 2005; Núñez et al., 2008; Cabral and Griffin-Thomas, 2009).

In the last decade, increasing evidence has shown that CB receptors may act as CB1-CB2 receptor heteromers in the brain (Callén et al., 2012). In fact, the expression of CB1-CB2 receptor heteromers was determined in a variety of brain regions, such as the nucleus accumbens, pineal gland and globus pallidus (Callén et al., 2012). Due to this tight functional interaction between CB receptors, the response to molecules acting as agonists or antagonists may be different when a CB receptor is engaged in heteroreceptor complexes. Although the clinical relevance of this phenomenon is not entirely clear, additional studies are needed in order to shed further light on this important functional interaction.

eCBs after their actions are rapidly eliminated by cellular uptake and enzymatic hydrolysis. To this regard, AEA is mainly inactivated by fatty acid amide hydrolase (FAAH) (Cravatt et al., 1996; Dinh et al., 2002), whereas 2-AG is predominantly catalyzed by monoacylglycerol lipase (Dinh et al., 2002).

As previously reported, CB1 receptor expression is abundant in the CNS, where it seems to mediate the psychoactive effects of cannabis (Mackie, 2005). Therefore, the scarcity of CNS CB2 receptors makes CB2 selective drugs attractive as therapeutics as they would presumably invoke minimal psychoactive responses. In support of this hypothesis, CB2 knockout mice demonstrated typical behavioral responses to THC but lost their normal immune responsiveness to THC (Buckley et al., 2000). CB2 levels are also increased under certain conditions and disease states further adding to its attractiveness as a potential therapeutic target (Zhang et al., 2003; Wotherspoon et al., 2005; Yiangou et al., 2006).

Therefore, we will review the role of eCB system in two chronic neurodegenerative diseases, in which the neuroprotective effects following CB receptors modulation have been reported in different studies. Specifically, we will focus on the role of CB2 receptors and their agonists, as potential therapeutical targets in Alzheimer's disease (AD) and Parkinson's disease (PD).

ROLE OF CB2 RECEPTOR IN THE NEURODEGENERATION AND NEUROPROTECTION

Recently, much research has paid attention to the neuroprotective effects of compounds targeting the eCB system. In particular, these studies have focused on identifying molecular targets within the eCB system that may lead to neuroprotection against the most prevalent neurodegenerative disorders (Fernández-Ruiz et al., 2010, 2015).

One of the most important features of CBs as potential neuroprotectants is their broad-spectrum of activity. This aspect is particularly important in neurodegenerative diseases since declines in neural function are likely due to the concerted involvement of different insults including protein misfolding, neuroinflammation, excitotoxicity, oxidative stress and mitochondrial dysfunction (Serviddio et al., 2011; Cassano et al., 2012, 2016; Aureli et al., 2014). All these pathological processes appear to be modulated by the eCB signaling system. In fact, during aging and neuroinflammation (or when both are present together) there is a widespread disruption of brain tissue homeostasis that involves eCB signaling, and this contributes to specific dysfunctions in cell function.

Although the CNS is considered a relatively immune-privileged tissue, it is able to initiate an endogenous immune response. To this regard, astrocytes and microglia are the main innate immune response effectors in brain parenchyma (Halliday and Stevens, 2011).

The most extensively studied mechanism of neuroprotection includes the anti-inflammatory effects of the CB2 receptors, in which CB2 protects the brain by restraining inflammatory processes (Benito et al., 2008; Cabral and Griffin-Thomas, 2009). In particular, CB2 receptor activation modulates the release of

cytokines, protein molecules responsible for the regulation of immune function and inflammatory responses (Mecha et al., 2016; Turcotte et al., 2016). Differently, the CB1 receptor has been implicated in protection against cell death induced by an overstimulation of excitatory receptors and concurrent calcium release, also known as excitotoxicity (Vendel and de Lange, 2014). CB receptors, therefore, may have an impact on neurodegenerative diseases through two main ways, restraining exitotoxic and immunological processes (Di Iorio et al., 2013).

Moreover, it has been demonstrated that changes in the expression of CB receptors may be time-dependent and could occur both in the brain and peripheral tissues at different stages of the neurodegenerative process (Bedse et al., 2014, 2015; Di Marzo et al., 2015). For this reason, targeting the CB receptors for therapeutic benefit needs more caution. To this regard, CB1 activity was higher at earlier AD stages in limited hippocampal areas and internal layers of the frontal cortex, but a decrease was observed during the advanced stages (Lastres-Becker et al., 2001; Manuel et al., 2014; Rodríguez-Cueto et al., 2014). The increased CB1 receptor activity during the initial stages of AD may indicate neuroprotective action mediated by eCBs in response to initial neuronal damage.

However, CB1 receptors are not usually considered as realistic targets for neuroprotection, because during neurodegenerative processes it has been described a progressive loss of specific populations of neurons that express CB1 receptors (Ramírez et al., 2005; Solas et al., 2013). In line with these results, our group (Bedse et al., 2014), but also Kalifa et al. (2011) reported a decrease in CB1 protein expression in transgenic mice models of AD.

In contrast, CB2 receptors are generally less expressed in the neurons of healthy brains, but their expression increases dramatically in reactive microglia and activated astrocytes during neuroinflammation (Stella, 2010; Di Marzo et al., 2015; Fernández-Ruiz et al., 2015). Therefore, the CB2 receptors have the potential to restrain the inflammatory processes that contribute to the declines in neural function occurring in a number of neurodegenerative disorders.

CB2 RECEPTORS AND ALZHEIMER'S DISEASE

AD is a devastating neurodegenerative disease leading to progressive cognitive dysfunction. The iconic hallmarks of AD are Aβ plaques, neurofibrillary tangles (NFTs) and a deficiency in cholinergic neurotransmission. It is widely accepted that the deposition of Aβ initiates an inflammatory process leading to neurodegeneration (McGeer et al., 2000; Walsh and Selkoe, 2004). Microglial cells are the resident CNS phagocytes of the immune system that mediate inflammatory responses to pathogens and injury by inducing release of pro-inflammatory cytokines including interleukin (IL)-1β, IL-6, and tumor necrosis factor-α (TNF-α). IL-1β and TNF-α are considered as primary cytokines responsible for chronic inflammation in AD (Sastre et al., 2006). Microglia-derived pro-inflammatory cytokines, in turn, aggravate and propagate inflammation throughout the brain. In fact, IL-1β released from microglia can induce the upregulation of nuclear factor-kappa B (NFκB), MAPK, and Jun-N-terminal kinase (JNK) signaling in neurons and astrocytes, leading to increased inflammatory process and tau phosphorylation, respectively (Sastre et al., 2006; Munoz and Ammit, 2010). Additionally, Aβ oligomers can induce production of inducible nitric oxide synthase (iNOS), nitric oxide (NO), and TNF-α in astrocytes (White et al., 2005). NO secreted from astrocytes induces abnormal tau hyperphosphorylation in neurons, which prompts an accumulation of NFTs in axons, leading to a disruption of synaptic plasticity and neuronal death (Duan et al., 2012). Moreover, the activation of toll-like receptors (TLR; e.g., TLR-4), involved in pathogen recognition and activation of innate immunity, can also activate the MAPK and NFκB pathways, as well as members of the caspase family responsible for hyperphosphorylation of tau (Churcher, 2006; Reed-Geaghan et al., 2009; Rohn, 2010; Arroyo et al., 2011). Activation of these signaling cascades in neurons could further inhibit synaptic plasticity.

Support for the involvement of the CB2 receptors in AD pathology is provided by a number of preclinical and human studies. In particular, post-mortem brains from patients with AD have shown that CB2 receptors are upregulated in cells that are associated with Aβ-enriched neuritic plaques (Benito et al., 2003; Ramírez et al., 2005; Grünblatt et al., 2009; Halleskog et al., 2011; Mulder et al., 2011; Solas et al., 2013). Apart from human studies, transgenic models of AD have also revealed overexpression of CB2 receptors in brain areas affected by AD-pathology (Horti et al., 2010). Increased CB2 mRNA in peripheral blood has been suggested as a peripheral biomarker for the early diagnosis of AD (Grünblatt et al., 2009). Moreover, an increase in CB2 receptors was also observed in rats and C6 astroglioma cells pre-treated with Aβ42 (Esposito et al., 2007).

All these effects may be counteracted by the activation of CB2 receptors, and mechanistic insights of the beneficial effects provided by CB2 receptor stimulation in AD has been provided (Ehrhart et al., 2005; Ramírez et al., 2005; Sheng et al., 2005; Chen et al., 2010; Fakhfouri et al., 2012; Martin-Moreno et al., 2012) (**Table 1**). In particular, the CB2 agonist, JWH-015, significantly attenuated CD40-mediated inhibition of microglial phagocytosis of Aβ42 by interfering with the Janus kinase/Signal transducer and activator of transcription 1 (JAK/STAT1) pathway (Benveniste et al., 2004; Ehrhart et al., 2005). Interestingly, CP55940 (CB1/CB2 full agonist) and JWH-015 treatment significantly reduced the interferon-gamma- (IFN-γ)-induced CD40 expression in microglial cells (Ehrhart et al., 2005).

Ramírez and colleagues demonstrated the effects of CB receptor agonists on microglial activation (Ramírez et al., 2005). Authors studied *in vitro* the effects of WIN55,212-2, the mixed CB1/CB2 agonist devoid of antioxidant properties (Howlett et al., 2002; Marsicano et al., 2002), HU-210 and JWH-133, respectively CB1 and CB2 selective agonist, in Aβ-induced microglial cells (Ramírez et al., 2005). As expected, Aβ peptide activated microglial cells and this was associated with increased mitochondrial activity, TNF-α release, cellular morphological changes and secretion of pro-inflammatory

TABLE 1 | CB2 receptor agonists and their beneficial effects in neurodegenerative diseases (AD and PD).

Subjects	CB2 agonists	Effects and mechanisms involved	References
ALZHEIMER'S DISEASE (AD)			
IFN-γ-activated microglial cells (Aβ42 insult)	JWH-015	↓ CD40 expression induced by IFN-γ;	Ehrhart et al., 2005
		↓ JAK/STAT1 phosphorylation;	
	CP55940	↑ phagocytosis of Aβ42;	
		↓ TNF-α and NO release.	
Microglial cells (Aβ insult)	WIN55,212-2	↓ Microglial cell Aβ induced activation;	Ramírez et al., 2005
	JWH-133	↓ TNF-α release.	
Aβ-induced hippocampal neurodegeneration in adult rats	WIN55,212-2	↑ Memory functions;	Fakhfouri et al., 2012
		↓ TNF-α release;	
		↓ caspases-3 activation;	
		↓ nuclear NFκB levels.	
IL-1β-activated human fetal astrocytes	WIN55,212-2	↓ iNOS expression;	Sheng et al., 2005
		↓ TNF-α and NO release;	
		↓ chemokines release (CXCL10, CCL2, CCL5).	
Tg2576 mice	WIN55,212-2	↓ cognitive impairments;	Martin-Moreno et al., 2012
	JWH-133	↓ microglial activation;	
		↓ COX-2 expression;	
		↓ TNF-α release;	
		↓ cortical Aβ deposition.	
PARKINSON'S DISEASE (PD)			
MPTP-lesioned mice	WIN55,212-2	↓ microglial activation;	Price et al., 2009
	JWH-015	↓ degeneration of nigro-striatal DA neurons;	
		↓ MPTP-induced motor deficits;	
		↑ dopamine and 3,4-dihydroxyphenylacetic acid levels in SNc and dorsal striatum;	
		↑ TH^+ neurons in the SNc.	
IFN-γ-activated microglial cells	JWH-015	↓ CD40 expression induced by IFN-γ;	Ehrhart et al., 2005
	CP55940	↓ JAK/STAT1 phosphorylation;	
		↓ TNF-α and NO release.	
Human microglial cells (from temporal lobe)	JWH-015	↑ neuroprotective effects;	Klegeris et al., 2003
		↓ TNF-α and IL-1β release (JWH-015);	
	BML-190	↑ TNF-α release	
		(BML-190).	
Primary astrocyte cultures from 1 day-old CD1 mouse brains (LPS insult)	CP55940	↓ iNOS expression;	Molina-Holgado et al., 2002
	HU-210	↓ NO release.	
Primary glial cells and cerebrocortical neurons from 1 day-old mouse brains (LPS insult)	CP55940	↑ IL-1ra and NO release (primary glial cells);	Molina-Holgado et al., 2003
	HU-210	↑ neuroprotective effects.	
LPS-lesioned rats	HU-308	↑ neuroprotective effects;	García et al., 2011
		↑ TH^+ neurons in the substantia nigra.	
LPS-lesioned mice	HU-308	↓ CD68, iNOS, TNF-α and IL-1β expression in the striatum;	Gómez-Gálvez et al., 2016
		↑ TH^+ neurons in the substantia nigra;	
		↓ TNF-α expression in the substantia nigra.	
Drosophila melanogaster (paraquat insult)	CP55940	↑ fly survival and locomotor activities;	Jimenez-Del-Rio et al., 2008
		↓ activation of JNK signaling.	
6-OHDA-lesioned rats	HU-308	↓ dopamine depletion	García-Arencibia et al., 2007
		in caudate putamen;	
		↑ TH activity in caudate putamen (HU-308);	
	WIN55,212-2	= TH-mRNA levels in	
		the substantia nigra	
		(HU-308).	

IL-1ra, endogenous IL-1 receptor antagonist.

cytokines. Cannabinoid treatments prevented the enhancement of TNF-α release and counteracted Aβ-mediated activation of microglia (Ramírez et al., 2005).

The protective properties of WIN55,212-2 were also demonstrated in Aβ-induced neurodegeneration in rat hippocampus. WIN55,212-2 significantly improved memory functions and decreased the elevated levels of neuroinflammatory markers like TNF-α, activated caspase-3, and nuclear NFκB. The use of antagonists confirmed that these neuroprotective effects of WIN55,212-2 were partially mediated by CB1 and CB2 receptors (Fakhfouri et al., 2012). Moreover, WIN55,212-2, through CB2 receptors, inhibited iNOS and NO production, the release of chemokines (CXCL10, CCL2, and CCL5) and TNF-α from IL-1β-activated human fetal astrocytes (Sheng et al., 2005). The CB1 and CB2 receptor-specific antagonists SR141716A (Micale et al., 2013) and SR144528 (Saito et al., 2010), respectively, partially blocked this suppressive effect, which suggests the involvement of both receptors (Sheng et al., 2005).

Furthermore, the effects of cannabinoids were studied in transgenic murine models of AD treated chronically with WIN55,212-2 or JWH-133, a potent selective CB2 receptor agonist (Martin-Moreno et al., 2012). JWH-133 was able to reduce cognitive impairments and decrease microglial activation in Tg2576 mice, while WIN55,212-2 was ineffective. Moreover, both cannabinoids significantly reduced the increase of COX-2, TNF-α, and cortical Aβ levels, suggesting a critical role of CB2 in inflammatory processes in AD (Martin-Moreno et al., 2012) (**Figure 1**).

From this scenario has emerged that the pleiotropic effects of CB2 agonists and the growing number of preclinical effects on AD rodent models should engage the interest of the research community and be seen as a valuable potential alternative treatment strategy to slow the progression and reduce the symptoms of cognitive decline in AD.

CB2 RECEPTORS AND PARKINSON'S DISEASE

PD, the second most common neurodegenerative disease, is characterized by the progressive loss of dopaminergic neurons primarily in the *substantia nigra* (SN) affecting the circuits of the basal ganglia resulting in bradykinesia, rigidity and tremors (de Lau and Breteler, 2006; Branchi et al., 2008, 2010; Bartels and Leenders, 2009). Current treatments include dopaminergic replacement therapies, which do alleviate some of the symptoms but there are no available therapies that reverse any of the underlying pathological mechanisms (Calne et al., 2005; Trapani et al., 2011; Denora et al., 2012; Di Gioia et al., 2015).

Moreover, there is an urgent need for a novel intervention aimed at the prevention of dyskinesia induced by long-term treatment with levodopa. To this regard, a randomized double-blind crossover study showed that cannabis, which contains

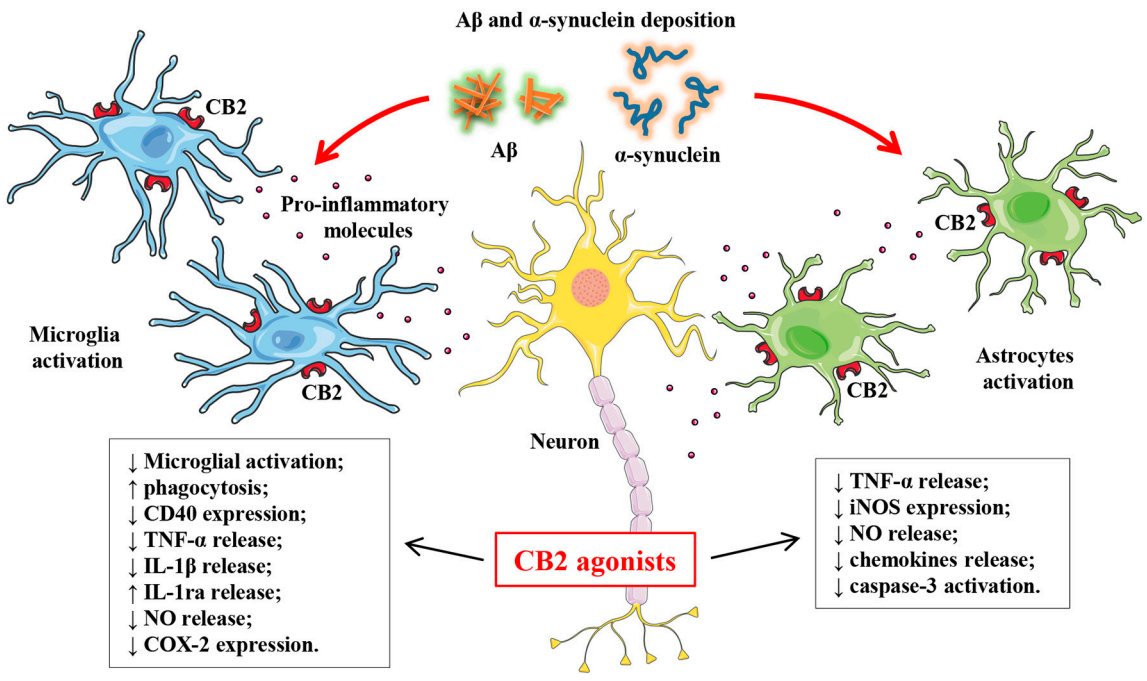

FIGURE 1 | Schematic representation of anti-inflammatory and neuroprotective actions of CB2 agonists in AD and PD. AD and PD are characterized respectively by the deposition of Aβ and α-synuclein proteins which in turn are directly or indirectly involved in microglial and astrocytic activation. This activation of microglia and astrocytes triggers a neuroinflammatory and immune response which contributes to the progression of AD and PD. The pharmacological activation of microglial and astrocytic CB2 cannabinoid receptors with CB2 agonists is a promising therapeutic approach because it promotes anti-inflammatory and neuroprotective effects such as the suppression of pro-inflammatory cytokine release and an increases in anti-inflammatory molecules.

more than 70 different cannabinoids (Mechoulam, 2005), failed to demonstrate efficacy in treating dyskinetic patients with PD (Carroll et al., 2004). Unfortunately, the latter study suffered from methodological issues such as including small numbers of patients, and having inadequate power to detect a small change in dyskinesia.

PD is accompanied by multiple changes in the brain that underlie the progression of the disease. In this context, inflammation is an important pathogenic factor in sporadic PD, where it is thought to disable or kill dopaminergic neurons of the SN, which contributes to the dopaminergic denervation of the striatum.

The involvement of inflammation in PD has been initially investigated by McGeer et al. (1988), who showed microglia activation in the SN of patients at post-mortem. Afterwards, more evidence has accumulated that highlights the role of the neuroinflammation in the pathogenesis of PD. In line with this, *in vivo* studies using structural brain imaging have demonstrated in the nigrostriatal system of PD patients the presence of activated microglia and an increase of proinflammatory cytokines, including TNF-α, IL-1β, IL-2, IL-4, and IL-6 (Ouchi et al., 2005; Gerhard et al., 2006; Taylor et al., 2013).

α-synuclein (α-syn), the major component of Lewy bodies, is another pre-disposing element in PD etiology (Spillantini et al., 1998; Aureli et al., 2014). Missense mutations in the α-syn gene have been identified to cause autosomal dominant familial PD (Polymeropoulos et al., 1997; Krüger et al., 1998; Zarranz et al., 2004). Several lines of evidence suggest that α-syn may play an important role in the microglia-mediated inflammatory response in PD (Zhang et al., 2005; Austin et al., 2006; Reynolds et al., 2007, 2008; Thomas et al., 2007; Gao et al., 2008; Klegeris et al., 2008; Aureli et al., 2014). It is believed that genetic and environmental factors may initiate the neurodegeneration, which is further sustained or exacerbated by neuroinflammation leading to a "self-sustaining" process (Tansey and Goldberg, 2010). Therefore, effective anti-inflammatory intervention may arrest this cyclical process and counteract the neuroinflammation-induced neuronal degeneration.

Recently, in post-mortem study it has been demonstrated that PD patients showed elevated expression of CB2 receptors in microglial cells of SN (Gómez-Gálvez et al., 2016). In this context, as for AD, converging evidence indicates that CB2 receptor may represent a promising anti-inflammatory target in PD (**Figure 1**, **Table 1**). This hypothesis comes from numerous studies where the pharmacological activation of microglial CB2 receptors produced a reduction of microglial activation and functional deficits in the 1-methyl-4-phenyl-1,2,3,6-tetrahydropyridine (MPTP) mouse model of PD (Price et al., 2009), the suppression of pro-inflammatory cytokine release (Molina-Holgado et al., 2002; Klegeris et al., 2003; Ehrhart et al., 2005), and an increase in anti-inflammatory cytokines (Molina-Holgado et al., 2003). Moreover, CB2 receptor–deficient mice have shown an exacerbation of the PD pathology with increased microglial activation, neural alterations and functional deficits. Similar effects were also observed in other models of PD, such as MPTP-lesioned and lipopolysaccharide- (LPS)-injected mice (Price et al., 2009; García et al., 2011; Gómez-Gálvez et al., 2016). Moreover, the genetic ablation of the CB2 receptor protects against nigro-striatal damage following 6-hydroxydopamine (6-OHDA) lesion in mice (Ternianov et al., 2012).

Neuroprotection has been provided by synthetic cannabinoids such as the CP55,940, CB1/CB2 full agonist (Jimenez-Del-Rio et al., 2008), which acts through CB receptor-independent mechanisms, and involves the control of endogenous antioxidant defenses. In particular, authors found that CP55,940 protects Drosophila melanogaster mutants which lack CB receptors (McPartland et al., 2001; Elphick and Egertová, 2005), and alleviates the toxicity induced by paraquat (Jimenez-Del-Rio et al., 2008). The latter effect was exerted by the inactivation of JNK signaling and CB receptors were not involved (Jimenez-Del-Rio et al., 2008). Other findings concerning the possible off-target effects of CB agonists were obtained also from *in vivo* studies, in which mice genetically deleted of CB receptors were treated with molecules targeting "non-cannabinoids" receptors (see for review Pertwee et al., 2010).

Selective CB2 receptor agonists induced gains of function in MPTP-lesioned mice (Price et al., 2009) and LPS-injected mice (García et al., 2011), but not in 6-OHDA-lesioned rats (García-Arencibia et al., 2007). The lack of effects of CB2 agonists may be due to a lower inflammatory response induced by 6-OHDA compared to that caused by LPS and MPTP (Price et al., 2009; García et al., 2011). In particular, HU-308, the selective CB2 agonist, reversed the LPS-induced reduction of tyrosine hydroxylase positive (TH^+) neurons and the elevation of CD68 immunostaining in the striatum, which identifies activated microglia and infiltrated peripheral macrophages. Moreover, authors found that HU-308 significantly reduced increases in striatal iNOS gene expression following an LPS insult (Gómez-Gálvez et al., 2016). In line with these results, García and colleagues found that HU-308 preserved TH^+ neurons in the SN of LPS-injected mice (García et al., 2011).

A comprehensive study conducted by Price et al. (2009) demonstrated that the chronic treatment with the non-selective CB receptor agonist WIN55,212-2 protected against MPTP-induced loss of TH^+ neurons in the SN pars compacta (SNc), independently of CB1 receptor activation. In fact, the authors found that WIN55,212-2 was still able to protect TH^+ neurons from MPTP-lesioned CB1 receptor–deficient mice. Moreover, WIN55,212-2 increased the levels of dopamine and 3,4-dihydroxyphenylacetic acid in the SNc and dorsal striatum of MPTP-lesioned mice and reversed MPTP-associated motor deficits. WIN55,212-2 or JWH015, agonist of CB2 receptor, reduced MPTP-induced microglial infiltration. The suppressive effect of WIN55,212-2 and JWH015 on microglia was due specifically to CB2 activation as it was reversed by the CB2 antagonist JTE (Price et al., 2009).

Unlike targeting CB2 receptor signaling, the activation of CB1 receptors may cause hypokinetic side effects that could aggravate the major symptoms of PD, such as bradykinesia (García-Arencibia et al., 2009). Therefore, the modulation of CB1 receptors seems not to be a promising target for therapeutic intervention in PD. However, CB1 activation may

alleviate the levodopa-induced dyskinesia, a motor complication resulting from long-term use of levodopa (Morgese et al., 2007, 2009).

Taken together these results demonstrate that CB2 receptors play an important role in the pathophysiology of PD and that their activation with selective agonist may lead to neuroprotective effect in the neurodegenerative processes of PD.

CONCLUSIONS

Several lines of evidence suggest a major involvement of inflammation in the neurodegenerative process and therapeutic intervention strategies limiting the inflammatory responses secondary to microglial activation have been proposed by different authors based on many preclinical researches. Furthermore, recent approaches to the development of novel therapeutic strategies for neurodegenerative diseases have focused on their neuroprotective properties rather than concentrating on palliating symptoms of the diseases. Because cannabinoids possess both anti-inflammatory and neuroprotective actions, the use of CB2 receptor agonists offers an interesting, novel and promising therapeutic approach for a range of neurodegenerative disorders.

Moreover, modulation of CB2 receptor function has considerable therapeutic advantages over the modulation of the CB1 receptor, since the selective expression of CB2 receptors on the microglial cells provides a highly specialized target, without the psychoactivity due to CB1 activation. Although more studies are necessary to dissect the molecular mechanisms which lead to changes in CB2 receptor expression in AD and PD, these studies suggest that CB2 receptors may be key regulators of neuroinflammation and may be successfully targeted by therapeutic intervention.

AUTHOR CONTRIBUTIONS

All authors have contributed to the writing, design and preparation of figures. Coordination of efforts has been carried out by the senior authors (TC and SG) of the three participating laboratories.

FUNDING

This study was supported by Grant PRIN 2012 (to SG) (PRIN: 2012JTX3KL_002) and the Post-Doctoral fellowship of Dr Adele Romano (FIR: RBFR12DELS_003).

REFERENCES

Arroyo, D. S., Soria, J. A., Gaviglio, E. A., Rodriguez-Galan, M. C., and Iribarren, P. (2011). Toll-like receptors are key players in neurodegeneration. *Int. Immunopharmacol.* 11, 1415–1421. doi: 10.1016/j.intimp.2011.05.006

Aureli, C., Cassano, T., Masci, A., Francioso, A., Martire, S., Cocciolo, A., et al. (2014). 5-S-cysteinyldopamine neurotoxicity: influence on the expression of α-synuclein and ERp57 in cellular and animal models of Parkinson's disease. *J. Neurosci. Res.* 92, 347–358. doi: 10.1002/jnr.23318

Austin, S. A., Floden, A. M., Murphy, E. J., and Combs, C. K. (2006). Alpha-synuclein expression modulates microglial activation phenotype. *J. Neurosci.* 26, 10558–10563. doi: 10.1523/JNEUROSCI.1799-06.2006

Bartels, A. L., and Leenders, K. L. (2009). Parkinson's disease: the syndrome, the pathogenesis and pathophysiology. *Cortex* 45, 915–921. doi: 10.1016/j.cortex.2008.11.010

Bedse, G., Romano, A., Cianci, S., Lavecchia, A. M., Lorenzo, P., Elphick, M. R., et al. (2014). Altered expression of the CB1 cannabinoid receptor in the triple transgenic mouse model of Alzheimer's disease. *J. Alzheimers. Dis.* 40, 701–712. doi: 10.3233/JAD-131910

Bedse, G., Romano, A., Lavecchia, A. M., Cassano, T., and Gaetani, S. (2015). The role of endocannabinoid signaling in the molecular mechanisms of neurodegeneration in Alzheimer's disease. *J. Alzheimers. Dis.* 43, 1115–1136. doi: 10.3233/JAD-141635

Benito, C., Núñez, E., Tolón, R. M., Carrier, E. J., Rábano, A., Hillard, C. J., et al. (2003). Cannabinoid CB2 receptors and fatty acid amide hydrolase are selectively overexpressed in neuritic plaque-associated glia in Alzheimer's disease brains. *J. Neurosci.* 23, 11136–11141.

Benito, C., Tolón, R. M., Pazos, M. R., Núñez, E., Castillo, A. I., and Romero, J. (2008). Cannabinoid CB2 receptors in human brain inflammation. *Br. J. Pharmacol.* 153, 277–285. doi: 10.1038/sj.bjp.0707505

Benveniste, E. N., Nguyen, V. T., and Wesemann, D. R. (2004). Molecular regulation of CD40 gene expression in macrophages and microglia. *Brain Behav. Immun.* 18, 7–12. doi: 10.1016/j.bbi.2003.09.001

Bonnet, A. E., and Marchalant, Y. (2015). Potential therapeutical contributions of the endocannabinoid system towards aging and Alzheimer's disease. *Aging Dis.* 6, 400–405. doi: 10.14336/AD.2015.0617

Branchi, I., D'Andrea, I., Armida, M., Carnevale, D., Ajmone-Cat, M. A., Pèzzola, A., et al. (2010). Striatal 6-OHDA lesion in mice: investigating early neurochemical changes underlying Parkinson's disease. *Behav. Brain Res.* 208, 137–143. doi: 10.1016/j.bbr.2009.11.020

Branchi, I., D'Andrea, I., Armida, M., Cassano, T., Pèzzola, A., Potenza, R. L., et al. (2008). Nonmotor symptoms in Parkinson's disease: investigating early-phase onset of behavioral dysfunction in the 6-hydroxydopamine-lesioned rat model. *J. Neurosci. Res.* 86, 2050–2061. doi: 10.1002/jnr.21642

Brown, S. M., Wager-Miller, J., and Mackie, K. (2002). Cloning and molecular characterization of the rat CB2 cannabinoid receptor. *Biochim. Biophys. Acta* 1576, 255–264. doi: 10.1016/S0167-4781(02)00341-X

Buckley, N. E., McCoy, K. L., Mezey, E., Bonner, T., Zimmer, A., Felder, C. C., et al. (2000). Immunomodulation by cannabinoids is absent in mice deficient for the cannabinoid CB(2) receptor. *Eur. J. Pharmacol.* 396, 141–149. doi: 10.1016/S0014-2999(00)00211-9

Cabral, G. A., and Griffin-Thomas, L. (2009). Emerging role of the cannabinoid receptor CB2 in immune regulation: therapeutic prospects for neuroinflammation. *Expert. Rev. Mol. Med.* 11:e3. doi: 10.1017/S1462399409000957

Callén, L., Moreno, E., Barroso-Chinea, P., Moreno-Delgado, D., Cortés, A., Mallol, J., et al. (2012). Cannabinoid receptors CB1 and CB2 form functional heteromers in brain. *J. Biol. Chem.* 287, 20851–20865. doi: 10.1074/jbc.M111.335273

Calne, D., Schulzer, M., Mak, E., and Stoessl, A. J. (2005). Treatment for the progression of Parkinson's disease. *Lancet Neurol.* 4, 206. doi: 10.1016/S1474-4422(05)70026-0

Carroll, C. B., Bain, P. G., Teare, L., Liu, X., Joint, C., Wroath, C., et al. (2004). Cannabis for dyskinesia in Parkinson disease: a randomized double-blind crossover study. *Neurology* 63, 1245–1250. doi: 10.1212/01.WNL.0000140288.48796.8E

Cassano, T., Pace, L., Bedse, G., Lavecchia, A. M., De Marco, F., Gaetani, S., et al. (2016). Glutamate and mitochondria: two prominent players in the oxidative stress-induced neurodegeneration. *Curr. Alzheimer Res.* 13, 185–197. doi: 10.2174/1567205013666151218132725

Cassano, T., Serviddio, G., Gaetani, S., Romano, A., Dipasquale, P., Cianci, S., et al. (2012). Glutamatergic alterations and mitochondrial impairment

in a murine model of Alzheimer disease. *Neurobiol. Aging* 33, 1121.e1-12. doi: 10.1016/j.neurobiolaging.2011.09.021

Chen, B., Bromley-Brits, K., He, G., Cai, F., Zhang, X., and Song, W. (2010). Effect of synthetic cannabinoid HU210 on memory deficits and neuropathology in Alzheimer's disease mouse model. *Curr. Alzheimer Res.* 7, 255–261. doi: 10.2174/156720510791050948

Churcher, I. (2006). Tau therapeutic strategies for the treatment of Alzheimer's disease. *Curr. Top. Med. Chem.* 6, 579–595. doi: 10.2174/156802606776743057

Cravatt, B. F., Giang, D. K., Mayfield, S. P., Boger, D. L., Lerner, R. A., and Gilula, N. B. (1996). Molecular characterization of an enzyme that degrades neuromodulatory fatty-acid amides. *Nature* 384, 83–87. doi: 10.1038/384083a0

D'Addario, C., Micioni Di Bonaventura, M. V., Pucci, M., Romano, A., Gaetani, S., Ciccocioppo, R., et al. (2014). Endocannabinoid signaling and food addiction. *Neurosci. Biobehav. Rev.* 47:203–224. doi: 10.1016/j.neubiorev.2014.08.008

de Lau, L. M., and Breteler, M. M. (2006). Epidemiology of Parkinson's disease. *Lancet Neurol.* 5, 525–535. doi: 10.1016/S1474-4422(06)70471-9

Denora, N., Cassano, T., Laquintana, V., Lopalco, A., Trapani, A., Cimmino, C. S., et al. (2012). Novel codrugs with GABAergic activity for dopamine delivery in the brain. *Int. J. Pharm.* 437, 221–231. doi: 10.1016/j.ijpharm.2012.08.023

Devane, W. A., Hanus, L., Breuer, A., Pertwee, R. G., Stevenson, L. A., Griffin, G., et al. (1992). Isolation and structure of a brain constituent that binds to the cannabinoid receptor. *Science* 258, 1946–1949. doi: 10.1126/science.1470919

Di Gioia, S., Trapani, A., Mandracchia, D., De Giglio, E., Cometa, S., Mangini, V., et al. (2015). Intranasal delivery of dopamine to the striatum using glycol chitosan/sulfobutylether-β-cyclodextrin based nanoparticles. *Eur. J. Pharm. Biopharm.* 94, 180–193. doi: 10.1016/j.ejpb.2015.05.019

Di Iorio, G., Lupi, M., Sarchione, F., Matarazzo, I., Santacroce, R., Petruccelli, F., et al. (2013). The endocannabinoid system: a putative role in neurodegenerative diseases. *Int. J. High Risk Behav. Addict.* 2, 100–106. doi: 10.5812/ijhrba.9222

Di Marzo, V., Stella, N., and Zimmer, A. (2015). Endocannabinoid signalling and the deteriorating brain. *Nat. Rev. Neurosci.* 16, 30–42. doi: 10.1038/nrn3876

Dinh, T. P., Freund, T. F., and Piomelli, D. (2002). A role for monoglyceride lipase in 2-arachidonoylglycerol inactivation. *Chem. Phys. Lipids.* 121, 149–158. doi: 10.1016/S0009-3084(02)00150-0

Duan, Y., Dong, S., Gu, F., Hu, Y., and Zhao, Z. (2012). Advances in the pathogenesis of Alzheimer's disease: focusing on tau-mediated neurodegeneration. *Transl. Neurodegener.* 1:24. doi: 10.1186/2047-9158-1-24

Egertová, M., Cravatt, B. F., and Elphick, M. R. (2003). Comparative analysis of fatty acid amide hydrolase and cb(1) cannabinoid receptor expression in the mouse brain: evidence of a widespread role for fatty acid amide hydrolase in regulation of endocannabinoid signaling. *Neuroscience* 119, 481–496. doi: 10.1016/S0306-4522(03)00145-3

Ehrhart, J., Obregon, D., Mori, T., Hou, H., Sun, N., Bai, Y., et al. (2005). Stimulation of cannabinoid receptor 2 (CB2) suppresses microglial activation. *J. Neuroinflammation.* 2:29. doi: 10.1186/1742-2094-2-29

Elphick, M. R., and Egertová, M. (2005). The phylogenetic distribution and evolutionary origins of endocannabinoid signalling. *Handb. Exp. Pharmacol.* 168, 283–297. doi: 10.1007/3-540-26573-2_9

Esposito, G., Iuvone, T., Savani, C., Scuderi, C., De Filippis, D., Papa, M., et al. (2007). Opposing control of cannabinoid receptor stimulation on amyloid-beta-induced reactive gliosis: *in vitro* and *in vivo* evidence. *J. Pharmacol. Exp. Ther.* 322, 1144–1152. doi: 10.1124/jpet.107.121566

Fagan, S. G., and Campbell, V. A. (2014). The influence of cannabinoids on generic traits of neurodegeneration. *Br. J. Pharmacol.* 171, 1347–1360. doi: 10.1111/bph.12492

Fakhfouri, G., Ahmadiani, A., Rahimian, R., Grolla, A. A., Moradi, F., and Haeri, A. (2012). WIN55212-2 attenuates amyloid-beta-induced neuroinflammation in rats through activation of cannabinoid receptors and PPAR-γ pathway. *Neuropharmacology* 63, 653–666. doi: 10.1016/j.neuropharm.2012.05.013

Fernández-Ruiz, J., García, C., Sagredo, O., Gómez-Ruiz, M., and de Lago, E. (2010). The endocannabinoid system as a target for the treatment of neuronal damage. *Expert Opin. Ther. Targets* 14, 387–404. doi: 10.1517/14728221003709792

Fernández-Ruiz, J., Moro, M. A., and Martínez-Orgado, J. (2015). Cannabinoids in neurodegenerative disorders and stroke/brain trauma: from preclinical models to clinical applications. *Neurotherapeutics* 12, 793–806. doi: 10.1007/s13311-015-0381-7

Freund, T. F., Katona, I., and Piomelli, D. (2003). Role of endogenous cannabinoids in synaptic signaling. *Physiol. Rev.* 83, 1017–1066. doi: 10.1152/physrev.00004.2003

Gao, H. M., Kotzbauer, P. T., Uryu, K., Leight, S., Trojanowski, J. Q., and Lee, V. M. (2008). Neuroinflammation and oxidation/nitration of alpha-synuclein linked to dopaminergic neurodegeneration. *J. Neurosci.* 28, 7687–7698. doi: 10.1523/JNEUROSCI.0143-07.2008

García, C., Palomo-Garo, C., García-Arencibia, M., Ramos, J., Pertwee, R., and Fernández-Ruiz, J. (2011). Symptom-relieving and neuroprotective effects of the phytocannabinoid Δ^9-THCV in animal models of Parkinson's disease. *Br. J. Pharmacol.* 163, 1495–1506. doi: 10.1111/j.1476-5381.2011.01278.x

García-Arencibia, M., García, C., Kurz, A., Rodríguez-Navarro, J. A., Gispert-Sáchez, S., Mena, M. A., et al. (2009). Cannabinoid CB1 receptors are early downregulated followed by a further upregulation in the basal ganglia of mice with deletion of specific park genes. *J. Neural. Transm. Suppl.* 73, 269–275. doi: 10.1007/978-3-211-92660-4_22

García-Arencibia, M., González, S., de Lago, E., Ramos, J. A., Mechoulam, R., and Fernández-Ruiz, J. (2007). Evaluation of the neuroprotective effect of cannabinoids in a rat model of Parkinson's disease: importance of antioxidant and cannabinoids receptor-independent properties. *Brain Res.* 1134, 162–170. doi: 10.1016/j.brainres.2006.11.063

Gerhard, A., Pavese, N., Hotton, G., Turkheimer, F., Es, M., Hammers, A., et al. (2006). *In vivo* imaging of microglial activation with [11C](R)-PK11195 PET in idiopathic Parkinson's disease. *Neurobiol. Dis.* 21, 404–412. doi: 10.1016/j.nbd.2005.08.002

Gómez-Gálvez, Y., Palomo-Garo, C., Fernández-Ruiz, J., and García, C. (2016). Potential of the cannabinoid CB(2) receptor as a pharmacological target against inflammation in Parkinson's disease. *Prog. Neuropsychopharmacol. Biol. Psychiatry* 64, 200–208. doi: 10.1016/j.pnpbp.2015.03.017

Griffin, G., Tao, Q., and Abood, M. E. (2000). Cloning and pharmacological characterization of the rat CB(2) cannabinoid receptor. *J. Pharmacol. Exp. Ther.* 292, 886–894.

Grünblatt, E., Bartl, J., Zehetmayer, S., Ringel, T. M., Bauer, P., Riederer, P., et al. (2009). Gene expression as peripheral biomarkers for sporadic Alzheimer's disease. *J. Alzheimers. Dis.* 16, 627–634. doi: 10.3233/JAD-2009-0996

Halleskog, C., Mulder, J., Dahlström, J., Mackie, K., Hortobágyi, T., Tanila, H., et al. (2011). WNT signaling in activated microglia is proinflammatory. *Glia* 59, 119–131. doi: 10.1002/glia.21081

Halliday, G. M., and Stevens, C. H. (2011). Glia: initiators and progressors of pathology in Parkinson's disease. *Mov. Disord.* 26, 6–17. doi: 10.1002/mds.23455

Horti, A. G., Gao, Y., Ravert, H. T., Finley, P., Valentine, H., Wong, D. F., et al. (2010). Synthesis and biodistribution of [11C]A-836339, a new potential radioligand for PET imaging of cannabinoid type 2 receptors (CB2). *Bioorg. Med. Chem.* 18, 5202–5207. doi: 10.1016/j.bmc.2010.05.058

Howlett, A. C., Barth, F., Bonner, T. I., Cabral, G., Casellas, P., Devane, W. A., et al. (2002). International union of pharmacology. XXVII. Classification of cannabinoid receptors. *Pharmacol. Rev.* 54, 161–202. doi: 10.1124/pr.54.2.161

Jimenez-Del-Rio, M., Daza-Restrepo, A., and Velez-Pardo, C. (2008). The cannabinoid CP55,940 prolongs survival and improves locomotor activity in Drosophila melanogaster against paraquat: implications in Parkinson's disease. *Neurosci. Res.* 61, 404–411. doi: 10.1016/j.neures.2008.04.011

Kalifa, S., Polston, E. K., Allard, J. S., and Manaye, K. F. (2011). Distribution patterns of cannabinoid CB1 receptors in the hippocampus of APPswe/PS1ΔE9 double transgenic mice. *Brain Res.* 1376, 94–100. doi: 10.1016/j.brainres.2010.12.061

Klegeris, A., Bissonnette, C. J., and McGeer, P. L. (2003). Reduction of human monocytic cell neurotoxicity and cytokine secretion by ligands of the cannabinoid-type CB2 receptor. *Br. J. Pharmacol.* 139, 775–786. doi: 10.1038/sj.bjp.0705304

Klegeris, A., Pelech, S., Giasson, B. I., Maguire, J., Zhang, H., McGeer, E. G., et al. (2008). Alpha-synuclein activates stress signaling protein kinases in THP-1 cells and microglia. *Neurobiol. Aging* 29, 739–752. doi: 10.1016/j.neurobiolaging.2006.11.013

Klein, T. W., Newton, C., Larsen, K., Lu, L., Perkins, I., Nong, L., et al. (2003). The cannabinoid system and immune modulation. *J. Leukoc. Biol.* 74, 486–496. doi: 10.1189/jlb.0303101

Krüger, R., Kuhn, W., Müller, T., Woitalla, D., Graeber, M., Kösel, S., et al. (1998). Ala30Pro mutation in the gene encoding alpha-synuclein in Parkinson's disease. *Nat. Genet.* 18, 106–108. doi: 10.1038/ng0298-106

Lastres-Becker, I., Cebeira, M., de Ceballos, M. L., Zeng, B. Y., Jenner, P., Ramos, J. A., et al. (2001). Increased cannabinoid CB1 receptor binding and activation of GTP-binding proteins in the basal ganglia of patients with Parkinson's syndrome and of MPTP-treated marmosets. *Eur. J. Neurosci.* 14, 1827–1832. doi: 10.1046/j.0953-816x.2001.01812.x

Liu, Q. R., Pan, C. H., Hishimoto, A., Li, C. Y., Xi, Z. X., Llorente-Berzal, A., et al. (2009). Species differences in cannabinoid receptor 2 (CNR2 gene): identification of novel human and rodent CB2 isoforms, differential tissue expression and regulation by cannabinoid receptor ligands. *Genes Brain Behav.* 8, 519–530. doi: 10.1111/j.1601-183X.2009.00498.x

Lu, H. C., and Mackie, K. (2015). An introduction to the endogenous cannabinoid system. *Biol. Psychiatry* 79, 516–525. doi: 10.1016/j.biopsych.2015.07.028

Maccarrone, M., Bari, M., Battista, N., Di Rienzo, M., and Finazzi-Agrò, A. (2001). Endogenous cannabinoids in neuronal and immune cells: toxic effects, levels and degradation. *Funct. Neurol.* 16(4 Suppl.), 53–60.

Maccarrone, M., Dainese, E., and Oddi, S. (2010). Intracellular trafficking of anandamide: new concepts for signaling. *Trends Biochem. Sci.* 35, 601–608. doi: 10.1016/j.tibs.2010.05.008

Mackie, K. (2005). Distribution of cannabinoid receptors in the central and peripheral nervous system. *Handb. Exp. Pharmacol.* 168, 299–325. doi: 10.1007/3-540-26573-2_10

Manuel, I., González de San Román, E., Giralt, M. T., Ferrer, I., and Rodríguez-Puertas, R. (2014). Type-1 cannabinoid receptor activity during Alzheimer's disease progression. *J. Alzheimers. Dis.* 42, 761–766. doi: 10.3233/JAD-140492

Marsicano, G., Moosmann, B., Hermann, H., Lutz, B., and Behl, C. (2002). Neuroprotective properties of cannabinoids against oxidative stress: role of the cannabinoid receptor CB1. *J. Neurochem.* 80, 448–456. doi: 10.1046/j.0022-3042.2001.00716.x

Martin-Moreno, A. M., Brera, B., Spuch, C., Carro, E., García-García, L., Delgado, M., et al. (2012). Prolonged oral cannabinoid administration prevents neuroinflammation, lowers β-amyloid levels and improves cognitive performance in Tg APP 2576 mice. *J. Neuroinflammation.* 9:8. doi: 10.1186/1742-2094-9-8

McGeer, P. L., Itagaki, S., Boyes, B. E., and McGeer, E. G. (1988). Reactive microglia are positive for HLA-DR in the substantia nigra of Parkinson's and Alzheimer's disease brains. *Neurology* 38, 1285–1291. doi: 10.1212/WNL.38.8.1285

McGeer, P. L., McGeer, E. G., and Yasojima, K. (2000). Alzheimer disease and neuroinflammation. *J. Neural Transm. Suppl.* 59, 53–57. doi: 10.1007/978-3-7091-6781-6_8

McPartland, J., Di Marzo, V., De Petrocellis, L., Mercer, A., and Glass, M. (2001). Cannabinoid receptors are absent in insects. *J. Comp. Neurol.* 436, 423–429. doi: 10.1002/cne.1078

Mecha, M., Carrillo-Salinas, F. J., Feliú, A., Mestre, L., and Guaza, C. (2016). Microglia activation states and cannabinoid system: therapeutic implications. *Pharmacol. Ther.* 166:40–55. doi: 10.1016/j.pharmthera.2016.06.011

Mechoulam, R. (1970). Marihuana chemistry. *Science* 168, 1159–1166. doi: 10.1126/science.168.3936.1159

Mechoulam, R. (2005). Plant cannabinoids: a neglected pharmacological treasure trove. *Br. J. Pharmacol.* 146, 913–915. doi: 10.1038/sj.bjp.0706415

Mechoulam, R., Ben-Shabat, S., Hanus, L., Ligumsky, M., Kaminski, N. E., Schatz, A. R., et al. (1995). Identification of an endogenous 2-monoglyceride, present in canine gut, that binds to cannabinoid receptors. *Biochem. Pharmacol.* 50, 83–90. doi: 10.1016/0006-2952(95)00109-D

Mechoulam, R., and Gaoni, Y. (1965). A total synthesis of DL-delta-1-tetrahydrocannabinol, the active constituent of hashish. *J. Am. Chem. Soc.* 87, 3273–3275. doi: 10.1021/ja01092a065

Mechoulam, R., and Parker, L. A. (2013). The endocannabinoid system and the brain. *Annu. Rev. Psychol.* 64, 21–47. doi: 10.1146/annurev-psych-113011-143739

Micale, V., Di Marzo, V., Sulcova, A., Wotjak, C. T., and Drago, F. (2013). Endocannabinoid system and mood disorders: priming a target for new therapies. *Pharmacol. Ther.* 138, 18–37. doi: 10.1016/j.pharmthera.2012.12.002

Molina-Holgado, F., Molina-Holgado, E., Guaza, C., and Rothwell, N. J. (2002). Role of CB1 and CB2 receptors in the inhibitory effects of cannabinoids on lipopolysaccharide-induced nitric oxide release in astrocyte cultures. *J. Neurosci. Res.* 67, 829–836. doi: 10.1002/jnr.10165

Molina-Holgado, F., Pinteaux, E., Moore, J. D., Molina-Holgado, E., Guaza, C., Gibson, R. M., et al. (2003). Endogenous interleukin-1 receptor antagonist mediates anti-inflammatory and neuroprotective actions of cannabinoids in neurons and glia. *J. Neurosci.* 23, 6470–6474.

Morgese, M. G., Cassano, T., Cuomo, V., and Giuffrida, A. (2007). Anti-dyskinetic effects of cannabinoids in a rat model of Parkinson's disease: role of CB(1) and TRPV1 receptors. *Exp. Neurol.* 208, 110–119. doi: 10.1016/j.expneurol.2007.07.021

Morgese, M. G., Cassano, T., Gaetani, S., Macheda, T., Laconca, L., Dipasquale, P., et al. (2009). Neurochemical changes in the striatum of dyskinetic rats after administration of the cannabinoid agonist WIN55,212-2. *Neurochem. Int.* 54, 56–64. doi: 10.1016/j.neuint.2008.10.007

Mulder, J., Zilberter, M., Pasquaré, S. J., Alpár, A., Schulte, G., Ferreira, S. G., et al. (2011). Molecular reorganization of endocannabinoid signalling in Alzheimer's disease. *Brain* 134(Pt 4), 1041–1060. doi: 10.1093/brain/awr046

Munoz, L., and Ammit, A. J. (2010). Targeting p38 MAPK pathway for the treatment of Alzheimer's disease. *Neuropharmacology* 58, 561–568. doi: 10.1016/j.neuropharm.2009.11.010

Nong, L., Newton, C., Friedman, H., and Klein, T. W. (2001). CB1 and CB2 receptor mRNA expression in human peripheral blood mononuclear cells (PBMC) from various donor types. *Adv. Exp. Med. Biol.* 493, 229–233. doi: 10.1007/0-306-47611-8_27

Núñez, E., Benito, C., Pazos, M. R., Barbachano, A., Fajardo, O., González, S., et al. (2004). Cannabinoid CB2 receptors are expressed by perivascular microglial cells in the human brain: an immunohistochemical study. *Synapse* 53, 208–213. doi: 10.1002/syn.20050

Núñez, E., Benito, C., Tolón, R. M., Hillard, C. J., Griffin, W. S., and Romero, J. (2008). Glial expression of cannabinoid CB(2) receptors and fatty acid amide hydrolase are beta amyloid-linked events in Down's syndrome. *Neuroscience* 151, 104–110. doi: 10.1016/j.neuroscience.2007.10.029

Ouchi, Y., Yoshikawa, E., Sekine, Y., Futatsubashi, M., Kanno, T., Ogusu, T., et al. (2005). Microglial activation and dopamine terminal loss in early Parkinson's disease. *Ann. Neurol.* 57, 168–175. doi: 10.1002/ana.20338

Pertwee, R. G., Howlett, A. C., Abood, M. E., Alexander, S. P., Di Marzo, V., Elphick, M. R., et al. (2010). International union of basic and clinical pharmacology. LXXIX. Cannabinoid receptors and their ligands: beyond CB1 and CB2. *Pharmacol Rev.* 62, 588–631. doi: 10.1124/pr.110.003004

Polymeropoulos, M. H., Lavedan, C., Leroy, E., Ide, S. E., Dehejia, A., Dutra, A., et al. (1997). Mutation in the alpha-synuclein gene identified in families with Parkinson's disease. *Science* 276, 2045–2047. doi: 10.1126/science.276.5321.2045

Price, D. A., Martinez, A. A., Seillier, A., Koek, W., Acosta, Y., Fernandez, E., et al. (2009). WIN55,212-2, a cannabinoid receptor agonist, protects against nigrostriatal cell loss in the 1-methyl-4-phenyl-1,2,3,6-tetrahydropyridine mouse model of Parkinson's disease. *Eur. J. Neurosci.* 29, 2177–2186. doi: 10.1111/j.1460-9568.2009.06764.x

Ramírez, B. G., Blázquez, C., Gómez del Pulgar, T., Guzmán, M., and de Ceballos, M. L. (2005). Prevention of Alzheimer's disease pathology by cannabinoids: neuroprotection mediated by blockade of microglial activation. *J. Neurosci.* 25, 1904–1913. doi: 10.1523/JNEUROSCI.4540-04.2005

Reed-Geaghan, E. G., Savage, J. C., Hise, A. G., and Landreth, G. E. (2009). CD14 and toll-like receptors 2 and 4 are required for fibrillar A{beta}-stimulated microglial activation. *J. Neurosci.* 29, 11982–11992. doi: 10.1523/JNEUROSCI.3158-09.2009

Reynolds, A. D., Glanzer, J. G., Kadiu, I., Ricardo-Dukelow, M., Chaudhuri, A., Ciborowski, P., et al. (2007). Nitrated alpha-synuclein-activated microglial profiling for Parkinson's disease. *J. Neurochem.* 104, 1504–1525. doi: 10.1111/j.1471-4159.2007.05087.x

Reynolds, A. D., Kadiu, I., Garg, S. K., Glanzer, J. G., Nordgren, T., Ciborowski, P., et al. (2008). Nitrated alpha-synuclein and microglial neuroregulatory activities. *J. Neuroimmune Pharmacol.* 3, 59–74. doi: 10.1007/s11481-008-9100-z

Rodríguez-Cueto, C., Benito, C., Fernández-Ruiz, J., Romero, J., Hernández-Gálvez, M., and Gómez-Ruiz, M. (2014). Changes in CB(1) and CB(2) receptors in the post-mortem cerebellum of humans affected by spinocerebellar ataxias. *Br. J. Pharmacol.* 171, 1472–1489. doi: 10.1111/bph.12283

Rohn, T. T. (2010). The role of caspases in Alzheimer's disease; potential novel therapeutic opportunities. *Apoptosis* 15, 1403–1409. doi: 10.1007/s10495-010-0463-2

Saito, V. M., Wotjak, C. T., and Moreira, F. A. (2010). Pharmacological exploitation of the endocannabinoid system: new perspectives for the treatment of depression and anxiety disorders? *Revista Brasileira de Psiquiatria* 32, S7–S14.

Sánchez, A. J., and García-Merino, A. (2012). Neuroprotective agents: cannabinoids. *Clin. Immunol.* 142, 57–67. doi: 10.1016/j.clim.2011.02.010

Sastre, M., Klockgether, T., and Heneka, M. T. (2006). Contribution of inflammatory processes to Alzheimer's disease: molecular mechanisms. *Int. J. Dev. Neurosci.* 24, 167–176. doi: 10.1016/j.ijdevneu.2005.11.014

Serviddio, G., Romano, A. D., Cassano, T., Bellanti, F., Altomare, E., and Vendemiale, G. (2011). Principles and therapeutic relevance for targeting mitochondria in aging and neurodegenerative diseases. *Curr. Pharm. Des.* 17, 2036–2055. doi: 10.2174/138161211796904740

Sheng, W. S., Hu, S., Min, X., Cabral, G. A., Lokensgard, J. R., and Peterson, P. K. (2005). Synthetic cannabinoid WIN55,212-2 inhibits generation of inflammatory mediators by IL-1beta-stimulated human astrocytes. *Glia* 49, 211–219. doi: 10.1002/glia.20108

Shire, D., Calandra, B., Rinaldi-Carmona, M., Oustric, D., Pessègue, B., Bonnin-Cabanne, O., et al. (1996). Molecular cloning, expression and function of the murine CB2 peripheral cannabinoid receptor. *Biochim. Biophys. Acta* 1307, 132–136. doi: 10.1016/0167-4781(96)00047-4

Solas, M., Francis, P. T., Franco, R., and Ramirez, M. J. (2013). CB2 receptor and amyloid pathology in frontal cortex of Alzheimer's disease patients. *Neurobiol. Aging* 34, 805–808. doi: 10.1016/j.neurobiolaging.2012.06.005

Spillantini, M. G., Crowther, R. A., Jakes, R., Hasegawa, M., and Goedert, M. (1998). alpha-Synuclein in filamentous inclusions of Lewy bodies from Parkinson's disease and dementia with lewy bodies. *Proc. Natl. Acad. Sci. U.S.A.* 95, 6469–6473. doi: 10.1073/pnas.95.11.6469

Spoto, B., Fezza, F., Parlongo, G., Battista, N., Sgro', E., Gasperi, V., et al. (2006). Human adipose tissue binds and metabolizes the endocannabinoids anandamide and 2-arachidonoylglycerol. *Biochimie* 88, 1889–1897. doi: 10.1016/j.biochi.2006.07.019

Stella, N. (2010). Cannabinoid and cannabinoid-like receptors in microglia, astrocytes, and astrocytomas. *Glia* 58, 1017–1030. doi: 10.1002/glia.20983

Sugiura, T., Kondo, S., Kishimoto, S., Miyashita, T., Nakane, S., Kodaka, T., et al. (2000). Evidence that 2-arachidonoylglycerol but not N-palmitoylethanolamine or anandamide is the physiological ligand for the cannabinoid CB2 receptor. Comparison of the agonistic activities of various cannabinoid receptor ligands in HL-60 cells. *J. Biol. Chem.* 275, 605–612. doi: 10.1074/jbc.275.1.605

Sugiura, T., Kondo, S., Sukagawa, A., Nakane, S., Shinoda, A., Itoh, K., et al. (1995). 2-Arachidonoylglycerol: a possible endogenous cannabinoid receptor ligand in brain. *Biochem. Biophys. Res. Commun.* 215, 89–97. doi: 10.1006/bbrc.1995.2437

Tansey, M. G., and Goldberg, M. S. (2010).Neuroinflammation in Parkinson's disease: its role in neuronal death and implications for therapeutic intervention. *Neurobiol. Dis.* 37, 510–518. doi: 10.1016/j.nbd.2009.11.004

Taylor, J. M., Main, B. S., and Crack, P. J. (2013). Neuroinflammation and oxidative stress: co-conspirators in the pathology of Parkinson's disease. *Neurochem. Int.* 62, 803–819. doi: 10.1016/j.neuint.2012.12.016

Ternianov, A., Pérez-Ortiz, J. M., Solesio, M. E., García-Gutiérrez, M. S., Ortega-Álvaro, A., Navarrete, F., et al. (2012). Overexpression of CB2 cannabinoid receptors results in neuroprotection against behavioral and neurochemical alterations induced by intracaudate administration of 6-hydroxydopamine. *Neurobiol. Aging* 33, 421.e1-16. doi: 10.1016/j.neurobiolaging.2010.09.012

Thomas, M. P., Chartrand, K., Reynolds, A., Vitvitsky, V., Banerjee, R., and Gendelman, H. E. (2007). Ion channel blockade attenuates aggregated alpha synuclein induction of microglial reactive oxygen species: relevance for the pathogenesis of Parkinson's disease. *J. Neurochem.* 100, 503–519. doi: 10.1111/j.1471-4159.2006.04315.x

Trapani, A., De Giglio, E., Cafagna, D., Denora, N., Agrimi, G., Cassano, T., et al. (2011). Characterization and evaluation of chitosan nanoparticles for dopamine brain delivery. *Int. J. Pharm.* 419, 1296–1307. doi: 10.1016/j.ijpharm.2011.07.036

Turcotte, C., Blanchet, M. R., Laviolette, M., and Flamand, N. (2016). The CB(2) receptor and its role as a regulator of inflammation. *Cell. Mol. Life Sci.* 73, 4449–4470. doi: 10.1007/s00018-016-2300-4

Van Sickle, M. D., Duncan, M., Kingsley, P. J., Mouihate, A., Urbani, P., Mackie, K., et al. (2005). Identification and functional characterization of brainstem cannabinoid CB2 receptors. *Science* 310, 329–332. doi: 10.1126/science.1115740

Vendel, E., and de Lange, E. C. (2014). Functions of the CB1 and CB2 receptors in neuroprotection at the level of the blood-brain barrier. *Neuromol. Med.* 16, 620–642. doi: 10.1007/s12017-014-8314-x

Viscomi, M. T., Oddi, S., Latini, L., Pasquariello, N., Florenzano, F., Bernardi, G., et al. (2009). Selective CB2 receptor agonism protects central neurons from remote axotomy-induced apoptosis through the PI3K/Akt pathway. *J. Neurosci.* 29, 4564–4570. doi: 10.1523/JNEUROSCI.0786-09.2009

Walsh, D. M., and Selkoe, D. J. (2004). Deciphering the molecular basis of memory failure in Alzheimer's disease. *Neuron* 44, 181–193. doi: 10.1016/j.neuron.2004.09.010

White, J. A., Manelli, A. M., Holmberg, K. H., Van Eldik, L. J., and Ladu, M. J. (2005). Differential effects of oligomeric and fibrillar amyloid-beta 1-42 on astrocyte-mediated inflammation. *Neurobiol. Dis.* 18, 459–465. doi: 10.1016/j.nbd.2004.12.013

Wotherspoon, G., Fox, A., McIntyre, P., Colley, S., Bevan, S., and Winter, J. (2005). Peripheral nerve injury induces cannabinoid receptor 2 protein expression in rat sensory neurons. *Neuroscience* 135, 235–245. doi: 10.1016/j.neuroscience.2005.06.009

Yiangou, Y., Facer, P., Durrenberger, P., Chessell, I. P., Naylor, A., Bountra, C., et al. (2006). COX-2, CB2 and P2X7-immunoreactivities are increased in activated microglial cells/macrophages of multiple sclerosis and amyotrophic lateral sclerosis spinal cord. *BMC Neurol.* 6:12. doi: 10.1186/1471-2377-6-12

Zarranz, J. J., Alegre, J., Gómez-Esteban, J. C., Lezcano, E., Ros, R., Ampuero, I., et al. (2004). The new mutation, E46K, of alpha-synuclein causes Parkinson and Lewy body dementia. *Ann. Neurol.* 55, 164–173. doi: 10.1002/ana.10795

Zhang, J., Hoffert, C., Vu, H. K., Groblewski, T., Ahmad, S., and O'Donnell, D. (2003). Induction of CB2 receptor expression in the rat spinal cord of neuropathic but not inflammatory chronic pain models. *Eur. J. Neurosci.* 17, 2750–2754. doi: 10.1046/j.1460-9568.2003.02704.x

Zhang, W., Wang, T., Pei, Z., Miller, D. S., Wu, X., Block, M. L., et al. (2005). Aggregated alpha-synuclein activates microglia: a process leading to disease progression in Parkinson's disease. *FASEB J.* 19, 533–542. doi: 10.1096/fj.04-2751com

Conflict of Interest Statement: The authors declare that the research was conducted in the absence of any commercial or financial relationships that could be construed as a potential conflict of interest.

Copyright © 2017 Cassano, Calcagnini, Pace, De Marco, Romano and Gaetani. This is an open-access article distributed under the terms of the Creative Commons Attribution License (CC BY). The use, distribution or reproduction in other forums is permitted, provided the original author(s) or licensor are credited and that the original publication in this journal is cited, in accordance with accepted academic practice. No use, distribution or reproduction is permitted which does not comply with these terms.

frontiers in Neuroscience

REVIEW
published: 31 May 2016
doi: 10.3389/fnins.2016.00243

CB_2 Cannabinoid Receptor As Potential Target against Alzheimer's Disease

Ester Aso[1,2]* *and Isidro Ferrer*[1,2]*

[1] *Institut de Neuropatologia, Servei d'Anatomia Patològica, Bellvitge Biomedical Research Institute (IDIBELL)-Hospital Universitari de Bellvitge, Universitat de Barcelona, L'Hospitalet de Llobregat, Spain,* [2] *CIBERNED - Centro de Investigación Biomédica en Red de Enfermedades Neurodegenerativas, Instituto Carlos III, Madrid, Spain*

The CB_2 receptor is one of the components of the endogenous cannabinoid system, a complex network of signaling molecules and receptors involved in the homeostatic control of several physiological functions. Accumulated evidence suggests a role for CB_2 receptors in Alzheimer's disease (AD) and indicates their potential as a therapeutic target against this neurodegenerative disease. Levels of CB_2 receptors are significantly increased in *post-mortem* AD brains, mainly in microglia surrounding senile plaques, and their expression levels correlate with the amounts of $A\beta_{42}$ and β-amyloid plaque deposition. Moreover, several studies on animal models of AD have demonstrated that specific CB_2 receptor agonists, which are devoid of psychoactive effects, reduce AD-like pathology, resulting in attenuation of the inflammation associated with the disease but also modulating Aβ and tau aberrant processing, among other effects. CB_2 receptor activation also improves cognitive impairment in animal models of AD. This review discusses available data regarding the role of CB_2 receptors in AD and the potential usefulness of specific agonists of these receptors against AD.

Keywords: CB_2 receptor, cannabinoids, Alzheimer, neuroinflammation, β-amyloid, tau, oxidative stress

OPEN ACCESS

Edited by:
Marialessandra Contino, Università degli Studi di Bari "Aldo Moro," Italy

Reviewed by:
Aurel Popa-Wagner, University of Medicine Rostock, Germany
Adam Denes, University of Manchester, UK
Andras Bilkei-Gorzo, University of Bonn, Germany
Julian Romero, Francisco de Vitoria University, Spain

***Correspondence:**
Ester Aso
aso@bellvitgehospital.cat;
Isidro Ferrer
8082ifa@gmail.com

Specialty section:
This article was submitted to Neurodegeneration, a section of the journal Frontiers in Neuroscience

Received: *29 March 2016*
Accepted: *17 May 2016*
Published: *31 May 2016*

Citation:
Aso E and Ferrer I (2016) CB_2 Cannabinoid Receptor As Potential Target against Alzheimer's Disease. Front. Neurosci. 10:243. doi: 10.3389/fnins.2016.00243

OVERVIEW OF ALZHEIMER'S DISEASE

Alzheimer's disease (AD) is an age-dependent neurodegenerative disorder characterized by slowly progressive cognitive decline with fatal outcome. To date, no effective treatment is available. Dementia due to AD occurs in one in nine people aged 65 and in about one in four at the age of 85 (Hebert et al., 2013). Prevalence is expected to grow in coming decades as the size and proportion of the older population continue to increase due to the rise in life expectancy in developed countries (Hebert et al., 2013).

AD is morphologically distinguished by the presence in the brain of senile plaques, mainly composed of different species of fibrillar β-amyloid (Aβ) produced by the cleavage of the β-amyloid precursor protein (APP), and neurofibrillary tangles composed of various isoforms of hyper-phosphorylated and truncated tau protein. Senile plaques are surrounded by dystrophic neurites, reactive astrocytes, and microglia. Neurofibrillary tangles first appear in selected nuclei of the brain stem, and entorhinal and transentorhinal cortex, and then progress to the hippocampus and limbic system, and finally to most of the telencephalon (Braak and Braak, 1991). The development and progression of senile plaques does not parallel the evolution of tau pathology in sporadic AD (Thal et al., 2002). Aβ and tau misfolded proteins compromise neural activity due to an increase in

toxic function and/or loss of their normal function, thus contributing to the decline of neuronal organization manifested as synaptic dysfunction and neuronal death (Duyckaerts and Dickson, 2011; Ferrer, 2012). A self-propagating process of misfolded proteins has been suggested to explain disease progression (Jucker and Walker, 2013). Aβ and misfolded tau aggregate into seeds that are able to modify native proteins causing them to aggregate and to form pathogenic assemblies in a prion-like way (Meyer-Luehmann et al., 2006; Clavaguera et al., 2009; Stöhr et al., 2012).

It is important to note that AD-related pathology begins more than 20 years before the onset of dementia. First stages of AD in which lesions are restricted to the brain stem and inner parts of the temporal lobe are usually asymptomatic. About 80% of individuals aged 65 present senile plaques and/or neurofibrillary tangles in specific brain areas but only about 5% of them suffer from dementia. This is an important point as AD-related pathology is common in the elderly but this does not inevitably lead to dementia. AD changes restricted to the inner temporal lobe can progress slowly and be well tolerated in some individuals. Only the accumulation of lesions in certain individuals determines a progression of the neurodegenerative disease, which leads to dementia once reached determinate threshold (Ferrer, 2012). The slow progression of the neurodegenerative process visualizes a putative temporal window for therapeutic intervention. However, to date most therapeutic interventions aimed at modifying a single pathological factor (e.g., cholinergic dysfunction, inflammation, Aβ and/or tau aberrant processing) have failed because of their limited benefit or for safety reasons (Scheltens et al., 2016). Considering that multiple alterations are concomitant to Aβ and tau aberrant processing in AD (Ferrer, 2012), compounds with pleiotropic activity which will target in parallel several processes that play key roles in AD are expected to yield greater benefits than those obtained by current therapies (Bolognesi et al., 2009; Frautschy and Cole, 2010). Inflammation, mitochondrial dysfunction, oxidative stress, and impaired function of degradation pathways are the most prominent concomitant pathological events (Keller et al., 2000; Ferrer, 2009; Sultana and Butterfield, 2010; López-González et al., 2015), as briefly described in the following paragraphs. These alterations are potential targets of therapeutic intervention.

Inflammation has been proposed as a key factor in the pathogenesis of AD. This is characterized by microglial activation, reactive astrocytes and elevated expression of cytokines and mediators of the inflammatory response. It has been proposed that microglial activation in AD can have beneficial and detrimental effects depending on the stage of the disease. Thus, the acute microglial reaction aims at removing the abnormal protein aggregates appearing at the early stages of the disease. However, cumulative formation of aberrant protein aggregates drives to chronic inflammation which has detrimental consequences due to the sustained exposure to chemokines, cytokines and other inflammatory mediators (Heneka et al., 2015). Conversion of microglia from detrimental (M1) to beneficial (M2) phenotype may be achieved by modulation of pro-inflammatory signaling pathways such as the NLRP3 inflammasome (Heneka et al., 2013). Similar to microglial cells, astrocytes contribute to inflammation in AD by releasing cytokines, interleukins, nitric oxide (NO), and other toxic molecules in response to Aβ exposure at the time they also participate in the internalization and degradation of Aβ (Heneka et al., 2015). However, anti-inflammatory treatments failed to produce beneficial effects in patients with severe cognitive impairment and dementia. This fact is probably due to the fact that inflammatory responses in AD differ not only depending on the stage of the disease but also on the region involved (López-González et al., 2015). That means that inflammatory responses in some regions have a beneficial phenotype whereas they have a deleterious phenotype in other regions in the same individual, thus stressing the need to identify new regulators or modulators of the inflammatory response that can be adapted to specific molecular targets (López-González et al., 2015).

Altered mitochondria are also key factors in the pathogenesis of AD. This includes impaired energy metabolism and increased production of free radicals with subsequent oxidative and nitrosative damage affecting lipids, proteins and nucleic acids (Sultana and Butterfield, 2010). These alterations are already observed in the entorhinal cortex at early stages of AD ultimately leading to neuron exhaustion (Ferrer, 2009). Several studies in AD transgenic mouse models support the potential beneficial effect of compounds targeting mitochondrial dysfunction although the clinical benefit of such drugs in humans is still not known (Onyango et al., 2016).

Finally, another prominent concomitant pathological event in AD is impaired function of degradation pathways (Keller et al., 2000). Oxidative damage and some other pathological events may alter protein structure and function in AD. These modified proteins have to be removed to prevent their toxic accumulation. However, the ubiquitin-proteasome system and autophagy mechanisms are impaired due to the toxic effects of Aβ and oxidative stress damage thus leading to the accumulation of oxidized/unfolded proteins that may contribute to neuronal loss (Tramutola et al., 2016).

ENDOGENOUS CANNABINOID SYSTEM: A ROLE IN NEURODEGENERATIVE DISEASES

Among the candidates to fulfill the requirements for novel effective multi-target therapies against neurodegenerative diseases are newly emerging compounds that target the endogenous cannabinoid system (ECS; Aso and Ferrer, 2014; Fagan and Campbell, 2014; Fernández-Ruiz et al., 2015). Interest in the ECS derives from the pleiotropic activity of this complex network of lipid molecules and receptors, which is involved in homeostatic control of several physiological functions in brain and other organs (Iannotti et al., 2016). The ECS is composed of (i) at least two subtypes of cannabinoid $G_{i/o}$-coupled receptors, CB_1 and CB_2 (Pertwee et al., 2010), (ii) certain endogenous ligands, mainly arachidonoylethanolamine or anandamide (AEA) and 2-arachidonoylglycerol (2-AG) derived from the membrane phospholipids (Pertwee, 2015), (iii) several enzymes

responsible for endocannabinoid biosynthesis and metabolism (Ligresti et al., 2005), and (iv) molecules linked to the cellular uptake and transport of certain endocannabinoids (Fowler, 2013). CB_1 receptors are the most abundant cannabinoid receptors and are located in brain, mainly in neurons but also in glial cells, and in peripheral tissues (Hu and Mackie, 2015). CB_1 activity regulates important brain functions including cognition and memory, emotion, motor control, feeding, and pain perception, by modulating excitatory and inhibitory neurotransmission (Wilson and Nicoll, 2002; Howlett, 2005). Moreover, CB_1 receptors mediate psychoactive effects of cannabis derivatives (Maldonado et al., 2011). In contrast, activation of CB_2 receptors is not accompanied by psychoactive effects (Buckley et al., 2000). CB_2 was initially considered a peripheral cannabinoid receptor because *in situ* hybridization analysis revealed high levels of CB_2 mRNA in spleen but levels below the detection thresholds in brain. CB_2 receptors were demonstrated to modulate immune cell migration and the release of cytokines in cells of the immune system (Cabral and Griffin-Thomas, 2009). However, more recent findings have shown that CB_2 receptors are also present in other tissues including the central nervous system (Atwood and Mackie, 2010). CB_2 receptors are highly inducible and under certain conditions are expressed in brain, mainly by microglia, with levels increasing as these immune cells are activated. CB_2 modulates microglial migration and infiltration into brain areas with active neuroinflammation and degeneration (Walter et al., 2003; Fernández-Ruiz et al., 2008). Moreover, CB_2 receptors are also present at detectable and functional levels in a subset of neurons with increasing expression levels following injury (Atwood and Mackie, 2010). Apart from the regulation of inflammatory processes, some experimental designs also suggest that CB_2 receptors may play a role in nociception (Jhaveri et al., 2007; Whiteside et al., 2007), gastrointestinal function (Wright et al., 2008), neural progenitor cell proliferation and axon guidance (Palazuelos et al., 2012; Duff et al., 2013), and synaptic transmission (Kim and Li, 2015; Li and Kim, 2016), among other functions. Most of the evidence comes from pharmacological studies using specific CB_2 agonists and antagonists, and from genetically manipulated mice. However, the location of CB_2 receptors mediating such effects is not conclusively documented.

As mentioned before, the ECS has a pleiotropic activity and is able to modulate several alterations occurring during normal and pathological aging, including protein misfolding, inflammation, excitotoxicity, mitochondrial dysfunction, and oxidative stress (Bilkei-Gorzo, 2012; Aso and Ferrer, 2014; Fagan and Campbell, 2014; Fernández-Ruiz et al., 2015). Evidence about the role of ECS on aging derives from observations in genetic models. Thus, deficiency in CB_1 receptors contributes to acceleration of aging (Bilkei-Gorzo et al., 2005, 2012) whereas deletion of the endocannabinoid degrading enzyme FAAH enhances age-related microglial activity and concomitant inflammatory responses in brain (Ativie et al., 2015). In contrast, stimulation of certain ECS components produces beneficial effects in experimental models of neurodegenerative diseases (Aso and Ferrer, 2014; Fagan and Campbell, 2014; Fernández-Ruiz et al., 2015). These findings demonstrate a role for ECS in normal and pathological aging that has sustained interest in developing therapies against neurodegenerative diseases based on ECS modulation. Major attention has been focused on the use of cannabinoid agonists, but the psychoactive effects elicited by compounds targeting CB_1 receptors have served to limit their potential development in clinical practice. For this reason, the study of specific CB_2 agonists which are devoid of psychoactive effects is promising, although detailed clinical evaluation is still needed (Atwood et al., 2012).

CB_2 RECEPTORS IN AD BRAINS

A few studies have addressed the analysis of CB_2 contents in AD brain but all of them have resulted in similar findings. A significant increase in CB_2 receptor levels has been found in *post-mortem* AD brains mainly expressed in microglia surrounding senile plaques (Benito et al., 2003; Ramírez et al., 2005; Solas et al., 2013). Similarly, enhanced CB_2 PET binding has been reported in the brain in an animal model of AD (Savonenko et al., 2015). In addition, CB_2-specific staining is also observed in tangle-like bearing neurons and in dystrophic neurites from frontal cortex in AD (Ramírez et al., 2005). Interestingly, expression levels of CB_2 receptors correlate with $A\beta_{42}$ levels and plaque deposition although not with cognitive status (Solas et al., 2013), thus suggesting that these pathogenic events induce CB_2 receptor expression. The strong induction of CB_2 receptors in affected microglia is therapeutically advantageous since it would permit their selective activation in damaged tissues, thereby minimizing the possibility of deleterious side effects. However, CB_2 receptors in AD brain are nitrosylated, probably as a consequence of microglial activation and peroxynitrite radical formation, and this may contribute to the impaired coupling of these receptors to downstream effector signaling molecules (Ramírez et al., 2005). Nevertheless, the functionality of CB_2 receptors seems to be at least partially preserved in AD according to the results of pharmacological experiments carried out in AD models, as described in the following sections.

CB_2 RECEPTOR AS A THERAPEUTIC TARGET IN AD: EVIDENCE FROM EXPERIMENTAL MODELS

During the last decade, a number of studies have provided experimental evidence about the potential therapeutic properties of compounds targeting CB_2 receptors in cellular and animal models that mimic a variety of AD-related changes. A summary of pharmacological findings supporting this hypothesis is shown in **Table 1**. Moreover, at least three different genetically manipulated murine models have recently been created to further demonstrate a role for CB_2 receptors in this neurodegenerative disease (**Table 2**). Most of these assays are focused on the potential benefit derived from the well-known anti-inflammatory properties of CB_2 agonists, but some of them also reveal the capacity of CB_2 receptors to modulate Aβ and hyper-phosphorylated tau levels, among other molecular alterations.

TABLE 1 | Pharmacological evidence of CB_2 receptor as a therapeutic target in AD.

References	AD model	Compound acting on CB_2 receptors	CB_2-mediated effect
Ehrhart et al., 2005	$A\beta_{1-42}$ Microglial cells culture	JWH-015	↓ IFN-γ-mediated CD40 expression ↓ TNF-α production ↑ Phagocytosis of Aβ ↓ NO
Ramírez et al., 2005	$A\beta_{25-35}$ and $A\beta_{1-40}$ Microglial rat primary culture Neuronal rat primary culture Adult rats (i.c.v. injection)	HU-210 WIN55,212-2 JWH-133	↑ Neuronal survival ↓ Microglial reactivity to Aβ ↓ TNF-α levels ↑ Cognitive performance
Eubanks et al., 2006	$A\beta_{1-40}$	Δ^9-THC	AchE inhibition ↓ Aβ aggregation (No direct demonstration of CB_2 involvement)
Esposito et al., 2006	$A\beta_{1-42}$ C6 rat glioma cells PC12 neurons	WIN55,212-2 JWH015 SR144528	= iNOS levels = NO production = Phosphorylated tau levels
Esposito et al., 2007	$A\beta_{1-42}$ C6 rat glioma cells Adult rats (cortical injection)	JWH-015 SR144528	↑ Aβ-induced astrocytic proliferation (CB_2 agonist) ↓ Aβ-induced astrocytic proliferation (CB_2 antagonist)
Tolón et al., 2009	$A\beta_{1-42}$ THP1 human macrophages U373 human astrocytoma Human AD tissue sections	JWH-015 SR144528	↑ Aβ plaque removal ↑ Aβ Phagocytosis
Martín-Moreno et al., 2011	$A\beta_{1-42}$ N13 and BV-2 microglial cells Rat primary microglia culture Adult mice (i.c.v. injection)	JWH-133 WIN55,212-2 HU-308 SR144528	↓ ATP-induced increase in $[Ca^{2+}]_i$ ↑ Microglia migration ↓ NO production ↑ Cognitive performance (no direct demonstration of CB_2 involvement) ↓ TNF-α and IL-6 expression (no direct demonstration of CB_2 involvement)
Fakhfouri et al., 2012	$A\beta_{1-42}$ Adult rats (hippocampal injection)	WIN55,212-2 SR144528	↑ Cognitive performance ↓ TNF-α and nuclear NF-kB levels ↓ Active caspase 3 levels and TUNEL-positive neurons
Martín-Moreno et al., 2012	TgAPP-2576 mice	JWH-133 WIN55,212-2	↑ Cognitive performance ↑ Glucose uptake in brain ↓ Microglial response to Aβ ↓ Aβ deposition ↓ TNF-α and COX-2 levels ↑ Aβ transport across choroid plexus
Aso et al., 2013	APP/PS1 mice	JWH-133	↑ Cognitive performance ↓ Microglial response to Aβ ↓ Pro-inflammatory cytokines (IL-1β, IL-6, TNF-α, and IFN-γ) ↓ Tau hyperphosphorylation around plaques ↓ Oxidative stress damage around plaques
Wu et al., 2013	$A\beta_{1-40}$ Adult rats (hippocampal injection)	MDA7	↓ Expression of microglia and astrocyte markers ↓ Secretion of interleukin-1β

(Continued)

TABLE 1 | Continued

References	AD model	Compound acting on CB_2 receptors	CB_2-mediated effect
			↓ Upsurge of CB_2 receptors ↑ Aβ clearance ↑ Synaptic plasticity ↑ Cognitive performance
Bachmeier et al., 2013	Primary human brain microvascular endothelial cells	CB13 AM630	↑ Aβ transport across blood brain barrier
Chen et al., 2013	Adult mice (Caudate putamen injection) 5xFAD APP mice	Δ^9-THC	↓ Aβ deposition ↓ Number of degenerated neurons (No direct demonstration of CB_2 involvement)
Janefjord et al., 2014	$A\beta_{1-42}$ Neuroblastoma SH-SY5Y cells BV-2 microglial cells	JWH-015 Δ^9-THC	↓ Aβ fibrillisation (no direct demonstration of CB_2 involvement) = Cell viability after $A\beta_{1-42}$ exposure ↑ Cell viability after LPS exposure
Cao et al., 2014	N2a/APPswe cells	Δ^9-THC	↓ Aβ levels ↓ Aβ aggregation ↓ Tau phosphorylation ↑ Mitochondria function (No direct demonstration of CB_2 involvement)
Aso et al., 2015	APP/PS1 mice	Δ^9-THC	↑ Cognitive performance ↓ Astroglial response to Aβ (No direct demonstration of CB_2 involvement)
Köfalvi et al., 2016	TgAPP-2576 mice	JWH-133 WIN55,212-2 AM630	↑ Glucose uptake in brain

Anti-Inflammatory Effects of CB_2 Receptor Activity

Inflammation is common in most neurodegenerative diseases including AD, and it may contribute to progressive neuronal damage. Microglia play a major role in neuroinflammation. Activated microglia produce cytokines and mediators of inflammatory response which, in combination with neurons and astrocytes, create a complex cytokine cycle with deleterious consequences in brain when sustained over time (Heneka et al., 2014; McGeer and McGeer, 2015). CB_2 receptors, mainly expressed in microglia, inhibit microglia-mediated neurotoxicity by reducing the production of pro-inflammatory molecules and by modulating macrophage migration in several pathological conditions (Cabral and Griffin-Thomas, 2009). In addition, CB_2 activity facilitates the transformation of microglial cells from the M1 to M2 phenotype which is suggested to favor phagocytosis and reparative mechanisms (Mecha et al., 2015). As summarized in **Table 1**, a number of studies have shown anti-inflammatory effects of CB_2 agonists in different models of AD. Thus, *in vitro* experiments have demonstrated that the selective agonists JWH-015, JWH-133, and HU-308, and the mixed CB_1–CB_2 receptor agonists WIN55,212-2 and HU-210 reduce the release of pro-inflammatory cytokines in microglial cell cultures exposed to different species of the toxic Aβ peptide (Ehrhart et al., 2005; Ramírez et al., 2005; Martín-Moreno et al., 2011). These findings may be the result of CB_2 agonists reducing microglial activation by decreasing intracellular calcium concentration, as demonstrated in microglial cell cultures (Martín-Moreno et al., 2011). Moreover, JWH-133 and WIN55,212-2 promote microglial migration, which facilitates the phagocytosis of aggregated Aβ (Martín-Moreno et al., 2011). CB_2 agonist JWH-015 facilitates Aβ-induced astrocytic proliferation in cell culture which participates in the inflammatory process as well (Esposito et al., 2007). These findings have been corroborated *in vivo* by the administration of selective CB_2 and mixed CB_1–CB_2 receptor agonists to rats and mice inoculated with Aβ into the brain, resulting in reduced levels of several pro-inflammatory cytokines and decreased microglia reactivity to the Aβ insult (Ramírez et al., 2005; Esposito et al., 2007; Martín-Moreno et al., 2011; Fakhfouri et al., 2012; Wu et al., 2013). In some cases, the specificity of CB_2-induced effects has been demonstrated by the co-administration of the selective CB_2 antagonist SR144528

TABLE 2 | Evidence about the role of CB_2 receptors in AD obtained from genetically modified mice.

References	Animal model	AD-related characteristics
Chen et al., 2012	5xFAD/CB_2(−/−)	= Effect of a MAGL inhibitor on reducing astrocytes Around plaques
Koppel et al., 2014	J20 APP/CB_2(−/−)	↑ Soluble $A\beta_{1-42}$ ↑ Plaque deposition ↓ Total tau ↑ Microglia associated to plaques
Schmöle et al., 2015	APP/PS1/CB_2(−/−)	= Cognitive performance = Plaque deposition ↓ Concentrations of soluble $A\beta_{1-40}$and $A\beta_{1-42}$ ↓ Microglial cells and infiltrated macrophages ↓ Levels of pro-inflammatory chemokines and cytokines
Aso et al., 2016	APP/PS1/CB_2(−/−)	= Cognitive performance = Cognitive improvement induced by Δ^9-THC+CBD ↑ Soluble $A\beta_{1-40}$ ↑ Plaque deposition = Tau phosphorylation around plaques ↓ Effect of Δ^9-THC+CBD on reducing microglia around plaques

(Esposito et al., 2007; Martín-Moreno et al., 2011; Fakhfouri et al., 2012). Moreover, transgenic mice bearing APP mutations linked to familial AD exhibit a reduction in the number of activated microglial cells surrounding Aβ deposits and in the levels of pro-inflammatory cytokines after chronic treatment with the selective CB_2 receptor agonist JWH-133 (Martín-Moreno et al., 2012; Aso et al., 2013). Considering that systemic inflammation may exacerbate the progression of AD (Lim et al., 2015) and that CB_2 receptor is highly expressed in the peripheral immune system (Atwood and Mackie, 2010), it can be speculated that systemic CB_2-driven actions may be also beneficial in AD.

Genetic models designed to unravel the role of CB_2 receptors in AD progression have produced divergent findings regarding inflammatory responses (**Table 2**). A significant increase in the number of activated microglia associated with plaques has been reported in J20 APP transgenic AD mice lacking, in addition, the CB_2 receptor (Koppel et al., 2014). Knocking down CB_2 receptor gene in APP/PS1 mice results in a reduction of microglia reactivity and in the levels of pro-inflammatory chemokines and cytokines (Schmöle et al., 2015; Aso et al., 2016). Inhibition of monoacylglycerol lipase (MAGL), one of the main enzymes responsible for endocannabinoids degradation, results effective at reducing astroglial reaction to amyloid plaques in 5xFAD mice lacking CB_2 receptor (Chen et al., 2012). However, the effect induced by the combination of Δ^9-THC+CBD is reduced in APP/PS1 mice knockout for CB_2 receptor (Aso et al., 2016). Divergent results may be related to the differing genetic backgrounds of mouse models, but in any case they point to a role for CB_2 receptors in the control of microglial and inflammatory responses to Aβ insults.

Modulation of Aβ and Hyper-Phosphorylated Tau Processing

A number of studies have proposed a direct role for CB_2 receptors in the modulation of Aβ peptide levels in brain. Most of them suggest the participation of CB_2 receptors in Aβ clearance rather than in Aβ production and aggregation. In this sense, activation of CB_2 receptors with the specific agonist JWH-015 facilitates Aβ phagocytosis by human macrophages in brain sections obtained from AD cases (Tolón et al., 2009) and by microglia in cell culture (Ehrhart et al., 2005). Similarly, MDA7, another potent synthetic CB_2 agonist, promotes Aβ clearance in the brains of Aβ-injected rats (Wu et al., 2013). JWH-133 and WIN55,212-2 favor Aβ transport through the choroid plexus *in vitro* (Martín-Moreno et al., 2012). The facilitation of Aβ clearance across the blood brain barrier has also been demonstrated using the synthetic CB_1–CB_2 receptor agonist CB13 in *in vitro* and *in vivo* models (Bachmeier et al., 2013). These findings may explain, at least in part, the reduction in Aβ levels in APP transgenic mice after chronic treatment with the agonists JWH-133 and WIN55,212-2 (Martín-Moreno et al., 2012). A few reports have also suggested a direct effect of the mixed CB_1–CB_2 agonist Δ^9-THC on the reduction of Aβ aggregation (Eubanks et al., 2006; Cao et al., 2014; Janefjord et al., 2014) and on the promotion of Aβ degradation (Chen et al., 2013). However, demonstration of a direct involvement of CB_1 or CB_2 receptors is lacking in these studies.

Further evidence of CB_2 participation in Aβ processing derives from the study of AD models with genetic deletion of this receptor (**Table 2**). Two of the three models had increased soluble Aβ levels and increased numbers of amyloid plaques in adult mouse brains (Koppel et al., 2014; Aso et al.,

2016). In the case of APP/PS1 mice lacking CB_2 receptors, the increased Aβ deposition observed may be related to the reduced microglial reaction in their brains (Aso et al., 2016), considering the role of CB_2 activity in promoting microglial-induced Aβ phagocytosis (Ehrhart et al., 2005; Tolón et al., 2009). These observations reinforce the hypothesis that CB_2 receptors facilitate Aβ clearance whereas their absence results in greater Aβ accumulation in brain. However, a slight reduction in soluble Aβ and plaque content has been reported in aged AD mice lacking CB_2 receptors (Schmöle et al., 2015), suggesting that CB_2 receptor participation in Aβ processing may vary along with the progression of the neurodegenerative process.

A role for CB_2 receptors in the modulation of tau hyper-phosphorylation has also been proposed. Early studies performed in cell cultures demonstrated that the mixed CB_1–CB_2 agonist WIN55,212-2 inhibited tau protein hyper-phosphorylation in Aβ-stimulated PC12 neuronal cells, but that this effect was mediated mainly by CB_1 receptors (Esposito et al., 2006). Moreover, a specific CB_2 agonist failed to modify tau hyper-phosphorylation in the same experimental conditions (Esposito et al., 2006). Δ^9-THC, a mixed CB_1–CB_2 agonist, is able to reduce tau phosphorylation in N2a/APPswe cells (Cao et al., 2014) but no direct evidence has been found about the specific involvement of CB_2 receptors in such effect. It is worth noting that *in vivo* experiments have demonstrated that chronic treatment with the specific CB_2 agonist JWH-133 significantly reduces tau hyper-phosphorylation at the Thr181 site in the vicinity of Aβ plaques in APP/PS1 mice (Aso et al., 2013). This effect may be explained by concomitant decreased expression of active forms of GSK3β, p38 and SAPK/JNK in the vicinity of Aβ plaques in JWH-133-treated APP/PS1 mice (Aso et al., 2013). In contrast, no difference in tau hyper-phosphorylation at site Thr181 was observed in APP/PS1 mice lacking CB_2 receptors (Aso et al., 2016), suggesting that the activation of these receptors may avoid tau phosphorylation but their absence does not alter the process of tau phosphorylation. Yet J20 APP mice knocked out for the CB_2 receptor gene show decreased levels of total tau protein without modifications of its phosphorylation state (Koppel et al., 2014). Considering all these observations, it is clear that the role of CB_2 receptors in tau processing requires further investigation, as the available information is variegated and not conclusive.

Other Effects: Neuronal Survival, Anti-Oxidative, Glucose Metabolism, and Cognition

Targeting CB_2 receptors produces additional benefits in AD. Thus, CB_2 receptor agonists promote cell survival in the face of Aβ insults in *in vitro* and *in vivo* models (Ramírez et al., 2005; Fakhfouri et al., 2012; Chen et al., 2013; Janefjord et al., 2014). Moreover, anti-oxidant effects have been reported for compounds activating CB_2 receptors. Specifically, two studies have demonstrated that specific CB_2 agonists reduce the production of free radical NO induced by Aβ exposure in microglial cell culture (Ehrhart et al., 2005; Martín-Moreno et al., 2011), although these results have not been replicated in a glioma cell line (Esposito et al., 2006). *In vivo* experiments also show that activation of CB_2 receptors reduces oxidative stress damage and promotes anti-oxidative stress responses; chronic treatment with JWH-133 reduces hydroxynonenal adducts derived from lipid peroxidation and enhances the levels of superoxide dismutase 1 and superoxide dismutase 2 in the vicinity of plaques in APP/PS1 mice (Aso et al., 2013). The mechanisms by which CB_2 receptors mediate these anti-oxidant effects remain elusive. It has been reported that the CB_1–CB_2 agonist Δ^9-THC improves mitochondrial function (Cao et al., 2014), thus presumably contributing to a reduction in the production of free radicals, but further study is needed to support this hypothesis. Additional benefits of the activation of CB_2 receptors in AD may derive from the ability of these receptors to mediate glucose uptake in brain (Martín-Moreno et al., 2012; Köfalvi et al., 2016), which may counteract the well-known glucose metabolism deficit in AD brains (Mosconi et al., 2008; Cohen and Klunk, 2014).

More importantly, CB_2 selective and CB_1–CB_2 mixed agonists prevent memory deficits in Aβ-injected rats and mice after chronic administration (Ramírez et al., 2005; Martín-Moreno et al., 2011; Fakhfouri et al., 2012; Wu et al., 2013) and improve cognitive performance in two different transgenic mouse models of AD (Martín-Moreno et al., 2012; Aso et al., 2013). The mechanisms of action underlying cognitive improvement are assumed to be multiple and likely related mainly to the capacity of CB_2 receptors to mitigate the harmful effects of several molecules produced in AD brains. In fact, AD-like mice lacking CB_2 receptors display the same cognitive performance as the corresponding transgenic control mice (Schmöle et al., 2015; Aso

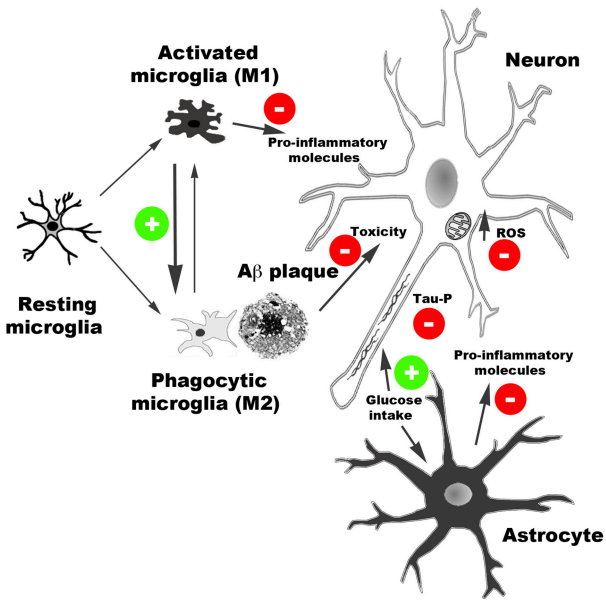

FIGURE 1 | Schematic representation of main effects of CB_2 receptor activation reported in AD models. CB_2 receptor agonists reduce the release of pro-inflammatory molecules, facilitate Aβ clearance by promoting microglia phagocytic phenotype, reduce Aβ neurotoxicity, and facilitate glucose uptake. Moreover, CB_2-mediated activity reduces oxidative stress damage produced by reactive oxidative species (ROS) and tau hyper-phosphorylation.

et al., 2016), suggesting that CB_2 receptors may not play a direct role on cognition.

CONCLUSIONS AND FUTURE PERSPECTIVES

Taken together, the experimental observations discussed in the present review indicate that AD induces CB_2 receptor expression and that targeting CB_2 receptors has beneficial effects in AD. Specifically, CB_2 receptor agonists reduce inflammatory responses linked to Aβ production and deposition, facilitate Aβ clearance, increase cell viability in the presence of Aβ, and promote glucose uptake in brain. Moreover, CB_2 activity likely reduces tau hyper-phosphorylation and oxidative stress damage caused by Aβ peptides (**Figure 1**). As a result of the combination of these effects, among others, CB_2 receptor agonists induce cognitive improvement in AD models.

Considering the evidence of pleiotropic activity and lack of undesirable psychoactive effects of CB_2 receptors, compounds acting on such cannabinoid receptors represent a promising therapy against AD. Nevertheless, there is still no information regarding the efficacy or toxicity in human beings of compounds specifically targeting CB_2 receptors, which might exhibit some side effects such as immune suppression (Pertwee, 2005). For these reasons, progress toward clinical practice requires further investigation.

AUTHOR CONTRIBUTIONS

EA and IF contributed equally to writing this review. Both authors give final approval of the text.

FUNDING

The authors' work is supported by CIBERNED, Institute of Health Carlos III (Spanish Ministry of Economy and Competitiveness) and confunded by FEDER funds/European Regional Development Fund (ERDF) - a way to build Europe (PI14/00757 to IF).

ACKNOWLEDGMENTS

We thank T. Yohannan for editorial assistance.

REFERENCES

Aso, E., Andrés-Benito, P., Carmona, M., Maldonado, R., and Ferrer, I. (2016). Cannabinoid receptor 2 participates in amyloid-β processing in a mouse model of Alzheimer's disease but plays a minor role in the therapeutic properties of a cannabis-based medicine. *J. Alzheimers Dis.* 51, 489–500. doi: 10.3233/JAD-150913

Aso, E., and Ferrer, I. (2014). Cannabinoids for treatment of Alzheimer's disease: moving toward the clinic. *Front. Pharmacol.* 5:37. doi: 10.3389/fphar.2014.00037

Aso, E., Juvés, S., Maldonado, R., and Ferrer, I. (2013). CB2 cannabinoid receptor agonist ameliorates Alzheimer-like phenotype in AßPP/PS1 mice. *J. Alzheimers Dis.* 35, 847–858. doi: 10.3233/JAD-130137

Aso, E., Sánchez-Pla, A., Vegas-Lozano, E., Maldonado, R., and Ferrer, I. (2015). Cannabis-based medicine reduces multiple pathological processes in AßPP/PS1 mice. *J. Alzheimers Dis.* 43, 977–991. doi: 10.3233/JAD-141014

Ativie, F., Albayram, O., Bach, K., Pradier, B., Zimmer, A., and Bilkei-Gorzo, A. (2015). Enhanced microglial activity in FAAH(−/−) animals. *Life Sci.* 138, 52–56. doi: 10.1016/j.lfs.2014.12.016

Atwood, B. K., and Mackie, K. (2010). CB2: a cannabinoid receptor with an identity crisis. *Br. J. Pharmacol.* 160, 467–479. doi: 10.1111/j.1476-5381.2010.00729.x

Atwood, B. K., Straiker, A., and Mackie, K. (2012). CB_2: therapeutic target-in-waiting. *Prog. Neuropsychopharmacol. Biol. Psychiatry* 38, 16–20. doi: 10.1016/j.pnpbp.2011.12.001

Bachmeier, C., Beaulieu-Abdelahad, D., Mullan, M., and Paris, D. (2013). Role of the cannabinoid system in the transit of beta-amyloid across the blood-brain barrier. *Mol. Cell. Neurosci.* 56, 255–262. doi: 10.1016/j.mcn.2013.06.004

Benito, C., Núñez, E., Tolón, R. M., Carrier, E. J., Rábano, A., Hillard, C. J., et al. (2003). Cannabinoid CB2 receptors and fatty acid amide hydrolase are selectively overexpressed in neuritic plaque-associated glia in Alzheimer's disease brains. *J. Neurosci.* 23, 11136–11141.

Bilkei-Gorzo, A., Drews, E., Albayram, Ö., Piyanova, A., Gaffal, E., Tueting, T., et al. (2012). Early onset of aging-like changes is restricted to cognitive abilities and skin structure in Cnr1(−/−) mice. *Neurobiol. Aging* 33, e11–e22. doi: 10.1016/j.neurobiolaging.2010.07.009

Bilkei-Gorzo, A., Racz, I., Valverde, O., Otto, M., Michel, K., Sastre, M., et al. (2005). Early age-related cognitive impairment in mice lacking cannabinoid CB1 receptors. *Proc. Natl. Acad. Sci. U.S.A.* 102, 15670–15675. doi: 10.1073/pnas.0504640102

Bilkei-Gorzo, A. (2012). The endocannabinoid system in normal and pathological brain ageing. *Philos. Trans. R. Soc. Lond. B Biol. Sci.* 367, 3326–3341. doi: 10.1098/rstb.2011.0388

Bolognesi, M. L., Matera, R., Minarini, A., Rosini, M., and Melchiorre, C. (2009). Alzheimer's disease: new approaches to drug discovery. *Curr. Opin. Chem. Biol.* 13, 303–308. doi: 10.1016/j.cbpa.2009.04.619

Braak, H., and Braak, E. (1991). Neuropathological stageing of Alzheimer-related changes. *Acta Neuropathol.* 82, 239–259. doi: 10.1007/BF00308809

Buckley, N. E., McCoy, K. L., Mezey, E., Bonner, T., Zimmer, A., Felder, C. C., et al. (2000). Immunomodulation by cannabinoids is absent in mice deficient for the cannabinoid CB(2) receptor. *Eur. J. Pharmacol.* 396, 141–149. doi: 10.1016/S0014-2999(00)00211-9

Cabral, G. A., and Griffin-Thomas, L. (2009). Emerging role of the cannabinoid receptor CB2 in immune regulation: therapeutic prospects for neuroinflammation. *Expert Rev. Mol. Med.* 11:e3. doi: 10.1017/S1462399409000957

Cao, C., Li, Y., Liu, H., Bai, G., Mayl, J., Lin, X., et al. (2014). The potential therapeutic effects of THC on Alzheimer's disease. *J. Alzheimers Dis.* 42, 973–984. doi: 10.3233/JAD-140093

Chen, R., Zhang, J., Wu, Y., Wang, D., Feng, G., Tang, Y. P., et al. (2012). Monoacylglycerol lipase is a therapeutic target for Alzheimer's disease. *Cell Rep.* 2, 1329–1339. doi: 10.1016/j.celrep.2012.09.030

Chen, R., Zhang, J., Fan, N., Teng, Z. Q., Wu, Y., Yang, H., et al. (2013). Δ(9)-THC-caused synaptic and memory impairments are mediated through COX-2 signaling. *Cell* 155, 1154–1165. doi: 10.1016/j.cell.2013.10.042

Clavaguera, F., Bolmont, T., Crowther, R. A., Abramowski, D., Frank, S., Probst, A., et al. (2009). Transmission and spreading of tauopathy in transgenic mouse brain. *Nat. Cell Biol.* 11, 909–913. doi: 10.1038/ncb1901

Cohen, A. D., and Klunk, W. E. (2014). Early detection of Alzheimer's disease using PiB and FDG PET. *Neurobiol. Dis.* 72, 117–122. doi: 10.1016/j.nbd.2014.05.001

Duff, G., Argaw, A., Cecyre, B., Cherif, H., Tea, N., Zabouri, N., et al. (2013). Cannabinoid receptor CB2 modulates axon guidance. *PLoS ONE* 8:e70849. doi: 10.1371/journal.pone.0070849

Duyckaerts, C., and Dickson, D. (2011). "Neuropathology of Alzheimer's disease and its variants," *in Neurodegeneration: The Molecular Pathology of Dementia and Movement Disorders, 2*nd *Edn.,* eds D. Dickson and R. Weller (West Sussex: Wiley-Blackwell), 62–91.

Ehrhart, J., Obregon, D., Mori, T., Hou, H., Sun, N., Bai, Y., et al. (2005). Stimulation of cannabinoid receptor 2 (CB2) suppresses microglial activation. *J. Neuroinflammation* 2:29. doi: 10.1186/1742-2094-2-29

Esposito, G., De Filippis, D., Steardo, L., Scuderi, C., Savani, C., Cuomo, V., et al. (2006). CB1 receptor selective activation inhibits beta-amyloid-induced iNOS protein expression in C6 cells and subsequently blunts tau protein hyperphosphorylation in co-cultured neurons. *Neurosci. Lett.* 404, 342–346. doi: 10.1016/j.neulet.2006.06.012

Esposito, G., Iuvone, T., Savani, C., Scuderi, C., De Filippis, D., Papa, M., et al. (2007). Opposing control of cannabinoid receptor stimulation on amyloid-beta-induced reactive gliosis: *in vitro* and *in vivo* evidence. *J. Pharmacol. Exp. Ther.* 322, 1144–1152. doi: 10.1124/jpet.107.121566

Eubanks, L. M., Rogers, C. J., Beuscher, A. E. IV, Koob, G. F., Olson, A. J., Dickerson, T. J., et al. (2006). A molecular link between the active component of marijuana and Alzheimer's disease pathology. *Mol. Pharm.* 3, 773–777. doi: 10.1021/mp060066m

Fagan, S. G., and Campbell, V. A. (2014). The influence of cannabinoids on generic traits of neurodegeneration. *Br. J. Pharmacol.* 171, 1347–1360. doi: 10.1111/bph.12492

Fakhfouri, G., Ahmadiani, A., Rahimian, R., Grolla, A. A., Moradi, F., and Haeri, A. (2012). WIN55212-2 attenuates amyloid-beta-induced neuroinflammation in rats through activation of cannabinoid receptors and PPAR-γ pathway. *Neuropharmacology* 63, 653–666. doi: 10.1016/j.neuropharm.2012.05.013

Fernández-Ruiz, J., Pazos, M. R., García-Arencibia, M., Sagredo, O., and Ramos, J. A. (2008). Role of CB2 receptors in neuroprotective effects of cannabinoids. *Mol. Cell. Endocrinol.* 286, S91–S96. doi: 10.1016/j.mce.2008.01.001

Fernández-Ruiz, J., Romero, J., and Ramos, J. A. (2015). Endocannabinoids and neurodegenerative disorders: Parkinson's disease, Huntington's chorea, Alzheimer's disease, and others. *Handb. Exp. Pharmacol.* 231, 233–259. doi: 10.1007/978-3-319-20825-1_8

Ferrer, I. (2009). Altered mitochondria, energy metabolism, voltage-dependent anion channel, and lipid rafts converge to exhaust neurons in Alzheimer's disease. *J. Bioenerg. Biomembr.* 41, 425–431. doi: 10.1007/s10863-009-9243-5

Ferrer, I. (2012). Defining Alzheimer as a common age-related neurodegenerative process not inevitably leading to dementia. *Prog. Neurobiol.* 397, 38–51. doi: 10.1016/j.pneurobio.2012.03.005

Fowler, C. J. (2013). Transport of endocannabinoids across the plasma membrane and within the cell. *FEBS. J.* 280, 1895–1904. doi: 10.1111/febs.12212

Frautschy, S. A., and Cole, G. M. (2010). Why pleiotropic interventions are needed for Alzheimer's disease. *Mol. Neurobiol.* 41, 392–409. doi: 10.1007/s12035-010-8137-1

Hebert, L. E., Weuve, J., Scherr, P. A., and Evans, D. A. (2013). Alzheimer disease in the United States (2010-2050) estimated using the 2010 census. *Neurology* 80, 1778–1783. doi: 10.1212/WNL.0b013e31828726f5

Heneka, M. T., Carson, M. J., El Khoury, J., Landreth, G. E., Brosseron, F., Feinstein, D. L., et al. (2015). Neuroinflammation in Alzheimer's disease. *Lancet Neurol.* 14, 388–405. doi: 10.1016/S1474-4422(15)70016-5

Heneka, M. T., Kummer, M. P., Stutz, A., Delekate, A., Schwartz, S., Vieira-Saecker, A., et al. (2013). NLRP3 is activated in Alzheimer's disease and contributes to pathology in APP/PS1 mice. *Nature* 493, 674–678. doi: 10.1038/nature11729

Heneka, M. T., Kummer, M. P., and Latz, E. (2014). Innate immune activation in neurodegenerative disease. *Nat. Rev. Immunol.* 14, 463–477. doi: 10.1038/nri3705

Howlett, A. C. (2005). Cannabinoid receptor signaling. *Handb. Exp. Pharmacol.* 168, 53–79. doi: 10.1007/3-540-26573-2_2

Hu, S. S., and Mackie, K. (2015). Distribution of the endocannabinoid system in the central nervous system. *Handb. Exp. Pharmacol.* 231, 59–93. doi: 10.1007/978-3-319-20825-1_3

Iannotti, F. A., Di Marzo, V., and Petrosino, S. (2016). Endocannabinoids and endocannabinoid-related mediators: targets, metabolism and role in neurological disorders. *Prog. Lipid Res.* 62, 107–128. doi: 10.1016/j.plipres.2016.02.002

Janefjord, E., Mååg, J. L., Harvey, B. S., and Smid, S. D. (2014). Cannabinoid effects on β amyloid fibril and aggregate formation, neuronal and microglial-activated neurotoxicity *in vitro*. *Cell. Mol. Neurobiol.* 34, 31–42. doi: 10.1007/s10571-013-9984-x

Jhaveri, M. D., Sagar, D. R., Elmes, S. J., Kendall, D. A., and Chapman, V. (2007). Cannabinoid CB2 receptor-mediated anti-nociception in models of acute and chronic pain. *Mol. Neurobiol.* 36, 26–35. doi: 10.1007/s12035-007-8007-7

Jucker, M., and Walker, L. C. (2013). Self-propagation of pathogenic protein aggregates in neurodegenerative diseases. *Nature* 501, 45–51. doi: 10.1038/nature12481

Keller, J. N., Hanni, K. B., and Markesbery, W. R. (2000). Impaired proteasome function in Alzheimer's disease. *J. Neurochem.* 75, 436–439. doi: 10.1046/j.1471-4159.2000.0750436.x

Kim, J., and Li, Y. (2015). Chronic activation of CB2 cannabinoid receptors in the hippocampus increases excitatory synaptic transmission. *J. Physiol.* 593, 871–886. doi: 10.1113/jphysiol.2014.286633

Köfalvi, A., Lemos, C., Martín-Moreno, A. M., Pinheiro, B. S., García-García, L., Pozo, M. A., et al. (2016). Stimulation of brain glucose uptake by cannabinoid CB(2) receptors and its therapeutic potential in Alzheimer's disease. *Neuropharmacology.* doi: 10.1016/j.neuropharm.2016.03.015. [Epub ahead of print].

Koppel, J., Vingtdeux, V., Marambaud, P., d'Abramo, C., Jimenez, H., Stauber, M., et al. (2014). CB2 receptor deficiency increases amyloid pathology and alters tau processing in a transgenic mouse model of Alzheimer's disease. *Mol. Med.* 20, 29–36. doi: 10.2119/molmed.2013.00140

Li, Y., and Kim, J. (2016). Deletion of CB2 cannabinoid receptors reduces synaptic transmission and long-term potentiation in the mouse hippocampus. *Hippocampus* 26, 275–281. doi: 10.1002/hipo.22558

Ligresti, A., Cascio, M. G., and Di Marzo, V. (2005). Endocannabinoid metabolic pathways and enzymes. *Curr. Drug Targets CNS Neurol. Disord.* 4, 615–623. doi: 10.2174/156800705774933104

Lim, S. L., Rodriguez-Ortiz, C. J., and Kitazawa, M. (2015). Infection, systemic inflammation, and Alzheimer's disease. *Microbes Infect.* 17, 549–556. doi: 10.1016/j.micinf.2015.04.004

López-González, I., Schlüter, A., Aso, E., Garcia-Esparcia, P., Ansoleaga, B., Llorens, F., et al. (2015). Neuroinflammatory signals in Alzheimer disease and APP/PS1 transgenic mice: correlations with plaques, tangles, and oligomeric species. *J. Neuropathol. Exp. Neurol.* 74, 319–344. doi: 10.1097/NEN.0000000000000176

Maldonado, R., Berrendero, F., Ozaita, A., and Robledo, P. (2011). Neurochemical basis of cannabis addiction. *Neuroscience* 181, 1–17. doi: 10.1016/j.neuroscience.2011.02.035

Martín-Moreno, A. M., Brera, B., Spuch, C., Carro, E., García-García, L., Delgado, M., et al. (2012). Prolonged oral cannabinoid administration prevents neuroinflammation, lowers β-amyloid levels and improves cognitive performance in Tg APP 2576 mice. *J. Neuroinflammation* 9:8. doi: 10.1186/1742-2094-9-8

Martín-Moreno, A. M., Reigada, D., Ramírez, B. G., Mechoulam, R., Innamorato, N., Cuadrado, A., et al. (2011). Cannabidiol and other cannabinoids reduce microglial activation *in vitro* and *in vivo*: relevance to Alzheimer's disease. *Mol. Pharmacol.* 79, 964–973. doi: 10.1124/mol.111.071290

McGeer, P. L., and McGeer, E. G. (2015). Targeting microglia for the treatment of Alzheimer's disease. *Expert Opin. Ther. Targets* 19, 497–506. doi: 10.1517/14728222.2014.988707

Mecha, M., Feliú, A., Carrillo-Salinas, F. J., Rueda-Zubiaurre, A., Ortega-Gutiérrez, S., de Sola, R. G., et al. (2015). Endocannabinoids drive the acquisition of an alternative phenotype in microglia. *Brain Behav. Immun.* 49, 233–245. doi: 10.1016/j.bbi.2015.06.002

Meyer-Luehmann, M., Coomaraswamy, J., Bolmont, T., Kaeser, S., Schaefer, C., Kilger, E., et al. (2006). Exogenous induction of cerebral beta-amyloidogenesis is governed by agent and host. *Science* 313, 1781–1784. doi: 10.1126/science.1131864

Mosconi, L., Pupi, A., and De Leon, M. J. (2008). Brain glucose hypometabolism and oxidative stress in preclinical Alzheimer's disease. *Ann. N.Y. Acad. Sci.* 1147, 180–195. doi: 10.1196/annals.1427.007

Onyango, I. G., Dennis, J., and Khan, S. M. (2016). Mitochondrial dysfunction in Alzheimer's disease and the rationale for bioenergetics based therapies. *Aging Dis.* 7, 201–214. doi: 10.14336/AD.2015.1007

Palazuelos, J., Ortega, Z., Díaz-Alonso, J., Guzmán, M., and Galve-Roperh, I. (2012). CB2 cannabinoid receptors promote neural progenitor cell proliferation via mTORC1 signaling. *J. Biol. Chem.* 287, 1198–1209. doi: 10.1074/jbc.M111.291294

Pertwee, R. G., Howlett, A. C., Abood, M. E., Alexander, S. P., Di Marzo, V., Elphick, M. R., et al. (2010). International union of basic and clinical pharmacology. LXXIX. Cannabinoid receptors and their ligands: beyond CB_1 and CB_2. *Pharmacol. Rev.* 62, 588–631. doi: 10.1124/pr.110.003004

Pertwee, R. G. (2015). Endocannabinoids and their pharmacological actions. *Handb. Exp. Pharmacol.* 231, 1–37. doi: 10.1007/978-3-319-20825-1_1

Pertwee, R. G. (2005). Pharmacological actions of cannabinoids. *Handb. Exp. Pharmacol.* 168, 1–51. doi: 10.1007/b137831

Ramírez, B. G., Blázquez, C., Gómez del Pulgar, T., Guzmán, M., and de Ceballos, M. L. (2005). Prevention of Alzheimer's disease pathology by cannabinoids: neuroprotection mediated by blockade of microglial activation. *J. Neurosci.* 25, 1904–1913. doi: 10.1523/JNEUROSCI.4540-04.2005

Savonenko, A. V., Melnikova, T., Wang, Y., Ravert, H., Gao, Y., Koppel, J., et al. (2015). Cannabinoid CB2 receptors in a mouse model of Aβ amyloidosis: immunohistochemical analysis and suitability as a PET biomarker of neuroinflammation. *PLoS ONE* 10:e0129618. doi: 10.1371/journal.pone.0129618

Scheltens, P., Blennow, K., Breteler, M. M., de Strooper, B., Frisoni, G. B., Salloway, S., et al. (2016). Alzheimer's disease. *Lancet*. doi: 10.1016/S0140-6736(15)01124-1. [Epub ahead of print].

Schmöle, A. C., Lundt, R., Ternes, S., Albayram, Ö., Ulas, T., Schultze, J. L., et al. (2015). Cannabinoid receptor 2 deficiency results in reduced neuroinflammation in an Alzheimer's disease mouse model. *Neurobiol. Aging* 36, 710–719. doi: 10.1016/j.neurobiolaging.2014.09.019

Solas, M., Francis, P. T., Franco, R., and Ramírez, M. J. (2013). CB2 receptor and amyloid pathology in frontal cortex of Alzheimer's disease patients. *Neurobiol. Aging* 34, 805–808. doi: 10.1016/j.neurobiolaging.2012.06.005

Stöhr, J., Watts, J. C., Mensinger, Z. L., Oehler, A., Grillo, S. K., DeArmond, S. J., et al. (2012). Purified and synthetic Alzheimer's amyloid beta (Aβ) prions. *Proc. Natl. Acad. Sci. U.S.A.* 109, 11025–11030. doi: 10.1073/pnas.1206555109

Sultana, R., and Butterfield, D. A. (2010). Role of oxidative stress in the progression of Alzheimer's disease. *J. Alzheimers Dis.* 19, 341–353. doi: 10.3233/JAD-2010-1222

Thal, D. R., Rüb, U., Orantes, M., and Braak, H. (2002). Phases of A beta-deposition in the human brain and its relevance for the development of AD. *Neurology* 58, 1791–1800. doi: 10.1212/WNL.58.12.1791

Tolón, R. M., Núñez, E., Pazos, M. R., Benito, C., Castillo, A. I., Martínez-Orgado, J. A., et al. (2009). The activation of cannabinoid CB2 receptors stimulates *in situ* and *in vitro* beta-amyloid removal by human macrophages. *Brain Res.* 1283, 148–154. doi: 10.1016/j.brainres.2009.05.098

Tramutola, A., Di Domenico, F., Barone, E., Perluigi, M., and Butterfield, D. A. (2016). It is all about (U)biquitin: role of altered ubiquitin-proteasome system and UCHL1 in Alzheimer Disease. *Oxid. Med. Cell. Longev.* 2016:2756068. doi: 10.1155/2016/2756068

Walter, L., Franklin, A., Witting, A., Wade, C., Xie, Y., Kunos, G., et al. (2003). Nonpsychotropic cannabinoid receptors regulate microglial cell migration. *J. Neurosci.* 23, 1398–1405.

Whiteside, G. T., Lee, G. P., and Valenzano, K. J. (2007). The role of the cannabinoid CB2 receptor in pain transmission and therapeutic potential of small molecule CB2 receptor agonists. *Curr. Med. Chem.* 14, 917–936. doi: 10.2174/092986707780363023

Wilson, R. I., and Nicoll, R. A. (2002). Endocannabinoid signaling in the brain. *Science* 296, 678–682. doi: 10.1126/science.1063545

Wright, K. L., Duncan, M., and Sharkey, K. A. (2008). Cannabinoid CB2 receptors in the gastrointestinal tract: a regulatory system in states of inflammation. *Br. J. Pharmacol.* 153, 263–270. doi: 10.1038/sj.bjp.0707486

Wu, J., Bie, B., Yang, H., Xu, J. J., Brown, D. L., and Naguib, M. (2013). Activation of the CB2 receptor system reverses amyloid-induced memory deficiency. *Neurobiol. Aging* 34, 791–804. doi: 10.1016/j.neurobiolaging.2012.06.011

Conflict of Interest Statement: The authors declare that the research was conducted in the absence of any commercial or financial relationships that could be construed as a potential conflict of interest.

Copyright © 2016 Aso and Ferrer. This is an open-access article distributed under the terms of the Creative Commons Attribution License (CC BY). The use, distribution or reproduction in other forums is permitted, provided the original author(s) or licensor are credited and that the original publication in this journal is cited, in accordance with accepted academic practice. No use, distribution or reproduction is permitted which does not comply with these terms.

frontiers in Neuroscience

ORIGINAL RESEARCH
published: 02 August 2016
doi: 10.3389/fnins.2016.00321

Cannabinoid Type 2 (CB_2) Receptors Activation Protects against Oxidative Stress and Neuroinflammation Associated Dopaminergic Neurodegeneration in Rotenone Model of Parkinson's Disease

Hayate Javed[1], *Sheikh Azimullah*[2], *M. Emdadul Haque*[1]* *and Shreesh K. Ojha*[2]*

[1] Departments of Biochemistry, College of Medicine and Health Sciences, United Arab Emirates University, Al Ain, UAE,
[2] Department of Pharmacology and Therapeutics, College of Medicine and Health Sciences, United Arab Emirates University, Al Ain, UAE

The cannabinoid type two receptors (CB_2), an important component of the endocannabinoid system, have recently emerged as neuromodulators and therapeutic targets for neurodegenerative diseases including Parkinson's disease (PD). The downregulation of CB_2 receptors has been reported in the brains of PD patients. Therefore, both the activation and the upregulation of the CB_2 receptors are believed to protect against the neurodegenerative changes in PD. In the present study, we investigated the CB_2 receptor-mediated neuroprotective effect of β-caryophyllene (BCP), a naturally occurring CB_2 receptor agonist, in, a clinically relevant, rotenone (ROT)-induced animal model of PD. ROT (2.5 mg/kg BW) was injected intraperitoneally (i.p.) once daily for 4 weeks to induce PD in male Wistar rats. ROT injections induced a significant loss of dopaminergic (DA) neurons in the substantia nigra pars compacta (SNpc) and DA striatal fibers, following activation of glial cells (astrocytes and microglia). ROT also caused oxidative injury evidenced by the loss of antioxidant enzymes and increased nitrite levels, and induction of proinflammatory cytokines: IL-1β, IL-6 and TNF-α, as well as inflammatory mediators: NF-κB, COX-2, and iNOS. However, treatment with BCP attenuated induction of proinflammatory cytokines and inflammatory mediators in ROT-challenged rats. BCP supplementation also prevented depletion of glutathione concomitant to reduced lipid peroxidation and augmentation of antioxidant enzymes: SOD and catalase. The results were further supported by tyrosine hydroxylase immunohistochemistry, which illustrated the rescue of the DA neurons and fibers subsequent to reduced activation of glial cells. Interestingly, BCP supplementation demonstrated the potent therapeutic effects against ROT-induced neurodegeneration, which was evidenced by BCP-mediated CB_2 receptor activation and the fact that, prior administration of the CB_2 receptor antagonist AM630 diminished the beneficial effects of BCP. The present study suggests that BCP has the potential therapeutic efficacy to elicit significant neuroprotection by its anti-inflammatory and antioxidant activities mediated by activation of the CB_2 receptors.

Keywords: AM630, β-caryophyllene, cannabinoid agonist, neurodegeneration, neuroprotection, Parkinson's disease, rotenone, Trans-caryophyllene

OPEN ACCESS

Edited by:
Ashley Ian Bush,
Florey Institute of Neuroscience and Mental Health, Australia

Reviewed by:
David Mazzocchi-Jones,
Keele University, UK
Maria Grazia Perrone,
University of Bari Aldo Moro, Italy

***Correspondence:**
M. Emdadul Haque
ehaque@uaeu.ac.ae
Shreesh K. Ojha
shreeshojha@uaeu.ac.ae

Specialty section:
This article was submitted to Neurodegeneration, a section of the journal Frontiers in Neuroscience

Received: *24 January 2016*
Accepted: *27 June 2016*
Published: *02 August 2016*

Citation:
Javed H, Azimullah S, Haque ME and Ojha SK (2016) Cannabinoid Type 2 (CB_2) Receptors Activation Protects against Oxidative Stress and Neuroinflammation Associated Dopaminergic Neurodegeneration in Rotenone Model of Parkinson's Disease. Front. Neurosci. 10:321. doi: 10.3389/fnins.2016.00321

INTRODUCTION

The endocannabinoid system, consisting of cannabinoid receptors type 1 and 2 (CB_1 and CB_2), their endogenous ligands, and the enzymes for synthesis, reuptake and metabolism of the endocannabinoids, has emerged as an important neuromodulator system for many brain functions such as learning, memory, mood, addiction, and reward processing (Hill et al., 2009; Zanettini et al., 2011). Among the cannabinoid receptors, the CB_2 receptor subtype has recently gained attention as an important therapeutic target for the modulation of neuroinflammation and attenuation of activated microglia and astrocytes in the substantia nigra and striatum (Bento et al., 2008; Concannon et al., 2015). The pharmacological activation of the CB_2 receptors has been shown to reduce microglial activation and improve functional deficits in neurodegenerative diseases including Alzheimer's disease (Ramírez et al., 2005), Huntington's disease (Palazuelos et al., 2009; Sagredo et al., 2009), multiple sclerosis (Palazuelos et al., 2008), and PD (Price et al., 2009). In addition to the pharmacological studies, genetic studies also demonstrate enhanced microglial activation, neural pathology and inflammation in CB_2 receptor knock-out mice (Palazuelos et al., 2008; Price et al., 2009). These studies indicated that cannabinoid-related compounds activating CB_2 receptors may preserve neuronal homeostasis and survival in neurodegenerative disorders, including PD (Fernandez-Ruiz et al., 2007).

Furthermore, the CB_2 receptor activation has been shown to be devoid of psychotropic, adverse effects, which are frequently observed with CB_1 receptor modulation. Among the cannabinoid ligands, β-caryophyllene (BCP) generated enormous therapeutic interest due to its noteworthy identification as a fully selective agonist of CB_2 receptors, its affinity and binding with CB_2, receptors along with favorable physicochemical and pharmacokinetic properties (**Figure 1**; Gertsch et al., 2008). It is one of the widely available dietary phytocannabinoids and is commonly used as a preservative, additive, and flavoring in food and cosmetics. It has been recently added to the list of "generally regarded as safe" compounds for dietary use by the United States Food and Drug Administration (Gertsch et al., 2008). Chemically, BCP is a bicyclic sesquiterpene abundantly found in the essential oils of different species such as *Cinnamomum* spp. and *Piper* spp (Passos et al., 2004; Medeiros et al., 2007). BCP is a secondary metabolite predominantly found in many dietary plants that exhibits potent and long-lasting antioxidant and anti-inflammatory properties in different models of human diseases (Sharma et al., 2016). BCP is also an important constituent of *Cannabis sativa that* makes one of the major ingredients of Sativex, an approved drug for multiple sclerosis in European countries and Canada (Sibbald, 2005). BCP has been shown to elicit potent pharmacological properties such as anti-inflammatory (Gertsch et al., 2008), antioxidant (Singh et al., 2006), antispasmodic (Leonhardt et al., 2010), antidepressant and anxiolytic (Galdino et al., 2012; Al Mansouri et al., 2014), and anti-addictive (Bahi et al., 2014). Pharmacologically, it has been reported to be a CB_2 receptor-selective agonist with a Ki value of 155 nmol/L for human CB_2 receptors, with no affinity for CB_1 receptors, which causes activation of Gi/Go subtype of G-proteins (Gertsch et al., 2008). The identification and participation of CB_2 receptors in mediating neuroprotection has driven special interest in the pharmacological investigation of BCP for neurodegenerative disorders including PD.

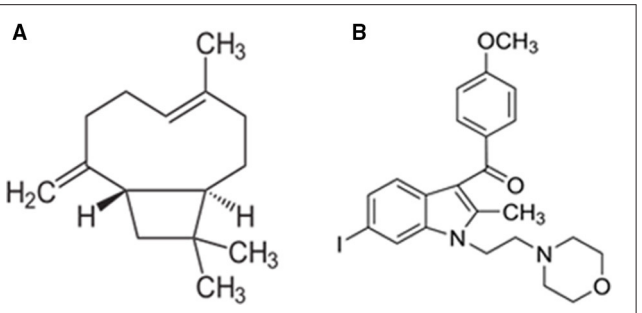

FIGURE 1 | Chemical structure of β-caryophyllene (A) and AM630 (B).

Among the neurodegenerative diseases, PD is the second most common progressive disease. It is characterized by the selective degeneration of dopaminergic neurons in the substantia nigra pars compacta (SNpc) and depletion of dopamine neurotransmitter in the striatum (Shimohama et al., 2003). The pathogenesis of PD involves enhanced oxidative stress and mitochondrial dysfunction caused by the selective inhibition of the activity of complex I of the mitochondrial respiratory chain (Hu et al., 2010). The available evidence has shown that the decreased activity of the mitochondrial complex I has been observed in the SNpc of PD patients (Schapira, 1989) accompanied by increased oxidative/nitrosative stress (Jenner, 2003). The reactive oxygen species (ROS) generated from unregulated dopamine metabolism and auto-oxidation (Cadet and Brannock, 1998) further impair mitochondrial function (Tapias et al., 2009) and alter defensive endogenous antioxidant systems together leading to oxidative stress and contributing to progressive loss of dopaminergic neurons. Numerous studies have demonstrated that increased production of cytokines and ROS as well as induction of NADPH oxidase and inducible nitric oxide synthase (iNOS) leads to glial cells activation that contributes to PD pathology (Chen and Tansey, 2011). Therefore, interplay between the oxidative stress and subsequent neuroinflammation perpetuates neurodegeneration in PD (Lee et al., 2009).

Rotenone (ROT) induced rat model of PD was employed in the present study to investigate the therapeutic effects of BCP. ROT is a rotenoid pesticide used for understanding the pathogenesis of PD and evaluation of pharmacotherapeutic agents. It causes selective nigrostriatal degeneration, accumulation and aggregation of α-synuclein, oxidative stress, inflammation, microglial activation, abnormal locomotor activity, impaired motor functions, and disrupts mitochondrial complex I activity resulting in pathology strikingly similar to that observed in human PD patients (Betarbet et al., 2006; Cannon et al., 2009; Thakur and Nehru, 2013; Tapias et al., 2014). In the present study, we have investigated the

neuroprotective effects of BCP in ROT induced rat model of PD, via CB_2 receptor-dependent mechanism by using a selective CB_2 receptor antagonist AM630 (**Figure 1**). AM630 (iodopravadoline) is a novel aminoalkylindole and a competitive cannabinoid receptor antagonist in the brain that is commonly employed as a pharmacological challenge to demonstrate the CB_2 receptor dependent mechanisms (Hosohata et al., 1997). BCP has potential anti-inflammatory and anti-oxidant activity and is widely accessible for dietary intervention. We believe that our present findings may have important pharmacotherapeutic significance in the treatment/prevention of PD.

MATERIALS AND METHODS

Drugs and Chemicals

Polyclonal rabbit anti-cyclo-oxygenase-2 (COX-2), anti-inducible nitric oxide synthase (iNOS), anti-glial fibrillary acidic protein (GFAP), anti-cannabinoid receptor type 2 (CB_2) and anti-NF-kB p65 antibodies were purchased from Abcam, Cambridge, MA, USA. Anti-ionized calcium binding adaptor molecule-1 (Iba-1) polyclonal rabbit antibody was purchased from Wako Chemicals, Richmond, VA, USA. Polyclonal rabbit anti-tyrosine hydroxylase (TH) antibody was obtained from Novus Biologicals, Littleton, CO, USA. Alexa Fluor® 488 and 594 conjugated secondary goat anti-rabbit antibodies were purchased from Life Technologies, Grand Island, NY, USA. CB_2 receptor antagonist, AM630 ([6-Iodo-2-methyl-1-[2-(4-morpholinyl) ethyl]-1*H*-indol-3-yl] (4-methoxyphenyl) methanone) was purchased from Tocris Bioscience, Ellisville, MO, USA. The lipid peroxidation kit for estimation of malondialdehyde (MDA) was obtained from North West Life science (Vancouver, WA, USA). The compounds: ROT, BCP and the assay kit for GSH were procured from Sigma-Aldrich, St. Louis, MO, USA. All the reagents used in the study were of analytical grade.

Experimental Animals

Six to seven months-old male Wistar rats (275–300 g), bred in the animal research facility of the College of Medicine and Health Sciences, United Arab Emirates University, were used. A maximum of four rats were housed per cage and were acclimatized for 1 week to the laboratory conditions prior to the start of the experiment. The animals were housed under standard laboratory conditions of 12/12 h of light and dark cycle. The animals had access to commercially available rodent food and water *ad libitum*. All the experiments were performed between 09:00 and 15:00 h. The experimental protocol for animal experimentation was approved by the Animal Ethics Committee of United Arab Emirates University, UAE.

Experimental Design

For the induction of PD in rats, ROT (2.5 mg/kg BW) was administered intraperitoneally (i.p.) once daily for 4 weeks. ROT was first dissolved in dimethyl sulfoxide (DMSO) at 50X stock solution and further diluted in sunflower oil to obtain a final concentration of 2.5 mg/ml. The regimen used in the current study for the induction of Parkinsonism in rats by ROT administration was described in a previous report (Ojha et al., 2015). To test the neuroprotective efficacy of CB_2 receptor agonist, BCP, it was diluted in olive oil and administered i.p. at a dose of 50 mg/kg BW once daily for 4 weeks, 30 min prior to ROT administration in the presence or absence of AM630, a CB_2 receptor antagonist. The dose of BCP was selected based on our previous study, in which a different set of experiments showed this dose to be pharmacologically optimal and devoid of any *in vivo* toxicity (Al Mansouri et al., 2014). The control group received a similar volume of vehicle. AM630 was dissolved in normal saline with 2.5% DMSO and tween 80 and injected 1 mg/kg BW i.p. 30 min prior to BCP treatment. The rats were divided into five groups as follows: Group I: Rats were injected vehicle only and abbreviated as control group (CONT), Group II: Rats were injected AM630 only and abbreviated as group AM630, Group III: Rats were injected rotenone dissolved in the vehicle and abbreviated as group ROT, Group IV: Rats were administered BCP, 30 min prior to rotenone injections and abbreviated as group ROT+BCP, Group V: Rats were administered AM630, 30 min prior to BCP treatment and rotenone and abbreviated as (ROT-BCP+AM630).

Tissue Preparation for Biochemical Studies

At the end of the 4 weeks, the animals were anesthetized with pentobarbital (40 mg/kg BW) and cardiac perfusion was performed using phosphate-buffered saline (PBS, 0.01 M, pH 7.4) to wash out the blood. The brains were quickly removed and placed on an ice plate to separate the two hemispheres. The midbrain and striatum were dissected from one hemisphere and immediately frozen in liquid nitrogen for further use. The other hemisphere was post-fixed first in paraformaldehyde solution (4%) for 48 h and subsequently in a series of sucrose solutions (10%) at 4°C changed three times a day for up to three consecutive days prior to cryostat sectioning.

Biochemical Studies

The midbrains of the rats collected from each group were homogenized in potassium chloride buffer at pH 8.0 (Tris-HCl 10 mM, NaCl 140 mM, KCl 300 mM, EDTA 1 mM, Triton X-100 0.5%) and supplemented with protease and phosphatase inhibitor. The tissue homogenates of the samples were centrifuged at 14000 g for 20 min at 4°C to obtain the post-mitochondrial supernatant (PMS) for estimation of antioxidant enzymes, lipid peroxidation product, and proinflammatory cytokines using spectrophotometric measurements and enzyme-linked immunosorbent assay (ELISA).

Estimation of Lipid Peroxidation Product

The extent of lipid peroxidation was measured by estimation of malondialdehyde (MDA). Briefly, the samples or calibrators (250 μl) were incubated in the presence of acid reagent and thiobarbituric acid (250 μl) and mixed vigorously using a vortex mixer. The samples were incubated for 60 min at 60°C and then centrifuged at 10,000 g for 2–3 min. The resultant reaction mixture was transferred to a cuvette and the absorbance was

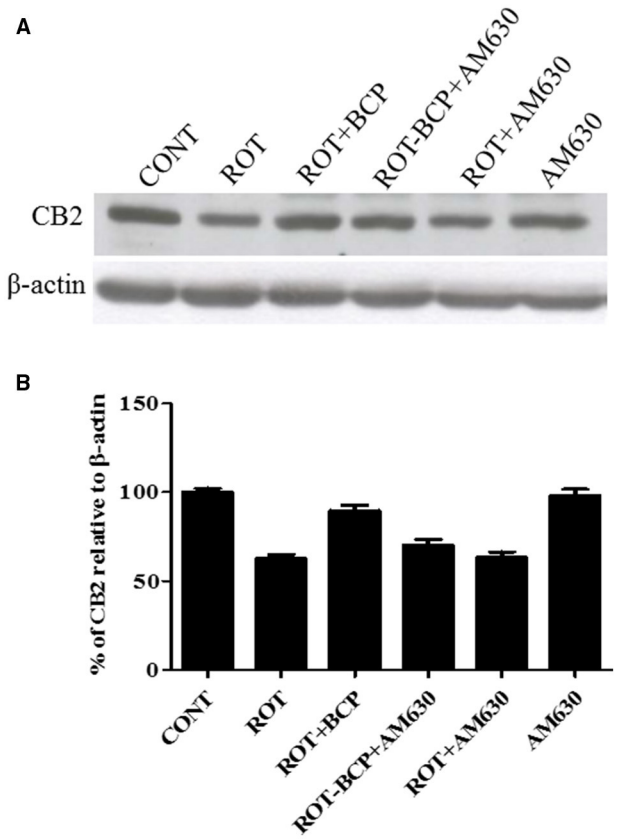

FIGURE 2 | The expression level of cannabinoid receptor 2 (CB_2) measured by western blot in the striatum. (A) The western blot showing CB_2 expression. **(B)** CB_2 expression was decreased in the ROT group as compared to the CONT group rats. However, BCP supplementation of ROT injected rats showed increased expression of CB_2 receptors. Selective antagonist of CB_2 receptors, AM630 administration prior to BCP supplementation decreased the expression of CB_2 receptors. AM630 administration to ROT injected rats has not shown any noticeable difference in the expression of CB_2. Finally, AM630 alone had no effect on the level of CB_2 expression as compared to control rats. Values are expressed as percent (%) mean ± SEM ($n = 3$).

recorded at 532 nm. The results were expressed as μM MDA/mg protein.

Estimation of GSH

The amount of GSH was estimated following the manufacturer's instructions for the commercially available kit. Briefly, the samples were first de-proteinized with 5-sulfosalicylic acid solution (5%) and centrifuged to remove the precipitated protein. The supernatant was used to estimate the amount of GSH. The samples or standards (10 μl) were incubated with 150 μl of working mixture (assay buffer with 5,5′-Dithiobis (2-nitrobenzoic acid) and glutathione reductase) in a 96-well plate for 5 min. Diluted NADPH solution (50 μl) was added to each well and mixed thoroughly. The absorbance of the samples was recorded at 412 nm using the microplate reader after 5 min incubation period. The results were expressed as μM GSH/mg protein.

Antioxidant Enzymes Activity

The activities of antioxidant enzymes: superoxide dismutase (SOD) and catalase (CAT) were estimated using assay kits (Cayman Chemicals Co., Ann Arbor, MI, USA). Briefly, the activity of SOD was estimated by adding samples or standards (10 μl) to a 96-well plate. Xanthine oxidase (20 μl) was added to each well to initiate the reaction and the plate was shaken for a few seconds, afterwards it was covered and incubated for 30 min at room temperature. The absorbance was recorded using the microplate reader at 450 nm. The activity of CAT was estimated by adding samples or standards (20 μl) to the assay buffer (100 μl) and methanol (30 μl) in a 96-well plate. Hydrogen peroxide solution (20 μl) was added to initiate the reaction and incubated for 20 min at room temperature. Potassium hydroxide (30 μl) was added to terminate the reaction, subsequently catalase purpald (30 μl) and catalase potassium periodate (10 μl) were added. The plate was incubated for 5 min at room temperature on a shaker and absorbance was read at 540 nm using the microplate reader. The SOD activity was expressed as U/mg protein and the CAT activity was expressed as nmol·min^{-1}·mg^{-1} protein.

Estimation of Nitrite Levels

The nitrite levels were estimated using a commercially available kit (R&D system, Minneapolis, MN, USA). Briefly, the sample or nitrite standard (50 μl) was added with reaction diluent (50 μl) to a 96-well plate supplied by the manufacturer. Subsequently, Griess reagent (50 μl) was added to each well and mixed by gentle tapping on the side of the plate. The plate was incubated for 10 min at room temperature and the absorbance was measured at 540 nm using the microplate reader. The nitrite levels were expressed as μmol/mg protein.

Estimation of Proinflammatory Cytokines

The levels of proinflammatory cytokines: interleukin-1β (IL-1β), interleukin-6 (IL-6), and tumor necrosis factor-alpha (TNF-α) were estimated using the commercially available ELISA kits purchased from R&D system (Minneapolis, MN, USA). Briefly, a 96-well plate was coated with the diluted capture antibody (100 μl) overnight at room temperature. Each well was aspirated and washed with the wash buffer (0.05% tween 20 in PBS 0.01M pH7.4). The plate was blocked by adding reagent diluent [containing 1% bovine serum albumin in PBS (300 μl)] for 1 h and washed with wash buffer. The samples or standards (100 μl) were added to the well and incubated for 2 h. The detection antibody (100 μl) was added to each well and then incubated for 2 h at room temperature. A working solution of streptavidin horseradish peroxidase (100 μl in ratio of 1:200) was added to each well and further incubated for 20 min. The contents of the wells were exchanged with substrate solution (100 μl) and incubated for 20 min. Stop solution containing 2N H_2SO_4 (50 μl) was added and the plate was gently tapped to ensure proper mixing. The absorbance of each well was measured immediately at 450 nm using a microplate reader. The results were expressed as pg/mg protein.

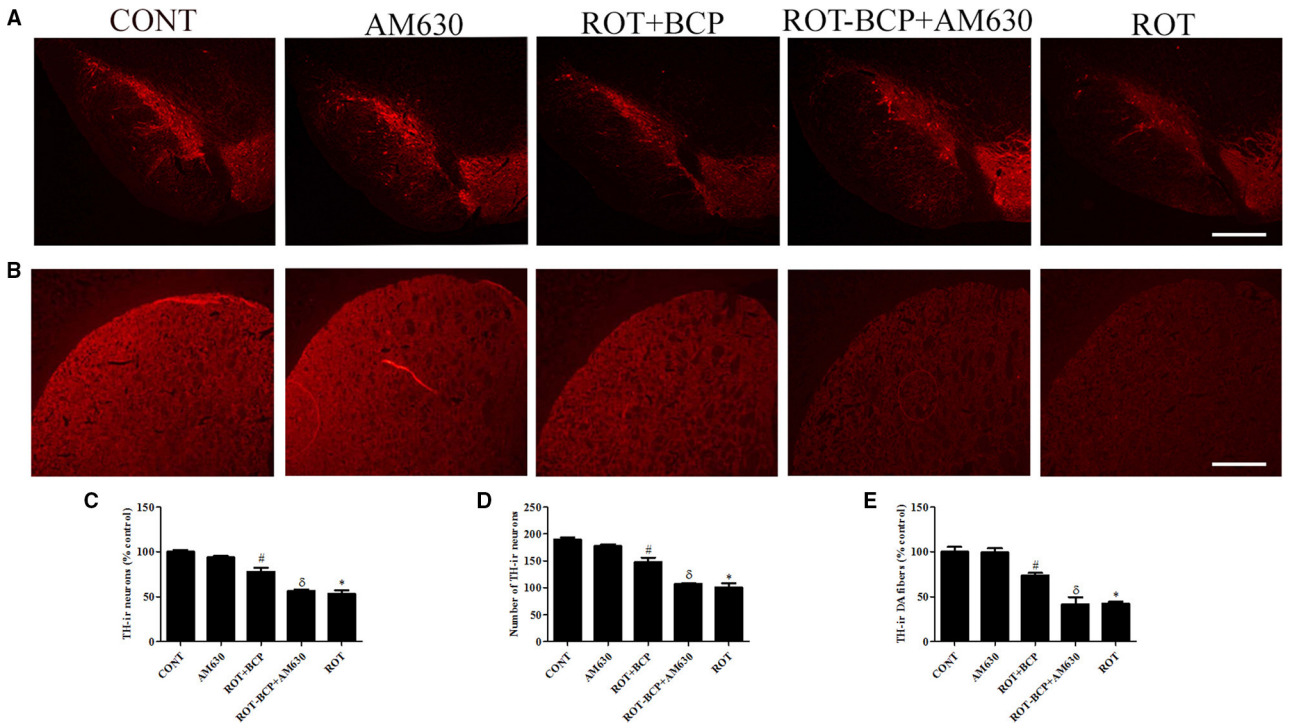

FIGURE 3 | The immunohistochemistry for tyrosine hydroxylase (TH) to detect the expression of the TH-immunoreactive (TH-ir) dopaminergic (DA) neurons in the substantia nigra pars compacta (SNpc) and the TH-ir dopamine nerve fibers in the striatum. Values are expressed as percent mean ± SEM ($n = 3$). The scale bar is 100 μm. **(A)** The number of TH-ir neurons was decreased in the SNpc of ROT-injected rats as compared to control (CONT) group. While, BCP supplementation leads to increased expression of TH-ir neurons in ROT+BCP group as compared to ROT group. Furthermore, the ROT-BCP+AM630 group showed decreased expression of TH-ir neurons as compared to ROT+BCP group. **(B)** Similarly, TH-ir DA nerve fibers immunofluorescence was also decreased in the ROT group in comparison to the CONT group rats. Moreover, BCP supplementation increased the immunoreactivity of DA fibers as compared to ROT group. The ROT-BCP+AM630 group showed TH-ir DA fibers expression similar to ROT group. **(C,D)** The number of TH-ir DA neurons in the SNpc was counted from each group. A significant (*$p < 0.05$) decrease in the number of DA neurons was observed in the SNpc of the ROT group when compared to the CONT group. BCP treatment to ROT administered rats significantly (#$p < 0.05$) protected the DA neurons from the ROT-induced neuronal death in the ROT+BCP group. The ROT-BCP+AM630 group also showed significantly ($^{\delta}p < 0.05$) decreased number of DA neurons as compared to the ROT+BCP group. No significant differences were observed between the DA neurons of the CONT and AM630-only group. **(E)** Immunofluorescence of the TH-ir DA fibers was observed in the striatum of different groups. Significant (*$p < 0.05$) decrease in the TH-ir striatal DA fibers was observed in the ROT group as compared to the CONT group. Although, BCP supplementation of ROT treated rats significantly (#$p < 0.05$) inhibited the loss of the TH-ir DA fibers in the ROT+BCP group as compared to the ROT group. ROT-BCP+AM630 group showed significant ($^{\delta}p < 0.05$) loss of the TH-ir DA fibers when compared to the ROT+BCP group. CONT and AM630-only group did not show any apparent loss of TH-ir DA fibers.

Immunofluorescence Staining of TH

The brain from each rat was collected as described above and sectioned for TH staining. Briefly, 14 μm coronal brain sections were cut at the levels of the striatum and the SNpc using a cryostat (Leica, Wetzlar, Germany). The sections were washed twice with PBS (0.01 M, pH 7.4) and then incubated with blocking reagent (10% normal goat serum in PBS, 0.3% Triton-X 100) for 1 h. Further, the sections were incubated with the primary polyclonal rabbit antibody against TH (1:500) overnight at 4°C. The sections were washed and incubated with fluorescent secondary antibody Alexa Fluor® 594 anti-rabbit (1:1000) for 1 h at room temperature. The sections were then washed and mounted using mounting medium Fluoroshield™ (Sigma Aldrich, MO, USA). Digital images of the sections were captured using a fluorescence microscope (Olympus, Hamburg, Germany).

Immunofluorescence Staining of GFAP and Iba-1

Immunofluorescence staining of the striatum was performed to examine the activation of GFAP positive astrocytes and Iba-1 positive microglia. Brain sections were washed twice with PBS and incubated with blocking reagent containing 10% normal goat serum and 0.3% Triton-X 100 in PBS for 1 h. The sections were then incubated with the primary polyclonal rabbit antibody against GFAP (1:1000) and Iba-1 (1:1000) overnight at 4°C. The sections were washed and incubated with fluorescent secondary antibody Alexa Fluor® 488 anti-rabbit for 1 h at room temperature. Sections were then washed and mounted using mounting medium Fluoroshield™. Images were captured using a fluorescence microscope, EVOS FL (Thermo Fisher Scientific, Waltham, MA, USA).

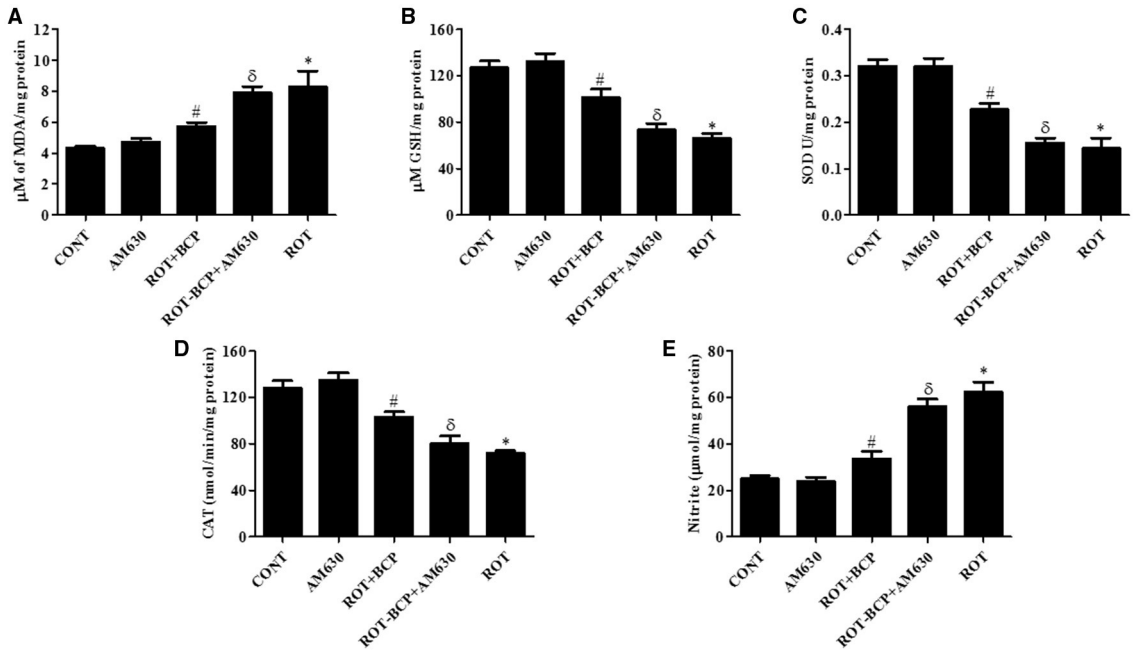

FIGURE 4 | The levels of malondialdehyde (MDA), glutathione (GSH), superoxide dismutase (SOD), catalase (CAT), and nitrite in the midbrain tissue. Values are expressed as mean ± SEM ($n = 6$–8). ROT treatment caused significant (*$p < 0.01$) increase in MDA **(A)** and decrease in GSH level **(B)** in ROT challenged rats as compared to vehicle injected control (CONT) rats. BCP treatment of ROT challenged rats showed significantly (#$p < 0.05$) decreased level of MDA and increased (#$p < 0.01$) GSH level. However, CB_2 antagonist AM630 administration prior to BCP treatment to ROT challenged rats significantly ($^{\delta}p < 0.05$) augmented the level of MDA and GSH as compared to ROT+BCP group rats. The activity of the antioxidant enzymes: SOD **(C)** and CAT **(D)** was significantly (*$p < 0.05$) decreased and nitrite **(E)** level was increased in the ROT group rats as compared to CONT group rats. BCP treatment of ROT administered ROT+BCP group rats significantly (#$p < 0.05$) augmented the SOD and CAT activity and nitrite level in comparison to the ROT group. ROT-BCP+AM630 group rats showed significant ($^{\delta}p < 0.05$) decline in SOD and CAT activity and rise in nitrite level as compared to ROT+BCP group rats.

Assessment of Tyrosine Hydroxylase-Immunoreactive (TH-ir) Dopaminergic (DA) Neurons and TH-ir DA Fibers

To determine the loss of the TH-ir neurons in the SNpc area, three different levels of the SNpc region (−4.8, −5.04, and −5.28 mm of bregma) were counted and the average was presented as a percentage. Loss of striatal fibers was evaluated by measuring the optical density of TH-ir DA fibers in the striatum (adjacent to 0.3 mm of bregma) using Image J software (NIH, Bethesda, MD, USA). For each rat, the optical density of TH-ir fibers within the striatum was measured in three different, equally sized fields of each section (three sections/rat). An average of the three areas was calculated and presented as a percentage with reference to the control. The optical density of the overlying cortex was taken as a background measurement and subtracted from the value generated from the striatum. The counting of TH-ir neurons and measurement of optical density of the TH-ir fibers were performed by an investigator blind to the experimental groups.

Assessment of Activated Astrocytes and Microglia

A minimum of three coronal sections, from each animal, at similar levels of the striatum were used to analyze the number of activated astrocytes and microglia. Activation of astrocytes and microglia was judged based on the intensity of the immunofluorescence and the presences of extended glial processes. Activated astrocytes and microglia were counted in three, randomly chosen, different, equally sized fields, using Image J software.

Western Blot Analysis of NF-κB, COX-2, iNOS, and CB_2

The striatal tissues from each experimental group were homogenized in the buffer to prepare the cytoplasmic and nuclear extracts as previously described by Arumugam et al. (2011). The samples of the cytoplasmic and nuclear fractions containing equal amounts of protein (35 µg) were separated by gel electrophoresis using SDS-polyacrylamide (10%). The proteins were transferred onto PVDF membrane and incubated overnight at 4°C with specific primary rabbit polyclonal antibodies against NF-κB p65 (1:500), COX-2 (1:1000), iNOS (1:500), and CB_2 (1:500) followed by horseradish peroxidase-conjugated secondary anti-rabbit antibody. The protein recognized by the antibody was visualized using an enhanced chemiluminescence pico kit (Thermo Fisher Scientific, Rockford, IL, USA). The obtained blots were stripped and re-probed for β-actin (1:5000; monoclonal mouse, Millipore, MA, USA) as

a loading control. The intensity of bands was measured by densitometry and quantified using Image J software.

Estimation of Protein Concentration

The protein contents in the sample were estimated using the Pierce™ BCA protein assay kit (Thermo Fisher Scientific, Rockford, IL, USA) following the manufacturer's instructions.

Statistical Analyses

The data were expressed as the mean value ± SEM. The data for all parameters, unless otherwise stated, were analyzed using one-way analysis of variance (ANOVA), followed by Tukey's test to calculate the statistical significance between various groups, using software obtained from GraphPad InStat, La Jolla, CA, USA. In all the tests, the criterion for statistical significance was set at $p < 0.05$.

RESULTS

BCP Treatment Upregulates Expression of CB_2 Receptors

First, using western blot, we investigated, whether BCP treatment is capable of selectively enhancing the expression of CB_2 receptors in the striatum region (**Figures 2A,B**). ROT administration decreased the expression of CB_2 receptors as compared to CONT rats (62.56 vs. 100% control). BCP administration prior to ROT increased the expression of CB_2 receptors in comparison to ROT-injected rats with no pretreatment (89.67 vs. 62.56%). However, AM630, a selective CB_2 receptor antagonist, administered prior to BCP in ROT-injected rats caused a noticeable decline in the expression of CB_2 receptors as compared to ROT+BCP group rats (70.22 vs. 89.67%). Further, we observed that AM630 administration to ROT-injected rats did not cause any change in the expression of CB_2 receptors when compared to ROT-injected rats (63.28 vs. 62.56%). Additionally, the CONT and AM630-only groups of rats also did not show any marked differences in the expression level of CB_2 receptors (98.19 vs. 100% control).

CB_2 Receptor Activation Prevents Loss of TH-ir DA Neurons in SNpc and TH-ir DA Fibers in Striatum

To assess the neuroprotection afforded by BCP against the neurodegeneration caused by ROT, we determined the TH-ir DA neurons in the SNpc and optical density of TH-ir DA fibers in the striatum (**Figures 3A–E**). ROT administration to rats caused significant ($p < 0.05$) loss of DA neurons in the SNpc and striatal DA fibers in comparison with vehicle-injected control animals. However, BCP significantly ($p < 0.05$) prevented loss of DA neurons induced by ROT in the SNpc and striatal DA fibers compared to the ROT group of animals. Interestingly, this protective effect of BCP was significantly ($p < 0.05$) reversed by the prior administration of CB_2 antagonist AM630 to rats administered with ROT and BCP. These results are indicative of the CB_2 receptor-mediated neuroprotective effects of BCP. In contrast, AM630 administration alone did not show any deleterious effects on the DA neurons and striatal fibers.

CB_2 Receptor Activation Attenuates the Level of MDA and GSH in the Midbrain

ROT administration significantly ($p < 0.01$) increased MDA content (**Figure 4A**) and decreased ($p < 0.01$) the level of GSH (**Figure 4B**) as compared to control group animals. However, BCP pretreatment of ROT-administered rats caused a significant ($p < 0.05$) reduction in MDA level and prevented ($p < 0.01$) decline of GSH level. In contrast, in ROT-challenged rats, administration of AM630 before BCP significantly ($p < 0.05$) diminished the effect of BCP on MDA reduction and GSH restoration (**Figures 4A,B**). Interestingly, the AM630-only group did not show alteration in the level of either MDA or GSH as compared to control animals.

CB_2 Receptors Activation Augments Antioxidant Enzymes Activity in the Midbrain

The activities of antioxidant enzymes: SOD (**Figure 4C**) and CAT (**Figure 4D**) was significantly ($p < 0.05$) decreased in ROT-injected rats compared to control rats. However, a significant ($p < 0.05$) increase in the activity of SOD and CAT was observed in BCP-treated rats as compared to ROT-injected rats. In contrast, AM630 administration diminished the effects of BCP in ROT-challenged rats (**Figures 4C,D**). The antioxidant enzyme activity of SOD and CAT was unaltered in the AM630-only group of animals.

CB_2 Receptors Activation Inhibits Increased Nitrite Level in the Midbrain

The nitrite levels were significantly ($p < 0.05$) increased in the ROT-administered rats as compared to control rats (**Figure 4E**). However, treatment with BCP produced a significant ($p < 0.05$) decrease in the level of nitrite and that in turn was significantly ($p < 0.05$) attenuated by the CB_2 receptor antagonist, AM630 (**Figure 4E**). In contrast, administration of CB_2 receptor antagonist AM630-only did not cause any significant change in the nitrite level.

CB_2 Receptor Activation Alleviates ROT-Induced Glial Cell Activation in the Striatum

Immunofluorescence staining of GFAP and Iba-1 was carried out to determine the morphological changes in astrocytes and microglia, respectively. In the ROT-administered rats, a noticeable rise in immunofluorescence of GFAP and Iba-1 was observed, which is indicative of the activation of astrocytes and microglia, the features observed in PD neurodegeneration. However, BCP treatment showed a comparatively decreased immunofluorescence of GFAP and Iba-1 (**Figures 5A,B**). Additionally, a quantitative evaluation for GFAP-positive astrocytes and Iba-1-positive microglia was performed in the rats of different experimental groups (**Figures 5C,D**). ROT-injected rats showed a significantly ($p < 0.05$) higher number of activated astrocytes and microglia compared to control animals, whereas BCP pretreatment of ROT-injected rats created a significant ($p < 0.05$) reduction in the number of activated astrocytes

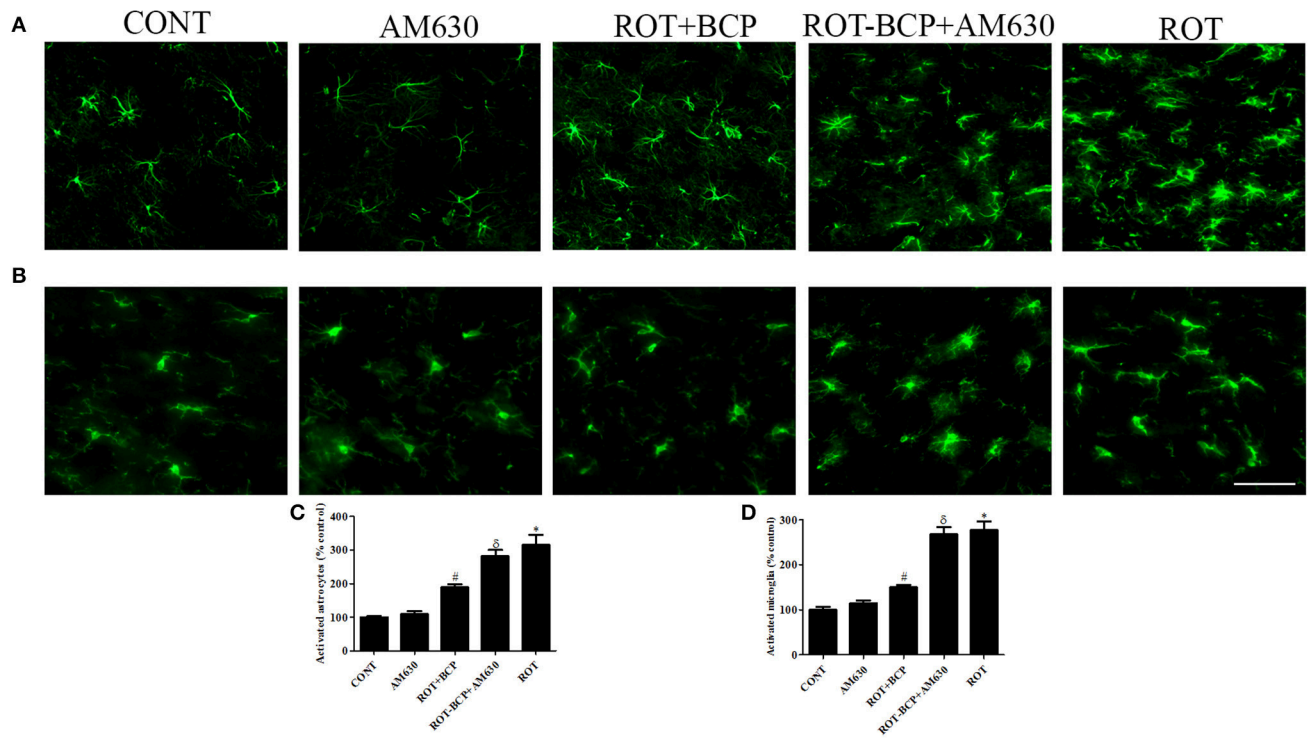

FIGURE 5 | The immunofluorescence staining to detect the expression of glial fibrillary acidic protein (GFAP) positive astrocyte and ionized calcium binding adaptor molecule-1 (Iba-1) positive microglia in the striatum. Values are expressed as percent mean ± SEM ($n = 3$). The scale bar is 200 μm. Profound expression of GFAP positive astrocytes **(A)** and Iba-1 positive microglia **(B)** was found in the ROT-administered and ROT-BCP+AM630 groups as compared to the vehicle-injected CONT and AM630-only groups. While BCP supplementation to ROT-injected rats showed moderate staining of GFAP and Iba-1 as compared to ROT-injected rats. Quantitative analysis of activated astrocytes **(C)** and microglia **(D)** has shown that significant (*$p < 0.05$) increase in number of activated astrocytes and microglia was observed in the ROT group as compared to the CONT group. However, BCP supplementation significantly (#$p < 0.05$) reduced the number of activated astrocytes and microglia in the ROT+BCP group as compared to the ROT group. The ROT-BCP+AM630 group also showed significantly ($^{\delta}p < 0.05$) increased number of activated astrocytes and microglia when compared to the ROT+BCP group. The CONT and AM630-only groups did not show any marked difference in the activation of astrocytes and microglia.

and microglia as compared to ROT-challenged rats. Further, AM630 administration prior to BCP supplementation to ROT injected animals showed increase in the number of activated astrocytes and microglia clearly demonstrating the CB_2 receptor-mediated activity of BCP. However, AM630 alone did not have a significant effect on the activation or number of astrocytes and microglia.

CB_2 Receptors Improve the Level of Proinflammatory Cytokines in the Midbrain

ROT administration created a significant ($p < 0.05$) increase in the level of proinflammatory cytokines such as IL-1β (**Figure 6A**), IL-6 (**Figure 6B**), and TNF-α (**Figure 6C**) as compared to the control group while treatment with BCP significantly ($p < 0.05$) attenuated the rise of these proinflammatory cytokines in ROT-injected rats (**Figures 6A–C**). However, AM630 administration before BCP abrogated the protective effects of BCP against ROT-induced elevated levels of proinflammatory cytokines. The CB_2 receptor antagonist AM630 alone, did not have any effect on the level of proinflammatory cytokines.

CB_2 Receptor Activation Attenuates Inflammatory Mediators NF-κB, COX-2 and iNOS

To detect and quantify the activation of NF-κB, the translocation of NF-κB p65 subunit to the nucleus was assayed in the striatal nuclear extracts using a subunit specific anti-NF-κB p65 antibody. As depicted in **Figures 7A,C**, the rats injected with ROT showed a remarkably higher level of NF-κB p65 as compared to the controls (171.7 vs. 100% control). However, treatment with BCP to ROT-administered rats produced a decrease in NF-κB p65 levels as compared to the ROT group (112.38 vs. 171.7%). In contrast, the CB_2 receptor antagonist AM630 administered prior to BCP in ROT-injected rats increased the level of NF-κB p65 expression as compared to the ROT+BCP group (171.55 vs. 112.38%).

We further investigated the protein expression level of NF-κB responsive genes such as COX-2 and iNOS in the cytoplasmic fraction of the striatal tissue (**Figure 7B**). Similar to NF-κB p65, the expression level of COX-2 and iNOS increased in ROT-challenged rats as compared to control rats (COX-2: 213.48 vs. 100% control; iNOS: 251.56 vs. 100% control). However, BCP

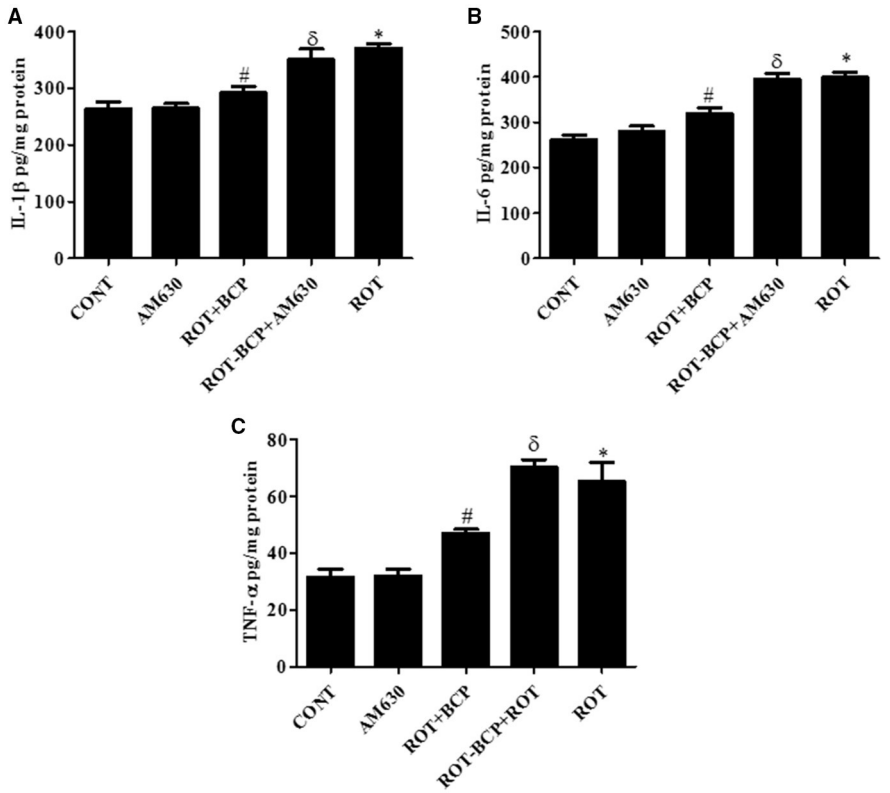

FIGURE 6 | The pro-inflammatory cytokines: IL-1β, IL-6, and TNF-α were measured by enzyme linked immunosorbent assay (ELISA) in the midbrain. Values are expressed as mean ± SEM ($n = 6$–8). The level of IL-1β **(A)**, IL-6 **(B)**, and TNF-α **(C)** was significantly ($^*p < 0.05$) increased in the ROT group when compared to the CONT group. Although, BCP supplementation significantly ($\#p < 0.05$) decreased the ROT-induced increase of these proinflammatory cytokines in the ROT+BCP group. The ROT-BCP+AM630 group showed significantly ($^{\delta}p < 0.05$) increased level of IL-1β, IL-6, and TNF-α as compared to the ROT+BCP group. There is no significant difference in these cytokines between the CONT and the AM630-only group.

pretreatment of ROT-challenged rats decreased the elevated level of COX-2 and iNOS as compared to ROT injected animals (COX-2: 143.6 vs. 213.48%; iNOS: 158.12 vs. 251.56%). However, AM630 administration before BCP has abrogated the beneficial effect of BCP against COX-2 and iNOS in animals treated with ROT (COX-2: 205.6 vs. 143.6%; iNOS: 247.18 vs. 158.12%) (**Figures 7D,E**). Similar to oxidative stress and morphological parameters, no significant changes in the levels of NF-κB, COX-2 and iNOS were observed in the AM630-alone group of rats.

DISCUSSION

The current therapies for PD are still inadequate. Therefore, intensive efforts are made to identify promising new targets for the treatment of PD. Until now, the exact cause of PD has yet to be established even though environmental factors, in addition to genetic factors, have been demonstrated to play a significant role in the causation of PD. Based on the environmental factors, the present study employed the ROT-induced rat model of PD that is widely used for the evaluation of novel pharmacotherapeutic agents and understanding of etiopathogensis. ROT has been shown to cause PD with the inhibition of mitochondrial complex I of the respiratory chain and activation of abnormal dopamine metabolism (Betarbet et al., 2000; Sherer et al., 2007), along with oxidative stress and inflammation, which causes neurodegeneration of DA neurons in the SNpc region of the PD brain (Johnson and Johnson, 2015). The results from the present study showed that ROT causes loss of dopaminergic neurons in the SNpc and the striatal dopaminergic nerve terminals. This correlates with the degeneration of the nigrostriatal pathway, which plays an important role in the co-ordination of motor functions. The degeneration of nigrostriatal pathways has been shown to be associated with the occurrence of oxidative/nitrosative stress, which subsequently leads to the induction of neuroinflammation and subsequent neurodegeneration (Hald and Lotharius, 2005; Cannon et al., 2009; Lee et al., 2009). In recent years, the cannabinoid receptors, specifically activating CB_2 receptors, appear to represent a novel therapeutic target for neurodegenerative diseases, including PD, because of their role in counteracting oxidative stress and inflammation. The CB_2 receptors have recently emerged as a potential anti-inflammatory target, to break the self-sustaining

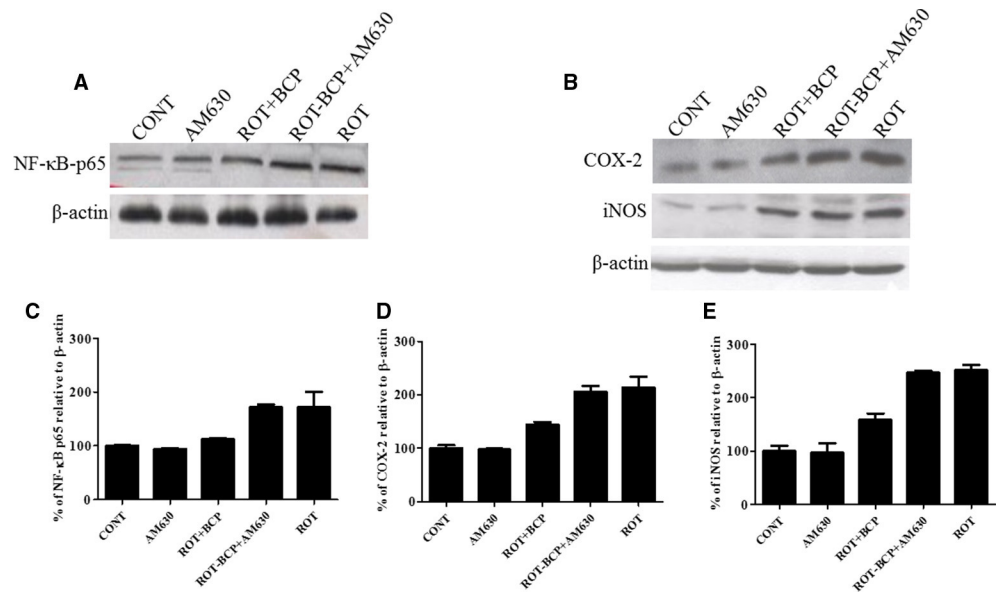

FIGURE 7 | Western blot analysis of NF-κB p65, COX-2, and iNOS in the striatal tissue. Values are expressed as percent (%) mean ± SEM ($n = 3$). Expression level of NF-κB p65 **(A)** COX-2 and iNOS **(B)** was carried out by western blot. **(C)** ROT-administered group rats showed increase in nuclear NF-κB p65 level as compared to control group (171.7 vs. 100% control). BCP treatment of the ROT-challenged rats decreased the NF-κB p65 expression when compared to the ROT group (112.38 vs. 171.7%). The ROT-BCP+AM630 group had shown increased expression of NF-κB p65 as compared to the ROT+BCP group (171.55 vs. 112.38%). **(D)** ROT-injected rats showed increased COX-2 level as compared to the CONT rats (213.48 vs. 100% control). BCP supplementation to ROT-injected rats showed decreased expression of COX-2 as compared to ROT group rats (143.6 vs. 213.48%). ROT-BCP+AM630 group rats showed increase in COX-2 expression as compared to the ROT+BCP group rats (205.6 vs. 143.6%). **(E)** Likewise, iNOS expression was increased in the ROT group rats as compared to the CONT group rats (251.56 vs. 100% control). BCP treatment decreased iNOS expression as compared to the ROT group rats (158.12 vs. 251.56%). The ROT-BCP+AM630 group showed increase in iNOS expression when compared to the ROT+BCP group (247.18 vs. 158.12%).

cycle of neuroinflammation and preserve neuronal homeostasis, and survival in neurodegenerative disorders (Ramírez et al., 2005; Palazuelos et al., 2008; Price et al., 2009; Sagredo et al., 2009; Gómez-Gálvez et al., 2016). The activity of CB_2 receptors is implicated in the reduction of proinflammatory mediators in response to noxious stimuli and in control of neuronal survival (Fernandez-Ruiz et al., 2007). Recently, changes in CB_2 receptors have been shown in the mice model of PD induced by intrastriatal lesions with lipopolysaccharides (García et al., 2011). Genetic studies have also shown that CB_2 receptor knockout-mice display microglial activation, neural pathology, and functional deficits in the MPTP-induced mice model of PD (Price et al., 2009). The CB_2 receptor expression has been demonstrated in the central nervous system, including the SNpc area of PD brains (García et al., 2015). A recent report also suggests that CB_2 receptors modulate the dopamine dependent neuronal activity and behavior in mice (Zhang et al., 2014). Because of potent anti-inflammatory and antioxidant action, and no psychoactive adverse reactions caused by CB_2 receptor activation, the therapeutic targeting of CB_2 receptor appears to be promising for modulation of neuroinflammation and disease modification in PD.

In addition, ROT has been reported to inhibit complex I of the mitochondrial respiratory chain, which consequently leads to the formation of ROS, such as superoxide, hydroxyl radical and peroxynitrite. The induction of ROS is critical in the SNpc because of low levels of antioxidant defenses corresponding to a very high level of dopamine metabolism in this region (Thakur and Nehru, 2013). To determine antioxidant tissue defense, we assessed the oxidative/nitrosative stress parameters such as activities of antioxidant enzymes like SOD and CAT; and the levels of GSH, total nitrite, and MDA, in the midbrain tissues. The occurrence of lipid peroxidation is a key pathogenic event in tissues, resulting from an imbalance between ROS generation and the availability of endogenous cellular antioxidant defense. We observed that the ROT-challenge caused a significant rise in the MDA level, with a concomitant decline in the GSH level in the midbrain tissues. Interestingly, treatment with BCP of ROT-injected rats inhibited lipid peroxidation evidenced by the reduced MDA levels followed by restoration of the GSH content. The decline in the MDA content and concomitant restoration of GSH content by BCP can be ascribed to the potent chain breaking, free radical scavenging, and antioxidant activity of BCP (Chang et al., 2007).

Apart from non-enzymatic antioxidants, the cells are also equipped with the enzymatic defense system, which includes SOD and CAT, as an important component in neutralizing the ROS load. The present study showed that ROT caused a significant reduction in the activities of SOD and CAT enzymes as compared to control rats. However, BCP treatment of ROT-challenged rats showed a significant restoration of SOD and CAT activities. Furthermore, in ROT-challenged rats, we

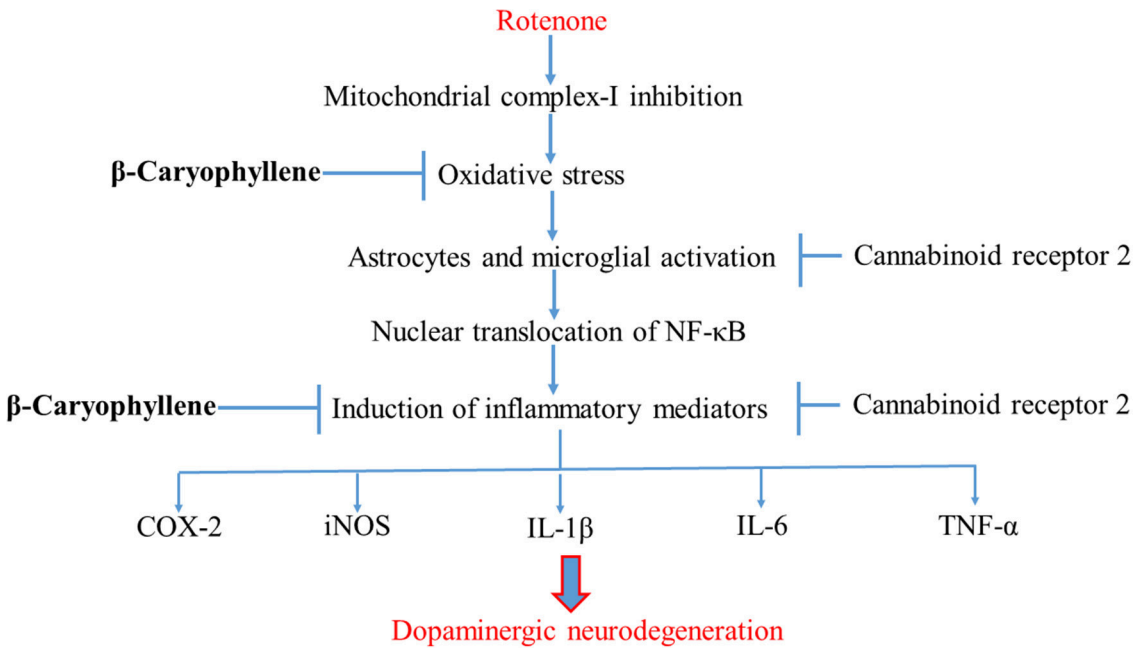

FIGURE 8 | Schematic representation of the neuroprotective mechanism of action of BCP.

observed a significant rise in the total nitrite levels, due to the production of nitric oxide that generates peroxynitrite on reaction with superoxide anion leading to robust neurotoxicity (Beckman et al., 1990). BCP treatment of ROT-challenged rats significantly counteracted any rise in nitrite levels. The reversal of these beneficial effects of BCP against oxidative stress by prior administration of AM630, a selective CB_2 receptor antagonist, clearly demonstrates CB_2 receptor-dependent activity of BCP. To our knowledge, the present study is the first to report that BCP reduces oxidative stress in ROT-induced dopaminergic neurodegeneration by activating CB_2 receptors.

Previous studies have demonstrated gliosis with increased expression of GFAP and Iba-1 in human PD brains that appears to be age dependent and related to the disease progression (Yan et al., 2014). The glial cells mediating neuroinflammation have recently emerged as key players in the pathogenesis of PD; and the activation of microglia in the nigrostriatal regions of the PD brains is believed to be a rapid cellular response to inflammation (Hirsch et al., 2003; Gordon et al., 2012). In our study, the hypertrophy with long processes, along with the increased immunofluorescence of GFAP and Iba-1, represents activated astrocytes and microglia, respectively. However, BCP treatment reduced the activation of astrocytes and microglia, which supports its anti-inflammatory action in-line with the reported activity of several other agonists of the CB_2 receptors (Marchalant et al., 2008). Furthermore, it was expected that a CB_2 receptor antagonist should reverse or abolish the protective effects of BCP, as indeed was the case, as the administration of AM630, abrogated the effects of BCP regarding glial cell activation. The findings clearly demonstrate a functional CB_2 receptor dependent mechanism in the protective effects of BCP.

Moreover, microglia activation leads to the nuclear translocation of transcription factor NF-κB, which upregulates the release of inflammatory mediators such as COX-2 and iNOS as well as induction of proinflammatory cytokines such as IL-1β, IL-6, and TNF-α in PD (Mosley et al., 2006). The transcription factor NF-κB also plays an important role in the regulation of several proinflammatory mediators that are directly involved in the initiation of neuroinflammation and subsequent neurodegeneration. The inactive form of NF-κB is present in the cytoplasm in association with the inhibitory protein IκB, which prevents its nuclear translocation that is required for transcriptional activity. The IκB phosphorylation followed by proteolytic degradation results in the translocation of a free p65 subunit of NF-κB to the nucleus where it binds to target DNA elements (gene promoters containing κB binding sites) and regulates transcription of several proinflammatory genes such as iNOS, COX-2, IL-1β, IL-6, and TNF-α (Shen et al., 2010). These inflammatory enzymes (COX-2 and iNOS and proinflammatory cytokines IL-1β, IL-6 and TNF-α) are known to be cytotoxic to neurons and to lead to neuronal cell death (Hald and Lotharius, 2005). Numerous studies have reported that cannabinoid ligands inhibit the production of proinflammatory cytokines such as TNF-α, IL-1β, and IL-6; and suppress production of proinflammatory mediators by microglia and macrophages, by CB2 receptor modulation (Correa et al., 2005; Klein, 2005; Zhao et al., 2010).

Our study demonstrates that BCP inhibited the ROT-induced nuclear translocation of NF-κB p65, whereas administration of AM630 prior to BCP supplementation to ROT-injected rats diminished the beneficial effects of BCP. We also observed elevated expression of inflammatory mediators COX-2 and iNOS

in ROT-challenged rats. BCP treatment of ROT-challenged rats modestly decreased the expression of COX-2 and iNOS, which supports its anti-inflammatory activity as reported by others (Cho et al., 2007; Bento et al., 2011). In contrast, the anti-inflammatory effect of BCP against increased expression of COX-2 and iNOS was abolished by prior administration of AM630. Additionally, proinflammatory cytokines (IL-1β, IL-6, and TNF-α) were also found significantly increased after ROT-challenge of the rats. BCP treatment significantly decreased the elevated levels of these proinflammatory cytokines in ROT-injected rats. In contrast, AM630 antagonized the protective effect of BCP against the proinflammatory cytokines. Taken together, these results demonstrate that the beneficial effects of BCP were reversed by AM630. To conclude, the abrogation of the BCP effects by AM630 clearly demonstrates that the activity of the central cannabinoid receptors plays an important role in mediating of the neuroprotective action of BCP in ROT-induced PD.

Further, the observed neuroprotective activity of BCP in the present study was also supported by a previous *in vitro* study, where BCP (among a group of triterpenoids screened for pharmacological activity) showed the highest neuroprotective effects due to favorable physicochemical properties, including high lipophilicity (Chang et al., 2007). The lipophilicity of BCP and AM630 are both more than four, which is strongly indicative of their ability to permeate the blood brain barrier and of their bioavailability in the brain. The CB_2 receptor antagonist AM630 is a protean ligand and inverse agonist that targets a constitutively active form of CB_2 receptor in the brain (Bolognini et al., 2012). The CB_2 receptor ligands are generally classified as agonists, antagonists and inverse agonists showing positive, neutral and negative efficacy, respectively, for a particular signaling pathway. They show varying potency and efficacy termed as "functional selectivity" or "biased agonism" (Pertwee et al., 2010), and pave the way to the design of agents, which may activate the specific pathways required for therapeutic benefit. The abrogation of CB_2 receptor mediated effects by AM630 demonstrates the CB_2 receptor dependent mechanism and has been shown in a number of studies (Hosohata et al., 1997).

The data in our study is in agreement with previous studies of the action of BCP and AM630 at CNS level (Choi et al., 2013). The previous report of the effects of BCP in enhancing cognition, preventing dependence and alleviating anxiety, depression, and compulsion is further supported by our current findings (Al Mansouri et al., 2014). Taken together, the abrogation of the protective effects of BCP by AM630 demonstrates the CB_2 receptor-dependent mechanism of BCP and the findings can be extrapolated to the neuroprotective properties of CB_2 agonism in PD.

CONCLUSION

In conclusion, the present study demonstrates that the plant-derived, sesquiterpene compound, BCP, exhibits potent anti-inflammatory and antioxidant effects in the ROT-induced rat model of PD. The major underlying mechanism is the activation of CB_2 receptors, which results in attenuation of oxidative/nitrosative stress and neuroinflammation, inhibition of gliosis and pro-inflammatory cytokine release, and decline in the nigrostriatal degeneration. A diagram of the proposed underlying mechanism has been shown in **Figure 8**. Our findings clearly demonstrate that CB_2 receptors may be an attractive therapeutic target for PD and BCP could be an attractive candidate molecule for the treatment of PD. Furthermore, BCP may be the first CB_2 receptor agonist and plant derived cannabinoid to be developed in the quest for novel compounds that might improve conventional therapies as well as provide novel disease-modifying agents.

AUTHOR CONTRIBUTIONS

All the authors provided important intellectual input, reviewed the content, and approved the final version of the manuscript. HJ, ME, SO: contributed significantly, conceived and designed the experiments, analyzed the data, read, wrote, and approved the manuscript. SA, HJ: performed the experiments. ME, SO: contributed reagents/materials/analysis tools. All the authors are agreed to be accountable for all aspects of the work in ensuring that questions related to the accuracy or integrity of any part of the work are appropriately investigated and resolved.

ACKNOWLEDGMENTS

The research grant support to the authors, SO (Grant number: 31M278) and ME (Grant number: 31M123) from United Arab Emirates University and the National Research foundation, United Arab Emirates are gratefully acknowledged. The authors also acknowledge help of Mahmoud Hag Ali, Animal Research Facility Controller for animal care and welfare. The authors sincerely thank Dr. Keith Bagnall, Professor of Anatomy, College of Medicine and Health Sciences, UAE University, UAE for proofreading the manuscript.

REFERENCES

Al Mansouri, S., Ojha, S., Al Maamari, E., Al Ameri, M., Nurulain, S. M., and Bahi, A. (2014). The cannabinoid receptor 2 agonist, β-caryophyllene, reduced voluntary alcohol intake and attenuated ethanol-induced place preference and sensitivity in mice. *Pharmacol. Biochem. Behav.* 124, 260–268. doi: 10.1016/j.pbb.2014.06.025

Arumugam, T. V., Cheng, Y. L., Choi, Y., Choi, Y. H., Yang, S., Yun, Y. K., et al., (2011). Evidence that γ-secretase-mediated notch signaling induces neuronal cell death via the nuclear factor-κB-Bcl-2- interacting mediator of cell death pathway in ischemic stroke. *Mol. Pharmacol.* 80, 23–31. doi: 10.1124/mol.111.071076

Bahi, A., Al Mansouri, S., Al Memari, E., Al Ameri, M., Nurulain, S. M., and Ojha, S. (2014). β-Caryophyllene, a CB2 receptor agonist produces multiple behavioral changes relevant to anxiety and depression in mice. *Physiol. Behav.* 135, 119–124. doi: 10.1016/j.physbeh.2014.06.003

Beckman, J. S., Beckman, T. W., Chen, J., Marshall, P. A., and Freeman, B. A. (1990). Apparent hydroxyl radical production by peroxynitrite: implications

for endothelial injury from nitric oxide and superoxide. *Proc. Natl. Acad. Sci. U.S.A.* 87, 1620–1624.

Bento, A. F., Leite, D. F., Claudino, R. F., Hara, D. B., Leal, P. C., and Calixto, J. B. (2008). The selective nonpeptide CXCR2 antagonist SB225002 ameliorates acute experimental colitis in mice. *J. Leukoc. Biol.* 84, 1213–1221. doi: 10.1189/jlb.0408231

Bento, A. F., Marcon, R., Dutra, R. C., Claudino, R. F., Cola, M., Leite, D. F., et al. (2011). Caryophyllene inhibits dextran sulfate sodium-induced colitis in mice through CB2 receptor activation and PPARγ pathway. *Am. J. Pathol.* 178, 1153–1166. doi: 10.1016/j.ajpath.2010.11.052

Betarbet, R., Canet-Aviles, R. M., Sherer, T. B., Mastroberardino, P. G., McLendon, C., Kim, J. H., et al. (2006). Intersecting pathways to neurodegeneration in Parkinson's disease: effects of the pesticide rotenone on DJ-1, alpha-synuclein, and the ubiquitin-proteasome system. *Neurobiol. Dis.* 22, 404–420. doi: 10.1016/j.nbd.2005.12.003

Betarbet, R., Sherer, T. B., MacKenzie, G., Garcia-Osuna, M., Panov, A. V., and Greenamyre, J. T. (2000). Chronic systemic pesticide exposure reproduces features of Parkinson's disease. *Nat. Neurosci.* 3, 1301–1306. doi: 10.1038/81834

Bolognini, D., Cascio, M. G., Parolaro, D., and Pertwee, R. G. (2012). AM630 behaves as a protean ligand at the human cannabinoid CB2 receptor. *Br. J. Pharmacol.* 165, 2561–2574. doi: 10.1111/j.1476-5381.2011.01503.x

Cadet, J. L., and Brannock, C. (1998). Free radicals and the pathobiology of brain dopamine systems. *Neurochem. Int.* 32, 117–131. doi: 10.1016/S0197-0186(97)00031-4

Cannon, J. R., Tapias, V., Na, H. M., Honick, A. S., Drolet, R. E., and Greenamyre, J. T. (2009). A highly reproducible rotenone model of Parkinson's disease. *Neurobiol. Dis.* 34, 279–290. doi: 10.1016/j.nbd.2009.01.016

Chang, H. J., Kim, H. J., and Chun, H. S. (2007). Quantitative Structure-Activity Relationship (QSAR) for neuroprotective activity of terpenoids. *Life Sci.* 80, 835–841. doi: 10.1016/j.lfs.2006.11.009

Chen, X., and Tansey, M. G. (2011). "The role of neuroinflammation in Parkinson's disease," in *Neuroinflammation,* ed A. Minagar (London: Elsevier), 403–421.

Cho, J., Chang, H. J., Lee, S. K., Kim, H. J., Hwang, J. K., and Chun, H. S. (2007). Amelioration of dextran sulfate sodium-induced colitis in mice by oral administration of beta-caryophyllene, a sesquiterpene. *Life Sci.* 80, 932–939. doi: 10.1016/j.lfs.2006.11.038

Choi, I. Y., Ju, C., Anthony Jalin, A. M., Lee da, I., Prather, P. L., and Kim, W. K. (2013). Activation of cannabinoid CB2 receptor-mediated AMPK/CREB pathway reduces cerebral ischemic injury. *Am. J. Pathol.* 182, 928–939. doi: 10.1016/j.ajpath.2012.11.024

Concannon, R. M., Okine, B. N., Finn, D. P., and Dowd, E. (2015). Differential upregulation of the cannabinoid CB_2 receptor in neurotoxic and inflammation-driven rat models of Parkinson's disease. *Exp. Neurol.* 269, 133–141. doi: 10.1016/j.expneurol.2015.04.007

Correa, F., Mestre, L., Molina-Holgado, E., Arevalo-Martin, A., Docagne, F., Romero, E., et al. (2005). The role of cannabinoid system on immune modulation: therapeutic implications on CNS inflammation. *Mini Rev. Med. Chem.* 5, 671–675. doi: 10.2174/1389557054368790

Fernandez-Ruiz, J., Romero, J., Velasco, G., Tolon, R. M., Ramos, J. A., and Guzman, M. (2007). Cannabinoid CB2 receptor: a new target for controlling neural cell survival? *Trends Pharmacol. Sci.* 28, 39–45. doi: 10.1016/j.tips.2006.11.001

Galdino, P. M., Nascimento, M. V., Florentino, I. F., Lino, R. C., Fajemiroye, J. O., Chaibub, B. A., et al. (2012). The anxiolytic-like effect of an essential oil derived from Spiranthera odoratissima A. St. Hil. leaves and its major component, β-caryophyllene, in male mice. *Prog. Neuropsychopharmacol. Biol. Psychiatry* 38, 276–284. doi: 10.1016/j.pnpbp.2012.04.012

García, C., Palomo-Garo, C., García-Arencibia, M., Ramos, J., Pertwee, R., and Fernández-Ruiz, J. (2011). Symptom-relieving and neuroprotective effects of the phytocannabinoid Δ^9-THCV in animal models of Parkinson's disease. *Br. J. Pharmacol.* 163, 1495–1506. doi: 10.1111/j.1476-5381.2011.01278.x

García, M. C., Cinquina, V., Palomo-Garo, C., Rábano, A., and Fernández-Ruiz, J. (2015). Identification of CB_2 receptors in human nigral neurons that degenerate in Parkinson's disease. *Neurosci. Lett.* 587, 1–4. doi: 10.1016/j.neulet.2014.12.003

Gertsch, J., Leonti, M., Raduner, S., Racz, I., Chen, J. Z., Xie, X. Q., et al. (2008). Beta-caryophyllene is a dietary cannabinoid. *Proc. Natl. Acad. Sci. U.S.A.* 105, 9099–9104. doi: 10.1073/pnas.0803601105

Gómez-Gálvez, Y., Palomo-Garo, C., Fernández-Ruiz, J., and García, C. (2016). Potential of the cannabinoid CB2 receptor as a pharmacological target against inflammation inParkinson's disease. *Prog. Neuropsychopharmacol. Biol. Psychiatry* 64, 200–208. doi: 10.1016/j.pnpbp.2015.03.017

Gordon, R., Anantharam, V., Kanthasamy, A. G., and Kanthasamy, A. (2012). Proteolytic activation of proapoptotic kinase protein kinase Cdelta by tumor necrosis factor alpha death receptor signaling in dopaminergic neurons during neuroinflammation. *J. Neuroinflammation* 9:82. doi: 10.1186/1742-2094-9-82

Hald, A., and Lotharius, J. (2005). Oxidative stress and inflammation in Parkinson's disease: is there a causal link? *Exp. Neurol.* 193, 279–290. doi: 10.1016/j.expneurol.2005.01.013

Hill, M. N., Hillard, C. J., Bambico, F. R., Patel, S., Gorzalka, B. B., and Gobbi, G. (2009). The therapeutic potential of the endocannabinoid system for the development of a novel class of antidepressants. *Trends Pharmacol. Sci.* 30, 484–493. doi: 10.1016/j.tips.2009.06.006

Hirsch, E. C., Breidert, T., Rousselet, E., Hunot, S., Hartmann, A., and Michel, P. P. (2003). The role of glial reaction and inflammation in Parkinson's disease. *Ann. N.Y. Acad. Sci.* 991, 214–228. doi: 10.1111/j.1749-6632.2003.tb07478.x

Hosohata, K., Quock, R. M., Hosohata, Y., Burkey, T. H., Makriyannis, A., Consroe, P., et al. (1997). AM630 is a competitive cannabinoid receptor antagonist in the guinea pig brain. *Life Sci.* 61, PL115–PL118. doi: 10.1016/S0024-3205(97)00596-1

Hu, L. F., Lu, M., Tiong, C. X., Dawe, G. S., Hu, G., and Bian, J. S. (2010). Neuroprotective effects of hydrogen sulfide on Parkinson's disease rat models. *Aging Cell* 9, 135–146. doi: 10.1111/j.1474-9726.2009.00543.x

Jenner, P. (2003). Oxidative stress in Parkinson's disease. *Ann. Neurol.* 53, S26–S36. doi: 10.1002/ana.10483

Johnson, D. A., and Johnson, J. A. (2015). Nrf2-a therapeutic target for the treatment of neurodegenerative diseases. *Free Radic. Biol. Med.* 88(Pt B), 253–267. doi: 10.1016/j.freeradbiomed.2015.07.147

Klein, T. W. (2005). Cannabinoid-based drugs as anti-inflammatory therapeutics. *Nat. Rev. Immunol.* 5, 400–411. doi: 10.1038/nri1602

Lee, J. K., Tran, T., and Tansey, M. G. (2009). Neuroinflammation in Parkinson's disease. *J. Neuroimmune. Pharmacol.* 4, 419–429. doi: 10.1007/s11481-009-9176-0

Leonhardt, V., Leal-Cardoso, J. H., Lahlou, S., Albuquerque, A. A., Porto, R. S., Celedonio, N. R., et al. (2010). Antispasmodic effects of essential oil of Pterodon polygalaeflorus and its main constituent β-caryophyllene on rat isolated ileum. *Fundam. Clin. Pharmacol.* 24, 749–758. doi: 10.1111/j.1472-8206.2009.00800.x

Marchalant, Y., Cerbai, F., Brothers, H. M., and Wenk, G. L. (2008). Cannabinoid receptor stimulation is antiinflammatory and improves memory in old rats. *Neurobiol. Aging* 29, 1894–1901. doi: 10.1016/j.neurobiolaging.2007.04.028

Medeiros, R., Passos, G. F., Vitor, C. E., Koepp, J., Mazzuco, T. L., Pianowski, L. F., et al. (2007). Effect of two active compounds obtained from the essential oil of *Cordia verbenacea* on the acute inflammatory responses elicited by LPS in the rat paw. *Br. J. Pharmacol.* 151, 618–627. doi: 10.1038/sj.bjp.0707270

Mosley, R. L., Benner, E. J., Kadiu, I., Thomas, M., Boska, M. D., Hasan, K., et al. (2006). Neuroinflammation, oxidative stress and the pathogenesis of Parkinson's Disease. *Clin. Neurosci. Res.* 6, 261–281. doi: 10.1016/j.cnr.2006.09.006

Ojha, S., Javed, H., Azimullah, S., Abul Khair, S. B., and Haque, M. E. (2015). Glycyrrhizic acid attenuates neuroinflammation and oxidative stress in rotenone model of Parkinson's disease. *Neurotox. Res.* 29, 275–287. doi: 10.1007/s12640-015-9579-z

Palazuelos, J., Aguado, T., Pazos, M. R., Julien, B., Carrasco, C., Resel, E., et al. (2009). Microglial CB_2 cannabinoid receptors are neuroprotective in Huntington's disease excitotoxicity. *Brain* 132(Pt 11), 3152–3164. doi: 10.1093/brain/awp239

Palazuelos, J., Davoust, N., Julien, B., Hatterer, E., Aguado, T., Mechoulam, R., et al. (2008). The CB_2 cannabinoid receptor controls myeloid progenitor trafficking: involvement in the pathogenesis of an animal model of multiple sclerosis. *J. Biol. Chem.* 283, 13320–13329. doi: 10.1074/jbc.M707960200

Passos, G. F., Fernandes, E. S., Campos, M. M., Araujo, J. G., Pesquero, J. L., Souza, G. E., et al. (2004). Kinin B1 receptor up-regulation after lipopolysaccharide administration: role of proinflammatory cytokines and neutrophil influx. *J. Immunol.* 172, 1839–1847. doi: 10.4049/jimmunol.172.3.1839

Pertwee, R. G., Howlett, A. C., Abood, M. E., Alexander, S. P. H., Di Marzo, V., Elphick, M. R., et al. (2010). International union of basic and clinical

pharmacology. LXXIX. Cannabinoid receptors and their ligands: beyond CB_1 and CB_2. *Pharmacol. Rev.* 62, 588–631. doi: 10.1124/pr.110.003004

Price, D. A., Martinez, A. A., Seillier, A., Koek, W., Acosta, Y., Fernandez, E., et al. (2009). WIN55, 212–2, a cannabinoid receptor agonist, protects against nigrostriatal cell loss in the MPTP mouse model of Parkinson's disease. *Eur. J. Neurosci.* 29, 2177–2186. doi: 10.1111/j.1460-9568.2009.06764.x

Ramírez, B. G., Blázquez, C., Gómez del Pulgar, T., Guzmán, M., and de Ceballos, M. L. (2005). Prevention of Alzheimer's disease pathology by cannabinoids: neuroprotection mediated by blockade of microglial activation. *J. Neurosci.* 25, 1904–1913. doi: 10.1523/JNEUROSCI.4540-04.2005

Sagredo, O., González, S., Aroyo, I., Pazos, M. R., Benito, C., Lastres-Becker, I., et al. (2009). Cannabinoid CB2 receptor agonists protect the striatum against malonate toxicity: relevance for Huntington's disease. *Glia* 57, 1154–1167. doi: 10.1002/glia.20838

Schapira, A. H. (1989). Mitochondrial complex I deficiency in Parkinson's disease. *Lancet* 1, 1269. doi: 10.1016/s0140-6736(89)92366-0

Sharma, C., Al Kaabi, J. M., Nurulain, S. M., Goyal, S. N., Kamal, M. A., and Ojha, S. (2016). Polypharmacological properties and therapeutic potential of β-Caryophyllene: a dietary phytocannabinoid of pharmaceutical promise. *Curr. Pharm. Des.* 22, 3237–3264.

Shen, H., Hu, X., Liu, C., Wang, S., Zhang, W., Gao, H., et al. (2010). Ethyl pyruvate protects against hypoxic-ischemic brain injury via anti-cell death and anti-inflammatory mechanisms. *Neurobiol. Dis.* 37, 711–722. doi: 10.1016/j.nbd.2009.12.010

Sherer, T. B., Richardson, J. R., Testa, C. M., Seo, B. B., Panov, A. V., Yagi, T., et al. (2007). Mechanism of toxicity of pesticides acting at complex I: relevance to environmental etiologies of Parkinson's disease. *J. Neurochem.* 100, 1469–1479. doi: 10.1111/j.1471-4159.2006.04333.x

Shimohama, S., Sawada, H., Kitamura, Y., and Taniguchi, T. (2003). Disease model: Parkinson's disease. *Trends Mol. Med.* 9, 360–365. doi: 10.1016/S1471-4914(03)00117-5

Sibbald, B. (2005). Conditional okay for cannabis prescription drug. *CMAJ* 172, 1672. doi: 10.1503/cmaj.050628

Singh, G., Marimuthu, P., de Heluani, C. S., and Catalan, C. A. (2006). Antioxidant and biocidal activities of Carum nigrum (seed) essential oil, oleoresin, and their selected components. *J. Agric. Food Chem.* 54, 174–181. doi: 10.1021/jf0518610

Tapias, V., Cannon, J. R., and Greenamyre, J. T. (2014). Pomegranate juice exacerbates oxidative stress and nigrostriatal degeneration in Parkinson's disease. *Neurobiol. Aging.* 35, 1162–1176. doi: 10.1016/j.neurobiolaging.2013.10.077

Tapias, V., Escames, G., López, L. C., López, A., Camacho, E., Carrión, M. D., et al. (2009). Melatonin and its brain metabolite N(1)-acetyl-5-methoxykynuramine prevent mitochondrial nitric oxide synthase induction in parkinsonian mice. *J. Neurosci. Res.* 87, 3002–3010. doi: 10.1002/jnr.22123

Thakur, P., and Nehru, B. (2013). Anti-inflammatory properties rather than anti-oxidant capability is the major mechanism of neuroprotection by sodium salicylate in a chronic rotenone model of Parkinson's disease. *Neuroscience* 231, 420–431. doi: 10.1016/j.neuroscience.2012.11.006

Yan, J., Fu, Q., Cheng, L., Zhai, M., Wu, W., Huang, L., et al. (2014). Inflammatory response in Parkinson's disease (Review). *Mol. Med. Rep.* 10, 2223–2233. doi: 10.3892/mmr.2014.2563

Zanettini, C., Panlilio, L. V., Alicki, M., Goldberg, S. R., Haller, J., and Yasar, S. (2011). Effects of endocannabinoid system modulation on cognitive and emotional behavior. *Front. Behav. Neurosci.* 5:57. doi: 10.3389/fnbeh.2011.00057

Zhang, H. Y., Gao, M., Liu, Q. R., Bi, G. H., Li, X., Yang, H. J., et al. (2014). Cannabinoid CB2 receptors modulate midbrain dopamine neuronal activity and dopamine-related behavior in mice. *Proc. Natl. Acad. Sci. U.S.A.* 111, E5007–E5015. doi: 10.1073/pnas.1413210111

Zhao, Y., Liu, Y., Zhang, W., Xue, J., Wu, Y. Z., Xu, W., et al. (2010). WIN55212-2 ameliorates atherosclerosis associated with suppression of pro-inflammatory responses in ApoE-knockout mice. *Eur. J. Pharmacol.* 649, 285–292. doi: 10.1016/j.ejphar.2010.09.027

Conflict of Interest Statement: The authors declare that the research was conducted in the absence of any commercial or financial relationships that could be construed as a potential conflict of interest.

Copyright © 2016 Javed, Azimullah, Haque and Ojha. This is an open-access article distributed under the terms of the Creative Commons Attribution License (CC BY). The use, distribution or reproduction in other forums is permitted, provided the original author(s) or licensor are credited and that the original publication in this journal is cited, in accordance with accepted academic practice. No use, distribution or reproduction is permitted which does not comply with these terms.

frontiers in Neuroscience

ORIGINAL RESEARCH
published: 06 October 2016
doi: 10.3389/fnins.2016.00449

Mild Traumatic Brain Injury Produces Neuron Loss That Can Be Rescued by Modulating Microglial Activation Using a CB2 Receptor Inverse Agonist

*Wei Bu[1], Huiling Ren[1], Yunping Deng[1], Nobel Del Mar[1], Natalie M. Guley[1], Bob M. Moore[2], Marcia G. Honig[1] and Anton Reiner[1,3]**

[1] Department of Anatomy and Neurobiology, University of Tennessee Health Science Center, Memphis, TN, USA, [2] Department of Pharmaceutical Sciences, University of Tennessee Health Science Center, Memphis, TN, USA, [3] Department of Ophthalmology, University of Tennessee Health Science Center, Memphis, TN, USA

We have previously reported that mild TBI created by focal left-side cranial blast in mice produces widespread axonal injury, microglial activation, and a variety of functional deficits. We have also shown that these functional deficits are reduced by targeting microglia through their cannabinoid type-2 (CB2) receptors using 2-week daily administration of the CB2 inverse agonist SMM-189. CB2 inverse agonists stabilize the G-protein coupled CB2 receptor in an inactive conformation, leading to increased phosphorylation and nuclear translocation of the cAMP response element binding protein (CREB), and thus bias activated microglia from a pro-inflammatory M1 to a pro-healing M2 state. In the present study, we showed that SMM-189 boosts nuclear pCREB levels in microglia in several brain regions by 3 days after TBI, by using pCREB/CD68 double immunofluorescent labeling. Next, to better understand the basis of motor deficits and increased fearfulness after TBI, we used unbiased stereological methods to characterize neuronal loss in cortex, striatum, and basolateral amygdala (BLA) and assessed how neuronal loss was affected by SMM-189 treatment. Our stereological neuron counts revealed a 20% reduction in cortical and 30% reduction in striatal neurons bilaterally at 2–3 months post blast, with SMM-189 yielding about 50% rescue. Loss of BLA neurons was restricted to the blast side, with 33% of Thy1+ fear-suppressing pyramidal neurons and 47% of fear-suppressing parvalbuminergic (PARV) interneurons lost, and Thy1-negative fear-promoting pyramidal neurons not significantly affected. SMM-189 yielded 50–60% rescue of Thy1+ and PARV neuron loss in BLA. Thus, fearfulness after mild TBI may result from the loss of fear-suppressing neuron types in BLA, and SMM-189 may reduce fearfulness by their rescue. Overall, our findings indicate that SMM-189 rescues damaged neurons and thereby alleviates functional deficits resulting from TBI, apparently by selectively modulating microglia to the beneficial M2 state. CB2 inverse agonists thus represent a promising therapeutic approach for mitigating neuroinflammation and neurodegeneration.

Keywords: traumatic brain injury, neuron loss, neuron rescue, cerebral cortex, striatum, basolateral amygdala, cannabinoid type-2 receptor inverse agonist

OPEN ACCESS

Edited by:
Ashley Ian Bush,
University of Melbourne, Australia

Reviewed by:
Zemin Wang,
Harvard Medical School, USA
Corinne Lasmezas,
Scripps Florida, USA

****Correspondence:***
Anton Reiner
areiner@uthsc.edu

Specialty section:
This article was submitted to Neurodegeneration, a section of the journal Frontiers in Neuroscience

Received: *27 July 2016*
Accepted: *20 September 2016*
Published: *06 October 2016*

Citation:
Bu W, Ren H, Deng Y, Del Mar N, Guley NM, Moore BM, Honig MG and Reiner A (2016) Mild Traumatic Brain Injury Produces Neuron Loss That Can Be Rescued by Modulating Microglial Activation Using a CB2 Receptor Inverse Agonist. Front. Neurosci. 10:449. doi: 10.3389/fnins.2016.00449

INTRODUCTION

Mild traumatic brain injury (TBI) occurs frequently as an outcome from military, sports, and recreational activities, and vehicular accidents, and can lead to a variety of adverse sensory, motor, cognitive and emotional outcomes (Faul et al., 2010; Risdall and Menon, 2011; Johnson et al., 2013). Mild TBI involves either brief or no loss of consciousness and causes minimal overt brain destruction, but produces widespread axonal injury that is commonly referred to as "diffuse" axonal injury, and sets in motion subsequent secondary degenerative events (Bazarian et al., 2013; Johnson et al., 2013; Smith et al., 2013b). The initial injury appears to stem from the compressive, tensile, and shear forces exerted on neural tissue by the concussive force created by a blow to the head with a blunt object, a blast shock wave, or a rapid head acceleration—deceleration (Namjoshi et al., 2013). Although a variety of treatments have been tested in animal models and human clinical trials (Xiong et al., 2013), effective therapies have not been developed. Since microglial activation is one of the secondary events that appears to worsen the outcome after mild TBI (Kelley et al., 2007; Redell and Dash, 2007; Cao et al., 2012; Das et al., 2012; Kumar and Loane, 2012; Patterson and Holahan, 2012; Perez-Polo et al., 2013; Smith et al., 2013a), we have evaluated the benefits of a novel pharmacological approach for reducing the harmful effects of activated microglia (Reiner et al., 2015).

We created mild TBI in mice using a focal blast model (Heldt et al., 2014; Guley et al., 2016). As our pharmacological approach, we modulated activated microglia via their cannabinoid type 2 receptors (CB2) (Schomberg and Olson, 2012; Cherry et al., 2014). CB2 receptors are typically expressed at very low levels in brain, are more concentrated in microglia than neurons, and are thus non-psychotropic, in contrast to cannabinoid type 1 (CB1) receptors (Benito et al., 2003; Stella, 2010; Baek et al., 2013). Activated microglia, however, rapidly increase their expression of CB2 receptors (Benito et al., 2003; Ashton and Glass, 2007; Stella, 2010; Schomberg and Olson, 2012; Baek et al., 2013; Donat et al., 2014), and so drugs acting on CB2 are especially promising for selectively targeting microglia for therapeutic purposes. CB2 inverse agonists in particular represent a unique class of ligands with promise for beneficially modulating microglia to treat TBI (Lunn et al., 2006, 2008). CB2 inverse agonists stabilize CB2 receptors in an inactive state, which are otherwise constitutively active, and reduce adenylyl cyclase inhibition and thereby increase cAMP production (Atwood et al., 2012). This in turn leads to downstream activation of protein kinase A, which phosphorylates the cAMP response element binding protein (CREB). Increased phosphorylation and nuclear translocation of CREB appear to bias activated microglia from the M1 toward the M2 state, and thus underlie the anti-inflammatory and pro-repair effects of CB2 inverse agonists (Lunn et al., 2006, 2008; Lawrence and Natoli, 2011; Presley et al., 2015).

We have previously tested if the selective CB2 inverse agonist SMM-189, which was developed in one of our laboratories and has striking efficacy in reducing the M1 features and increasing the M2 features of human and murine microglia *in vitro* (Presley et al., 2015; Reiner et al., 2015), could improve the outcome after mild TBI in our mouse model. We have shown that a 2-week daily treatment with SMM-189 after mild TBI greatly attenuates the motor deficits, visual deficits and increased fearfulness that are otherwise evident 2–6 weeks after the traumatic event (Reiner et al., 2015). We have also found that the decrease in some of these functional abnormalities was associated with reduced pathology in neural structures associated with these functions. For example, rescue of visual deficits was associated with reduced thinning of the retina, and the attenuation in fearfulness was associated with the rescue of at least one population of neurons in the basolateral amygdala (BLA) that promotes fear. Our previous work has thus shown that treatment with a CB2 receptor inverse agonist that biases brain microglia from a pro-inflammatory M1 phenotype to a pro-healing M2 phenotype is beneficial after mild TBI (Reiner et al., 2015).

The present study had two goals. First, we sought to determine if mild TBI resulted in the loss of neurons in brain regions linked to motor functions and fear control, to better understand the basis of the motor and emotional deficits observed in our model. To this end, we used blinded stereology in mice 2–3 months after mild TBI to analyze neuron loss in cerebral cortex and striatum because of their role in motor control, and several neuron types in the BLA that are differentially involved in fear regulation and expression. Secondly, we evaluated the efficacy of SMM-189 in rescuing these neuron types, both to better understand the basis of the functional recovery SMM-189 provides, and also to further assess the contributions of the neuronal loss to the functional deficits. As part of this, we confirmed that SMM-189 treatment increased levels of nuclear pCREB in microglia in the brain systems under study, which would thereby bias the microglia toward an M2 state. Overall, our findings indicate diffuse neuron loss as a contributor to functional deficits in our TBI model, and they support the use of CB2 inverse agonists as an approach for reducing neuron loss and/or injury after mild TBI and attenuating functional deficits.

MATERIALS AND METHODS

Animals

Three-month old male mice were subjected to single left-side blasts of 0-psi (sham) or 50–60-psi above atmospheric pressure and the outcome evaluated in two sets of studies. In one set of studies, we assessed if SMM-189 treatment increases nuclear pCREB levels in microglia, using pCREB/CD68 double immunofluorescent labeling of brain sections from mice 3 days either after blast alone or after blast followed by SMM-189 treatment. In a second set of studies, we evaluated the TBI outcome for neuron abundance in cerebral cortex, striatum and BLA histologically 2–3 months after blast, to allow time for any neuron loss to develop, comparing mice with and without SMM-189 treatment. Two strains of mice were used, C57BL/6 mice and reporter mice (on a C57BL/6 background) conditionally expressing enhanced yellow fluorescent protein (EYFP) in Thy1-expressing telencephalic neurons of the *emx1* lineage (Gorski et al., 2002; Bareyre et al., 2005). The EYFP reporter mice were used to histologically evaluate the effects of blast on the Thy1+ vs. Thy1−negative subset of functionally

distinct excitatory pyramidal neurons of BLA (Heldt et al., 2014; Reiner et al., 2015). The C57BL/6 mice were either purchased from Jackson Laboratories (JAX; Bar Harbor, ME), and/or taken from a colony maintained from C57BL/6 founders from JAX at the University of Tennessee Health Science Center (UTHSC). Floxed Thy1-EYFP reporter mice (purchased from JAX) and *emx1*-Cre driver mice (purchased from the Mutant Mouse Regional Resource Consortium) were maintained as colonies at the UTHSC, and bred to one another to produce the Thy1-EYFP+/emx1-cre+ progeny used for the experiments. Mice were injected intraperitoneally daily with 6 mg/kg SMM-189 or vehicle (ethanol:Cremophor:0.9% saline; 5:5:90) for 14 days beginning 2 h after 50–60 psi or 0-psi (sham) blast in the case of neuronal loss studies and for 3 days in the case of pCREB studies. The dose used was chosen based on studies of uptake in rodent brain of structurally similar tri-aryl CB2 compounds (Fujinaga et al., 2010), which proved effective in our prior study (Reiner et al., 2015), and which is more than adequate for CB2 receptor activation given its 121.3 nM affinity (Presley et al., 2015). Note that although Cremophor has been linked to neuropathy when used as a vehicle for anti-cancer drugs (Gelderblom et al., 2001), the dose of Cremophor used here was below the maximum recommended dose for rodents, which is not known to have side effects (Neervannan, 2006). Consistent with this, no abnormalities were seen in optic nerve of mice following 2 weeks of Chremophor vehicle treatment in a prior study by us (Reiner et al., 2015). In addition, the number of cortical and striatal neurons in mice that received sham blast and Cremophor vehicle in the present study did not differ from those in our prior study (Guley et al., 2016) that received sham blast and no vehicle, and there were also no differences in body weight. All studies were performed in accordance with an UTHSC Institutional Animal Care and Use Committee approved protocol and complied with the National Institutes of Health and Society for Neuroscience guidelines. The mice analyzed here for neuron loss included some that had been used in our initial study of functional and morphological aspects of SMM-189 benefit (16; Reiner et al., 2015). For studies of neuron loss in cortex and striatum, 3 mice were analyzed per group (0-psi vehicle, 50-psi vehicle, and 50-psi, SMM-189), with a mean post-blast survival of 75.3, 75.7, and 77.0 days, respectively, per group. For BLA neuron loss, 4 mice were analyzed per group, with a mean post-blast survival of 69.3, 67.5, and 58.0 days, respectively, per group.

TBI Methods

The overpressure air blast was delivered by a small horizontally mounted air cannon system (Heldt et al., 2014; Guley et al., 2016), consisting of a modified paintball gun (Invert Mini, Empire Paintball, Sewell NJ), pressurized air tank, and x-y table secured onto a medium-density fiberboard. The original paintball gun barrel with a 13 mm aperture was replaced with a machined barrel with a 6.5 mm diameter aperture, to increase output pressure. The air blast pressures from the paintball gun were controlled by adjusting the output from a pressurized air tank, as monitored by a gun input pressure gauge. The part of the mouse exposed to the blast was restricted to a 7.5 mm diameter mid-cranial territory, as described previously (Guley et al., 2016). The exposed region was the parietal area of the left side of the head between the ear and the eye, encompassing that part of the skull overlying the forebrain. A foam rubber sleeve surrounding the mouse cushioned the non-blast side of the mouse, to stabilize it and minimize head displacement. Prior to blast exposure, mice were anesthetized with avertin (400 mg/kg body weight), the fur of the parietal region of the left side of the head shaved, and the mouse secured in a holder as described previously (Guley et al., 2016). TBI mice used for study of cortex and striatum received 50-psi blast, while TBI mice used for study of BLA received 60-psi blast. All of the same procedures were followed for sham-blast mice (0-psi), except that the mouse was shielded from the blast by a metal plate inserted between it and the gun nozzle. Mice received 35 mg/ml Tylenol in their drinking water for 24 h after blast.

Morphological Methods

Histological analysis was carried out on fixed brain tissue to determine the effects of TBI on the brain, and the remedial effects of SMM-189. Either 3 days or 2–3 months after blast, mice were deeply anesthetized (avertin; 0.2 ml/g body weight), the chest opened, and 0.1 ml of heparinized saline (800 U.S.P. units/ml) injected into the heart. Mice were then perfused transcardially with 40 ml of 0.9% NaCl in 0.1 M sodium phosphate buffer at pH 7.4 (PB), followed by 200 ml of 4% paraformaldehyde, 0.1 M lysine-0.1 M sodium periodate in 0.1 M PB at pH 7.4 (PLP). The brain was removed, post-fixed overnight, a pin inserted longitudinally into the right side to distinguish left blast-exposed side from right non-exposed side, and then stored in a 20% sucrose/10% glycerol solution at 4°C. The fixed brains were sectioned frozen on a sliding microtome in the transverse plane at 35 μm, and each brain collected as either 6 (for BLA) or 12 separate series (for cortex and striatum) in 0.1 M PB with 0.02% sodium azide. At least one series of brain sections from each mouse was mounted as sectioned and stained with cresyl violet. One or more series were immunostained for the pan-neuronal marker NeuN using a mouse monoclonal antibody (Millipore Corp., Billerica, MA) and peroxidase-antiperoxidase (PAP) procedures as described previously (Reiner et al., 2015; Guley et al., 2016), and in the case of 2–3 month survival mice employed to count all neuronal perikarya in cerebral cortex, striatum and BLA. Thy1+ pyramidal neurons of BLA in the Thy1 reporter mice were visualized for transmitted light microscopic study using a mouse monoclonal antibody against green fluorescent protein (Rockland Inc, Gilbertsville, PA), which crossreacts with EYFP due to the high similarity of their antigenic determinants. We detected PARV+ interneurons in BLA using a mouse monoclonal anti-PARV antibody (Sigma-Aldrich, St. Louis, MO), as described previously (Deng et al., 2007). Thy1+ pyramidal neurons and PARV+ interneurons in BLA were each visualized using PAP procedures in separate series of coronal sections. To evaluate CREB phosphorylation by SMM-189, we used a rabbit anti-pCREB antibody (#p1010-133; PhosphoSolutions, Aurora, CO) and anti-rabbit IgG conjugated to Alexa-594 (Molecular Probes; Eugene, OR), in conjunction with a rat anti-CD68 antibody (#ab53444; Abcam, Cambridge, MA) and anti-rat IgG conjugated to Alexa-647 (Molecular Probes; Eugene, OR) to

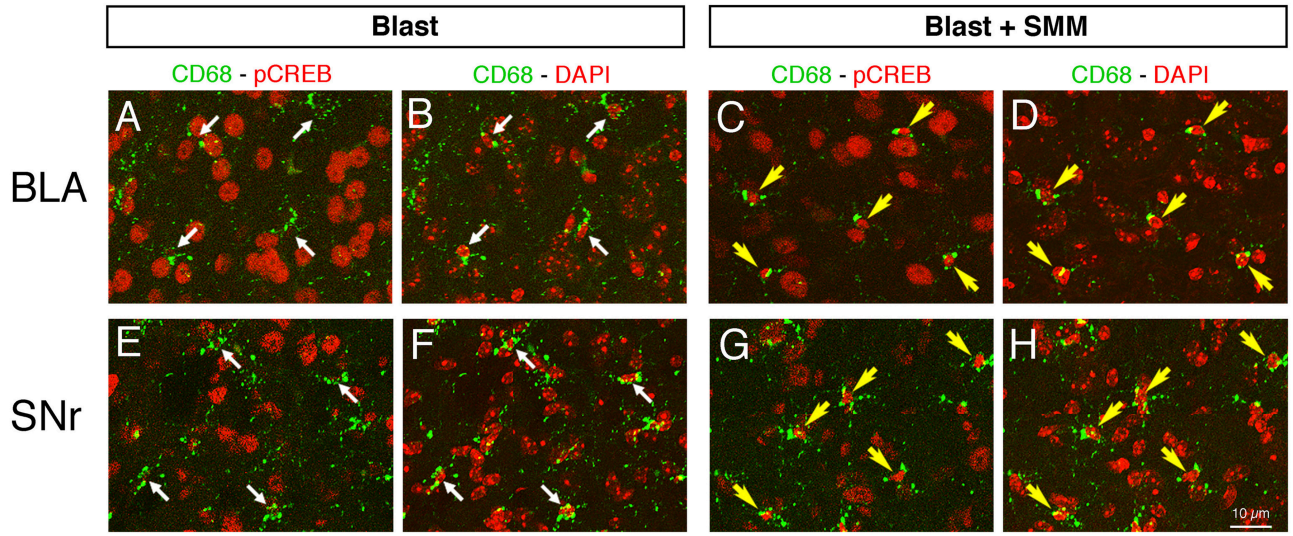

FIGURE 1 | Images showing the effect of SMM-189 treatment on pCREB expression in microglia after blast. Confocal image pairs, one showing immunostaining for pCREB and CD68 and the other showing pCREB and DAPI, in left BLA and SNr in a blast alone mouse **(A,B,E,F)** compared to a SMM-189 treated blast mouse **(C,D,G,H)** at 3 days post blast. The CD68/pCREB double labeling shows microglia with CREB activation (i.e., nuclear pCREB; yellow arrows). The DAPI staining (pseudo-colored red for ease of viewing) reveals nuclei. Note that the nuclei of neurons are distinctly larger than those of microglia. The nuclei of all microglia in the blast mouse lack prominent pCREB (thin white arrows), whereas in the SMM-189 treated blast mouse all microglia are rich in nuclear pCREB (yellow arrows). Thus, SMM-189 treatment after blast results in CREB activation in microglia in BLA and SNr.

identify microglia. Nuclei were visualized by DAPI staining. Sections were mounted on gelatin-coated slides and coverslipped with ProLong® antifade medium (Molecular Probes, Eugene, OR). Sections were viewed and images captured using a Zeiss 710 confocal laser-scanning microscope.

Neuron Counts

Unbiased, blinded stereological neuron counts were carried out using Stereo Investigator (Micro-Brightfield, Colchester, VT) with the optical fractionator method, as described previously (Reiner et al., 2012; Guley et al., 2016). Stereology also provided information on the volumes of the structures examined. The results for different groups of mice were compared using ANOVA followed by planned comparisons with post-hoc Bonferroni tests. No inhomogeneity of variances was detected by the Levene statistic for any of the data sets. Neuron counts for cortex and striatum were obtained using a one-in-twelve series of coronal sections immunolabeled for NeuN from C57BL/6 mice that had previously been used in rotarod assessments of motor performance (Reiner et al., 2015). The cortical field counted extended from the pial surface to the external capsule, and from the midline to the rhinal fissure. The striatum was defined by the contours of the external capsule and globus pallidus, and included nucleus accumbens. Cortex and striatum counts were performed from the rostral end of each to the level of the passage of the internal capsule into the thalamus, and thus included all but the most caudal ~25% of cortex and the most caudal ~10% of striatum. We have interpreted a reduction in the number of immunolabeled neurons at 2–3 months post-blast to represent neuron loss, as is routinely the case (Kordower et al., 2001; Shi et al., 2004; Unal-Cevik et al., 2004; Avramescu et al., 2009; Reiner et al., 2012; Zhang et al., 2015), although the possibility exists that the loss of immunolabeling could reflect neuronal dysfunction. To evaluate the impact of neuron loss/rescue on motor function, we used regression analysis to determine if neuron abundance was correlated with rotarod performance, as determined in the previously reported functional assessment at 2 weeks post-blast. Neuron counts for BLA were obtained from Thy1 reporter mice, which had not been tested for fearfulness, using separate one-in-six series of brain sections immunolabeled for NeuN, Thy1 (i.e. GFP) or PARV, and covered the full extent of rostral BLA.

RESULTS

Activation of CREB by SMM-189

As an inverse agonist, SMM-189 biases the CB2 receptor conformation to an inactive state (Presley et al., 2015), leading to phosphorylation of CREB, which, in turn, promotes transcription of M2 genes and represses transcription of M1 genes (Atwood et al., 2012). To examine the effects of SMM-189 on microglia in the brain, we immunolabeled for pCREB in conjunction with CD68 to visualize microglia. Confocal images from blast-alone mice 3 days after blast revealed no evident pCREB in the vast majority of microglia (>95%), with microglial cell bodies and nuclei confirmed as CD68+ and DAPI+. This was true for all brain regions examined, notably the BLA, the striatum and its major projection target, the substantia nigra pars reticulata (SNr), and for the axonal outflow of cerebral cortex in the internal capsule, as shown in **Figures 1**, **2**. By contrast, in mice 3 days after blast with daily SMM-189, most, if not all, microglia in

these brain regions were enriched in nuclear pCREB. Moreover, some microglia, notably in the internal capsule, had a rod-like morphology (**Figure 2C**). Some of the rod-like microglia were aligned parallel to axons in the internal capsule and some seemingly parallel to blood vessels. These rod-like microglia are reminiscent of microglia that become aligned along scratches in the tissue culture substratum, which are thought to correspond to an M2 state (Tam and Ma, 2014). Thus, SMM-189 acted on brain microglia as expected and consistent with its actions on microglia *in vitro* (Presley et al., 2015; Reiner et al., 2015).

Cortical and Striatal Neuron Loss after Mild TBI Is Rescued by SMM-189

Examination of cresyl violet or NeuN stained sections did not reveal any obvious foci of neuronal loss or generalized neuron loss in cerebral cortex or striatum on either side of the brain 2–3 months after a 50-psi blast (**Figure 3**). However, blinded stereological neuron counts showed a bilateral loss of about 20% of neurons in the cerebral cortex (left: $p = 0.025$; right: $p = 0.021$), and a bilateral loss of about 30% of striatal neurons (left: $p = 0.00048$; right: $p = 0.003$) in mice that had received 50-psi blasts compared to those that had received 0-psi blasts (**Figure 4A**). The overall volumes of the cerebral cortex and the striatum were slightly, but not significantly, less in mice with 50-psi blast than in sham mice (**Figure 4B**). Daily treatment with SMM-189 for the 2 weeks after blast significantly reduced the cortical and striatal neuron loss, by about 50% in both cases (**Figure 4A**). For cortex, neuron counts in SMM-189 treated mice with 50-psi blast were no longer significantly different than in the vehicle-treated sham blast mice (left: $p = 0.691$; right: $p = 0.745$), and trended toward being more than in vehicle-treated 50-psi mice (left: $p = 0.133$; right: $p = 0.103$). For left striatum, neuron counts in SMM-189 treated mice with 50-psi blast were significantly more than in vehicle-treated 50-psi mice (p=0.020), although they remained significantly less than in the vehicle-treated sham blast mice ($p = 0.015$). For right striatum as well, neuron counts in SMM-189 treated mice with 50-psi blast were significantly more than in vehicle-treated 50-psi mice ($p = 0.047$), but in this case they were also statistically indistinguishable from that in the vehicle-treated sham blast mice ($p = 0.094$).

We previously reported that blast resulted in impaired rotarod performance and that SMM-189 treatment produced partial rescue of this motor deficit (Reiner et al., 2015). We used regression analysis to examine the relationship between rotarod performance and the extent of neuronal loss and rescue, combining the data for all three groups of mice (i.e., sham mice, and the TBI mice, with and without SMM-189), as shown in **Figure 5**. We found that cortical neuron abundance for the two sides of the brain taken together was highly correlated with rotarod performance ($r = 0.6443$; $p = 0.032$). Similarly, striatal neuron abundance for both sides of the brain combined was also highly correlated with rotarod performance ($r = 0.5908$; $p = 0.047$). These results are consistent with the idea that the loss of cortical and striatal neurons contributed to the rotarod deficit produced by blast, and that their partial rescue by SMM-189 contributed to the partial rescue of rotarod performance.

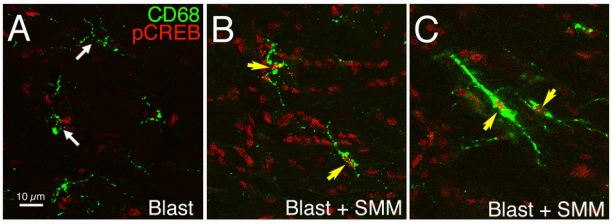

FIGURE 2 | Images showing the effect of SMM-189 treatment on pCREB expression in microglia in the left internal capsule after blast. Confocal images showing immunostaining for pCREB and CD68 in a blast alone mouse **(A)** compared to a SMM-189-treated blast mouse **(B,C)** at 3 days post blast. DAPI staining (not shown) was used to identify nuclei. The nuclei of all microglia lack prominent pCREB in the blast mouse (white arrows), but all are rich in pCREB in the SMM-189-treated mouse (yellow arrows). Note that some microglia exhibit prominent CD68 expression and a rod-like morphology **(C)** after SMM-189 treatment, and some of these are aligned parallel to axons descending from the cerebral cortex.

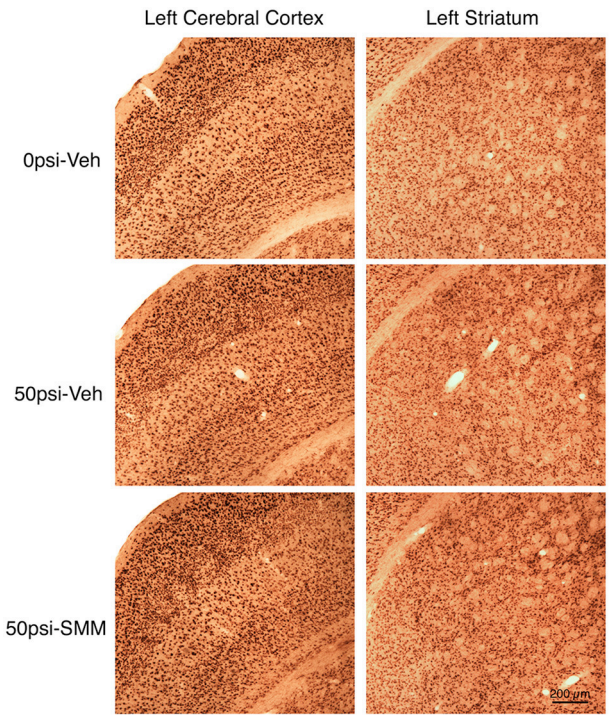

FIGURE 3 | Images showing the effect of TBI and SMM-189 on NeuN+ neurons in left cerebral cortex and striatum at 2–3 months post-blast. Neither focal nor diffuse neuron loss is evident in the 50-psi vehicle-treated cortex or striatum, compared to 0-psi vehicle-treated cortex and striatum. Similarly, the abundance of cortical and striatal neurons does not appear obviously different in the 50-psi SMM-189 treated mice from that in either of the other two groups. Magnification is the same for all panels. Stereology, nonetheless, revealed neuron loss in both in 50-psi vehicle-treated mice.

BLA Neuron Loss after TBI Is Rescued by SMM-189

BLA is composed primarily of Thy1+ and Thy1-negative pyramidal neurons, with several types of interneurons making

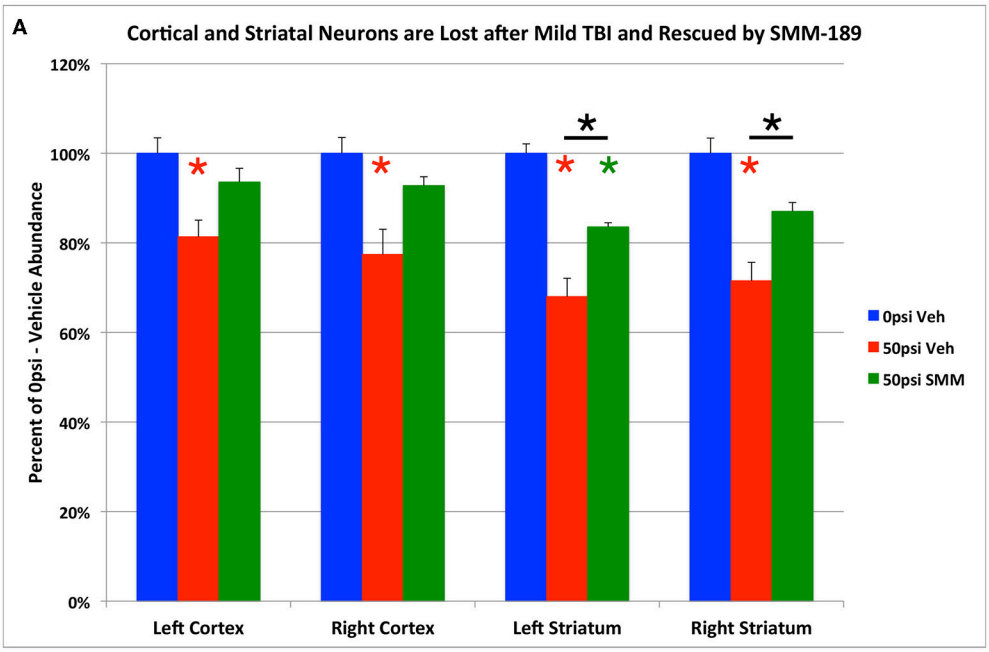

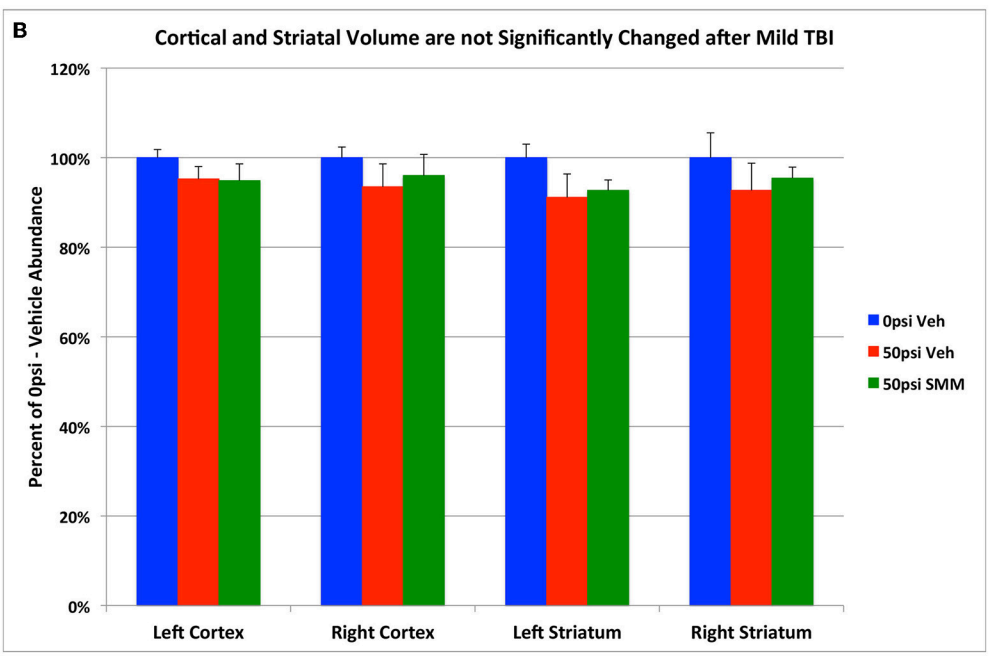

FIGURE 4 | Graphs showing the effect of TBI and SMM-189 on NeuN+ neurons (A) and on volumes (B) in cerebral cortex and striatum. Stereological counts **(A)** revealed bilateral neuron loss in the 50-psi vehicle-treated cortex and striatum, and significant rescue after SMM-189 treatment. Red asterisks indicate a significant difference between vehicle-treated 50-psi mice and vehicle-treated 0-psi mice. Green asterisks indicate a significant difference between SMM-189 and vehicle-treated 0-psi mice. Asterisks above bars spanning the SMM-189 and vehicle-treated 50-psi mice columns indicate a significant difference between these two conditions. No significant volume loss is evident in the 50-psi vehicle-treated cortex or striatum **(B)**, compared to 0-psi vehicle-treated cortex and striatum, although a trend toward reduction is seen.

up the remaining 10% of the total neuronal population. The Thy1+ pyramidal neurons and the PARV+ interneurons are both reported to play a role in suppressing fear (Myers et al., 2006; Herry et al., 2008; Heldt et al., 2012; Jasnow et al., 2013). For this reason, and because we had previously observed that mild TBI results in a loss of Thy1+ neurons (Reiner et al., 2015), in the present study we used stereological neuron counting methods to more fully analyze the effects of TBI and SMM-189 treatment on neuron-type specific pattern of loss in BLA. As a first step, we determined the relative abundance of

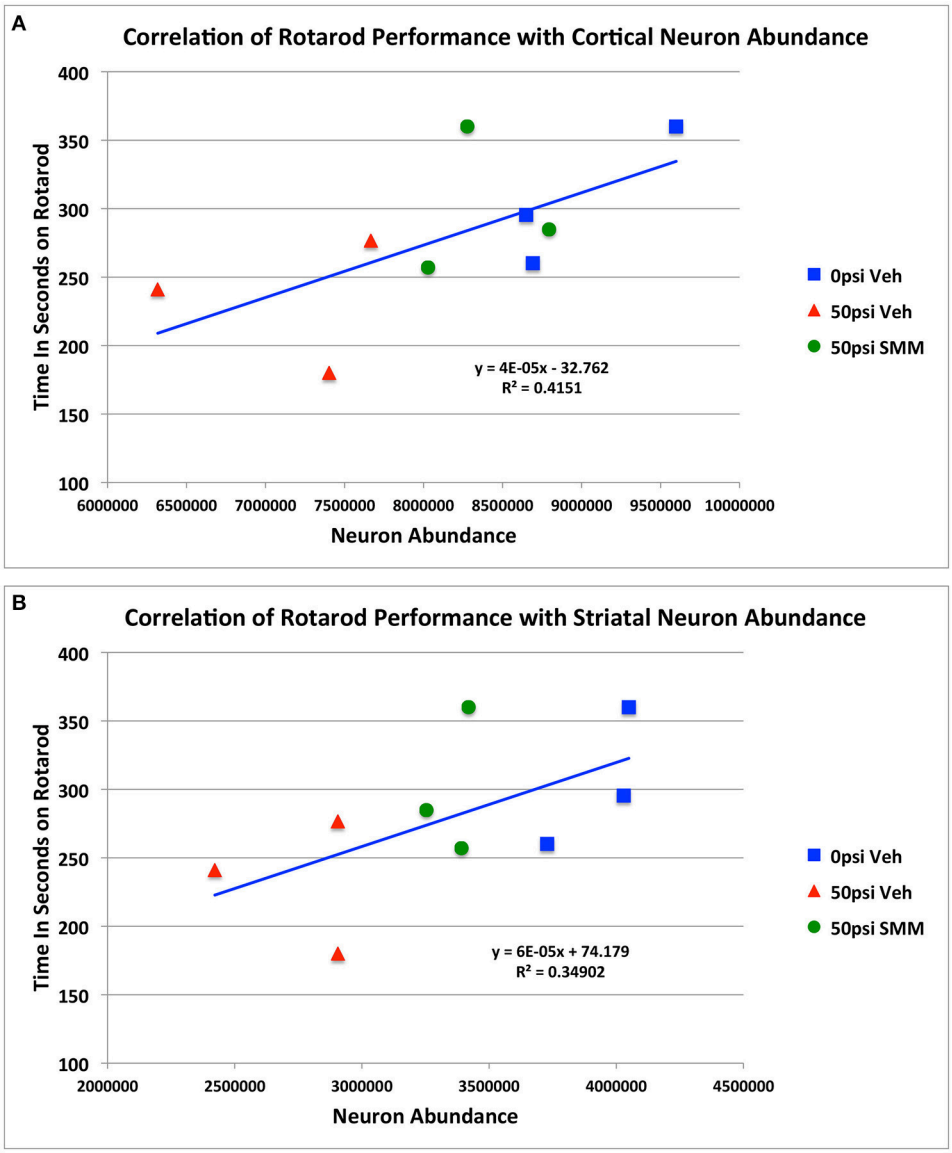

FIGURE 5 | Regression analysis showing the relationship between rotarod performance and the extent of cortical (A) and striatal (B) neuronal loss and rescue, combining the data for all three groups of mice.

several of the different major neuron types in BLA. Using a Thy1-EYFP reporter mouse to visualize the Thy1+ neurons, and immunostaining a separate series of sections for NeuN to visualize the total neuronal population, we found that 38.1% of BLA neurons are Thy1+ neurons. As pyramidal neurons are thought to make up about 90% of the total population of BLA neurons (Godavarthi et al., 2014; Wolff et al., 2014), this suggests that Thy1-poor pyramidal neurons constitute 51.9% of all BLA neurons (90–38.1%). We also found that 3.7% of all BLA neurons are PARV+. With interneurons representing about 10% of all BLA interneurons, 6.3% of BLA neurons must correspond to the separate interneuron types that contain somatostatin, cholecystokinin, or vasoactive intestinal polypeptide (Rainnie et al., 2006; Muller et al., 2007).

Blasts of 60-psi to the left side of the head resulted in 20.1% overall loss ($p = 0.000069$) of NeuN-immunostained neurons from the left BLA (**Figures 6A,B**, **7A**), with no significant change in the volume of left BLA. Thy1+ pyramidal neurons showed a 33.3% loss ($p = 0.000014$) in vehicle-treated 60-psi mice compared to vehicle-treated sham blast mice (**Figures 6D,E**, **7A**). Similarly, PARV+ interneurons showed a 42.1% neuron loss ($p = 0.00001$; **Figures 6G,H**, **7A**). As the Thy1+ pyramidal neurons and the PARV+ interneurons of BLA are involved in reduction and extinction of learned fear (Myers et al., 2006; Herry et al., 2008; Heldt et al., 2012; Jasnow et al., 2013), their loss is likely to contribute to the increased learned contextual fear and diminished fear extinction exhibited by mice that we had subjected to 50–60 psi blasts (Heldt et al.,

2014; Reiner et al., 2015). By contrast, the remaining neurons (i.e., Thy1-negative/PARV-negative), which largely constitute the Thy1-negative pyramidal neurons of BLA, showed only a small reduction that was not statistically significant (∼10% loss; $p = 0.109$; **Figure 7A**). Since the non-Thy1+ pyramidal neurons promote fear, their preferential preservation, together with the substantial loss of the Thy1-enriched fear-reducing pyramidal neurons may explain why TBI increases fear in our model (Haubensak et al., 2010; Herry and Johansen, 2014; Lüthi and Lüscher, 2014).

We found that SMM-189 treatment significantly rescued the TBI-related loss of both Thy1+ neurons and PARV+ interneurons, returning these to 80.3 and to 82.4% of sham abundance, respectively (**Figures 6D–I**, **7A**). The abundance of Thy1+ BLA neurons in SMM-189 treated 60-psi mice was significantly greater than in vehicle-treated 60-psi mice ($p = 0.010$), although it remained less than in vehicle-treated 0-psi mice ($p = 0.001$). Similarly, the abundance of PARV+ BLA neurons in SMM-189 treated 60-psi mice was greater than in vehicle-treated 60-psi mice ($p = 0.005$), but still less than in vehicle-treated 0-psi mice ($p = 0.034$). SMM-189 trended toward rescue of overall BLA neuron loss, as reflected in the NeuN immunolabeling (**Figures 6A–C**), reducing it from 79.9% to 87.2% ($p = 0.054842$). By contrast, with SMM-189 treatment, the Thy1-negative/PARV-negative BLA neurons were found to be 92.0% of sham-vehicle abundance—not significantly more than in vehicle-treated 60-psi mice ($p = 1.000$), nor significantly less than in vehicle-treated 0-psi mice ($p = 0.240$; **Figure 7A**).

In contrast to left BLA, no significant loss was observed in the right BLA for the Thy1+ neurons ($p = 1.000$), the PARV+ neurons ($p = 1.000$), or the Thy1-negative/PARV-negative NeuN neurons ($p = 0.611$; **Figure 7B**), or for right BLA volume as measured in the sections used for Thy1, PARV or NeuN neuron counts. Finally, the abundance of each of these three neuron types in right BLA did not differ significantly between SMM-189 treated blast mice and the sham mice.

DISCUSSION

Neuronal Loss with TBI

Cerebral Cortex and Striatum

We have previously reported that our model of mild TBI produces diffuse axonal injury, as evidenced by the presence of swollen axonal bulbs at a few days, and degenerating axons at 1–2 weeks after blast (Heldt et al., 2014; Guley et al., 2016). As in humans and in other animal models of TBI (Petras et al., 1997; Shitaka et al., 2001; Koliatsos et al., 2011; MacDonald et al., 2011; Johnson et al., 2013; Morey et al., 2013; Xu et al., 2016), damaged axons were most prevalent in the major white fiber tracts, where their parallel arrangement is thought to make them especially vulnerable to breakage by the stretch and shear forces produced when the blast pressure wave is conducted through the brain parenchyma (Smith et al., 2013b). In turn, this widespread axonal damage may contribute to the apparently diffuse loss of neurons we report here for the cerebral cortex and striatum, as well as to the neuron loss and atrophy observed in cortex and striatum after closed-head TBI in humans (Wilde et al., 2007; Maxwell et al., 2010; Leunissen et al., 2014) and after mild TBI in animal models (Smith et al., 1997; Cho et al., 2013; Sajja et al., 2013; Goddeyne et al., 2015). The observed neuronal loss in our study was not obviously localized to a restricted region and was not evident without stereological neuron counts. It thus seems unlikely that neuronal loss occurred disproportionately in a particular region (e.g., frontal, visual, somatosensory, motor, or medial vs. lateral) or layer of cerebral cortex, or in a particular region or compartment of the striatum. However, additional analysis and the use of cell-type specific markers would be required to determine if there was any loss of interneurons and/or any preferential loss of a specific subpopulation(s) of projection neurons from cortex or striatum (Reiner et al., 1998; Hattox and Nelson, 2007; DeFelipe et al., 2013; Deng et al., 2015). Prior studies have reported that projection neurons in cortex and striatum are vulnerable to TBI (Maxwell et al., 2010; Bales et al., 2011), but interneurons, at least those in the hippocampus, have been reported to also be vulnerable to TBI (Lowenstein et al., 1992; Hicks et al., 1993; Smith et al., 1997; Tsuda et al., 2016).

The loss of neurons in the cerebral cortex and striatum was not only seemingly distributed throughout each, but also was similar in extent for the two sides of the brain. It may be that the bilateral neuronal loss stems from bilateral axonal injury, as both cortex and striatum are composed primarily of projection neurons possessing long axons, which travel in the corpus callosum or pyramidal tract and in the ansa lenticularis or striatonigral tract, respectively (Reiner et al., 1998; Hattox and Nelson, 2007; Deng et al., 2015). The fact that the pyramidal tract, ansa lenticularis and striatonigral tract are juxtaposed at their entry into the thalamus and midbrain may make their axons subject to similar tensile and shear forces at this level of the brain, and thus bilaterally vulnerable. A possible reason for the greater extent of neuron loss we find for the striatum as compared to cortex (∼30 vs. ∼20%) may relate to the higher proportion of projection neurons in the striatum (∼95%) as compared to the cerebral cortex (∼80%) (Peters et al., 1985; Reiner et al., 1998; Bartolini et al., 2013), with all striatal projection neurons, but only about half of all cortical projection neurons, having axons that follow a longitudinal trajectory in the brain. Longitudinally running axons appear to be more susceptible to damage in our TBI model, in that we observed axonal bulbs and silver-stained degenerating axons more frequently in the pyramidal and optic tracts than in the corpus callosum (Heldt et al., 2014; Guley et al., 2016). Similarly, the pyramidal and optic tracts are especially vulnerable to axonal injury with closed skull impact TBI, for example the Marmarou impact acceleration approach, which also subjects axons to stretch and shear forces (Kallakuri et al., 2012; Zakaria et al., 2012). Based on published computer models of TBI biomechanics (Taylor and Ford, 2009; Laksari et al., 2014), the blast wave created using our system would be expected to also compress the brain, first on the targeted left side and then on the contrecoup side as the brain moves within the skull, and this may further contribute to the generalized bilateral neuron loss we found. Relatively little is known, however, about the long-term deleterious consequences of compressive forces on axons and neuronal cell bodies (Meaney and Smith, 2011).

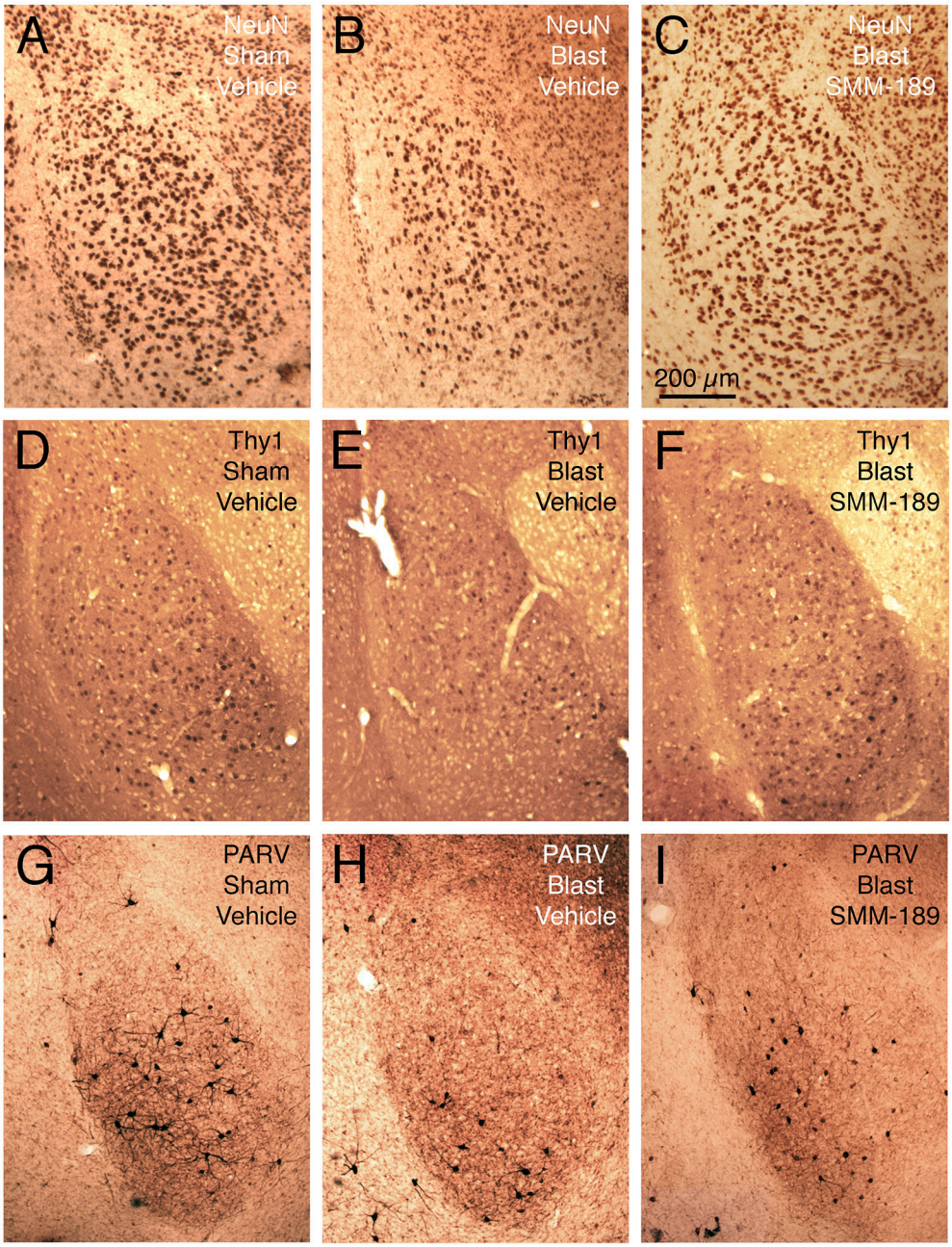

FIGURE 6 | Images showing the effect of TBI and SMM-189 on NeuN+ neurons in left BLA (A–C), on Thy1+ fear-suppressing pyramidal neurons in left BLA in a Thy1-EYFP reporter mouse (D–F), and on PARV+ interneurons in left BLA (G–I). A reduction in NeuN+ neurons is seen in the 60-psi blast mice (**B** compared to **A**), which trended toward being rescued by SMM-189 treatment **(C)**. Similarly, Thy1+ neurons of left BLA are reduced in the 60-psi blast mice **(E)**, and rescued in the SMM-189 treated 60-psi blast mice **(F)**, as also true for the PARV+ neurons of left BLA **(G–I)**. Medial is to the right and magnification is the same in all images.

It should be noted that we previously reported an ∼10% loss of axons in the dorsal corticospinal (CST) axons at thoracic spinal cord levels on the right side as compared to the left side following left side cranial blast (Guley et al., 2016). We also observed an asymmetry in signs of axonal injury along the descending pyramidal tracts at the level of the pons, with more on the left side (Guley et al., 2016). As axons arising from corticospinal motoneurons (CSMNs) on the left side of the brain cross the midline at the spinomedullary junction, the results for CST axons might suggest that damage was limited to the left side of motor cortex, and at first glance, appear to contradict the bilateral loss of cortical neurons reported here. However, our analysis of axon loss, which compared the areas of axons immunostained for protein kinase C gamma on the two sides, would not rule out the

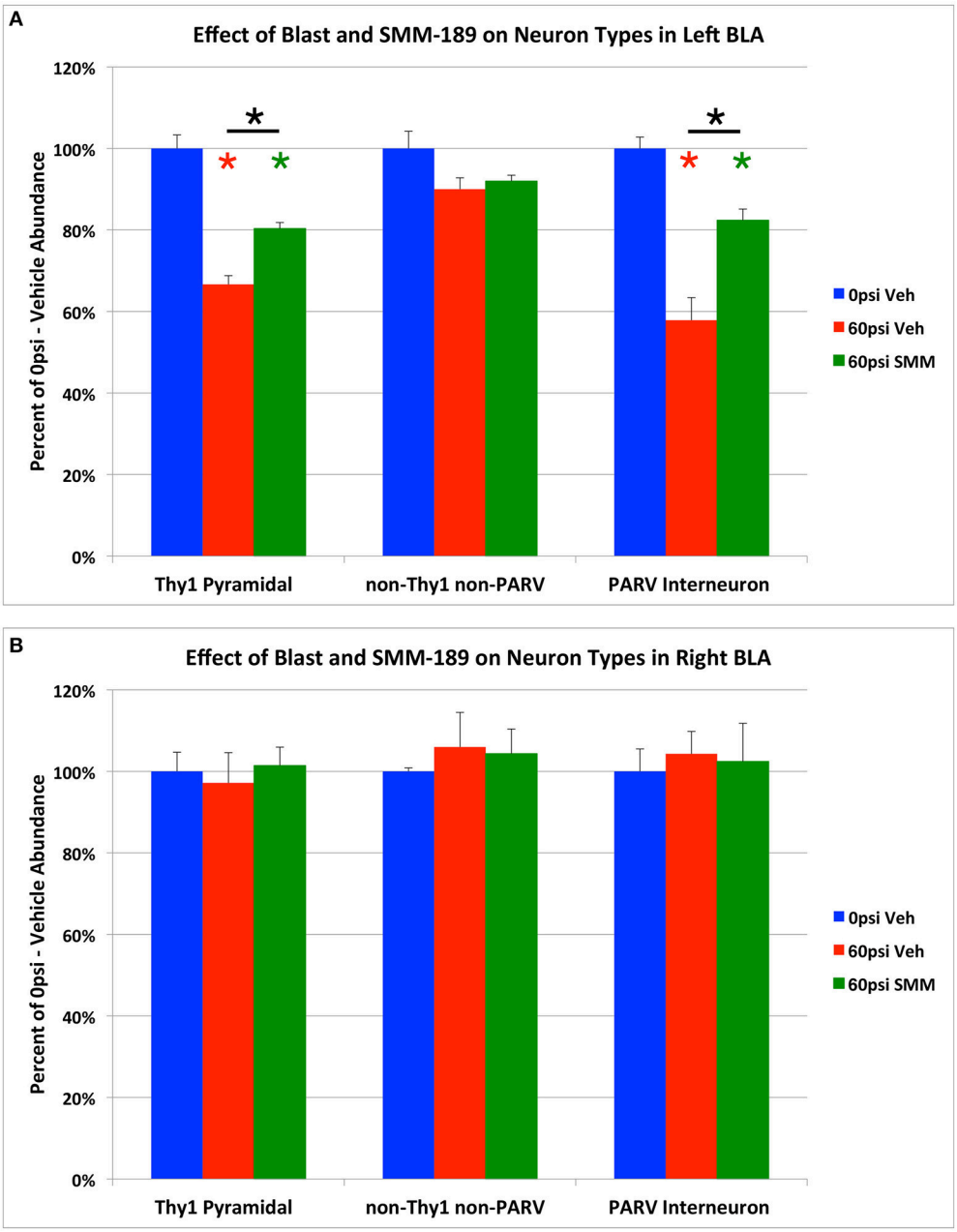

FIGURE 7 | Graphs showing the effect of TBI and SMM-189 on neuron types in left BLA (A), and in right BLA (B). Thy1+ pyramidal neurons and PARV+ interneurons are decreased in number in the left BLA of 60-psi blast mice, and are both rescued in the SMM-189 treated mice. By contrast, there was no significant change in the non-Thy1/non-PARV neurons of left BLA (which are mainly fear-promoting pyramidal neurons) of BLA after TBI. Red asterisks indicate a significant difference between vehicle-treated 60-psi mice and vehicle-treated 0-psi mice. Green asterisks indicate a significant difference between SMM-189 and vehicle-treated 0-psi mice. Asterisks above bars spanning the SMM-189 and vehicle-treated 60-psi mice columns indicate a significant difference between these two conditions. No significant changes in Thy1+ pyramidal neurons, PARV+ inhibitory interneurons, or non-Thy1/non-PARV neurons were seen for the right BLA following TBI, with or without treatment **(B)**.

possibility that CST axons on the left side of the spinal cord were also lost, just that loss was greater for the right side. Moreover, CSMNs are estimated to comprise less than 5% of the neurons in motor cortex (Özdinler et al., 2011) and so a preferential loss of CSMNs from left but not right motor cortex, would not significantly affect the overall cortical counts reported here.

The injury produced in our blast model is classified as mild TBI, based on the absence of obvious contusion or hemorrhaging, the rapidity with which animals awaken from anesthesia after TBI, and the absence of any post-TBI torpor. It thus is surprising to find that 20–30% of neurons had been lost by 2–3 months after the injury. Few other studies of mild TBI have, however,

examined this issue. Although some published reports have shown dying neurons by immunolabeling for activated caspase, or staining using fluorojade or TUNEL (e.g., Raghupathi et al., 2002; Longhi et al., 2005; Sajja et al., 2015), these approaches do not provide information about the ultimate extent of neuronal loss. Further, in many cases, histological examination of the brain has been limited to 10 days or less after the TBI event. The main exceptions are several studies in which researchers, having observed extensive axonal injury in the optic tract and nerve, have then counted surviving retinal ganglion cells (Tzekov et al., 2014; Xu et al., 2016). For example, Xu et al. (2016) reported 30% retinal ganglion cell loss by 10 weeks after impact TBI. Interestingly this is similar to the amount of loss we found for the striatum, with its 95% complement of projection neurons, and is consistent with observations that the majority of axons are not injured by mild TBI. Other studies have shown substantial cortical thinning, striatal atrophy, and up to 40% hippocampal neuron loss as long-term consequences of contusive cortical injury (Baldwin et al., 1997; Smith et al., 1997). This type of TBI is, however, severe in that the skull is open and the exposed dura is impacted. Thus, to the best of our knowledge, no studies other than our own have examined the consequence of mild TBI for neuron loss in the brain. It may be that the 20–30% loss we observed occurs over a time frame of several weeks and that diffuse neuron loss goes undetected unless stereological analysis is performed.

Basolateral Amygdala

Neuronal loss in BLA varied in several ways from that in cerebral cortex and striatum. Most strikingly, it was limited to the targeted side of the brain rather than occurring bilaterally. BLA is situated slightly deep and anterior to the center of the area targeted by the blast region, which corresponds to the thalamus. The presence of the fluid-filled lateral and third ventricles at this level may alter the transmission of tensile, shear, and compressive forces from one side of the brain to the other, and may thereby "protect" deeper neural structures such as the amygdala on the non-blast side, as may also the transverse course of its efferent axons (Gupta and Przekwas, 2013). In addition, the left BLA neuron loss involved 33.3% reduction in one population of pyramidal projection neurons (Thy1+) but no significant loss in the other major population of BLA pyramidal projection neurons (i.e., the Thy1-negative), as well as a 42.1% loss of PARV interneurons. The present results are consistent with our prior report of Thy1 neuron loss in BLA after mild TBI (Heldt et al., 2014; Reiner et al., 2015), and with reports of GABAergic neuron loss from BLA after controlled cortical impact TBI (Almeida-Suhett et al., 2014). Although we did not observe neuron loss in the right BLA, it is nonetheless possible that functional changes occurred in Thy1 and PARV neurons in right BLA, given that neurons can be dysfunctional after brain injury or in neurodegenerative diseases, in the absence of or prior to overt neuron loss (Cohen et al., 2007; Smith et al., 2013a; Deng et al., 2014).

Mechanisms of Neuron Loss

Taken together, our results for cortex and striatum suggest that axonal injury may contribute to subsequent neuron death after TBI, whereas our results for PARV+ interneurons of BLA indicate that axonal injury is not necessary for neuronal loss for at least some neuron types in our model. Moreover, the basis of the differential vulnerability of Thy1+ vs. Thy1-negative pyramidal neurons of left BLA is uncertain, as both send axons to the nearby central amygdala, as well as more distantly to the medial prefrontal cortex (Lüthi and Lüscher, 2014). A variety of cellular characteristics confer susceptibility to neuronal death after trauma, for example, a limited ability to buffer calcium or a high vulnerability to excitotoxic or oxidative injury (McGinn and Povlishock, 2015; Jayakumar et al., 2016; Tovar-y-Romo et al., 2016). In addition, neuroinflammation often has detrimental effects in the aftermath of TBI (Brown and Vilalta, 2015; Loane and Kumar, 2016) and is likely to contribute to the neuron loss we find here. Consistent with this possibility, neuron loss appears to be progressive in our model, as we previously found ∼12% cortical neuron loss at 45 days after blast (Guley et al., 2016), as compared to the ∼20% loss at 2–3 months post-blast reported here. We do not know if cortical and/or striatal neurons continue to die beyond the 3-month time point and, if so, at what rate. Moreover, we do we know if neuronal death occurs and is progressive in other regions as well. The additional loss of ∼8% of cortical neurons between 6 and 10 weeks after the initial traumatic event cannot readily be explained by damage to the neurons themselves. Moreover, as will be discussed in more detail below, that SMM-189 treatment rescued roughly half of the neurons that would have otherwise been lost, suggests that the rescued neurons died as consequence of neuroinflammatory processes. It is possible that yet more neurons may be capable of rescue, since we do not know if the dose or timing of SMM-189 treatment we used could be further optimized.

Neuronal Loss and Rescue in Cerebral Cortex and Striatum and Relation to Motor Deficits

The neuronal loss we find in cerebral cortex and striatum at 3–4 months is correlated with the rotarod deficits these mice exhibited at 2 weeks post blast (Guley et al., 2016), indicating that the injury severity in the 2 weeks after blast and its rescue with SMM-189 predict the deficits and ultimate neuron loss. Consistent with this, treatment for 2 weeks after blast with the CB2 inverse agonist SMM-189 rescues about half the total number of cortical and striatal neurons that would have otherwise died, and significantly reduces rotarod deficits (Reiner et al., 2015). Whether the rescue of cortical neurons with SMM-189 treatment is the cause or consequence of the rescue of CST axons that we previously reported (Reiner et al., 2015) is uncertain. The present results extend on our prior findings, in that they show that rescue of sensorimotor deficits causing impaired rotarod performance may be due to the preservation of cortical and striatal neurons. Much of the area of the cortex for which counts were obtained corresponds to somatosensory and motor regions and staying on rotarod requires sensory-motor coordination. Similarly, the correlation of striatal neuron abundance with rotarod performance is consistent with role of striatum, as it is important in movement

initiation, action sequence coordination, and motor learning (Deng et al., 2015; Yttri and Dudman, 2016). It is likely that TBI in our model produces cortical neuron loss throughout the entire cortex and deficits in functions that we have not assayed, such as in somesthesis, audition, and memory. Consistent with this, we have detected electrophysiological abnormalities in prefrontal cortex, hippocampus, visual cortex and somatosensory cortex as early as 1 month after blast (Liu et al., 2016). Whether deficits in memory and in sensory modalities other than vision occur after blast in our model and are also rescued by SMM-189 treatment requires further study.

Neuronal Loss and Rescue in BLA and Relation to Fearfulness

We previously reported that mild TBI with our model causes an increase in fearfulness as assessed in an auditory fear conditioning paradigm, as well as a reduction in the Thy1+ neurons of BLA (as determined from confocal microscopy), and that both are rescued with SMM-189 treatment (Reiner et al., 2015). The increased fearfulness manifests as both an increase in freezing (freezing being the standard indicator of fear in rodents) to a learned auditory fear stimulus that signals impending shock, and an enhancement of contextual fear when the mice are placed in the fear-training chamber (Heldt et al., 2014). Moreover, the TBI mice exhibit greater resistance to extinction of the learned fear, in that more extinction trials are needed to extinguish the learned fear response than is the case for sham blast mice. The fear is perseverative and progressive, as contextual fear persists and learned fear is even more resistant to extinction in TBI mice at 1 year after blast (Heck et al., 2015). In the present study, stereological neuron counts showed a 33.3% loss of the Thy1+ fear-suppressing pyramidal neurons and a 42.1% loss of PARV+ fear-suppressing interneurons in BLA, but no significant loss of the fear-promoting Thy1-negative pyramidal neurons of BLA. Together, these findings help explain the increased fearfulness occurring in our TBI model, as preferential loss of fear-suppressing neurons should lead to increased fear responses. Moreover, SMM-189 treatment significantly reduced the Thy1 and PARV neuron loss in BLA, with the rescue of these neuron types most likely representing the means by which SMM-189 reduces post-TBI fearfulness.

The amygdala contributes to fear via the interplay of three cell groups, BLA, the lateral anterior nucleus (LA), and the central nucleus (CeA) (**Figure 8**; Ehrlich et al., 2009; Ciocchi et al., 2010; Morozov et al., 2011; Janak and Tye, 2015). The LA and BLA each contain about 90% excitatory pyramidal neurons and about 10% GABAergic inhibitory interneurons. The CeA consists mainly of GABAergic inhibitory neurons, some of which are projection neurons while others are local circuit neurons. Fear associations are learned by LA neurons via their inputs from sensory and pain regions. Learned fear is then signaled to BLA neurons that activate an intrinsic fear circuit in the CeA that provides output to various brainstem sites mediating the affective, autonomic and motor components of fear behavior. This fear output from BLA appears to occur via Thy1-negative pyramidal neurons that receive input from LA neurons that learn to associate a neutral stimulus with a given aversive event. These Thy1-negative fear-promoting neurons in BLA project to GABAergic neurons of CeA that promote fear (Herry et al., 2008; Haubensak et al., 2010; Jasnow et al., 2013; Herry and Johansen, 2014; Lüthi and Lüscher, 2014). By contrast, the Thy1-enriched pyramidal neurons in BLA suppress fear and project to CeA neurons that suppress fear. BLA in rodents appears to receive its main excitatory drive via cortical inputs from different parts of the ventral medial prefrontal cortex (mPFC), which is specialized for the integration of emotional states with environmental stimuli. Projections from the fear-promoting prelimbic part of mPFC mainly target the fear-promoting pyramidal BLA neurons, while the fear-reducing infralimbic part of mPFC targets fear-suppressing pyramidal neurons and GABAergic inhibitory BLA interneurons (Rosenkranz and Grace, 2001; Paré et al., 2004; Herry et al., 2008; Jasnow et al., 2013). To better understand how mild TBI increases fearfulness, and how SMM-189 rescues this deficit, it would be valuable to know how the inputs from the prelimbic and infralimbic parts of mPFC, as well as the input from ventral hippocampus, to BLA are affected by mild TBI.

The BLA contains four major types of GABAergic inhibitory interneurons constituting about 10% of its total neuronal population - a parvalbuminergic (PARV) type, a somatostatinergic (SST) type, a large-sized type containing cholecystokinin (CCK), and a small-sized type containing vasoactive intestinal polypeptide (VIP) (Rainnie et al., 2006;

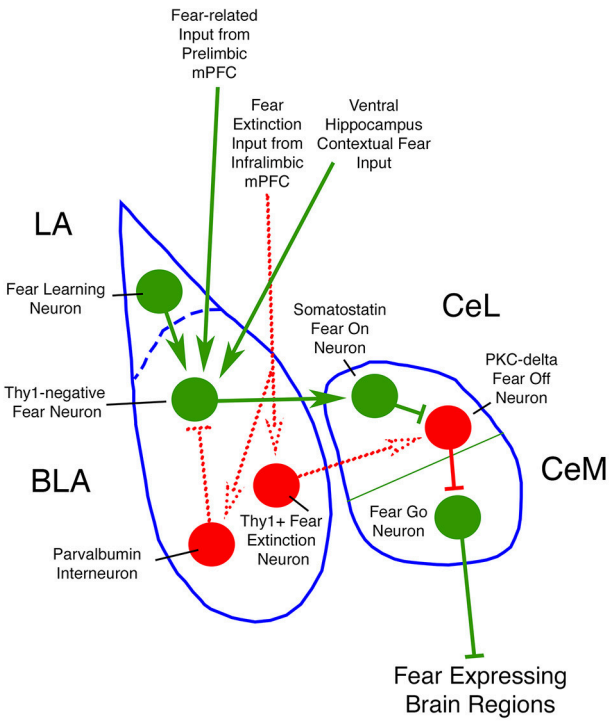

FIGURE 8 | Circuit diagram of neuron types of amygdala of interest to the present study. Neurons and inputs shown in green promote fear, while those shown in red reduce fear. Dotted lines represent connections that are less firmly established in the literature than are the connections shown by solid lines.

Muller et al., 2007). The PARV interneurons primarily target pyramidal BLA neurons, making up half of their inhibitory input (Muller et al., 2006; Wolff et al., 2014), with the other types of interneurons providing the other half (Mascagni and McDonald, 2003; Muller et al., 2003, 2007). Both the PARV interneurons (Godavarthi et al., 2014; Wolff et al., 2014) and the CCK interneurons (Truitt et al., 2009) appear to reduce fear and anxiety, while the SST interneurons appear to increase fear (Wolff et al., 2014). One simple way in which PARV and CCK interneurons may reduce fear and anxiety, and SST neurons may increase fear, is if the PARV and CCK interneurons preferentially innervate the Thy1-negative fear-promoting BLA neurons, and SST interneurons preferentially innervate the Thy1-rich fear suppressing neurons of BLA. Future studies will be needed to characterize the connectivity of these other interneuron types with pyramidal neurons, and to determine how each type is affected by mild TBI, to more fully understand how mild TBI increases fearfulness, and how SMM-189 treatment produces its rescue of fearfulness.

Microglial Activation and SMM-189 Therapy

We previously showed that the axonal injury in major fiber tracts resulting from blast in our TBI model is accompanied by microglial activation along those fiber tracts and in brain regions where the damaged axons terminate (Guley et al., 2016). It is known that injured axons and their myelin sheaths release molecules that can bind to damage-associated molecular pattern molecule receptors, which include Toll-like receptors expressed on microglia, thereby activating them (Kumar and Loane, 2012). The activated microglia then typically release pro-inflammatory factors that have toxic effects on nearby neurons, may help recruit other immune cells to the region, and can compromise the integrity of the blood-brain barrier, leaving the central nervous system vulnerable to molecules in the systemic circulation (Brown and Vilalta, 2015; Loane and Kumar, 2016). Thus, an initial injury has the potential to lead to a continuing cascade of deleterious effects. Our present finding that blast TBI yields substantial neuron loss in cortex, striatum, and amygdala thus indicates that the initial trauma and the cascade it initiates leads not only to axonal injury but also neuron loss, perhaps in some cases secondary to axonal injury.

The rapid upregulation of CB2 by microglia after TBI allows them to be specifically targeted by SMM-189 for therapeutic purposes. Our prior *in vitro* analysis has shown that SMM-189 biases microglia from a pro-inflammatory M1 phenotype to a pro-healing M2 phenotype (Presley et al., 2015; Reiner et al., 2015). In addition, we have previously shown that treatment with SMM-189 reduces microglial activation in the right optic tract and retina, as assessed with IBA1 immunolabeling, and biases microglia away from the M1 state toward the M2 state, as indicated by increased pCREB immunolabeling (Reiner et al., 2015; Guley et al., 2016). In the present study, we have extended this observation to several additional brain regions, including BLA, the striatum, the terminal projection field of the striatum in the substantia nigra pars reticulata, and the white matter tract passing from cerebral cortex to brainstem. In all cases, microglia in these regions in blast-only mice rarely possessed evident nuclear pCREB, whereas in the SMM-189-treated mice, all the microglia showed prominent nuclear pCREB staining. Interestingly, the CD68 immunolabeling revealed some rod-like microglia in the internal capsule in mice with blast plus SMM-189, all with prominent nuclear pCREB. The presence of rod-like microglia is of interest because we have previously shown that SMM-189 promotes a rod-like morphology in microglia *in vitro* (Presley et al., 2015). Moreover, others have demonstrated that rod-shaped microglia show increased M2 marker expression after stable alignment with their substrate (Tam and Ma, 2014), suggesting that such microglia play a role in repairing nervous system damage.

Overall then, our results show that SMM-189 acts on brain microglia and biases them to the beneficial M2 state in the brain regions (and/or their fiber tracts) where SMM-189 rescues TBI-related neuron loss. Our present finding that SMM-189 treatment for the 2 weeks after blast yields substantial neuron rescue in cortex, striatum, and amygdala thus indicates that M1 microglial activation during the aftermath of mild TBI worsens the outcome, and that biasing toward M2 microglial activation during this same time period allows the survival of many of the neurons that would have otherwise died. It is likely that the observed neuronal rescue contributed to the reduction of motor deficits and fearfulness that mild TBI normally produces. Note that treatment with a CB2 agonist instead would reduce M1 activation but not promote M2 activation, which may explain why CB2 agonists have not consistently shown strong benefit in treating TBI (Mechoulam et al., 2002; Meyer et al., 2010; Elliott et al., 2011; Amenta et al., 2012, 2014; Firsching et al., 2012). Our results thus support further testing of CB2 inverse agonists as a useful therapeutic approach for reducing neural injury and functional deficits after mild TBI. It is possible that further optimization of dosage and timing would produce even greater benefit than we found here and that there is a critical time window during which treatment would be most effective. It will also be important to extend testing the efficacy of SMM-189 to additional neuronal populations and functions in our TBI model, as well as determine its usefulness in other TBI models.

AUTHOR CONTRIBUTIONS

WB, HR, YD, ND, and NG carried out research. BM developed, characterized and provided SMM-189. WB, HR, YD, MH, and AR analyzed data. BM, MH, and AR wrote the manuscript.

FUNDING

Supported by the Neuroscience Institute and the Office of the Dean of the College of Medicine, both at UTHSC, The Methodist Hospitals Endowed Professorship in Neuroscience (AR), NIH grant NS-081370 (AR), and the College of Pharmacy at UTHSC (BM).

ACKNOWLEDGMENTS

We thank Marion Joni, Rhonda Williams, and Josh Rogers for technical assistance.

REFERENCES

Almeida-Suhett, C. P., Prager, E. M., Pidoplichko, V., Figueiredo, T. H., Marini, A. M., Li, Z., et al. (2014). Reduced GABAergic inhibition in the basolateral amygdala and the development of anxiety-like behaviors after mild traumatic brain injury. *PLoS ONE* 9:e102627. doi: 10.1371/journal.pone.0102627

Amenta, P. S., Jallo, J. A., Tuma, R. F., Hooper, D. C., and Elliott, M. B. (2014). Cannabinoid receptor type-2 stimulation, blockade, and deletion alter the vascular inflammatory responses to traumatic brain injury. *J. Neuroinflammation* 11, 191. doi: 10.1186/s12974-014-0191-6

Amenta, P. S., Jallo, J. I., Tuma, R. F., and Elliott, M. B. (2012). A cannabinoid type-2 receptor agonist attenuates blood-brain barrier damage and neurodegeneration in a murine model of traumatic brain injury. *J. Neurosci.* 90, 2293–2305. doi: 10.1002/jnr.23114

Ashton, J. C., and Glass, M. (2007). The cannabinoid CB_2 receptor as a target for inflammation-dependent neurodegeneration. *Curr. Neuropharmacol.* 5, 73–80. doi: 10.2174/157015907780866884

Atwood, B. K., Straiker, A., and Mackie, K. (2012). CB_2 therapeutic target-in-waiting. *Prog. Neuropsychopharmacol. Biol. Psychiat.* 38, 16–20. doi: 10.1016/j.pnpbp.2011.12.001

Avramescu, S., Nita, D. A., and Timofeev, I. (2009). Neocortical post-traumatic epileptogenesis is associated with loss of GABAergic neurons. *J. Neurotrauma* 26, 799–812. doi: 10.1089/neu.2008.0739

Baek, J. H., Darlington, C. L., Smith, P. F., and Ashton, J. C. (2013). Antibody testing for brain immunohistochemistry: brain immunolabeling for the cannabinoid CB_2, receptor. *J. Neurosci. Methods* 216, 87–95. doi: 10.1016/j.jneumeth.2013.03.021

Baldwin, S. A., Gibson, T., Callihan, C. T., Sullivan, P. G., Palmer, E., and Scheff, S. W. (1997). Neuronal cell loss in the CA3 subfield of the hippocampus following cortical contusion utilizing the optical disector method for cell counting. *J. Neurotrauma* 14, 385–398. doi: 10.1089/neu.1997.14.385

Bales, J. W., Yan, H. Q., Ma, X., Li, Y., Samarasinghe, R., and Dixon, C. E. (2011). The dopamine and cAMP regulated phosphoprotein, 32 kDa (DARPP-32) signaling pathway: a novel therapeutic target in traumatic brain injury. *Exp. Neurol.* 229, 300–307. doi: 10.1016/j.expneurol.2011.02.013

Bareyre, F. M., Kerschensteiner, M., Misgeld, T., and Sanes, J. R. (2005). Transgenic labeling of the corticospinal tract for monitoring axonal responses to spinal cord injury. *Nat. Med.* 11, 1355–1360. doi: 10.1038/nm1331

Bartolini, G., Ciceri, G., and Marín, O. (2013). Integration of GABAergic interneurons into cortical cell assemblies: lessons from embryos and adults. *Neuron* 79, 849–864. doi: 10.1016/j.neuron.2013.08.014

Bazarian, J. J., Donnelly, K., Peterson, D. R., Warner, G. C., Zhu, T., and Zhong, J. (2013). The relation between posttraumatic stress disorder and mild traumatic brain injury acquired during operations Enduring Freedom and Iraqi Freedom. *J. Head Trauma Rehabil.* 28, 1–12. doi: 10.1097/HTR.0b013e318256d3d3

Benito, C., Nú-ez, E., Tolón, R. M., Carrier, E. J., Rábano, A., Hillard, C. J., et al. (2003). Cannabinoid CB_2 receptors and fatty acid amide hydrolase are selectively overexpressed in neuritic plaque-associated glia in Alzheimer's disease brains. *J. Neurosci.* 23, 11136–11141.

Brown, G. C., and Vilalta, A. (2015). How microglia kill neurons. *Brain Res.* 1628(Pt B), 288–297. doi: 10.1016/j.brainres.2015.08.031

Cao, T., Thomas, T. C., Ziebell, J. M., Pauly, J. R., and Lifshitz, J. (2012). Morphological and genetic activation of microglia after diffuse traumatic brain injury in the rat. *Neuroscience* 225, 65–75. doi: 10.1016/j.neuroscience.2012.08.058

Cherry, J. D., Olschowka, J. A., and O'Banion, M. K. (2014). Neuroinflammation and M2 microglia: the good, the bad, and the inflamed. *J. Neuroinflammation* 11:98. doi: 10.1186/1742-2094-11-98

Cho, H. J., Sajja, V. S., Vandevord, P. J., and Lee, Y. W. (2013). Blast induces oxidative stress, inflammation, neuronal loss and subsequent short-term memory impairment in rats. *Neuroscience* 253, 9–20. doi: 10.1016/j.neuroscience.2013.08.037

Ciocchi, S., Herry, C., Grenier, F., Wolff, S. B., Letzkus, J. J., Vlachos, I., et al. (2010). Encoding of conditioned fear in central amygdala inhibitory circuits. *Nature* 468, 277–282. doi: 10.1038/nature09559

Cohen, A. S., Pfister, B. J., Schwarzbach, E., Grady, M. S., Goforth, P. B., and Satin, L. S. (2007). Injury-induced alterations in CNS electrophysiology. *Prog. Brain Res.* 161, 143–169. doi: 10.1016/S0079-6123(06)61010-8

Das, M., Mohapatra, S., and Mohapatra, S. S. (2012). New perspectives on central and peripheral immune responses to acute traumatic brain injury. *J. Neuroinflammation* 9:236. doi: 10.1186/1742-2094-9-236

DeFelipe, J., López-Cruz, P. L., Benavides-Piccione, R., Bielza, C., Larra-aga, P., Anderson, S., et al. (2013). New insights into the classification and nomenclature of cortical GABAergic interneurons. *Nat. Rev. Neurosci.* 14, 202–216. doi: 10.1038/nrn3444

Deng, Y., Lanciego, J., Goff, L. K., Coulon, P., Salin, P., Kachidian, P., et al. (2015). Differential organization of cortical inputs to striatal projection neurons of the matrix compartment in rats. *Front. Syst. Neurosci.* 9:51. doi: 10.3389/fnsys.2015.00051

Deng, Y. P., Xie, J. P., Wang, H. B., Lei, W. L., Chen, Q., and Reiner, A. (2007). Differential localization of the GluR1 and GluR2 subunits of the AMPA-type glutamate receptor among striatal neuron types in rats. *J. Chem. Neuroanat.* 33, 167–192. doi: 10.1016/j.jchemneu.2007.02.008

Deng, Y., Wong, T., Wan, J. Y., and Reiner, A. (2014). Differential loss of thalamostriatal and corticostriatal input to striatal projection neuron types prior to overt motor symptoms in the Q140 knock-in mouse model of Huntington's disease. *Front. Syst. Neurosci.* 8:198. doi: 10.3389/fnsys.2014.00198

Donat, C. K., Fischer, F., Walter, B., Deuther-Conrad, W., Brodhun, M., Bauer, R., et al. (2014). Early increase of cannabinoid receptor density after experimental traumatic brain injury in the newborn piglet. *Acta Neurobiol. Exp. (Wars)* 74, 197–210.

Ehrlich, I., Humeau, Y., Grenier, F., Ciocchi, S., Herry, C., and Lüthi, A. (2009). Amygdala inhibitory circuits and the control of fear memory. *Neuron* 62, 757–771. doi: 10.1016/j.neuron.2009.05.026

Elliott, M. B., Tuma, R. F., Amenta, P. S., Barbe, M. F., and Jallo, J. I. (2011). Acute effects of a selective cannabinoid-2 receptor agonist on neuroinflammation in a model of traumatic brain injury. *J. Neurotrauma* 28, 973–981. doi: 10.1089/neu.2010.1672

Faul, M., Xu, L., Wald, M. M., and Coronado,VG. (2010). *Traumatic Brain Injury in the United States: Emergency Department Visits, Hospitalizations, and Deaths*. Atlanta, GA: Centers for Disease Control and Prevention. National Center for Injury Prevention and Control.

Firsching, R., Piek, J., Skalej, M., Rohde, V., Schmidt, U., Striggow F., et al. (2012). Early survival of comatose patients after severe traumatic brain injury with the dual cannabinoid CB1/CB2 receptor agonist KN38-7271: a randomized, double-blind, placebo-controlled phase II trial. *J. Neurol. Surg. A Cent. Eur. Neurosurg.* 73, 204–216. doi: 10.1055/s-0032-1304815

Fujinaga, M., Kumata, K., Yanamoto, K., Kawamura, K., Yamasaki, T., Yui, J., et al. (2010). Radiosynthesis of novel carbon-11- labeled triaryl ligands for cannabinoid-type 2 receptor. *Bioorg. Med. Chem. Lett.* 20, 1565–1568. doi: 10.1016/j.bmcl.2010.01.074

Gelderblom, H., Verweij, J., Nooter, K., and Sparreboom, A. (2001). Cremophor EL: the drawbacks and advantages of vehicle selection for drug formulation. *Eur J Cancer* 37, 1590–1598. doi: 10.1016/S0959-8049(01)00171-X

Godavarthi, S. K., Sharma, A., and Jana, N. R. (2014). Reversal of reduced parvalbumin neurons in hippocampus and amygdala of Angelman syndrome model mice by chronic treatment of fluoxetine. *J. Neurochem.* 130, 444–454. doi: 10.1111/jnc.12726

Goddeyne, C., Nichols, J., Wu, C., and Anderson, T. (2015). Repetitive mild traumatic brain injury induces ventriculomegaly and cortical thinning in juvenile rats. *J. Neurophysiol.* 113, 3268–3280. doi: 10.1152/jn.00970.2014

Gorski, J. A., Talley, T., Qiu, M., Puelles, L., Rubenstein, J. L., and Jones, K. R. (2002). Cortical excitatory neurons and glia, but not GABAergic neurons, are produced in the emx1-expressing lineage. *J. Neurosci.* 22, 6309–6314.

Guley, N. H., Rogers, J. T., Del Mar, N. A., Deng, Y., Islam, R. M., D'Surney, L., et al. (2016). A novel closed-head model of mild traumatic brain injury using focal primary overpressure blast to the cranium in mice. *J. Neurotrauma* 33, 403–422. doi: 10.1089/neu.2015.3886

Gupta, R. K., and Przekwas, A. (2013). Mathematical models of blast-induced TBI: current status, challenges, and prospects. *Front. Neurol.* 4:59. doi: 10.3389/fneur.2013.00059

Hattox, A. M., and Nelson, S. B. (2007). Layer V neurons in mouse cortex projecting to different targets have distinct physiological properties. *J. Neurophysiol.* 98, 3330–3340. doi: 10.1152/jn.00397.2007

Haubensak, W., Kunwar, P. S., Cai, H., Ciocchi, S., Wall, N. R., Ponnusamy, R., et al. (2010). Genetic dissection of an amygdala microcircuit that gates conditioned fear. *Nature* 468, 270–276. doi: 10.1038/nature09553

Heck, D. H., Liu, Y., Honig, M. G., Heldt, S., Del Mar, N., Guley, N. H., et al. (2015). Abnormalities in coherence of local field potential oscillations in medial prefrontal cortex are linked to lasting perseverative depression and fear following mild traumatic brain injury in a mouse model. *Soc. Neurosci. Abst.* 589.13.

Heldt, S. A., Elberger, A. J., Deng, Y., Guley, N. H., Del Mar, N., Rogers, J., et al. (2014). A novel closed-head model of mild traumatic brain injury caused by primary overpressure blast to the cranium produces sustained emotional deficits in mice. *Front. Neurol.* 5:2. doi: 10.3389/fneur.2014.00002

Heldt, S. A., Mou, L., and Ressler, K. J. (2012). *In vivo* knockdown of GAD67 in the amygdala disrupts fear extinction and the anxiolytic-like effect of diazepam in mice. *Transl. Psychiatry* 2, e181. doi: 10.1038/tp.2012.101

Herry, C., Ciocchi, S., Senn, V., Demmou, L., Müller, C., and Lüthi, A. (2008). Switching on and off fear by distinct neuronal circuits. *Nature* 454, 600–606. doi: 10.1038/nature07166

Herry, C., and Johansen, J. P. (2014). Encoding of fear learning and memory in distributed neuronal circuits. *Nat. Neurosci.* 17, 1644–1654. doi: 10.1038/nn.3869

Hicks, R. R., Smith, D. H., Lowenstein, D. H., Saint Marie, R., and McIntosh, T. K. (1993). Mild experimental brain injury in the rat induces cognitive deficits associated with regional neuronal loss in the hippocampus. *J. Neurotrauma* 10, 405–414. doi: 10.1089/neu.1993.10.405

Janak, P. H., and Tye, K. M. (2015). From circuits to behaviour in the amygdala. *Nature* 517, 284–292. doi: 10.1038/nature14188

Jasnow, A. M., Ehrlich, D. E., Choi, D. C., Dabrowska, J., Bowers, M. E., McCullough, K. M., et al. (2013). Thy1-expressing neurons in the basolateral amygdala may mediate fear inhibition. *J. Neurosci.* 33, 10396–10404. doi: 10.1523/JNEUROSCI.5539-12.2013

Jayakumar, A. R., Bak, L. K., Rama Rao, K. V., Waagepetersen, H. S., Schousboe, A., and Norenberg, M. D. (2016). Neuronal cell death induced by mechanical percussion trauma in cultured neurons is not preceded by alterations in glucose, lactate and glutamine metabolism. *Neurochem. Res.* 41, 307–315. doi: 10.1007/s11064-015-1801-0

Johnson, V. E., Stewart, W., and Smith, D. H. (2013). Axonal pathology in traumatic brain injury. *Exp. Neurol.* 246, 35–43. doi: 10.1016/j.expneurol.2012.01.013

Kallakuri, S., Li, Y., Zhou, R., Bandaru, S., Zakaria, N., Zhang, L., et al. (2012). Impaired axoplasmic transport is the dominant injury induced by an impact acceleration injury device: an analysis of traumatic axonal injury in pyramidal tract and corpus callosum of rats. *Brain Res.* 1452, 29–38. doi: 10.1016/j.brainres.2012.02.065

Kelley, B. J., Lifshitz, J., and Povlishock, J. T. (2007). Neuroinflammatory responses after experimental diffuse traumatic brain injury. *J. Neuropathol. Exp. Neurol.* 66, 989–1001. doi: 10.1097/NEN.0b013e3181588245

Koliatsos, V. E., Cernak, I., Xu, L., Song, Y., Savonenko, A., Crain, B. J., et al. (2011). A mouse model of blast injury to brain: initial pathological, neuropathological, and behavioral characterization. *J. Neuropathol. Exp. Neurol.* 70, 399–416. doi: 10.1097/NEN.0b013e3182189f06

Kordower, J. H., Chu, Y., Stebbins, G. T., DeKosky, S. T., Cochran, E. J., Bennett, D., et al. (2001). Loss and atrophy of layer II entorhinal cortex neurons in elderly people with mild cognitive impairment. *Ann. Neurol.* 49, 202–213 doi: 10.1002/1531-8249(20010201)49:2<202::AID-ANA40>3.0.CO;2-3

Kumar, A., and Loane, D. J. (2012). Neuroinflammation after traumatic brain injury: opportunities for therapeutic intervention. *Brain Behav. Immun.* 26, 1191–1201. doi: 10.1016/j.bbi.2012.06.008

Laksari, K., Sadeghipour, K., and Darvish, K. (2014). Mechanical response of brain tissue under blast loading. *J. Mech. Behav. Biomed. Mater.* 32, 132–144. doi: 10.1016/j.jmbbm.2013.12.021

Lawrence, T., and Natoli, G. (2011). Transcriptional regulation of macrophage polarization: enabling diversity with identity. *Nat. Rev. Immunol.* 11, 750–761. doi: 10.1038/nri3088

Leunissen, I., Coxon, J. P., Caeyenberghs, K., Michiels, K., Sunaert, S., and Swinnen, S. P. (2014). Subcortical volume analysis in traumatic brain injury: the importance of the fronto-striato-thalamic circuit in task switching. *Cortex* 51, 67–81. doi: 10.1016/j.cortex.2013.10.009

Liu, Y., McAfee, S. S., Guley, N. H., Honig, M. G., Del Mar, N., Bu, W., et al. (2016). Mild traumatic brain injury in mice causes region specific deficits in oscillatory neuronal activity and functional connectivity that are rescued by the novel cannabinoid type-2 receptor inverse agonist SMM-189. *Soc. Neurosci. Abst.* 607.14.

Loane, D. J., and Kumar, A. (2016). Microglia in the TBI brain: the good, the bad, and the dysregulated. *Exp. Neurol.* 275, 316–327. doi: 10.1016/j.expneurol.2015.08.018

Longhi, L., Saatman, K. E., Fujimoto, S., Raghupathi, R., Meaney, D. F., Davis, J., et al. (2005). Temporal window of vulnerability to repetitive experimental concussive brain injury. *Neurosurgery* 56, 364–374. doi: 10.1227/01.NEU.0000149008.73513.44

Lowenstein, D. H., Thomas, M. J., Smith, D. H., and McIntosh, T. K. (1992). Selective vulnerability of dentate hilar neurons following traumatic brain injury: a potential mechanistic link between head trauma and disorders of the hippocampus. *J. Neurosci.* 12, 4846–4853.

Lunn, C. A., Fine, J. S., Rojas-Triana, A., Jackson, J. V., Fan, X., Kung, T. T., et al. (2006). A novel cannabinoid peripheral cannabinoid receptor-selective inverse agonist blocks leukocyte recruitment *in vivo*. *J. Pharmacol. Exp. Ther.* 316, 780–788. doi: 10.1124/jpet.105.093500

Lunn, C. A., Reich, E. P., Fine, J. S., Lavey, B., Kozlowski, J. A., Hipkin, R. W., et al. (2008). Biology and therapeutic potential of cannabinoid CB_2 receptor inverse agonists. *Br. J. Pharmacol.* 153, 226–239. doi: 10.1038/sj.bjp.0707480

Lüthi, A., and Lüscher, C. (2014). Pathological circuit function underlying addiction and anxiety disorders. *Nat. Neurosci.* 17, 1635–1643. doi: 10.1038/nn.3849

MacDonald, C. L., Johnson, A. M., Cooper, D., Nelson, E. C., Werner, N. J., Shimony, J. S., et al. (2011). Detection of blast-related traumatic brain injury in U.S. military personnel. *N. Engl. J. Med.* 364, 2091–2100 doi: 10.1056/NEJMoa1008069

Mascagni, F., and McDonald, A. J. (2003). Immunohistochemical characterization of cholecystokinin containing neurons in the rat basolateral amygdala. *Brain Res.* 976, 171–184. doi: 10.1016/S0006-8993(03)02625-8

Maxwell, W. L., MacKinnon, M. A., Stewart, J. E., and Graham, D. I. (2010). Stereology of cerebral cortex after traumatic brain injury matched to the Glasgow outcome score. *Brain* 133(Pt 1), 139–160. doi: 10.1093/brain/awp264

McGinn, M. J., and Povlishock, J. T. (2015). Cellular and molecular mechanisms of injury and spontaneous recovery. *Handbook Clin Neurol.* 127, 67–87. doi: 10.1016/B978-0-444-52892-6.00005-2

Meaney, D. F., and Smith, D. H. (2011). Biomechanics of concussion. *Clin. Sports Med.* 30, 19–31. doi: 10.1016/j.csm.2010.08.009

Mechoulam, R., Spatz, M., and Shohami, E. (2002). Endocannabinoids and neuroprotection. *Science STKE* 2002:re5. doi: 10.1126/stke.2002.129.re5

Meyer, M. J., Megyesi, J., Meythaler, J., Murie-Fernandez, M., Aubut, J. A., Foley, N., et al. (2010). Acute management of acquired brain injury part II: an evidence-based review of pharmacological interventions. *Brain Injury* 24, 706–721. doi: 10.3109/02699051003692126

Morey, R. A., Haswell, C. C., Selgrade, E. S., Massoglia, D., Liu, C., Weiner, J., et al. (2013). Effects of chronic mild traumatic brain injury on white matter integrity in Iraq and Afghanistan war veterans. *Hum. Brain Mapp.* 34, 2986–2999. doi: 10.1002/hbm.22117

Morozov, A., Sukato, D., and Ito, W. (2011). Selective suppression of plasticity in amygdala inputs from temporal association cortex by the external capsule. *J. Neurosci.* 31, 339–345. doi: 10.1523/JNEUROSCI.5537-10.2011

Muller, J. F., Mascagni, F., and McDonald, A. J. (2003). Synaptic connections of distinct interneuronal subpopulations in the rat basolateral amygdalar nucleus. *J. Comp. Neurol.* 456, 217–236. doi: 10.1002/cne.10435

Muller, J. F., Mascagni, F., and McDonald, A. J. (2006). Pyramidal cells of the rat basolateral amygdala: synaptology and innervation by parvalbumin-immunoreactive interneurons. *J. Comp. Neurol.* 494, 635–650. doi: 10.1002/cne.20832

Muller, J. F., Mascagni, F., and McDonald, A. J. (2007). Postsynaptic targets of somatostatin-containing interneurons in the rat basolateral amygdala. *J. Comp. Neurol.* 500, 513–529. doi: 10.1002/cne.21185

Myers, K. M., Ressler, K. J., and Davis, M. (2006). Different mechanisms of fear extinction dependent on length of time since fear acquisition. *Learn. Mem.* 13, 216–223. doi: 10.1101/lm.119806

Namjoshi, D. R., Good, C., Cheng, W. H., Panenka, W., Richards, D., Cripton, P. A., et al. (2013). Towards clinical management of traumatic brain injury: a review of models and mechanisms from a biomechanical perspective. *Dis. Models Mech.* 6, 1325–1338. doi: 10.1242/dmm.011320

Neervannan, S. (2006). Preclinical formulations for discovery and toxicology: physicochemical challenges. *Expert Opin. Drug Metab. Toxicol.* 2, 715–731. doi: 10.1517/17425255.2.5.715

Özdinler, P. H., Benn, S., Yamamoto, T. H., Güzel, M., and Brown RH Jr, Macklis, J. D. (2011). Corticospinal motor neurons and related subcerebral projection neurons undergo early and specific neurodegeneration in hSOD1G93A transgenic ALS mice. *J. Neurosci.* 31, 4166–4177. doi: 10.1523/JNEUROSCI.4184-10.2011

Paré, D., Quirk, G. J., and Ledoux, J. E. (2004). New vistas on amygdala networks in conditioned fear. *J. Neurophysiol.* 92, 1–9. doi: 10.1152/jn.00153.2004

Patterson, Z. R., and Holahan, M. R. (2012). Understanding the neuroinflammatory response following concussion to develop treatment strategies. *Front. Cell. Neurosci.* 6:58. doi: 10.3389/fncel.2012.00058

Perez-Polo, J. R., Rea, H. C., Johnson, K. M., Parsley, M. A., Unabia, G. C., Xu, G., et al. (2013). Inflammatory consequences in a rodent model of mild traumatic brain injury. *J. Neurotrauma* 30, 727–740. doi: 10.1089/neu.2012.2650

Peters, A., Kara, D. A., and Harriman, K. M. (1985). The neuronal composition of area 17 of rat visual cortex. III. Numerical considerations. *J. Comp. Neurol.* 238, 263–274. doi: 10.1002/cne.902380303

Petras, J. M., Bauman, R. A., and Elsayed, N. M. (1997). Visual system degeneration induced by blast overpressure. *Toxicology* 121, 41–49. doi: 10.1016/S0300-483X(97)03654-8

Presley, C., Abidi, A., Suryawanshi, S., Mustafa, S., Meibohm, B., and Moore, B. M. (2015). Pre-clinical evaluation of SMM-189, a cannabinoid receptor-2 specific inverse agonist. *Pharmacol. Res. Perspect.* 3:e00159. doi: 10.1002/prp2.159

Raghupathi, R., Conti, A. C., Graham, D. I., Krajewski, S., Reed, J. C., Grady, M. S., et al. (2002). Mild traumatic brain injury induces apoptotic cell death in the cortex that is preceded by decreases in cellular Bcl-2 immunoreactivity. *Neuroscience* 110, 605–616. doi: 10.1016/S0306-4522(01)00461-4

Rainnie, D. G., Mania, I., Mascagni, F., and McDonald, A. J. (2006). Physiological and morphological characterization of parvalbumin-containing interneurons of the rat basolateral amygdala. *J. Comp. Neurol.* 498, 142–161. doi: 10.1002/cne.21049

Redell, J. B., and Dash, P. K. (2007). Traumatic brain injury stimulates hippocampal catechol-o-methyl transferase expression in microglia. *Neurosci. Lett.* 413, 36–41. doi: 10.1016/j.neulet.2006.11.060

Reiner, A., Heldt, S. A., Presley, C. S., Guley, N. H., Elberger, A. J., Deng, Y., et al. (2015). Emotional, sensory and motor deficits in mice after closed-head mild traumatic brain injury are alleviated by the novel CB_2 inverse agonist SMM-189. *Int. J. Mol. Sci.* 16, 758–787. doi: 10.3390/ijms16010758

Reiner, A., Lafferty, D. C., Wang, H. B., Del Mar, N., and Deng, Y. P. (2012). The group-2 metabotropic glutamate receptor agonist LY379268 rescues neuronal, neurochemical and motor abnormalities in R6/2 Huntington's disease mice. *Neurobiol. Dis.* 47, 75–91. doi: 10.1016/j.nbd.2012.03.025

Reiner, A., Medina, L., and Veenman, C. L. (1998). Structural and functional evolution of the basal ganglia in vertebrates. *Brain Res. Rev.* 28, 235–285. doi: 10.1016/S0165-0173(98)00016-2

Risdall, J. E., and Menon, D. K. (2011). Traumatic brain injury. *Philos Trans. R Soc. Lond B Biol. Sci.* 366, 241–250. doi: 10.1098/rstb.2010.0230

Rosenkranz, J. A., and Grace, A. A. (2001). Dopamine attenuates prefrontal cortical suppression of sensory inputs to the basolateral amygdala of rats. *J. Neurosci.* 21, 4090–4103.

Sajja, V. S., Galloway, M., Ghoddoussi, F., Kepsel, A., and VandeVord, P. (2013). Effects of blast-induced neurotrauma on the nucleus accumbens. *J. Neurosci. Res.* 91, 593–601. doi: 10.1002/jnr.23179

Sajja, V. S., Hubbard, W. B., Hall, C. S., Ghoddoussi, F., Galloway, M. P., and VandeVord, P. J. (2015). Enduring deficits in memory and neuronal pathology after blast induced traumatic brain injury. *Sci. Rep.* 5:15075. doi: 10.1038/srep15075

Schomberg, D., and Olson, J. (2012). Immune responses of microglia in the spinal cord: contribution to pain states. *Exp. Neurol.* 234, 262–270. doi: 10.1016/j.expneurol.2011.12.021

Shi, L., Argenta, A. E., Winseck, A. K., and Brunso-Bechtold, J. K. (2004). Stereological quantification of GAD-67-immunoreactive neurons and boutons in the hippocampus of middle-aged and old Fischer 344 x Brown Norway rats. *J. Comp. Neurol.* 478, 282–291. doi: 10.1002/cne.20303

Shitaka, Y., Tran, H. T., Bennett, R. E., Sanchez, L., Levy, M. A., Dikranian, K., et al. (2001). Repetitive closed-skull traumatic brain injury in mice causes persistent multifocal axonal injury and microglial reactivity. *J. Neuropathol. Exp. Neurol.* 70, 551–567. doi: 10.1097/NEN.0b013e31821f891f

Smith, C., Gentleman, S. M., Leclercq, P. D., Murray, L. S., Griffin, W. S., Graham, D. I., et al. (2013a). The neuroinflammatory response in humans after traumatic brain injury. *Neuropathol. Appl. Neurobiol.* 39, 654–666. doi: 10.1111/nan.12008

Smith, D. H., Chen, X. H., Pierce, J. E., Wolf, J. A., Trojanowski, J. Q., Graham, D. I., et al. (1997). Progressive atrophy and neuron death for one year following brain trauma in the rat. *J. Neurotrauma* 14, 715–727. doi: 10.1089/neu.1997.14.715

Smith, D. H., Hicks, R., and Povlishock, J. T. (2013b). Therapy development for diffuse axonal injury. *J. Neurotrauma* 30, 307–323. doi: 10.1089/neu.2012.2825

Stella, N. (2010). Cannabinoid and cannabinoid-like receptors in microglia, astrocytes and astrocytomas. *Glia* 58, 1017–1030. doi: 10.1002/glia.20983

Tam, W. Y., and Ma, C. H. (2014). Bipolar/rod-shaped microglia are proliferating microglia with distinct M1/M2 phenotypes. *Sci. Rep.* 4:7279. doi: 10.1038/srep07279

Taylor, P. A., and Ford, C. C. (2009). Simulation of blast-induced early-time intracranial wave physics leading to traumatic brain injury. *J. Biomed. Eng.* 131, 061007. doi: 10.1115/1.3118765

Tovar-y-Romo, L. B., Penagos-Puig, A., and Ramírez-Jarquín, J. O. (2016). Endogenous recovery after brain damage: molecular mechanisms that balance neuronal life/death fate. *J. Neurochem.* 136, 13–27. doi: 10.1111/jnc.13362

Truitt, W. A., Johnson, P. L., Dietrich, A. D., Fitz, S. D., and Shekhar, A. (2009). Anxiety-like behavior is modulated by a discrete subpopulation of interneurons in the basolateral amygdala. *Neuroscience* 160, 284–294. doi: 10.1016/j.neuroscience.2009.01.083

Tsuda, S., Hou, J., Nelson, R. L., Wilkie, Z. J., Mustafa, G., Sinharoy, A., et al. (2016). Prolonged hippocampal cell death following closed-head traumatic brain injury in rats. *Neuroreport* 27, 724–729. doi: 10.1097/WNR.0000000000000598

Tzekov, R., Quezada, A., Gautier, M., Biggins, D., Frances, C., Mouzon, B., et al. (2014). Repetitive mild traumatic brain injury causes optic nerve and retinal damage in a mouse model. *J. Neuropathol. Exp. Neurol.* 73, 345–361. doi: 10.1097/NEN.0000000000000059

Unal-Cevik, I., Kilin,ç, M., Gürsoy-Ozdemir, Y., Gurer, G., and Dalkara, T. (2004). Loss of NeuN immunoreactivity after cerebral ischemia does not indicate neuronal cell loss: a cautionary note. *Brain Res.* 1015, 169–174. doi: 10.1016/j.brainres.2004.04.032

Wilde, E. A., Bigler, E. D., Hunter, J. V., Fearing, M. A., Scheibel, R. S., Newsome, M. R., et al. (2007). Hippocampus, amygdala, and basal ganglia morphometrics in children after moderate-to-severe traumatic brain injury. *Dev. Med. Child Neurol.* 49, 294–299. doi: 10.1111/j.1469-8749.2007.00294.x

Wolff, S. B., Gründemann, J., Tovote, P., Krabbe, S., Jacobson, G. A., Müller, C., et al. (2014). Amygdala interneuron subtypes control fear learning through disinhibition. *Nature* 509, 453–458. doi: 10.1038/nature13258

Xiong, Y., Mahmood, A., and Chopp, M. (2013). Animal models of traumatic brain injury. *Nat. Rev. Neurosci.* 14, 128–142. doi: 10.1038/nrn3407

Xu, L., Nguyen, J. V., Lehar, M., Menon, A., Rha, E., Arena, J., et al. (2016). Repetitive mild traumatic brain injury with impact acceleration in the mouse: multifocal axonopathy, neuroinflammation, and neurodegeneration in the visual system. *Exp. Neurol.* 275, 436–449. doi: 10.1016/j.expneurol.2014.11.004

Yttri, E. A., and Dudman, J. T. (2016). Opponent and bidirectional control of movement velocity in the basal ganglia. *Nature* 533, 402–406. doi: 10.1038/nature17639

Zakaria, N., Kallakuri, S., Bandaru, S., and Cavanaugh, J. M. (2012). Temporal assessment of traumatic axonal injury in the rat corpus callosum and optic chiasm. *Brain Res.* 1467, 81–90. doi: 10.1016/j.brainres.2012.05.046

Zhang, L., Guo, Y., Hu, H., Wang, J., Liu, Z., and Gao, F. (2015). FDG-PET and NeuN-GFAP immunohistochemistry of hippocampus at different phases of the pilocarpine model of temporal lobe epilepsy. *Int. J. Med. Sci.* 12, 288–294. doi: 10.7150/ijms.10527

Conflict of Interest Statement: The authors declare that the research was conducted in the absence of any commercial or financial relationships that could be construed as a potential conflict of interest.

Copyright © 2016 Bu, Ren, Deng, Del Mar, Guley, Moore, Honig and Reiner. This is an open-access article distributed under the terms of the Creative Commons Attribution License (CC BY). The use, distribution or reproduction in other forums is permitted, provided the original author(s) or licensor are credited and that the original publication in this journal is cited, in accordance with accepted academic practice. No use, distribution or reproduction is permitted which does not comply with these terms.

frontiers in Neuroscience

ORIGINAL RESEARCH
published: 16 September 2016
doi: 10.3389/fnins.2016.00422

Vascular Dysfunction in a Transgenic Model of Alzheimer's Disease: Effects of CB1R and CB2R Cannabinoid Agonists

Jorge Navarro-Dorado[1†], Nuria Villalba[2†], Dolores Prieto[2], Begoña Brera[3], Ana M. Martín-Moreno[3†], Teresa Tejerina[1] and María L. de Ceballos[3]*

[1] Department of Pharmacology, School of Medicine, Complutense University of Madrid, Madrid, Spain, [2] Department of Physiology, Faculty of Pharmacy, Complutense University of Madrid, Madrid, Spain, [3] Neurodegeneration Group, Cellular, Molecular and Developmental Neurobiology and CIBERNED, Cajal Institute, CSIC, Madrid, Spain

There is evidence of altered vascular function, including cerebrovascular, in Alzheimer's disease (AD) and transgenic models of the disease. Indeed vasoconstrictor responses are increased, while vasodilation is reduced in both conditions. β-Amyloid (Aβ) appears to be responsible, at least in part, of alterations in vascular function. Cannabinoids, neuroprotective and anti-inflammatory agents, induce vasodilation both *in vivo* and *in vitro*. We have demonstrated a beneficial effect of cannabinoids in models of AD by preventing glial activation. In this work we have studied the effects of these compounds on vessel density in amyloid precursor protein (APP) transgenic mice, line 2576, and on altered vascular responses in aortae isolated ring. First we showed increased collagen IV positive vessels in AD brain compared to control subjects, with a similar increase in TgAPP mice, which was normalized by prolonged oral treatment with the CB1/CB2 mixed agonist WIN 55,212-2 (WIN) and the CB2 selective agonist JWH-133 (JWH). In Tg APP mice the vasoconstriction induced by phenylephrine and the thromboxane agonist U46619 was significantly increased, and no change in the vasodilation to acetylcholine (ACh) was observed. Tg APP displayed decreased vasodilation to both cannabinoid agonists, which were able to prevent decreased ACh relaxation in the presence of Aβ. In summary, we have confirmed and extended the existence of altered vascular responses in Tg APP mice. Moreover, our results suggest that treatment with cannabinoids may ameliorate the vascular responses in AD-type pathology.

Keywords: Alzheimer's disease, β-amyloid, cannabinoid receptors, collagen IV, Tg APP, vascular dysfunction

OPEN ACCESS

Edited by:
Marialessandra Contino, University of Bari Aldo Moro, Italy

Reviewed by:
Rudolf Schubert, Heidelberg University, Germany
Claus Jürgen Scholz, University of Würzburg, Germany

***Correspondence:**
María L. de Ceballos
mceballos@cajal.csic.es

†Present Address:
Jorge Navarro-Dorado, Centre for Integrative Physiology, University of Edinburgh, Edinburgh, UK
Nuria Villalba, Department of Pharmacology, College of Medicine, University of Vermont, Burlington, VT, USA
Ana M. Martín-Moreno, Pathology Department, MD Anderson Cancer Center, Madrid, Spain

Specialty section:
This article was submitted to Neurodegeneration, a section of the journal Frontiers in Neuroscience

Received: *05 May 2016*
Accepted: *29 August 2016*
Published: *16 September 2016*

Citation:
Navarro-Dorado J, Villalba N, Prieto D, Brera B, Martín-Moreno AM, Tejerina T and de Ceballos ML (2016) Vascular Dysfunction in a Transgenic Model of Alzheimer's Disease: Effects of CB1R and CB2R Cannabinoid Agonists. Front. Neurosci. 10:422. doi: 10.3389/fnins.2016.00422

INTRODUCTION

Alzheimer's disease (AD) is the major cause of dementia. This neurologic condition is characterized pathologically by β-amyloid (Aβ) deposition, neurofibrillary tangles, composed of hypophosphorylated tau, the degeneration of particular subsets of neurons and neuroinflammation, as a consequence of glial activation. Although the existence of hereditary AD,

with early onset, has been described, it only accounts for a small percentage of cases (Hardy, 1996; Campion et al., 1999). The actual cause of sporadic AD is unknown, but several risk factors have been recognized (Grammas, 2011; Carnevale et al., 2016; Hamel et al., 2016). Indeed, hypertension, hypercholesterolaemia, ischaemic stroke, the ApoE4 allele and diabetes, all characterized by a vascular pathology, constitute risk factors for AD. On the other hand, several abnormalities in cerebrovascular vessels have been observed, including amyloid cerebral angiopathy (Thomas et al., 2000; Hardy and Selkoe, 2002; Kalaria, 2002; Iadecola, 2010), with a prominent accumulation of Aβ in vessels, alterations in smooth muscle or endothelial cells, and thickening of basement membrane (Mancardi et al., 1980; Kalaria, 2002; Iadecola, 2010; Morris et al., 2014). Moreover, there are pathophysiological links among these actors, since increased hypertension in mice results in Aβ deposition and cognitive impairment (Carnevale et al., 2012). Similarly, in transgenic models of the disease exists angiopathy, alterations in cerebral microvasculature occur, with the presence of apoptotic vascular cells in brain (Christie et al., 2001; Miao et al., 2005; Tong et al., 2005).

Aβ induces several types of vessel dysfunctions. Indeed, preincubation of aortae rings with the peptide diminishes the vasodilator activity of acetylcholine (ACh), while the vasoconstrictor responses to phenylephrine (Thomas et al., 1996) and endothelin-1 (ET-1; Crawford et al., 1998) are enhanced. Free radical generation appeared to mediate the effects of Aβ, since the addition of the antioxidant enzyme superoxide dismutase (SOD) avoided Aβ effects (Thomas et al., 1996; Crawford et al., 1998). On the other hand, calcium channel blockers or calcium chelators fully abrogate the enhancement induced by Aβ on ET-1 vasoconstriction (Crawford et al., 1998). In regard to the chemical species, it has been reported that Aβ 1-40 appears to be the fragment inducing higher vasoactivity (Crawford et al., 1998; Smith et al., 2007), compared to fragments 1–42 or 25–35, both showing greater cytotoxicity. It should be noted that Aβ1-42, more prone to aggregation, along with the 1–40 peptide fragment are deposited in senile plaques. However, Aß1-40 is the chemical species present in blood. However, it is not clear whether the presence of endothelium is required for vasoactivity (Thomas et al., 1996; Crawford et al., 1998). Interestingly, Aβ intra-arterial infusion to rats decreased blood flow and increased vascular resistance specifically in cerebral cortex (Suo et al., 1998), and enhances mean arterial blood pressure (Arendash et al., 1999). In isolated middle cerebral arteries from amyloid precursor protein transgenic mice (Tg APP) the vasodilator responses to calcitonin gene related peptide (CGRP) and ACh were significantly reduced, although the vasoconstriction induced by ET-1 was preserved, and both catalase and SOD addition restored to control values ACh-induced vessel relaxation (Tong et al., 2005). Moreover, Tg APP mice showed selective impairment in endothelium-dependent regulation of the neocortical microcirculation, as measured by laser-Doppler, which was counteracted by SOD (Iadecola et al., 1999).

Cannabinoids are molecules interacting with cannabinoid receptors, or with similar chemical structure to tetrahydrocannabinol, the major constituent of *Cannabis sativa*. Thus, cannabinoid agonists comprise molecules derived from the plant, synthetic molecules, with higher potency, and the endocannabinoids, present in living animals. Anandamide (AEA) and 2-arachidonoylglycerol (2-AG) are the major endocannabinoids, which along with their synthetic and degrading enzymes, and specific cannabinoid receptors constitute the endocannabinoid system (Di Marzo and De Petrocellis, 2012; Pertwee, 2012), which has a modulatory role with pleiotropic actions. Cannabinoid agonists have shown neuroprotective and anti-inflammatory effects of interest for the treatment of different neurodegenerative (Baker et al., 2000; Glass et al., 2000; Arévalo-Martín et al., 2008; Fernández-Ruiz et al., 2011) and mental disorders (Marsicano et al., 2002; de Bitencourt et al., 2013; Leweke et al., 2016). We (Ramírez et al., 2005; Martín-Moreno et al., 2012) and others (Wu et al., 2013; Aso and Ferrer, 2014; Cheng et al., 2014) have described beneficial effects relevant for AD treatment. Indeed, cannabinoid agonists rescue the cognitive impairment in AD animal models, affording neuroprotection by decreasing neuroinflammation and Aβ levels. On the other hand, cannabinoid agonists are hypotensive agents. Their cardiovascular actions are complex (Randall et al., 2004; López-Miranda et al., 2008). They cause vasorelaxation of isolated vessels *in vitro*, and *in vivo* they induce multiphasic responses that lead to sustained hypotension. For instance, anandamide, the endocannabinoid, caused a triphasic response in anaesthesized rats: first, there is a hypotensive response, vagally mediated, followed by a pressor response and by a sustained hypotension (Varga et al., 1996). Moreover, WIN 55,212-2 and HU-210 in conscious rats induced pressor, and renal and mesenteric vasoconstrictor effects, but hindquarters vasodilator actions (Gardiner et al., 2001). Although in some instances the classical cannabinoid receptors, the well characterized CB_1 and CB_2 receptors, are involved in such responses, in other occasions different receptors are activated, the release of endothelial mediators may be implicated, or even direct effects on transduction mechanisms have been invoked.

Given the vascular alterations observed in AD and in its animal models, and that cannabinoid agonists show vascular effects, in this work we sought to investigate the vascular responses of two pharmacologically distinct cannabinoid agonists, the CB_1/CB_2 mixed agonist WIN 55,212-2 (WIN) and the CB_2 selective agonist JWH-133 (JWH). We selected WIN because it shows a slightly higher CB_2 selectivity compared to other mixed agonists, and JWH because it was one of the first CB_2 selective agonists synthesized and characterized (Huffman et al., 1999). Since we have been using both compounds for years, commencing with our seminal work on the cannabinoid receptor alterations in AD and the effects of cannabinoid agonists on its experimental *in vitro* and *in vivo* models (Ramírez et al., 2005), we have gathered a broad knowledge on their pharmacology. Furthermore, we tested whether they counteract the Aβ-induced alteration in vessel function and if they maintain their effects in vessels of a transgenic mouse model of the disease, Tg APP mice (line 2576). The possible beneficial effects of cannabinoid agonists on the vascular system may be of therapeutic interest in a multifactorial disease such as AD.

MATERIALS AND METHODS

Materials

ßA$_{1-40}$ (Polypeptide Group, France) was dissolved in PBS (1.72 mg/ml), aliquoted and stored at −80°C until used. WIN was purchased from Sigma, JWH was from Tocris (Cookson Ltd., UK), SR141716 (SR1; Rinaldi-Carmona et al., 1994) and SR144528 (SR2; Rinaldi-Carmona et al., 1998) were kindly donated by Sanofi-Synthelabo (Montpellier, France). For *in vitro* experiments each of these compounds was dissolved in DMSO at 10 mM, aliquoted and stored at −80°C. Before their use, drugs were diluted in appropriate solvent and DMSO never exceeded 0.1% in pharmacological experiments. For *in vivo* experiments, WIN and JWH were initially dissolved in chloroform (on ice), quickly aliquoted to prevent evaporation, dried under a stream of N_2, and aliquots stored desiccated. Before their use, drugs were diluted in ethanol and added to the drinking water. Salts and other reagents were analytical grade from Merck.

Human *Post-mortem* Brain Tissue

For immunocytochemistry, cryoprotected and fixed frozen frontal cortex samples were obtained from the Neurologic Tissue Bank, Hospital Clinic, Barcelona, Spain, and processed as previously described (Ramírez et al., 2005). Human brains were obtained by the Neurologic Tissue Bank following written consent. Controls consisted of 3 males and 2 females (median 70.0, range 38.0–0.0 years of age; median 17.0, range 3.5–21.0 h of *post-mortem* interval), and clinically diagnosed and neuropathologically defined AD patients consisted of 3 females and 3 males (median 74.0, range 66.0–88.0 years; median 5.5, range 4.0–9.0 h).

Animals and Treatments

Tg APP transgenic mice were obtained via heterozygous breeding of mice expressing the 695 aa long isoform of the human APP containing a double mutation Lys 670-Asn, Met 671-Leu (swedish mutation) under transcriptional control of the hamster prion promoter on a C57BL/6 breeding background (Hsiao et al., 1996). Male Tg APP, and wild type (wt) littermates, used as controls, were 7 months old at the beginning of the experiments. Mice were group-housed (4–5 animals per cage) under controlled temperature (23 ± 2°C), with a 12:12 h light/dark cycle and with *ad libitum* access to food and water. All of the experiments were performed according to ethical regulations on the use and welfare of experimental animals of the European Union and the Spanish Ministry of Agriculture, and the procedures were approved by the bioethical committee of the CSIC.

WIN and JWH were administered in the drinking water at a dose of 0.2 mg/Kg/day using ethanol (0.1%) as vehicle (Martín-Moreno et al., 2012). The amount of water drank by the animals was assessed every other day and the treatment was adjusted to their weight. There was no difference in the body weight or the ingested water between groups, all along the experiment, discarding a possible reinforcing effect of cannabinoids.

Animals were sacrificed by cervical dislocation followed by decapitation at 11 months of age after 4 months chronic treatment. The brain was sagittally divided. One brain hemisphere was rapidly dissected on a cold plate, frozen on dry ice and stored at −80°C until assayed. The other hemisphere was immersion fixed in 4% paraformaldehyde (4% PF) in sodium phosphate buffer (PB) 0.1 M for 24 h, cryoprotected in sucrose 15% (24 h) and 30% (24 h) in PB, snap frozen in hexane (−60°C), and stored at −20°C until cut with a sliding microtome.

For pharmacological studies male mice, wt used as control, or Tg APP mice (line 2576) (25–30 g, 12 months of age) were sacrificed by decapitation following cervical dislocation. The thoracic aorta was removed, cleaned and cut into segments of 2 mm length. Rings were mounted in Multy Myograph System 610M (Danish Myo Technology, Denmark) at 37 ± 0.5°C and gassed continuously with a mixture of 95% O_2-5% CO_2, in a solution of the following composition: PSS (mM): NaCl 140, KCl 5, $MgCl_2$ 1, $CaCl_2$ 1.5, HEPES 5, and glucose 10. After equilibration, arterial rings were mounted between two parallel tungsten wires under a resting tension of 2 g. The isometric force was digitalized by Myodaq 2.01 program (Danish Myo Technology, Denmark) and displayed on a personal computer.

Arteries were preconstricted with 123.5 mM K^+ (KPSS) for 4 min, washed, and then a) concentration-response curves for phenylephrine (Phe, 0.1-10 μM) and the thromboxane analog U46619 (0.01-0.1 μM) were performed; b) in a different set of experiments arterial rings were preconstricted with a submaximal concentration of U46619 (0.03 μM) for 15 min and then vasodilation to ACh 10 μM was assessed. After 2 washes vessels were incubated with Aβ (1 μM) for 15 min, and stimulated with U46619 (0.03 μM) for 15 min followed by relaxation with ACh 10 μM. To assess the vasodilatory effects of WIN and JWH concentration-response curves (1nM-10 μM) were performed in segments preconstricted with U46619. Concentration-response curves for WIN and JWH were performed in arterial segments treated with the selective CB_1 or CB_2 antagonists (SR1 and SR2), added 5 min before preconstriction with U46619. To investigate the effect of cannabinoid agonists on ACh-induced vasodilation, agonists were added to arterial rings at 0.5 μM after 15 min incubation with Aβ (1 μM). Given that the effect of Aβ is irreversible (Thomas et al., 1996) different arterial rings were used for each experiment. Tension was expressed as mN/mm artery length, or as a percentage of initial preconstriction (either with K^+ or U46619). Indeed each ring was its own control, avoiding the variance between the responses of different rings from the same animal (decreased responsivity as the rings approached the abdominal aortic region).

Immunohistochemistry

Immunostaining was performed on floating sections (30 μm thick) as described (Gómez Del Pulgar et al., 2002). Sections were incubated with the different antibodies overnight at 4°C. Dilutions of antibodies were as follow: polyclonal anti-CB1 (1:900, CC2, raised in our laboratory, De March et al., 2008), polyclonal anti-collagen IV (Col IV; 1: 400, ref. CR013X; Fitzgerald, MA, USA). The CC2 antibody was raised in rabbits using as immunogen the 15 aa N-terminal end of the CB_1 receptor protein coupled to keyhole limpet hemocyanin. The antiserum was affinity purified, and it was characterized in wt mice and in CB_1 KO mice brain. CB_1

immunoreactivity brain distribution was in agreement with previous studies (Tsou et al., 1997, 1999). The anti-collagen antibody has been raised in rabbits using as immunogen Col IV from human and bovine placenta. It shows negligible cross reaction with Col I, Col II, Col III, and Col V. Development was conducted by the Avidin-Biotin Complex (ABC) method (Pierce), and immunoreactivity was visualized by 3,3′-diaminobenzidine oxidation as chromogen, with (CB_1) or without nickel enhancement (Col IV). Omission of primary or secondary antibodies resulted in no immunostaining.

Images were acquired with a Zeiss Axiocam high resolution digital color camera, using the same settings and segmentation parameters (MCID software; InterFocus Imaging, UK) for a given marker and experiment. The mean value for each animal per region results from the analysis of 5–6 sections. The percentage of the brain area covered by Col IV positive vessels was assessed by image analysis with MCID software.

Analysis of mRNA Levels by RT-PCR

Total RNA from pooled aortae ($n = 3$–4) was extracted using TRIzol reagent according to the manufacturer's instructions (Invitrogen). To avoid interference with potential genomic DNA amplification 1 μg of total RNA was treated with 1 μl DNAse I (Invitrogen) plus 1 μl of 10X Buffer (Invitrogen) and incubated for 15 min at RT, then EDTA (25 mM) was added and incubated at 65°C for 15 min to inactivate DNAse I. For cDNA synthesis a total of 1 μg of RNA were reverse-transcribed for 75 min at 42°C using 5 U of avian myeloblastosis virus reverse transcriptase (Promega) in the presence of 20 U of RNAsin (Promega). The PCR reaction was performed using TaQ polymerase (TaQ DNA polymerase Sigma) and a mixture of reverse and forward primers (5 pmol). The primers used were CB_1 forward 5′-AGCTTTGTT GACTTCCAGTGT and CB_1 reverse 5′-CTGCCCACAGATGCT GTGAA, CB_2 forward 5′-AGGAGCTGTCAGCTCAGGGTAT and CB_2 reverse 5′-CTGCGCCCCTAAGGACCTA. The PCR reaction (final volume10 μl) was performed in a Veriti thermal cycler (Applied Biosystems) and the PCR program was as follows: initial denaturation for 10 min at 95°C, then 40 cycles of denaturation (15 s, 95°C), annealing (30 s, 60°C), and extension (30 s, 60°C). The PCR products were analyzed by standard agarose gel electrophoresis, and gene expression levels were detected by the use of ethidium bromide.

Electron Microscopy

Aortae 1–2 mm long rings were fixed in 4% PF/ 2.5% glutaraldehyde in cold 0.1 M Na cacodylate buffer immediately after dissection, for 6 h. The segments were washed five times with cacodylate buffer every 30 min, and left overnight at 4°C. The segments were postfixed with 1% osmium tetroxide and potassium ferrocyanide in distilled water for 1.5 h, they were washed with distilled water (3 × 10 min washes) and dehydrated in increasing acetone solutions (50–100% each for 15 min). The segments were then gradually embedded in resin (1:3, 1:1, 3:1 acetone:pure resin) and finally left in pure resin (TAAB 812 mix) at 60°C overnight. The resin embedded samples were sectioned by diamond knife, and the 80 nm sections were collected onto copper grids and post-stained with 1% uranyl acetate and Reynolds lead citrate for 4 and 3 min, respectively. Electron micrographs were obtained using a Jeol JEM-1010 high resolution transmission electronic microscope (Jeol, Tokyo, Japan).

Statistical Analysis

In pharmacological experiments we used one vessel per mouse, therefore n represents number of animals. In brief, each aorta was cut into 5 different rings and each ring was used for a given treatment to avoid artefactual results. Results are expressed as mean ± standard error mean (SEM) or as mean ± standard deviation (SD). Statistical analysis was assessed by using two-way or one-way analysis of variance (ANOVA) followed by Wilcoxon's test, if the data follow a Gaussian distribution (KS normality test), or by Kruskal-Wallis test, followed by Dunn's test (version 5.0, Prism software, GraphPad, USA). A value of $p < 0.05$ was considered significant.

RESULTS

Vascular Density is Increased in AD Frontal Cortex and Tg APP Mice

Previous studies have reported vascular alterations in the brain of AD affected individuals, such as increased vessel density and greater collagen deposition at the structural level. As shown in **Figures 1A,B**) we found an increase (≈30%) in Col IV positive vessel density in the gray matter of frontal cortex from AD patients compared with control subjects. Vessel density was significantly lower in the white matter compared to the gray matter. No difference in vessel density in the white matter was found between the control and AD group (**Figures 1A,B**). Vessel density in Tg APP mice was much higher (≈50%) in cortical areas compared to wt mice, however it showed similar density in the hippocampus (**Figures 1C,D**). Interestingly, prolonged *in vivo* oral treatment (0.2 mg/Kg/day) with both WIN, a mixed CB_1/CB_2 agonist, and JWH, a CB_2 selective agonist, counteracted the increased Col IV vessel density. In summary, similar vessel alterations were found in the neurologic condition and in the experimental model of AD, where a prolonged oral treatment of a cannabinoid agonist prevented vascular changes.

Vascular Dysfunction in Tg APP Mice, Contribution of β-Amyloid and Vasodilatory Effect of Cannabinoid Agonists

We next examined whether mice aortae expressed CB_1 and CB_2 receptors. CB_1 immunoreactivity has been previously reported in brain vessels (Ashton et al., 200), but the presence of CB_2 receptors is uncertain. CB_1 receptors were expressed in endothelial cells, at the *basal lamina*, but not in smooth muscle cells (**Figure 2A**, representative image of $n = 3$), while Col IV immunoreactivity just stained the *basal lamina* of the aorta (**Figure 2B**, representative image of $n = 3$). The immunostaining was very reproducible for both antibodies. There is debate on the specificity of CB_2 receptors antibody (Cécyre et al., 2014; Li and

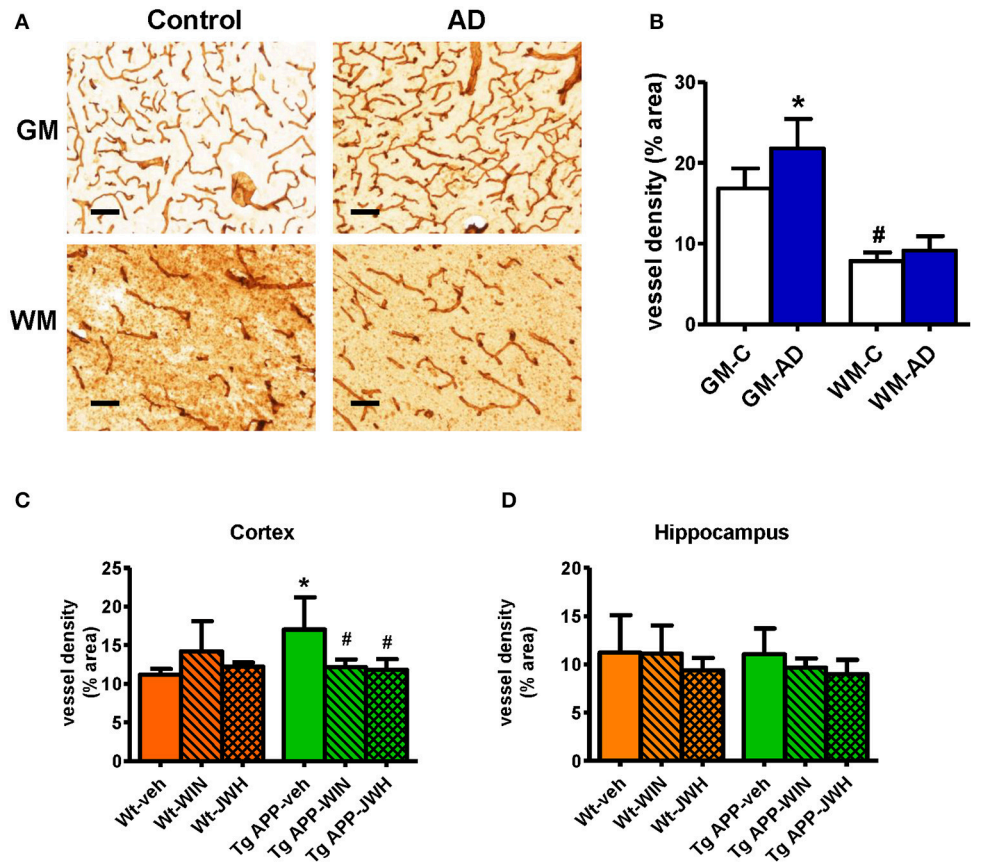

FIGURE 1 | Vessel density is altered in AD compared to controls. (A) Representative collagen IV immunostaining of cortical vessels in human controls ($n = 5$) and AD patients ($n = 6$). Scale bar, 100 μm. GM, gray matter; WM, white matter. **(B)** Collagen IV positive vessels are significantly increased in gray matter. Results are mean ± SD ($n = 5$–6) and they are expressed as percentage of area occupied by vessels. $^{*}p < 0.05$ versus controls, $^{\#}p < 0.05$ versus gray matter vessel density (Student's *t*-test). **(C)** Tg APP vehicle treated mice showed increased collagen IV vessel density in cortex vs. wild type (Wt) vehicle treated mice. Cannabinoid agonists normalized vessel density of Tg APP mice. Results are mean ± SD ($n = 7$–8) $^{*}p < 0.05$ vs. controls (Wt-veh), $^{\#}p < 0.05$ vs. Tg APP-veh (Kruskal-Wallis, followed by Dunn's test). **(D)** No changes in vessel density were found in hippocampus due to genotype and/or drug treatment.

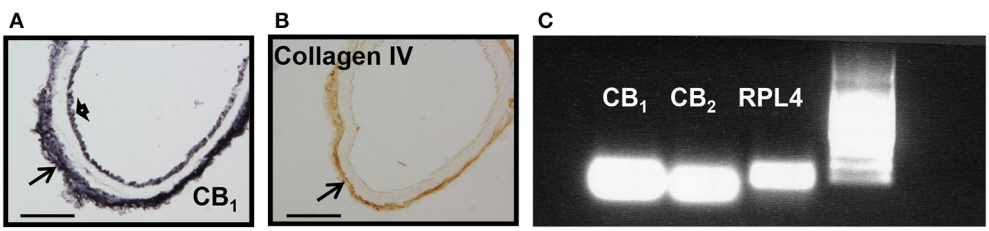

FIGURE 2 | CB_1, CB_2, and collagen IV expression in mouse aorta. (A) CB_1 immunostaining shown at endothelial cells (short arrow) and *basal lamina* (arrow), **(B)** while collagen IV is restricted to the *basal lamina* (arrow). Scale bar, 50 μm; representative images of $n = 3$ aortae for each immunostaining. **(C)** CB_1 and CB_2 mRNA expression in extracts from mouse aorta. RPL4 was used as control. Representative image of $n = 3$ independent experiments done with 3–4 pooled aortae.

Kim, 2015), therefore we used PCR to demonstrate CB_2 and CB_1 receptor expression in aorta extracts (**Figure 2C**).

Constriction of aorta rings with high potassium (123.5 mM K^+) was decreased by 50% in Tg APP mice aortae compared to those from wt mice (1.07 ± 0.13 and 2.25 ± 0.30 mN/mm respectively; $p < 0.01$, Student's *t*-test). Next, we tested two pharmacologically distinct vasoconstrictors: phenylephrine and the thromboxane analog U46619 (**Figure 3**). The vasoconstrictor response to 0.1 μM phenylephrine was enhanced by 2 fold in Tg APP compared to wt mice (**Figure 3A**), and that of 0.1 μM U46619 around a 50% (**Figure 3B**). We did not find any differences in the vasodilation induced by ACh

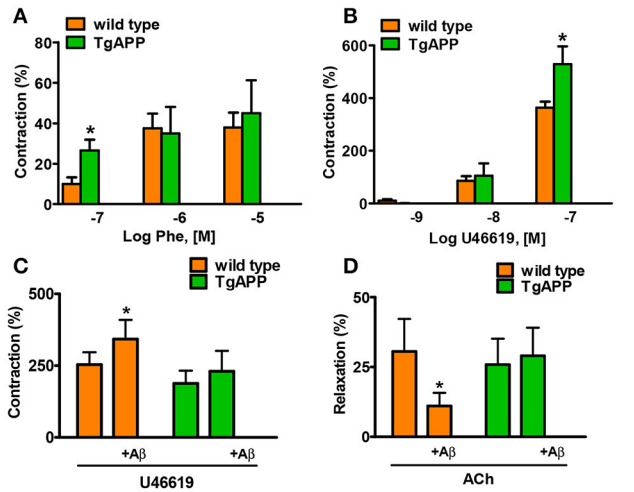

FIGURE 3 | Alterations in aorta contractility of Tg APP mice. Tg APP aortae showed increased phenylephrine **(A)** and U46619-induced **(B)** contraction compared to aortae from wt mice. Vessels were precontracted by 123.5 mM K^+ and washed before other treatment addition. Aβ (1 μM) incubation increased U46619 (0.03 μM) contraction **(C)** and decreased ACh (10 μM) relaxation **(D)** in wt aortae, but not in Tg APP aortae. Preconstriction levels were similar for all the vessels (approximately 5.44 mN). Results are mean ± SEM of $n = 7$ mice and are expressed as percentage of 123.5 mM K^+-induced contraction, considered 100%. $^*p < 0.05$ (Kruskal-Wallis, followed by Dunn's test).

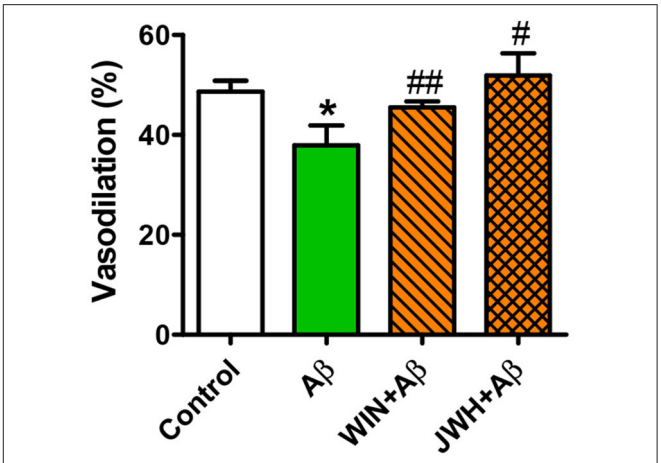

FIGURE 4 | Cannabinoid agonists prevent Aβ reduction of ACh relaxation. Vessels from wt mice were precontracted with U46619 (0.03 μM) and ACh (10 μM) vasodilation assessed in the absence and presence of WIN and JWH. Preconstriction levels were similar for all the vessels (approximately 5.44 mN). Results are mean ± SEM of $n = 6$ mice and are expressed as percentage of U46619 contraction. $^*p < 0.05$ vs. untreated-aortae; $^{\#}p < 0.05$; $^{\#\#}p < 0.01$ vs. Aβ treated alone (Kruskal-Wallis, followed by Dunn's test).

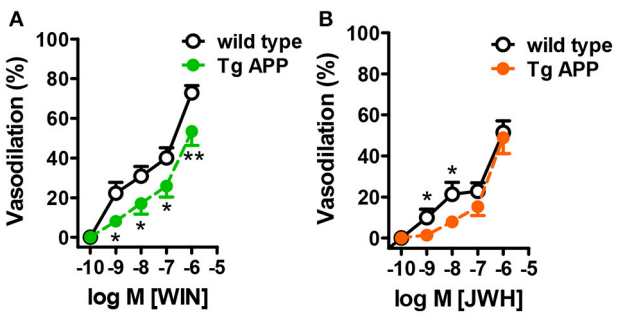

FIGURE 5 | Cannabinoid agonists induce dose-dependent vasodilation. Cannabinoid vasodilation was reduced in Tg APP aortae compared to wt **(A,B)**. Concentration-response curves (1 nM-10 μM) for WIN and JWH were performed in segments preconstricted with U46619 (0.03 μM). Preconstriction levels were similar for all the vessels (approximately 8.9 mN). Results are mean ± SEM of $n = 6$ mice and are expressed as percentage of U46619-induced contraction. $^*p < 0.05$, $^{**}p < 0.01$ (two way ANOVA).

(100 μM) between groups (data not shown). Furthermore, the cannabinoid agonists (15 min preincubation) under study did not change ACh vasodilation either (data not shown).

Given that Tg APP mice are continuously exposed to circulating Aβ we wondered whether the peptide would mediate those responses. Aβ (1 μM) preincubation increased vasoconstriction to 0.03 μM U46619 (**Figure 3C**) and decreased vasodilation to 10 μM ACh (**Figure 3D**), in aortae from wt mice, although the peptide alone did not show any vasoactivity. However, incubation with Aβ did not alter arterial vasoconstriction or vasodilation in Tg APP mice aortae (**Figures 3C,D**). Interestingly, both cannabinoid agonists rescued ACh-induced vasodilation in the presence of Aβ (**Figure 4**) in wt mice.

WIN concentration-dependently induced vasodilation in control mice, with a maximal effect of 80% at 1 μM (**Figure 5A**). The vasodilatory effect of JWH was smaller than the one induced by WIN, with a maximal effect of 56% at 1 μM (**Figure 5B**). In Tg APP aortae the vasodilation induced by WIN was significantly decreased at all the concentrations tested (**Figure 5A**), but in the case of JWH the effect at lower concentrations (1 and 10 nM) was decreased and at higher concentrations was similar between wt and Tg APP mice (**Figure 5B**).

Taken together these results show that vascular function is markedly altered in Tg APP mice and that Aβ may play a role in those altered responses. Furthermore, cannabinoid agonists induce vasodilation in aortic rings, which is partially preserved in Tg APP mice.

Ultrastructural Changes in Tg APP Aortae

Some reports have described changes in the structure of Tg APP vessels (Christie et al., 2001; Tong et al., 2005). Therefore, we sought to determine if changes at the ultrastructural level may explain the vessel dysfunction observed in Tg APP mice. Toluidine labeled vessels showed similar vessel structure (**Figures 6A,B**). Endothelial cells appeared unaltered in both strains (**Figures 6C,D**). Moreover, smooth muscle cells also appeared normal, with normal numbers of mitochondria (not shown). However, there was a great difference in *basal lamina* collagen that was markedly increased in Tg APP when compared with wt aortae (**Figures 6E,F**).

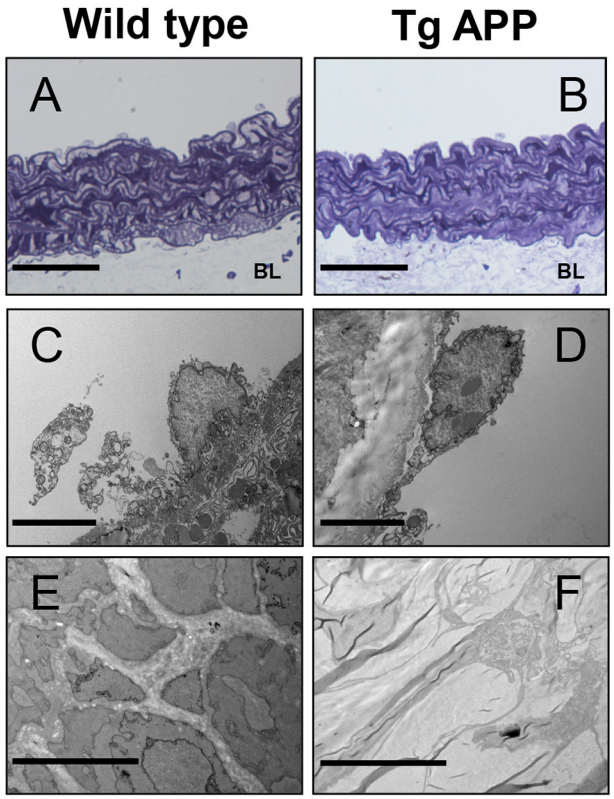

FIGURE 6 | Electron micrographs of wild type and Tg APP mice. Representative images are shown for wt **(A,C,E)** and Tg APP mice aortae **(B,D,F)**. **(A,B)** toluidine blue micrographs showing similar structure ($n = 20$ animals/per group). BL: *basal lamina,* **(C,D)** endothelial cells show similar appearance (wt $n = 4$, Tg APP $n = 6$). **(E)** smooth muscle cells surrounded by collagen in wt mice aorta, **(F)** muscle cells are embedded in collagen in Tg APP aorta (wt $n = 4$, Tg APP $n = 6$). Scale bars, 50 μm in (**A,B**); 100 nm in **(C–F)**.

DISCUSSION

In the present work we report that WIN, a mixed CB_1 and CB_2 agonist (Howlett et al., 2002), and JWH, a CB_2 selective agonist (Huffman et al., 1999), induce vasodilation of isolated aortae. Tg APP vessels show altered vascular responses, in which Aβ may play a role, that were restored by the cannabinoids under study. We found an enhancement of collagen in *basal lamina*, that may partly explain the vascular dysfunction in Tg APP mice. This collagen increase was found in AD cerebrocortical vessels, and in Tg APP mice as well, and was fully reverted by prolonged oral treatment with both cannabinoid agonists. Taken together these results suggest that cannabinoid have effects on vascular function that may be beneficial in the treatment of AD.

Vessel function is compromised in Tg APP mice. Indeed we have confirmed and extended previous reports on the increase in the vasoconstriction to phenylephrine in isolated aorta rings (Thomas et al., 1996), and we have found similar increases with U46619, that decreased cerebral blood flow *in vivo* (Iadecola et al., 1999). However, endothelium-independent vasoconstriction was markedly reduced in Tg APP aortae, as judged by the decreased vasoconstriction to high potassium. This change parallels the attenuation in the vasodilator response to sodium nitroprusside (an endothelial-independent vasodilator) observed *in vivo* by multiphoton microscopy in Tg APP mice (Christie et al., 2001). Although ACh vasodilation was decreased in cerebral arteries from Tg APP mice (Tong et al., 2005), and following topical application onto the brain (Christie et al., 2001), in our hands its vasodilatory response was similar in wt and in Tg APP aortae. These results may be explained by the different origin of the vessels, cerebral compared to peripheral vessels, or the age of the animals. In AD, vessels are continuously exposed to high circulating levels of soluble Aβ, in contrast to the insoluble form of the peptide present in senile plaques occurring in brain. In our hands incubation with Aβ up to 15 min did not alter mice vessel tone. This is in contrast with the results of Thomas et al. (1996) and Crawford et al. (1998) obtained in rat aorta. Given that the methods used were very similar, we speculate that the rodent species accounts for this difference. However, in wt mice Aβ significantly enhanced the vasoconstriction to the thromboxane analog, paralleling the results obtained with noradrenaline, phenylephrine or ET-1 reported by other authors (Thomas et al., 1996; Crawford et al., 1998; Smith et al., 2007). Similarly, in the present study the vasodilation to ACh was decreased by Aβ (Smith et al., 2007) in wt mice. In contrast, the vessel responses in Tg APP were not modified by Aβ. These results suggest that in Tg APP mice, that express high levels of APP in the brain and in peripheral organs, including cerebral microvessels and the aorta (Paris et al., 2004), there is tolerance to Aβ effects due to the continuous exposure to the peptide. More importantly, both cannabinoids were able to normalize the Tg APP dysfunctional responses.

Cannabinoids induce vasodilatory effects in different isolated vessels, but so far these responses have not been studied in Tg APP mice. The CB_1/CB_2 mixed agonist WIN induced a concentration-dependent vasodilation of wt mice aortae, reaching 80% decrease of the maximal constriction to U46619, and higher than the vasodilation to ACh at 10 μM. The maximal vasodilatory effect to JWH in wt aortae was smaller compared to WIN. Cannabinoid-induced vasodilation, in spite of the presence of both CB_1 (Ashton et al., 2004) and CB_2 receptors in aortae, was completely insensitive to either CB_1 or CB_2 antagonism (data not shown). This is not without precedent, since the vascular effects of cannabinoids in many instances have been shown to be resistant to antagonism by cannabinoid antagonists, and they may involve activation of other targets (Randall et al., 2004; López-Miranda et al., 2008). We did not intend to characterize the mechanism underlying the vasodilatory effects of WIN and JWH in this work, since the pharmacology of the effects of cannabinoids is increasingly complicated (Randall et al., 2004; Stanley and O'Sullivan, 2014). Several possible targets could be proposed such as the putative "endothelial" cannabinoid receptor, potassium channel activation and calcium channel blockade. On the other hand, several cannabinoid agonists, including WIN, interact with peroxisome proliferator-activated receptors (PPAR) (O'Sullivan, 2016), members of the family of nuclear receptors, exerting vasodilation (O'Sullivan, 2007). Importantly, the vasodilation to both WIN and JWH was partially preserved in Tg APP mice, suggesting its possible therapeutic endorsement in AD.

We observed increased Col IV vessel density in AD specimens compared to control subjects, with a similar increase in Tg APP brain. Previous works have reported increased thickening of basement membranes in AD (Mancardi et al., 1980; Kalaria, 2002; Miao et al., 2005), in particular Col IV (Miao et al., 2005; Tong et al., 2005), associated or not with differences in density. In Tg APP mice similar changes were observed (Tong et al., 2005). Although the exact cause of increased basement membrane is unknown, several factors could be involved such as soluble Aβ and its progressive deposition in vessels, inflammatory mediators derived from activated glial cells around vessels and chronic changes in levels of vasoactive mediators (Grammas, 2011). Cannabinoid agonists, in particular CB_2 selective agonists, impinge on several of these factors by decreasing glial activation, inflammation and Aβ levels (Ramírez et al., 2005; Martín-Moreno et al., 2012; Wu et al., 2013; Chiurchiù et al., 2015), explaining the normalization in vessel density following prolonged oral treatment with the drugs. At the ultrastructural level, aortic endothelial cells appeared normal in Tg APP aortae, in agreement with their preservation found in other works (Iadecola et al., 1999; Miao et al., 2005), which contrasts with the endothelial disruption in Aβ treated vessels (Thomas et al., 1996). Therefore, altered vessel function is not a consequence of endothelial disruption or death. Interestingly the major change observed in Tg APP aortae compared to wt mice was the increase in Col IV in the basement membrane, paralleling the changes in AD brain microvasculature, which may be involved in altered vessel contractility.

We have here described important pharmacological effects of cannabinoid agonists with relevance for the therapy of a devastating disorder such as AD. Prolonged oral treatment abrogated the changes in microvasculature that are important for vascular function and the perivascular drainage of Aβ from the parenchyma, that would initiate or worsen Aβ angiopathy, leading to a vicious circle toward further accumulation of the peptide. Moreover, both cannabinoids improved endothelial-dependent relaxations impaired by Aβ and showed vasodilatory effects that are maintained in Tg APP mice, albeit being reduced. Finally, the therapeutic activation of CB_2R is safe and it does not trigger psychoactivity (Atwood and Mackie, 2010; Pertwee, 2012).

AUTHOR CONTRIBUTIONS

MLC conceived the work. MLC, TT, and DP designed the study. JN-D, NV, BB, AM, and MLC performed the experiments and analyzed the data. MLC, JN-D, and NV wrote the article. All authors revised and approved the version to be published.

ACKNOWLEDGMENTS

This work was supported by the Council of Madrid (S-BIO/0170/2006 and P2010/BMD-2349 to MLC) and by Instituto de Salud Carlos III/FISS (PI12/00590 to TT). AM received a fellowship from the Spanish Ministry of Education and Science and JN-D from FISS. Dr. R. Martínez-Murillo is acknowledged for preliminary EM experiments.

REFERENCES

Arendash, G. W., Su, G. C., Crawford, F. C., Bjugstad, K. B., and Mullan, M. (1999). Intravascular beta-amyloid infusion increases blood pressure: implications for a vasoactive role of beta-amyloid in the pathogenesis of Alzheimer's disease. *Neurosci. Lett.* 268, 17–20.

Arévalo-Martín, A., García-Ovejero, D., Gómez, O., Rubio-Araiz, A., Navarro-Galve, B., Guaza, C., et al. (2008). CB2 cannabinoid receptors as an emerging target for demyelinating diseases: from neuroimmune interactions to cell replacement strategies. *Br. J. Pharmacol.* 153, 216–225. doi: 10.1038/sj.bjp.0707466

Ashton, J. C., Appleton, I., Darlington, C. L., and Smith, P. F. (2004). Immunohistochemical localization of cerebrovascular cannabinoid CB1 receptor protein. *J. Cardiovasc. Pharmacol.* 44, 517–519. doi: 10.1097/00005344-200411000-00001

Aso, E., and Ferrer, I. (2014). Cannabinoids for treatment of Alzheimer's disease: moving toward the clinic. *Front. Pharmacol.* 5:37. doi: 10.3389/fphar.2014.00037

Atwood, B. K., and Mackie, K. (2010). CB2: a cannabinoid receptor with an identity crisis. *Br. J. Pharmacol.* 160, 467–479. doi: 10.1111/j.1476-5381.2010.00729.x

Baker, D., Pryce, G., Croxford, J. L., Brown, P., Pertwee, R. G., Huffman, J. W., et al. (2000). Cannabinoids control spasticity and tremor in a multiple sclerosis model. *Nature* 404, 84–87. doi: 10.1038/35003583

Campion, D., Dumanchin, C., Hannequin, D., Dubois, B., Belliard, S., Puel, M., et al. (1999). Early-onset autosomal dominant Alzheimer disease: prevalence, genetic heterogeneity, and mutation spectrum. *Am. J. Hum. Genet.* 65, 664–670.

Carnevale, D., Mascio, G., D'Andrea, I., Fardella, V., Bell, R. D., Branchi, I., et al. (2012). Hypertension induces brain β-amyloid accumulation, cognitive impairment, and memory deterioration through activation of receptor for advanced glycation end products in brain vasculature. *Hypertension* 60, 188–197. doi: 10.1161/HYPERTENSIONAHA.112.195511

Carnevale, D., Perrotta, M., Lembo, G., and Trimarco, B. (2016). Pathophysiological links among hypertension and Alzheimer's disease. *High Blood Press. Cardiovasc. Prev.* 23, 3–7. doi: 10.1007/s40292-015-0108-1

Cécyre, B., Thomas, S., Ptito, M., Casanova, C., and Bouchard, J. F. (2014). Evaluation of the specificity of antibodies raised against cannabinoid receptor type 2 in the mouse retina. *Naunyn Schmiedebergs Arch. Pharmacol.* 387, 175–184. doi: 10.1007/s00210-013-0930-8

Cheng, Y., Dong, Z., and Liu, S. (2014). β-Caryophyllene ameliorates the Alzheimer-like phenotype in APP/PS1 Mice through CB2 receptor activation and the PPARγ pathway. *Pharmacology* 94, 1–12. doi: 10.1159/000362689

Chiurchiù, V., Leuti, A., and Maccarrone, M. (2015). Cannabinoid signaling and neuroinflammatory diseases: a melting pot for the regulation of brain immune responses. *J. Neuroimmune Pharmacol.* 10, 268–280. doi: 10.1007/s11481-015-9584-2

Christie, R., Yamada, M., Moskowitz, M., and Hyman, B. (2001). Structural and functional disruption of vascular smooth muscle cells in a transgenic mouse model of amyloid angiopathy. *Am. J. Pathol.* 158, 1065–1071. doi: 10.1016/S0002-9440(10)64053-9

Crawford, F., Suo, Z., Fang, C., and Mullan, M. (1998). Characteristics of the *in vitro* vasoactivity of beta-amyloid peptides. *Exp. Neurol.* 150, 159–168.

de Bitencourt, R. M., Pamplona., F. A., and Takahashi, R. N. (2013). A current overview of cannabinoids and glucocorticoids in facilitating extinction of aversive memories: potential extinction enhancers. *Neuropharmacology* 64, 389–395. doi: 10.1016/j.neuropharm.2012.05.039

De March, Z., Zuccato, C., Giampà, C., Patassini, S., Bari, M., Gasperi, V., de Ceballos, M. L., et al. (2008). Cortical expression of brain derived neurotrophic factor and type-1 cannabinoid receptor after striatal excitotoxic lesions. *Neuroscience* 152, 734–740. doi: 10.1016/j.neuroscience.2007.11.044

Di Marzo, V., and De Petrocellis, L. (2012). Why do cannabinoid receptors have more than one endogenous ligand? *Philos. Trans. R. Soc. Lond. B. Biol. Sci.* 367, 3216–3228. doi: 10.1098/rstb.2011.0382

Fernández-Ruiz, J., Moreno-Martet, M., Rodríguez-Cueto, C., Palomo-Garo, C., Gómez-Cañas, M., Valdeolivas, S., et al. (2011). Prospects for cannabinoid therapies in basal ganglia disorders. *Brit. J. Pharmacol.* 163, 1365–1378. doi: 10.1111/j.1476-5381.2011.01365.x

Gardiner, S. M., March, J. E., Kemp, P. A., and Bennett, T. (2001). Regional haemodynamic responses to the cannabinoid agonist, WIN 55212-2, in conscious, normotensive rats, and in hypertensive, transgenic rats. *Brit. J. Pharmacol.* 133, 445–453. doi: 10.1038/sj.bjp.0704100

Glass, M., Dragunow, M., and Faull, R. L. (2000). The pattern of neurodegeneration in Huntington's disease: a comparative study of cannabinoid, dopamine, adenosine and GABA(A) receptor alterations in the human basal ganglia in Huntington's disease. *Neuroscience* 97, 505–519. doi: 10.1016/S0306-4522(00)00008-7

Gómez Del Pulgar, T., de Ceballos, M. L., Guzmán, M., and Velasco, G. (2002). Cannabinoids protect astrocytes from ceramide-induced apoptosis through the phosphatidylinositol 3-kinase/protein kinase B pathway. *J. Biol. Chem.* 277, 36527–36533. doi: 10.1074/jbc.M205797200

Grammas, P. (2011). Neurovascular dysfunction, inflammation and endothelial activation: implications for the pathogenesis of Alzheimer's disease. *J. Neuroinflammation* 8:26. doi: 10.1186/1742-2094-8-26

Hamel, E., Royea, J., Ongali, B., and Tong, X. K. (2016). Neurovascular and cognitive failure in Alzheimer's disease: benefits of cardiovascular therapy. *Cell. Mol. Neurobiol.* 36, 219–232. doi: 10.1007/s10571-015-0285-4

Hardy, J. (1996). New insights into the genetics of Alzheimer's disease. *Ann. Med.* 28, 255–258.

Hardy, J., and Selkoe, D. J. (2002). The amyloid hypothesis of Alzheimer's disease: progress and problems on the road to therapeutics. *Science* 297, 353–356. doi: 10.1126/science.1072994

Howlett, A. C., Barth, F., Bonner, T. I., Cabral, G., Casellas, P., Devane, W., et al. (2002). International union of pharmacology. XXVII. Classification of cannabinoid receptors. *Pharmacol. Rev.* 54, 61–202. doi: 10.1124/pr.54.2.161

Hsiao, K., Chapman, P., Nilsen, S., Eckman, C., Harigaya, Y., Younkin, S., et al. (1996). Correlative memory deficits, Abeta elevation, and amyloid plaques in transgenic mice. *Science* 274, 99–102. doi: 10.1126/science.274.5284.99

Huffman, J. W., Liddle, J., Yu, S., Aung, M. M., Aboot, M. E., Wiley, J. L., et al. (1999). 3-(1′,1′-Dimethylbutyl)-1-deoxy-delta-8-THC and related compounds: synthesis and selective ligands for the CB2 receptor. *Bioorg. Med. Chem. Lett.* 7, 2905–2914.

Iadecola, C. (2010). The overlap between neurodegenerative and vascular factors in the pathogenesis of dementia. *Acta Neuropathol.* 120, 287–296. doi: 10.1007/s00401-010-0718-6

Iadecola, C., Zhang, F., Niwa, K., Eckman, C., Turner, S. K., Fischer, E., et al. (1999). SOD1 rescues cerebral endothelial dysfunction in mice overexpressing amyloid precursor protein. *Nat. Neurosci.* 2, 157–161.

Kalaria, R. N. (2002). Small vessel disease and Alzheimer's dementia: pathological considerations. *Cerebrovasc. Dis.* 13(Suppl. 2), 48–52. doi: 10.1159/000049150

Leweke, F. M., Mueller, J. K., Lange, B., and Rohleder, C. (2016). Therapeutic potential of cannabinoids in psychosis. *Biol. Psychiatry* 79, 604–612. doi: 10.1016/j.biopsych.2015.11.018

Li, Y., and Kim, J. (2015). Neuronal expression of CB2 cannabinoid receptor mRNAs in the mouse hippocampus. *Neuroscience* 311, 253–267. doi: 10.1016/j.neuroscience.2015.10.041

López-Miranda, V., Herradón, E., and Martín, M. I. (2008). Vasorelaxation caused by cannabinoids: mechanisms in different vascular beds. *Curr. Vasc. Pharmacol.* 6, 335–346. doi: 10.2174/157016108785909706

Mancardi, G. L., Perdelli, F., Rivan, C., Leonardi, A., and Bugiani, O. (1980). Thickening of the basement membrane of cortical capillaries in Alzheimer's disease. *Acta Neuropathol.* 49, 79–83.

Marsicano, G., Wotjak, C. T., Azad, S. C., Bisogno, T., Rammes, G., Cascio, M. G., et al. (2002). The endogenous cannabinoid system controls extinction of aversive memories. *Nature* 418, 530–534. doi: 10.1038/nature00839

Martín-Moreno, A. M., Brera, B., Spuch, C., Carro, E., García-García, L., Delgado, M., et al. (2012). Prolonged oral cannabinoid administration prevents neuroinflammation, lowers β-amyloid levels and improves cognitive performance in Tg APP 2576 mice. *J. Neuroinflammation* 9:8. doi: 10.1186/1742-2094-9-8

Miao, J., Xu, F., Davis, J., Otte-Höller, I., Verbeek, M. M., and Van Nostrand, W. E. (2005). Cerebral microvascular amyloid beta protein deposition induces vascular degeneration and neuroinflammation in transgenic mice expressing human vasculotropic mutant amyloid beta precursor protein. *Am. J. Pathol.* 167, 505–515. doi: 10.1016/S0002-9440(10)62993-8

Morris, A. W., Carare, R. O., Schreiber, S., and Hawkes, C. A. (2014). The cerebrovascular basement membrane: role in the clearance of β-amyloid and cerebral amyloid angiopathy. *Front. Aging Neurosci.* 6:251. doi: 10.3389/fnagi.2014.00251

O'Sullivan, S. E. (2007). Cannabinoids go nuclear: evidence for activation of peroxisome proliferator-activated receptors. *Br. J. Pharmacol.* 152, 576–582. doi: 10.1038/sj.bjp.0707423

O'Sullivan, S. E. (2016). An update on peroxisome proliferator-activated receptor (PPAR) activation by cannabinoids. *Br. J. Pharmacol.* 173, 1899–1910. doi: 10.1111/bph.13497

Paris, D., Patel, N., Delle Donne, A., Quadros, A., Smeed, R., and Mullan, M. (2004). Impaired angiogenesis in a transgenic mouse model of cerebral amyloidosis. *Neurosci. Lett.* 366, 80–85. doi: 10.1016/j.neulet.2004.05.017

Pertwee, R. G. (2012). Targeting the endocannabinoid system with cannabinoid receptor agonists: pharmacological strategies and therapeutic possibilities. *Philos. Trans. R. Soc. Lond. B. Biol. Sci.* 367, 3353–3363. doi: 10.1098/rstb.2011.0381

Ramírez, B. G., Blázquez, C., Gómez del Pulgar, T., Guzmán, M., and de Ceballos, M. L. (2005). Prevention of Alzheimer's disease pathology by cannabinoids: neuroprotection mediated by blockade of microglial activation. *J. Neurosci.* 25, 1904–1913. doi: 10.1523/JNEUROSCI.4540-04.2005

Randall, M. D., Kendall, D. A., and O'Sullivan, S. E. (2004). The complexities of the cardiovascular actions of cannabinoids. *Br. J. Pharmacol.* 142, 20–26. doi: 10.1016/j.neulet.2004.05.017

Rinaldi-Carmona, M., Barth, F., Héaulme, M., Shire, D., Calandra, B., Congy, C., et al. (1994). SR141716A, a potent and selective antagonist of the brain cannabinoid receptor. *FEBS Lett.* 350, 240–244.

Rinaldi-Carmona, M., Barth, F., Millan, J., Derocq, J.-M., Casellas, P., Congy, C., et al. (1998). SR144528, the first potent and selective antagonist of the CB2 cannabinoid receptor. *J. Pharmacol. Exp. Ther.* 284, 644–650.

Smith, C. C., Stanyer, L., Betteridge, D. J., and Cooper, M. B. (2007). Native and oxidized low-density lipoproteins modulate the vasoactive actions of soluble beta-amyloid peptides in rat aorta. *Clin. Sci.* 113, 427–434. doi: 10.1042/CS20070082

Stanley, C., and O'Sullivan, S. E. (2014). Vascular targets for cannabinoids: animal and human studies.*Br. J. Pharmacol.* 171, 1361–1378. doi: 10.1111/bph.12560

Suo, Z., Humphrey, J., Kundtz, A., Sethi, F., Placzek, A., Crawford, F., et al. (1998). Soluble Alzheimers beta-amyloid constricts the cerebral vasculature *in vivo*. *Neurosci. Lett.* 257, 77–80.

Thomas, A. J., Morris, C. M., Ferrier, I. N., and Kalaria, R. N. (2000). Distribution of amyloid beta 42 in relation to the cerebral microvasculature in an elderly cohort with Alzheimer's disease. *Ann. N. Y. Acad. Sci.* 903, 83–88. doi: 10.1111/j.1749-6632.2000.tb06353.x

Thomas, T., Thomas, G., McLendon, C., Sutton, T., and Mullan, M. (1996). β-Amyloid-mediated vasoactivity and vascular endothelial damage. *Nature* 380, 168–171.

Tong, X., and K., Nicolakakis, N., Kocharyan, A., Hamel, E. (2005). Vascular remodeling versus amyloid beta-induced oxidative stress in the cerebrovascular dysfunctions associated with Alzheimer's disease. *J. Neurosci.* 25, 11165–11174. doi: 10.1523/JNEUROSCI.4031-05.2005

Tsou, K., Brown, S., Sañudo-Peña, M. C., Mackie, K., and Walker, J. M. (1997). Immunohistochemical distribution of cannabinoid CB1 receptors in the rat central nervous system. *Neuroscience* 83, 393–411.

Tsou, K., Mackie, K., Sañudo-Peña, M. C., and Walker, J. M. (1999). Cannabinoid CB1 receptors are localized primarily on cholecystokinin-containing gabaergic interneurons in the rat hippocampal formation. *Neuroscience* 93, 969–975.

Varga, K., Lake, K. D., Huangfu, D., Guyenet, P. G., and Kunos, G. (1996). Mechanism of the hypotensive action of anandamide in anesthetized rats. *Hypertension* 28, 682–686.

Wu, J., Bie, B., Yang, H., Xu, J. J., Brown, D. L., and Naguib, M. (2013). Activation of the CB2 receptor system reverses amyloid-induced memory deficiency. *Neurobiol. Aging* 34, 791–804. doi: 10.1016/j.neurobiolaging.2012.06.011

Conflict of Interest Statement: The authors declare that the research was conducted in the absence of any commercial or financial relationships that could be construed as a potential conflict of interest.

Copyright © 2016 Navarro-Dorado, Villalba, Prieto, Brera, Martín-Moreno, Tejerina and de Ceballos. This is an open-access article distributed under the terms of the Creative Commons Attribution License (CC BY). The use, distribution or reproduction in other forums is permitted, provided the original author(s) or licensor are credited and that the original publication in this journal is cited, in accordance with accepted academic practice. No use, distribution or reproduction is permitted which does not comply with these terms.

frontiers in Neuroscience

REVIEW
published: 13 September 2016
doi: 10.3389/fnins.2016.00406

Targeting Cannabinoid CB_2 Receptors in the Central Nervous System. Medicinal Chemistry Approaches with Focus on Neurodegenerative Disorders

Gemma Navarro[1,2,3], *Paula Morales*[4,5], *Carmen Rodríguez-Cueto*[2,6,7], *Javier Fernández-Ruiz*[2,6,7], *Nadine Jagerovic*[4] *and Rafael Franco*[1,2,3]*

[1] Department of Biochemistry and Molecular Biomedicine, University of Barcelona, Barcelona, Spain, [2] Centro de Investigación en Red sobre Enfermedades Neurodegenerativas (CIBERNED), Instituto de Salud Carlos III, Madrid, Spain, [3] Cell and Molecular Neuropharmacology, Institut de Biomedicina (IBUB), Universitat de Barcelona, Barcelona, Spain, [4] Instituto de Química Médica, Consejo Superior de Investigaciones Científicas, Madrid, Spain, [5] Center for Drug Discovery, University of North Carolina at Greensboro, Greensboro, NC, USA, [6] Departamento de Bioquímica, Facultad de Medicina, Instituto Universitario de Investigación en Neuroquímica, Universidad Complutense, Madrid, Spain, [7] Instituto Ramón y Cajal de Investigación Sanitaria, Madrid, Spain

OPEN ACCESS

Edited by:
Marialessandra Contino, University of Bari Aldo Moro, Italy

Reviewed by:
Aurel Popa-Wagner, University of Rostock, Germany
Michael Decker, University of Würzburg, Germany
Claudia Mugnaini, University of Siena, Italy

***Correspondence:**
Rafael Franco
rfranco@ub.edu; rfranco123@gmail.com

Specialty section:
This article was submitted to Neurodegeneration, a section of the journal Frontiers in Neuroscience

Received: *25 May 2016*
Accepted: *22 August 2016*
Published: *13 September 2016*

Citation:
Navarro G, Morales P, Rodríguez-Cueto C, Fernández-Ruiz J, Jagerovic N and Franco R (2016) Targeting Cannabinoid CB_2 Receptors in the Central Nervous System. Medicinal Chemistry Approaches with Focus on Neurodegenerative Disorders. Front. Neurosci. 10:406. doi: 10.3389/fnins.2016.00406

Endocannabinoids activate two types of specific G-protein-coupled receptors (GPCRs), namely cannabinoid CB_1 and CB_2. Contrary to the psychotropic actions of agonists of CB_1 receptors, and serious side effects of the selective antagonists of this receptor, drugs acting on CB_2 receptors appear as promising drugs to combat CNS diseases (Parkinson's disease, Huntington's chorea, cerebellar ataxia, amyotrohic lateral sclerosis). Differential localization of CB_2 receptors in neural cell types and upregulation in neuroinflammation are keys to understand the therapeutic potential in *inter alia* diseases that imply progressive neurodegeneration. Medicinal chemistry approaches are now engaged to develop imaging tools to map receptors in the living human brain, to develop more efficacious agonists, and to investigate the possibility to develop allosteric modulators.

Keywords: heteromer, microglia, astroglia, M0/M1/M2 phenotype, neuroprotection, neurorestoration, GPCR, amyotrophic lateral sclerosis

INTRODUCTION

To date only two cannabinoid receptors have been identified and completely accepted as key members of the endocannabinoid signaling. The CB_1 receptor (CB_1R) is mainly expressed in the central nervous system (CNS) (Hu and Mackie, 2015), whereas, the CB_2 receptor (CB_2R) is mainly expressed in the periphery, especially in blood cells, and in blood-cell producing organs (Onaivi et al., 1999; Atwood and Mackie, 2010; Atwood et al., 2012). Other receptors, e.g., GPR55, the cation channel TRPV1 and the nuclear receptors of the PPAR family, are also under discussion as possible members of the endocannabinoid receptor family. CB_1R and CB_2R belong to the most populated family of the human proteome, i.e., to the family of receptors coupled to heterotrimeric G proteins (GPCRs). More specifically they are members of class A GPCRs, which are characterized by being structurally similar to rhodopsin, for having an extracellular N-terminal domain, a seven α-helical transmembrane domain, and a C-terminal domain of 73 (for CB_1R) or of 59 (for CB_2R) amino acids. Total length of the most common[1] protein products is 472 for CB_1R and 360 for CB_2R. The

[1] Isoforms of endocannabinoid receptors have been identified (details available at www.uniprot.org.)

difference in receptor length comes from the bigger N-terminal domain of the CB_1R (116 vs. 33 amino acids).

Soon after its discovery and the realization of the relevant role of endogenous cannabinoids, the CB_1R was considered a potential target to combat CNS diseases. In fact, the CB_1R is considered the class A GPCR member with the highest expression in the CNS. In sharp contrast, controversy surrounds expression of CB_2R in the CNS, and until recently this receptor was not considered as target for neurological or neuropsychiatric diseases (Atwood and Mackie, 2010; Atwood et al., 2012). This paper scans the literature that supports the view that CB_2R may have now more potential than CB_1R to combat some CNS disorders, in particular those related to neuroinflammatory, and neurodegenerative events. The paper also informs on current developments in medicinal chemistry aspects of CB_2R-based CNS drug discovery.

BETTER PROSPECTS FOR CB_2R THAN FOR CB_1R IN CNS DISEASES

GPCRs constitute the target of approximately 40% of approved drugs. Drug development programs are still heavily relying on the potential of GPCRs for a huge variety of diseases. Agonists, which are able to activate the receptor and compete with the endogenous agonist, and antagonists, which block the receptor and impede activation by the endogenous agonist, have therapeutic potential. However, the number of medications that consist of GPCR antagonists outnumbers that of GPCR agonists. In general terms, the higher success of antagonists means that they have fewer side effects than agonists, although other causes overlay. The endocannabinoid system is a very special case as endogenous compounds produced by neurons and acting on central CB_1Rs are absolutely required for higher brain functions, but any synthetic or natural (e.g., Δ^9-tetrahydrocannabinol) agonist reaching the brain and hitting CB_1R has proved to have psychotropic actions in animal models of disease and in humans. Therefore, the potential of CB_1Rs as targets for diseases of the CNS, and also peripheral disorders, has been limited by the psychoactive side effects derived from their agonists, and for the need to consider the risk-benefit balance. In this context, some researchers wanted to develop CB_1R antagonists (including inverse agonists) as a safer alternative in those pathologies having an overactivity of the endocannabinoid system (e.g., obesity, addiction, schizophrenia), although side effects were also evident with such strategy (see below).

The first two molecules targeting CB_1R that reached the therapeutic market (in the 80s) were Δ^9-tetrahydrocannabinol, also known as dronabinol (marketed as Marinol®), and nabilone (marketed as Cesamet®) (**Figure 1**), both prescribed to combat nausea and vomiting, as well anorexia, derived from cancer, and AIDS treatments, respectively (Green et al., 1989), but their use was limited. By contrast, a CB_1R antagonist/inverse agonist, rimonabant (Acomplia®), was approved in 2006 to treat obesity, and metabolic syndrome (Carai et al., 2006) and generated extremely high expectations. Unfortunately, the drug had to be retired due to side effects, especially due to reports of suicide (Sam et al., 2011). Consequently, chances, that other CB_1R selective drug may advance though regulatory bodies, and reach the market have dramatically diminished. In this context, the CB_2R has taken the lead in the race to find novel cannabinoid-related drugs for CNS diseases. On the one hand, CB_1R is expressed in almost any brain region, and in many neuronal cell types, whereas CB_2R expression in neurons is restricted to few areas. Accordingly, fewer side effects are expected when drugs are targeting receptors with restricted expression than when drugs are targeting receptors widely expressed in the CNS. Furthermore, CB_2R are upregulated in a variety of CNS diseases that course with activated microglia or astroglia. Then the CB_2R but not the CB_1R is a promising candidate to consider in diseases with a neuroinflammatory component. It is even possible that the activation of CB_2Rs may explain recent controversies in relation with the consumption of cannabis as a factor either increasing risk or preventing against spontaneous brain insults (e.g., intracerebral hemorrhage). Recent epidemiological studies suggest a potential protective effect of cannabis to the modulation of C-reactive protein response in intracerebral hemorrhage (Di Napoli et al., 2012, 2016; Alshaarawy and Anthony, 2015), an effect that could be possibly related to CB_2R activation, although this has not been investigated. Advantages of developing CB_2R selective drugs to prevent neurodegeneration in cases of neuroinflammation are presented later in this article.

As macrophages express CB_2R and microglia is somehow a similar cell type, these receptors were soon identified in microglial cells, but further research demonstrated that they can be also found in other types of glial cells (see below). There is however, some controversy on the degree of CB_2R expression in resting vs. activated microglial cells. Also the activated microglial phenotype is different in macrophages filtered from the blood into the CNS and in resident microglia that becomes activated due to, *inter alia*, accumulation of protein aggregates such as alpha-synuclein, or ß-amyloid. Remarkably, (see Franco and Fernández-Suárez, 2015 and references therein) a better understanding of the expression and role of CB_2R in the different microglial phenotypes (M0, M1, M2) will help in designing CB_2R selective ligands able to induce the neuroprotective/anti-inflammatory-skewed phenotype(s).

CB_2R may be also expressed by CNS neurons. The role of CB_2Rs in schizophrenia, depression, food consumption, and drug addiction has been demonstrated in different laboratories and the results are consistent with neuronal expression of the receptor (Onaivi et al., 2008a,b,c; Hu et al., 2009; García-Gutiérrez et al., 2010; Ishiguro et al., 2010a,b; García-Gutiérrez and Manzanares, 2011; Ortega-Alvaro et al., 2011; Aracil-Fernández et al., 2012; Navarrete et al., 2012, 2013; Bahi et al., 2014; Blanco-Calvo et al., 2014; Ortega-Álvaro et al., 2015; Rodríguez-Arias et al., 2015; García-Cabrerizo and García-Fuster, 2016). The receptor is significantly expressed in neurons in the brain stem (Van Sickle et al., 2005), in the cerebellum (Skaper et al., 1996; Ashton et al., 2006; Gong et al., 2006; Rodríguez-Cueto et al., 2014) in the internal and the external segments of the *globus pallidus* of the non-human primate (Lanciego et al., 2011), and in the *substantia nigra* (in humans, not in rodents) (García et al., 2016; Gómez-Gálvez et al., 2016).

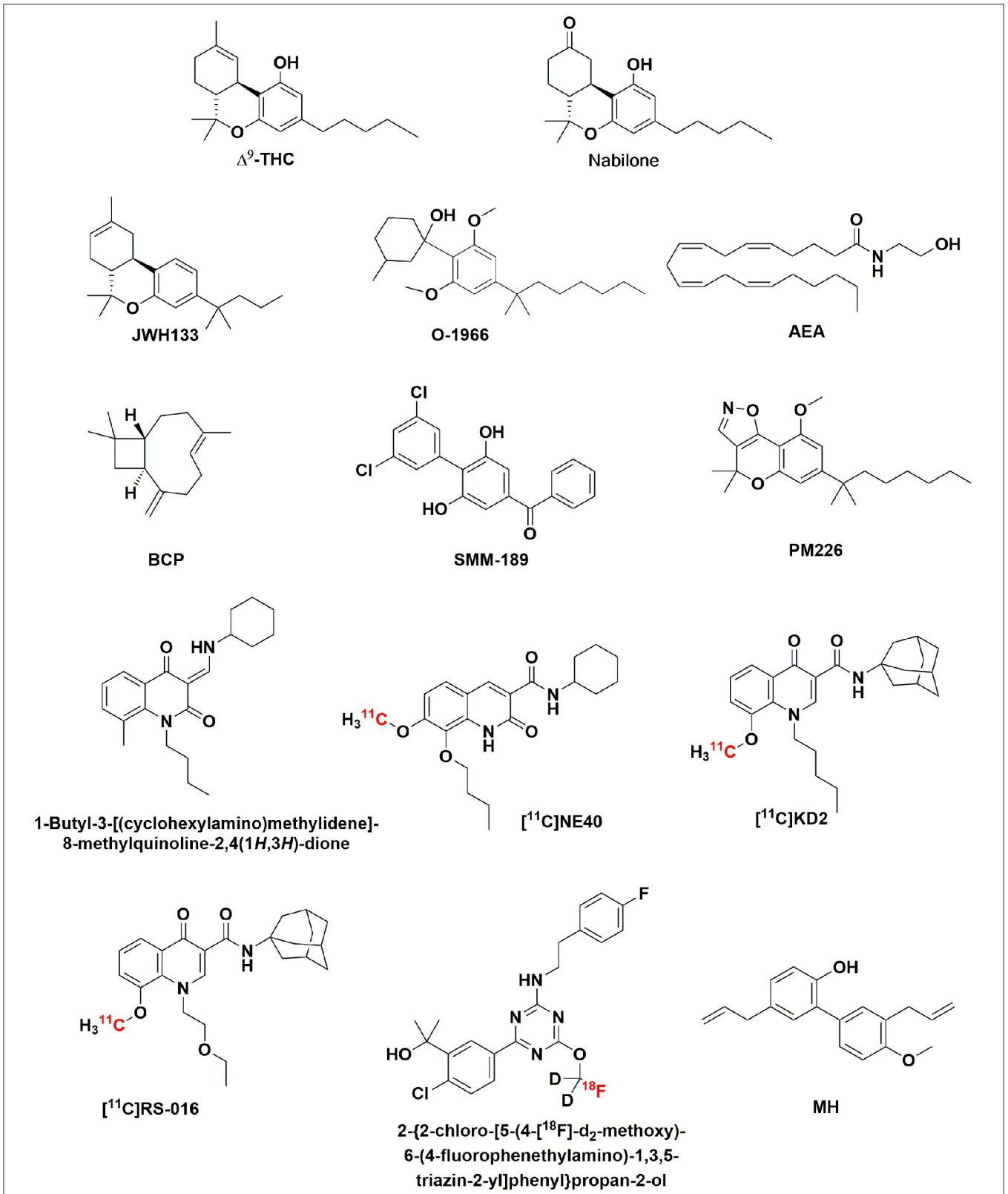

FIGURE 1 | Chemical structure of Δ^9-THC, nabilone, and the CB_2R ligands: JWH133, 0-1966, AEA, BCP, SMM-189, PM226, 1-butyl-3-[(cyclohexylamino)methylidene]-8-methylquinoline-2,4(1*H*,3*H*)-dione, [^{11}C]NE40, [^{11}C]KD2, [^{11}C]RS-016, 2-{2-chloro-[5-(4-[^{18}F]-d_2-methoxy)-6-(4-fluorophenethylamino)-1,3,5-triazin-2-yl]phenyl}propan-2-ol.

Different laboratories working with rodents or primates have also identified receptor expression in neurons of the prefrontal cortex and hippocampus (Callén et al., 2012; den Boon et al., 2012; Sierra et al., 2015; García-Cabrerizo and García-Fuster, 2016). Expression of CB_2R in the basal ganglia show promise in Parkinson's disease and Huntington's chorea; the presence of the receptor in hippocampus and prefrontal cortex makes it attractive for Alzheimer's disease and the expression in brain stem and cerebellum opens novel therapeutic avenues for a variety of diseases such as hereditary spinocerebellar ataxias. Last but not least, the data on CB_2R-mediated endocannabinoid regulation of microglial activation makes the receptor attractive for diseases with a neuroinflammatory component.

Cannabinoid neuroregulation is mainly based on retrograde signaling (Alger, 2002), i.e., endocannabinoids come from post-synaptic elements to activate presynaptic receptors. However, postsynaptic CB_2Rs have been also reported (Brusco et al., 2008). The combination of restricted neuronal expression with the possibility of targeting pre- or postsynaptic receptors, makes the CB_2R a really attractive target.

CB_2R IN NEURODEGENERATIVE DISORDERS. RELEVANCE OF DIFFERENTIAL EXPRESSION OF CB_2R IN NEURAL CELLS

The preservation of neuronal integrity and survival is one of the most promising therapeutic possibilities of CB_2R-targeting cannabinoids (Atwood et al., 2012). There is potential in pain and in numerous acute or chronic neurodegenerative/neuroinflammatory conditions (Jhaveri et al., 2007; Micale et al., 2007; Campillo and Páez, 2009). The neuroprotective potential of compounds targeting the CB_2R is, first of all, the logical consequence of their location in key cell types (e.g., in specific neuronal subsets, activated astrocytes, reactive microglia, perivascular microglia, oligodendrocytes, and neural progenitor cells), and also in some structures (e.g., the blood-brain barrier (BBB)) that are critical for the maintenance of the CNS integrity (Amenta et al., 2012; Chung et al., 2016) (**Figure 2A**). Such variety of locations enable compounds capable to selectively activate the CB_2R to exert a selective control over the specific functions fulfilled by these cells in degeneration, protection and/or repair (Fernández-Ruiz et al., 2014). For example, BBB function is under the control of CB_2R-mediated signals (Fujii et al., 2014), which maintain the integrity of tight junctions, inhibit leukocyte infiltration, and facilitate β-amyloid clearance (Vendel and de Lange, 2014).

CB_2Rs in glial cells recruited to the site of the neurodegeneration, appear to be critical for preserving the neuronal integrity and function (Savonenko et al., 2015). In fact, CB_2R may be absent of these cells in resting conditions, with a weak expression in the healthy brain. As the receptors are strongly up-regulated when glial cells are activated in conditions of neurodegeneration (Fernández-Ruiz et al., 2007, 2015), they have potential from a therapeutic point of view (**Figure 2B**). Up-regulation may occur in both astrocytes and microglial cells, but the CB_2R-mediated signaling may vary depending *inter alia* on the type of pathology and the experimental model. CB_2R-mediated neuroprotection/neurorestoration mechanisms are of special interest in disorders that affect movement-related areas, such as (i) Parkinson's and Huntington's diseases (affecting the basal ganglia, and producing rigidity, postural instability, bradykinesia, tremor, and chorea), (ii) autosomal dominant spinocerebellar ataxias (affecting the cerebellum and its afferent and efferent connections, and producing loss of balance, and motor incoordination), and (iii) amyotrophic lateral sclerosis (ALS) (affecting upper and lower spinal motor neurons, and producing muscle denervation and atrophy, which results in a progressive weakness and paralysis affecting voluntary muscles). For example, in this last disorder, CB_2Rs become up-regulated in microglial cells recruited at the spinal cord of patients (Yiangou et al., 2006), a fact corroborated by studies in the TDP-43 mouse model of the disease (Espejo-Porras et al., 2015). However, apart from microglial cells, other CB_2R-positive cells were found in this murine model (Espejo-Porras et al., 2015). In another murine model of ALS, (the SOD-1 mouse), CB_2R also become up-regulated, but the study did not characterize the type of cell that was expressing the receptors (Shoemaker et al., 2007).

Interestingly, microglial CB_2Rs appear up-regulated in the cerebellum of patients with different autosomal dominant cerebellar ataxias, but such trend was also found in activated astrocytes located in the cerebellar parenchyma and in the periphery of blood vessels, and in certain neuronal subpopulations (Rodríguez-Cueto et al., 2014). Similarly, increased levels of CB_2R are found in both striatal activated astrocytes and reactive microglial cells after an insult with malonate in rats, an experimental model of Huntington's disease (Sagredo et al., 2009). Although data collected from Huntington's disease patients or obtained in genetic models of the disease (e.g., R6/1, R6/2) indicated that CB_2R were located and up-regulated only in microglial cells (Palazuelos et al., 2009), a more recent study situated the up-regulation of these receptors in vascular cells, not in activated glial cells, in HD patients (Dowie et al., 2014).

In yet another neurodegenerative condition affecting the basal ganglia circuits, (Price et al., 2009) were the first to demonstrate up-regulation of CB_2R in microglial cells recruited at the *substantia nigra* in MPTP-lesioned mice. In the study it was not addressed whether there were other CB_2R-positive cells that do not correspond to reactive microglia. We investigated the issue in parkinsonian patients using *postmortem* samples and identified such up-regulation in microglial cells (labeled with Iba-1) and in another unidentified cell type (Gómez-Gálvez et al., 2016).

CB_2R has potential in demyelinating disorders (e.g., multiple sclerosis; Molina-Holgado et al., 2002; Gomez et al., 2010, 2011). In fact, CB_2R are present in oligodendrocytes, and more importantly, in their natural precursor cells, so that they may play a role in their survival, proliferation, and differentiation. CB_2Rs have been also identified in neural progenitor cells, and it appears that they can play a role in the proliferation and differentiation of these precursors (Palazuelos et al., 2006, 2012; Goncalves et al., 2008; Avraham et al., 2014), opening the possibility to

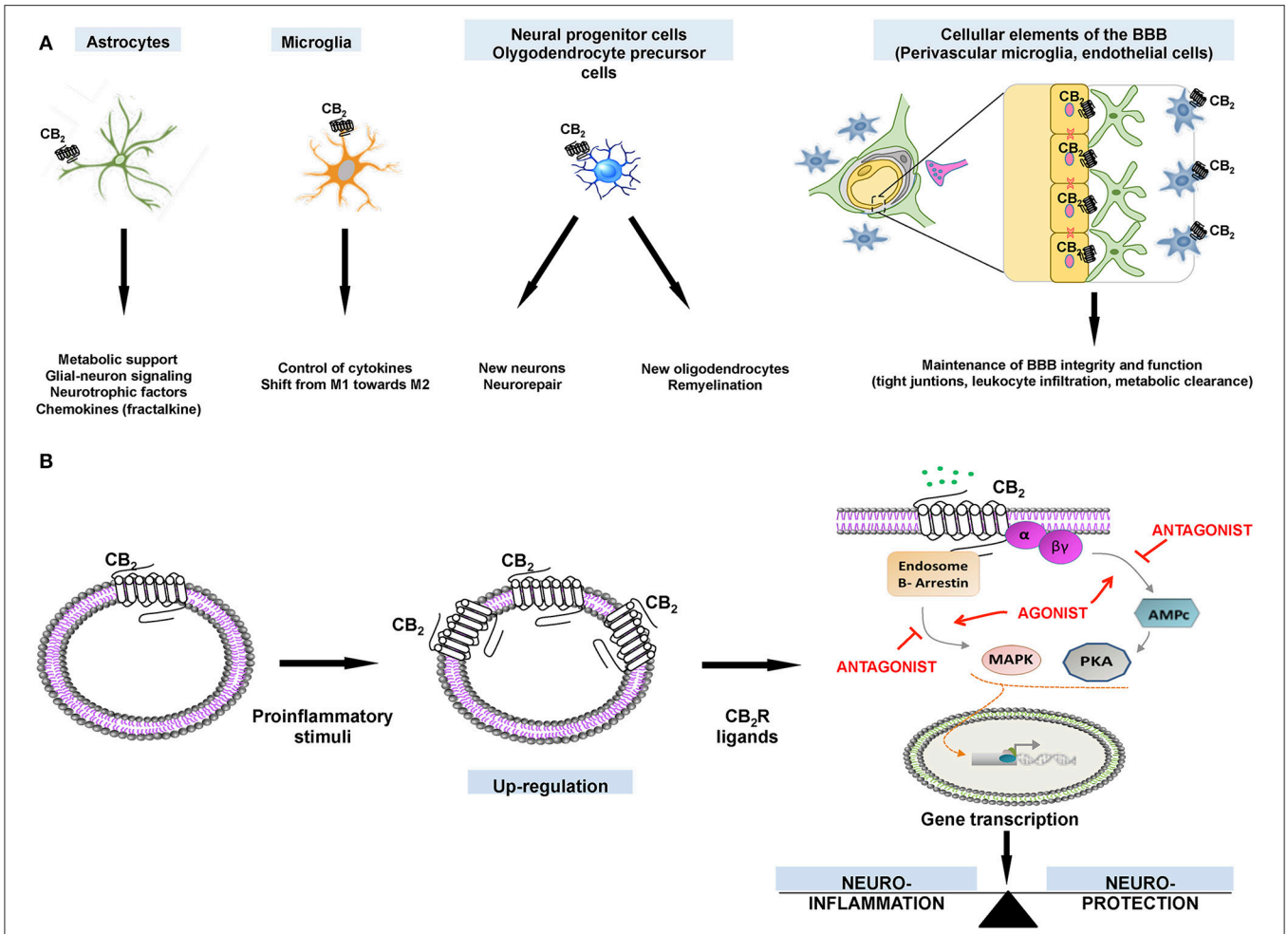

FIGURE 2 | (A). Expression of CB_2Rs in different neural cell types and how receptor activation may impact on cell-specific functions. **(B)** Cellular events that explain the therapeutic possibilities for ligands that target CB_2Rs, which are upregulated in activated glial cells.

facilitate neurorestoration by pharmacologically manipulating this receptor. Lastly, the identification of CB_2Rs in perivascular microglial cells in the cerebellum (Núñez et al., 2004) may be possibly related to the role attributed to these receptors at the level of the BBB (see above).

CHALLENGES IN CB_2R-BASED DRUG DESIGN

Pharmacology of cannabinoid receptors is complex due to the lipophilic nature of many natural and synthetic agonists. Endogenous agonists of many class A GPCRs are hydrophilic, which contrast with the lipophilic nature of endocannabinoids. Pharmacological characterization by radioligand binding to CB_2R is especially complex. On the one hand, the binding site extends deeply within the seven transmembrane domain of the receptor, and the two available radiolabeled ligands (tritiated CP-55940 and tritiated WIN-55212-2) do not interact with exactly the same amino acid residues in the orthosteric center; in particular CP-55940 does not interact with a conserved lysine residue in the binding site (Tao et al., 1999). Furthermore, it is hypothesized that cannabinoids may not reach the binding site from the outside of the cells but by lateral diffusion via the lipid bilayer of the plasma membrane (Guo et al., 2003; Makriyannis et al., 2005; Hurst et al., 2010). These features suggest that newly synthesized drugs or newly discovered natural cannabinoids have qualitatively different modes of binding to CB_2Rs. On the other hand, the nonspecific binding to membranes from natural CNS sources is high and leads to low-confidence values of the amount of receptor in neural cells. This problem is partially solved by performing the assays in heterologous cells expressing the human receptor; such approach provides reliable parameters for drug discovery. The complex pharmacology is also slowing the discovery of allosteric centers, and accordingly, of allosteric CB_2R modulators.

GPCR pharmacology must somehow be revisited due to the occurrence of receptor heteromers (Cordomí et al., 2015; Franco et al., 2016). Each heteromer is unique and functionally different from the two constituting receptors. In fact, affinity

of agonists/antagonists may change when a given receptor is forming heteroreceptor complexes, and more importantly, signaling cascades may be heteromer-specific (Ferré et al., 2009; Franco et al., 2016). Also relevant is the fact that presynaptic heteromers seem to be different from those in post-synaptic locations, i.e., a given GPCR may form different heteromers in pre- or post-synaptic membranes. Cannabinoid receptors may form a variety of heteromers with other class a GPCRs (see www.gpcr-hetnet.com; Borroto-Escuela et al., 2014). Interestingly, the two cannabinoid receptors may interact and give rise to CB_1R-CB_2R heteromers (Callén et al., 2012; Sierra et al., 2015). In agreement with the widespread distribution of CB_2Rs in brain and the robust expression of CB_2Rs in the *globus pallidus*, CB_1R-CB_2R heteromers are abundant in basal ganglia output neurons; available data indicate that these CB_1R-CB_2R heteromers are mainly post-synaptic. Pallidal expression of heteromers investigated in a primate model of Parkinson's disease was evident in naïve and parkinsonian animals, but it was markedly reduced in the levodopa-induced dyskinetic group (Sierra et al., 2015). Although likely, cannabinoid-receptor containing heteromers have not been identified and characterized in glial cells. Heteromer expression is worth considering on designing drugs targeting CB_2R. In particular pallidal CB_1R-CB_2R heteromers constitute a specific target in Parkinson's disease. A main advantage of selectively targeting GPCR heteromers, i.e., to use drugs that preferentially act on heteromer-expressing cells, is the reduction of side effects.

CB_2R LIGANDS AS THERAPEUTIC AGENTS IN CNS DISEASES

Positron Emission Tomography Reagents for Brain Imaging

Studies of CB_2R ligands as diagnostic agents for noninvasive brain imaging have been reported. Positron emission tomography (PET) provides a sensitive and non-invasive imaging technique to quantify CB_2R expression in the CNS. This technique requires radioligands with high affinity and high specificity toward CB_2R. Despite the development of highly selective CB_2R ligands (Han et al., 2014), a limited number of PET radiotracers for imaging CB_2R have been reported. Whereas, novel PET tracers for CB_1R in brain imaging have been evaluated in clinical trials, few CB_2R radioligands have been tested in humans. Few years ago, the first PET tracers for CB_2R were presented as candidates for the *in vivo* imaging of neuroinflammatory events (Evens and Bormans, 2010). Preliminary clinical assays of the first CB_2R radioligand, [^{11}C]NE40 (**Figure 1**), showed appropriate fast brain kinetics in the healthy human brain (Ahmad et al., 2013). A major challenge is the development of CB_2R PET agents with maximized brain penetration and minimized non-specific binding. In this sense, structural optimization of [^{11}C]KD2 (**Figure 1**) (Mu et al., 2013), a potential PET tracer with poor brain penetration, led to the discovery of [^{11}C]RS-016 (**Figure 1**), which showed slightly improved blood-brain penetration, and higher specific CB_2R binding in murine spleen tissues and *postmortem* ALS patient spinal cord tissues (Contartese et al., 2012; Slavik et al., 2015a,b). A promising PET tracer candidate for the *in vivo* evaluation of neuroinflammation and disease progression has been recently described (Hortala et al., 2014). A triazine derivative labeled with the long-lasting radionucleotide fluorine-18 (**Figure 1**), 2-{2-chloro-[5-(4-[^{18}F]-d2-methoxy)-6-(4-fluorophenethylamino)-1,3,5-triazin-2-yl]phenyl}propan-2-ol, showed in rhesus macaques, and baboons significant brain uptake and moderate washout.

Current Medicinal Chemistry Approaches

Often, increased levels of the endogenous cannabinoid, anandamide (AEA, **Figure 1**), correlate with neurodegenerative conditions. In recent studies, AEA has been shown to alleviate lipopolysaccharide-induced neuroinflammation in rat primary microglial cultures. Even though AEA can activate CB_1R, CB_2R, and other receptors such as GPR55, GPR18, TRPV1, or PPARs, the anti-inflammatory effects seem to be CB_2R-mediated, although a possible functional cross talk with GPR18/GPR55 cannot be ruled out (Malek et al., 2015). Accordingly, AEA may have potential therapeutic action on managing microglial-derived neuroinflammation and may regulate many aspects of the brain's inflammatory response. However, from a medicinal chemistry perspective, drug development is more securely based on designing novel and selective CB_2R ligands.

Despite the increasing number of reports on selective CB_2R ligands and the high expectations with this cannabinoid target, only a few synthetic CB_2R agonists have reached clinical trials (Han et al., 2014; Aghazadeh Tabrizi et al., 2016). CB_2R agonists, namely GW842166X, CP55940, S-777469, and JTE-907, completed phase II for treatment of different pain conditions, but none of them has been evaluated in humans for neurodegenerative or neuroinflammatory diseases. However, preclinical data of CB_2R agonists and inverse agonists have been described within this therapeutic perspective (Dhopeshwarkar and Mackie, 2014; Zhang et al., 2014).

Administration of a selective CB_2R agonist, JWH-133 (**Figure 1**), to an animal model of brain infarction improved infarct outcome and neurological impairment through inhibition of different subpopulations of microglia and macrophages (Zarruk et al., 2012). Repeated treatments with the resorcinol-based CB_2R agonist, O-1966, resulted in attenuated BBB disruption and neuronal degeneration as shown in a traumatic brain injury model (Amenta et al., 2012).

Trans-caryophyllene (BCP, **Figure 1**), a bicyclic sesquiterpene with selective CB_2R agonist properties, has been reported as a therapeutic target for the treatment of cerebral ischemia (Guo et al., 2014). This sesquiterpene suppressed hypoxia-induced neuroinflammatory responses by inhibiting NF-κB activation in microglia. Effectively, studies performed in the microglial cell line BV-2 and in primary cultures of microglia indicated that the inhibitory action of both cannabinoid receptor agonists and antagonists was mediated by extracellular signal regulated kinase 1/2 (ERK1/2), cytosolic phospholipase A2 (cPLA2), and activation of nuclear factor kappa (NF-κB) (Ribeiro et al., 2013).

New potentially neuroprotective CB_2R ligands have been recently described. Among them, the novel CB_2R inverse

agonist SMM-189 (**Figure 1**) ($K_i(CB_2)$ = 121 nM; $K_i(CB_1)$ = 4780 nM; EC_{50} = 153 nM) showed in a murine model of mild traumatic brain injury efficacy in reducing the motor, visual, and emotional deficits; such neuroprotection was seemingly achieved by modulating microglial activation (Reiner et al., 2015) and chemokine expression. Reduction of the proinflammatory markers, oetaxin, MCP-1, and IP-10 by SMM-189 suggests that SMM-189 would decrease infiltration of peripheral macrophage and other cells of the immune system implicated in neurodegeneration events (Presley et al., 2015). The chromenoisoxazole PM226 (**Figure 1**) has been described as a selective CB_2R agonist ($K_i(CB_2)$ = 13 nM; $K_i(CB_1R)$ > 40 μM; EC_{50} = 39 nM) with neuroprotective properties *in vitro* and *in vivo* evaluations (Gómez-Cañas et al., 2016). In this study, the beneficial effects of PM226 against the toxicity caused by conditioned media generated from LPS-treated cultured BV2 cells and exposed to a striatal neuron-derived cell line in culture was shown to be mediated by CB_2R. This neuroprotective potential was confirmed in an *in vivo* model of mitochondrial damage of striatal neurons in rats. Structure-activity relationship studies on the quinoline-2,4(1*H*,3*H*)-dione scaffold allowed the discovery of the CB_2R agonist 1-butyl-3-[(cyclohexylamino)methylidene]-8-methylquinoline-2,4(1*H*,3*H*)-dione (**Figure 1**) ($EC_{50}(CB_2)$ = 92 nM; $EC_{50}(CB_1)$ > 10 μM) that significantly reduced the clinical symptoms of experimental autoimmune encephalomyelitis in a mouse model of multiple sclerosis (Han et al., 2015). As shown by histological analysis, oral administration of this quinoline-2,4(1*H*,3*H*)-dione(10 mg/Kg) decreased leukocyte infiltration in the spinal cord and demyelination in white matter.

New strategies involving the targeting of CB_2R have been recently proposed for neurodegenerative and neuroinflammatory diseases. One of them has been proposed recently after reporting the mechanisms that could led to the beneficial effects of 4′-O-methylhokiol (MH, **Figure 1**), the major bioactive component of *Magnolia grandiflora L.*, in animal models of neurodegeneration (Chicca et al., 2015). MH exerts dual actions on the endocannabinoid system by acting as CB_2R modulator and COX-2 substrate-specific inhibitor.

Another strategy that needs to be explored is targeting CB_2R homo o heterodimers. Homobivalent and heterobivalent ligands have been explored for several GPCRs such as opioid (Fulton et al., 2010), dopamine (Gogoi et al., 2012), or histamine receptors (Birnkammer et al., 2012). CB_1R homobivalent and heterobivalent ligands have been designed and reported in the literature (Nimczick and Decker, 2015). In what concerns CB_2R dimers, the first structurally bivalent compounds was designed and synthesized in 2014 (Nimczick et al., 2014). Unfortunately, these molecules have less activity and selectivity compared to their monomeric compound. Bivalent molecules showed to be weak antagonists/inverse agonists of CB_1 and CB_2 receptors whereas the monomeric parent was selective CB_2R agonist (Nimczick et al., 2014). It appears that the development of bivalent drugs for CB_2Rs is still a complex task as commented very recently (Glass et al., 2016). Reported bivalent CB_1 receptor ligands are too short to bind both receptors simultaneously. The strategy for CB_1 or CB_2 receptor dimers need to be reviewed due to the fact that the ligand reaches the binding site through the lipid bilayer and the linkers are unlikely to be at the external receptor face.

Despite the promising therapeutic potential offered by CB_2R agonists, their translational success depends on overcoming some limitations, such as immune suppression upon chronic use- or pro-inflammatory actions. There is growing evidence that CB_1Rs are subject to ligand-biased signaling (Khajehali et al., 2015). However, ligand-biased signaling profiles of ligands at CB_2R are still under scrutiny; certainly, upon validation, they could open new therapeutic approaches. For example, the endocannabinoid 2-arachidonoylglycerol is very potent activating the ERK1/2-MAPK pathway at low concentration, whereas the inhibition of the adenylyl cyclase and calcium pathways needs higher concentrations (Dhopeshwarkar and Mackie, 2014). In the near future allosteric modulation at CB_2R may offer a novel therapeutic approach as allosteric modulators may both fine-tune the receptor response and minimize side-effects. Signaling-specific allosteric modulation as well as orthosteric probe dependence at CB_1R is currently under intense focus (Morales et al., 2016). In what concerns the CB_2R, positive and negative CB_2R allosteric modulators still need to be discovered.

TARGETING CB_2R IN NEURODEGENERATIVE DISORDERS

As above mentioned, drugs specifically targeting CB_2R in pallidal neurons may provide symptomatic relief in Parkinson's disease. However, neuroprotection is more likely afforded by guiding glial cells to protect or restore neuronal damage. The expression of CB_2R by glia enables these receptors to participate in the control by glial cells of the neuronal homeostasis, integrity and survival, particularly when glial cells become reactive (Fernández-Ruiz et al., 2007, 2015). Such potential situates cannabinoid ligands acting on CB_2Rs in a promising position for being used in neuroprotection (**Figure 2B**) (Fernández-Ruiz et al., 2015). Such pharmacological manipulations may be the best way to modulate the endogenous response provoked by these receptors, which are up-regulated in activated astrocytes and reactive microglia in response to inflammatory, excitotoxic and traumatic insults. Accordingly, preserving healthy neurons, or rescuing damaged neurons may be likely achieved by selecting the right agonist or allosteric modulator of CB_2R (see **Figure 2B**).

In the case of activated astrocytes, the benefits derived from the activation of CB_2R may be associated with: (i) increasing the trophic role exerted by these glial cells, including the supply of metabolic substrates to neurons (Köfalvi et al., 2016); (ii) enhancing the generation of neurotrophins (e.g., GDNF), anti-inflammatory mediators (e.g., interleukin-10, interleukin-1 receptor antagonist), and/or pro-survival factors (e.g., transforming growth factor-β) (Smith et al., 2000; Molina-Holgado et al., 2003); and (iii) inhibiting the production of chemokines (e.g., fractalkine) which contribute to neuronal damage (Sheng et al., 2009). All these effects should be likely dependent on the activation of CB_2R, either working alone or in conjunction with CB_1R (Stella, 2010).

Microglial cells have an added value as they are recruited to the lesion site where they become reactive and change morphology and molecular phenotype. Accordingly, CB_2Rs are concentrated surrounding the site of action of the therapeutic drug. The benefits derived from targeting CB_2R in activated microglia may be associated with: i) regulation of migration and proliferation at lesion sites (Walter et al., 2003; Carrier et al., 2004); (ii) regulation in the production of TNF-α and other microglia-derived neurotoxic factors (Fernández-Ruiz et al., 2007, 2015; Stella, 2010); and (iii) regulation of the balance M1 (pro-inflammatory) vs. M2 (neuroprotective) phenotypes (Mecha et al., 2013; Franco and Fernández-Suárez, 2015; Malek et al., 2015; Jia et al., 2016).

CONCLUDING REMARKS AND FUTURE PERSPECTIVES

The aim of this article was to collect evidence generated in the last years in support of the therapeutic potential of compounds selectively targeting the CB_2R. We placed emphasis in the potential relevance to provoke neuroprotection/neurorestoration in neurodegenerative disorders, particularly when activation of glial elements and occurrence of local inflammatory events are involved. We have compared the advantages of targeting CB_2Rs over targeting other elements of the endocannabinoid signaling, in particular the CB_1Rs. Right now there are a number of advantages based on the biochemical and signaling properties of CB_2Rs, the characteristics of the binding site, their capability to form heteromers, and very importantly, to their differential expression and function depending on the CNS region and the neural cell type. Knowledge of the exact role of CB_2R in activated glial cells will enhance the therapeutic potential of targeting these receptors in neuroinflammatory/neurodegenerative disorders.

It would be relevant to assess which among those disorders may receive more benefit from the targeting the receptor. Also relevant are the new perspectives in the design and development of novel ligands targeting the receptor. Other issues that require additional investigation are those related to the necessary developments to translate the preclinical potential of CB_2Rs and their ligands to the clinical scenario. This would be the major challenge in the next 5–10 years after which the first CB_2R-based medications will, hopefully, be available. Expectations are that new formulations of selective CB_2R ligands active at the orthosteric binding site, or acting as allosteric modulators, used alone or in combination with other licensed medicines, will be available to combat devastating neurological disorders such as Alzheimer's disease, Parkinson's disease, ataxias or amyotrophic lateral sclerosis.

AUTHOR CONTRIBUTIONS

All authors have contributed to the writing and to design and preparation of figures. Coordination of efforts has been carried out by the senior authors (NJ, JF, RF) of the three participating laboratories.

FUNDING

Open access partially supported by Grant 201413-30 from Fundació La Marató de TV3. Authors declare that personal funds are needed to carry out our research and/or to elaborate didactical materials/papers in some of our Institutions.

REFERENCES

Aghazadeh Tabrizi, M., Baraldi, P. G., Borea, P. A., and Varani, K. (2016). Medicinal chemistry, pharmacology, and potential therapeutic benefits of cannabinoid CB2 Receptor Agonists. *Chem. Rev.* 116, 519–560. doi: 10.1021/acs.chemrev.5b00411

Ahmad, R., Koole, M., Evens, N., Serdons, K., Verbruggen, A., Bormans, G., et al. (2013). Whole-body biodistribution and radiation dosimetry of the cannabinoid type 2 receptor ligand [11C]-NE40 in healthy subjects. *Mol. Imaging Bio.* 15, 384–390. doi: 10.1007/s11307-013-0626-y

Alger, B. E. (2002). Retrograde signaling in the regulation of synaptic transmission: focus on endocannabinoids. *Prog. Neurobiol.* 68, 247–286. doi: 10.1016/S0301-0082(02)00080-1

Alshaarawy, O., and Anthony, J. C. (2015). Cannabis smoking and serum C-reactive protein: a quantile regressions approach based on NHANES 2005-2010. *Drug Alcohol Depend.* 147, 203–207. doi: 10.1016/j.drugalcdep.2014.11.017

Amenta, P. S., Jallo, J. I., Tuma, R. F., and Elliott, M. B. (2012). A cannabinoid type 2 receptor agonist attenuates blood-brain barrier damage and neurodegeneration in a murine model of traumatic brain injury. *J. Neurosci. Res.* 90, 2293–2305. doi: 10.1002/jnr.23114

Aracil-Fernández, A., Trigo, J. M., García-Gutiérrez, M. S., Ortega-Álvaro, A., Ternianov, A., Navarro, D., et al. (2012). Decreased cocaine motor sensitization and self-administration in mice overexpressing cannabinoid CB2 receptors. *Neuropsychopharmacology* 37, 1749–1763. doi: 10.1038/npp.2012.22

Ashton, J. C., Friberg, D., Darlington, C. L., and Smith, P. F. (2006). Expression of the cannabinoid CB2 receptor in the rat cerebellum: an immunohistochemical study. *Neurosci. Lett.* 396, 113–116. doi: 10.1016/j.neulet.2005.11.038

Atwood, B. K., and Mackie, K. (2010). CB2: a cannabinoid receptor with an identity crisis. *Br. J. Pharmacol.* 160, 467–479. doi: 10.1111/j.1476-5381.2010.00729.x

Atwood, B. K., Straiker, A., and Mackie, K. (2012). CB2: therapeutic target-in-waiting. *Prog. Neuropsychopharmacol. Biol. Psychiatry* 38, 16–20. doi: 10.1016/j.pnpbp.2011.12.001

Avraham, H. K., Jiang, S., Fu, Y., Rockenstein, E., Makriyannis, A., Zvonok, A., et al. (2014). The cannabinoid CB2 receptor agonist AM1241 enhances neurogenesis in GFAP/Gp120 transgenic mice displaying deficits in neurogenesis. *Br. J. Pharmacol.* 171, 468–479. doi: 10.1111/bph.12478

Bahi, A., Al Mansouri, S., Al Memari, E., Al Ameri, M., Nurulain, S. M., and Ojha, S. (2014). β-Caryophyllene, a CB2 receptor agonist produces multiple behavioral changes relevant to anxiety and depression in mice. *Physiol. Behav.* 135, 119–124. doi: 10.1016/j.physbeh.2014.06.003

Birnkammer, T., Spickenreither, A., Brunskole, I., Lopuch, M., Kagermeier, N., Bernhardt, G., et al. (2012). The bivalent ligand approach leads to highly potent and selective acylguanidine-type histamine H 2 receptor agonists. *J. Med. Chem.* 55, 1147–1160. doi: 10.1021/jm201128q

Blanco-Calvo, E., Rivera, P., Arrabal, S., Vargas, A., Pavón, F. J., Serrano, A., et al. (2014). Pharmacological blockade of either cannabinoid CB1 or CB2 receptors prevents both cocaine-induced conditioned locomotion and cocaine-induced reduction of cell proliferation in the hippocampus of adult male rat. *Front. Integr. Neurosci.* 7:106. doi: 10.3389/fnint.2013.00106

Borroto-Escuela, D. O., Brito, I., Romero-Fernandez, W., Di Palma, M., Oflijan, J., Skieterska, K., et al. (2014). The G protein-coupled receptor heterodimer network (GPCR-HetNet) and its hub components. *Int. J. Mol. Sci.* 15, 8570–8590. doi: 10.3390/ijms15058570

Brusco, A., Tagliaferro, P., Saez, T., and Onaivi, E. S. (2008). Postsynaptic localization of CB2 cannabinoid receptors in the rat hippocampus. *Synapse* 62, 944–949. doi: 10.1002/syn.20569

Callén, L., Moreno, E., Barroso-Chinea, P., Moreno-Delgado, D., Cortés, A., Mallol, J., et al. (2012). Cannabinoid receptors CB1 and CB2 form functional heteromers in brain. *J. Biol. Chem.* 287, 20851–20865. doi: 10.1074/jbc.M111.335273

Campillo, N. E., and Páez, J. A. (2009). Cannabinoid system in neurodegeneration: new perspectives in Alzheimer's disease. *Mini Rev. Med. Chem.* 9, 539–559. doi: 10.2174/138955709788167628

Carai, M. A. M., Colombo, G., Maccioni, P., and Gessa, G. L. (2006). Efficacy of rimonabant and other cannabinoid CB1 receptor antagonists in reducing food intake and body weight: preclinical and clinical data. *CNS Drug Rev.* 12, 91–99. doi: 10.1111/j.1527-3458.2006.00091.x

Carrier, E. J., Kearn, C. S., Barkmeier, A. J., Breese, N. M., Yang, W., Nithipatikom, K., et al. (2004). Cultured rat microglial cells synthesize the endocannabinoid 2-arachidonylglycerol, which increases proliferation via a CB2 receptor-dependent mechanism. *Mol. Pharmacol.* 65, 999–1007. doi: 10.1124/mol.65.4.999

Chicca, A., Gachet, M. S., Petrucci, V., Schuehly, W., Charles, R.-P., and Gertsch, J. (2015). 4′-O-methylhonokiol increases levels of 2-arachidonoyl glycerol in mouse brain via selective inhibition of its COX-2-mediated oxygenation. *J. Neuroinflammation* 12, 89. doi: 10.1186/s12974-015-0307-7

Chung, Y. C., Shin, W.-H., Baek, J. Y., Cho, E. J., Baik, H. H., Kim, S. R., et al. (2016). CB2 receptor activation prevents glial-derived neurotoxic mediator production, BBB leakage and peripheral immune cell infiltration and rescues dopamine neurons in the MPTP model of Parkinson's disease. *Exp. Mol. Med.* 48:e205. doi: 10.1038/emm.2015.100

Contartese, A., Valoti, M., Corelli, F., Pasquini, S., Mugnaini, C., Pessina, F., et al. (2012). A novel CB2 agonist, COR167, potently protects rat brain cortical slices against OGD and reperfusion injury. *Pharmacol. Res.* 66, 555–563. doi: 10.1016/j.phrs.2012.08.003

Cordomí, A., Navarro, G., Aymerich, M. S., and Franco, R. (2015). Structures for G-protein-coupled receptor tetramers in complex with g proteins. *Trends Biochem. Sci.* 40, 548–551. doi: 10.1016/j.tibs.2015.07.007

den Boon, F. S., Chameau, P., Schaafsma-zhao, Q., Van Aken, W., Bari, M., Oddi, S., et al. (2012). Excitability of prefrontal cortical pyramidal neurons is modulated by activation of intracellular type-2 cannabinoid receptors. *Proc. Natl. Acad. Sci. U.S.A.* 109, 1–6. doi: 10.1073/pnas.1118167109

Dhopeshwarkar, A., and Mackie, K. (2014). CB2 Cannabinoid receptors as a therapeutic target-what does the future hold? *Mol. Pharmacol.* 86, 430–437. doi: 10.1124/mol.114.094649

Di Napoli, M., Godoy, D. A., Campi, V., Masotti, L., Smith, C. J., Parry Jones, A. R., et al. (2012). C-reactive protein in intracerebral hemorrhage: time course, tissue localization, and prognosis. *Neurology* 79, 690–699. doi: 10.1212/WNL.0b013e318264e3be

Di Napoli, M., Zha, A. M., Godoy, D. A., Masotti, L., Schreuder, F. H. B. M., Popa-Wagner, A., et al. (2016). Prior cannabis use is associated with outcome after intracerebral hemorrhage. *Cerebrovasc. Dis.* 41, 248–255. doi: 10.1159/000443532

Dowie, M. J., Grimsey, N. L., Hoffman, T., Faull, R. L. M., and Glass, M. (2014). Cannabinoid receptor CB2 is expressed on vascular cells, but not astroglial cells in the post-mortem human Huntington's disease brain. *J. Chem. Neuroanat.* 59, 62–71. doi: 10.1016/j.jchemneu.2014.06.004

Espejo-Porras, F., Piscitelli, F., Verde, R., Ramos, J. A., Di Marzo, V., de Lago, E., et al. (2015). Changes in the endocannabinoid signaling system in CNS structures of TDP-43 transgenic mice: relevance for a neuroprotective therapy in TDP-43-related disorders. *J. Neuroimmune Pharmacol.* 10, 233–244. doi: 10.1007/s11481-015-9602-4

Evens, N., and Bormans, G. M. (2010). Non-invasive imaging of the type 2 cannabinoid receptor, focus on positron emission tomography. *Curr. Top. Med. Chem.* 10, 1527–1543. doi: 10.2174/156802610793176819

Fernández-Ruiz, J., de Lago, E., Gómez-Ruiz, M., García, C., Sagredo, O., and García-Arencíbia, M. (2014). "Neurodegenerative disorders other than multiple sclerosis," in *Handbook of Cannabis*, ed R. Pertwee (Oxford: Oxford University Press), 505–525. doi: 10.1093/acprof:oso/9780199662685.003.0027

Fernández-Ruiz, J., Romero, J., and Ramos, J. A. (2015). Endocannabinoids and neurodegenerative disorders: Parkinson's Disease, Huntington's Chorea, Alzheimer's Disease, and Others. *Handb. Exp. Pharmacol.* 231, 233–259. doi: 10.1007/978-3-319-20825-1_8

Fernández-Ruiz, J., Romero, J., Velasco, G., Tolón, R. M., Ramos, J. A., and Guzmán, M. (2007). Cannabinoid CB2 receptor: a new target for controlling neural cell survival? *Trends Pharmacol. Sci.* 28, 39–45. doi: 10.1016/j.tips.2006.11.0 01

Ferré, S., Baler, R., Bouvier, M., Caron, M. G., Devi, L. A., Durroux, T., et al. (2009). Building a new conceptual framework for receptor heteromers. *Nat. Chem. Biol.* 5, 131–134. doi: 10.1038/nchembio0309-131

Franco, R., and Fernández-Suárez, D. (2015). Alternatively activated microglia and macrophages in the central nervous system. *Prog. Neurobiol.* 131, 65–86. doi: 10.1016/j.pneurobio.2015.05.003

Franco, R., Martínez-Pinilla, E., Lanciego, J. L., and Navarro, G. (2016). Basic pharmacological and structural evidence for class a g-protein-coupled receptor heteromerization. *Front. Pharmacol.* 7:76. doi: 10.3389/fphar.2016.00076

Fujii, M., Sherchan, P., Krafft, P. R., Rolland, W. B., and Soejima, Y., Z. J. (2014). Cannabinoid type 2 receptor stimulation attenuates brain edema by reducing cerebral leukocyte infiltration following subarachnoid hemorrhage in rats. *J. Neurol. Sci.* 342, 101–106. doi: 10.1016/j.jns.2014.04.034

Fulton, B. S., Knapp, B. L., Bidlack, J. M., and Neumeyer, J. L. (2010). Effect of linker substitution on the binding of butorphan univalent and bivalent ligands to opioid receptors. *Bioorganic Med. Chem. Lett.* 20, 1507–1509. doi: 10.1016/j.bmcl.2010.01.101

García, C., Palomo-Garo, C., Gómez-Gálvez, Y., and Fernández-Ruiz, J. (2016). Cannabinoid-dopamine interactions in the physiology and physiopathology of the basal ganglia. *Br. J. Pharmacol.* 173, 2069–2079. doi: 10.1111/bph.13215

García-Cabrerizo, R., and García-Fuster, M. J. (2016). Opposite regulation of cannabinoid CB1 and CB2 receptors in the prefrontal cortex of rats treated with cocaine during adolescence. *Neurosci. Lett.* 615, 60–65. doi: 10.1016/j.neulet.2016.01.018

García-Gutiérrez, M. S., and Manzanares, J. (2011). Overexpression of CB2 cannabinoid receptors decreased vulnerability to anxiety and impaired anxiolytic action of alprazolam in mice. *J. Psychopharmacol.* 25, 111–120. doi: 10.1177/0269881110379507

García-Gutiérrez, M. S., Pérez-Ortiz, J. M., Gutiérrez-Adán, A., and Manzanares, J. (2010). Depression-resistant endophenotype in mice overexpressing cannabinoid CB(2) receptors. *Br. J. Pharmacol.* 160, 1773–1784. doi: 10.1111/j.1476-5381.2010.00819.x

Glass, M., Govindpani, K., Furkert, D. P., Hurst, D. P., Reggio, P. H., and Flanagan, J. U. (2016). One for the Price of two...are bivalent ligands targeting cannabinoid receptor dimers capable of simultaneously binding to both receptors? *Trends Pharmacol. Sci.* 37, 353–363. doi: 10.1016/j.tips.2016.01.010

Gogoi, S., Biswas, S., Modi, G., Antonio, T., Reith, M. E. A., and Dutta, A. K. (2012). Novel bivalent ligands for D2/D3 dopamine receptors: significant cooperative gain in D2 affinity and potency. *ACS Med. Chem. Lett.* 3, 991–996. doi: 10.1021/ml3002117

Gómez-Cañas, M., Morales, P., García-Toscano, L., Navarrete, C., Muñoz, E., Jagerovic, N., et al. (2016). Biological characterization of PM226, a chromenoisoxazole, as a selective CB2 receptor agonist with neuroprotective profile. *Pharmacol. Res.* 110, 205–215. doi: 10.1016/j.phrs.2016.03.021

Gómez-Gálvez, Y., Palomo-Garo, C., Fernández-Ruiz, J., and García, C. (2016). Potential of the cannabinoid CB2 receptor as a pharmacological target against inflammation in Parkinson's disease. *Prog. Neuropsychopharmacol. Biol. Psychiatry* 64, 200–208. doi: 10.1016/j.pnpbp.2015.03.017

Gomez, O., Arevalo-Martin, A., Garcia-Ovejero, D., Ortega-Gutierrez, S., Cisneros, J. A., Almazan, G., et al. (2010). The constitutive production of the endocannabinoid 2-arachidonoylglycerol participates in oligodendrocyte differentiation. *Glia* 58, 1913–1927. doi: 10.1002/glia.21061

Gomez, O., Sanchez-Rodriguez, A., Le, M., Sanchez-Caro, C., Molina-Holgado, F., and Molina-Holgado, E. (2011). Cannabinoid receptor agonists modulate oligodendrocyte differentiation by activating PI3K/Akt and the mammalian target of rapamycin (mTOR) pathways. *Br. J. Pharmacol.* 163, 1520–1532. doi: 10.1111/j.1476-5381.2011.01414.x

Goncalves, M. B., Suetterlin, P., Yip, P., Molina-Holgado, F., Walker, D. J., Oudin, M. J., et al. (2008). A diacylglycerol lipase- CB2 cannabinoid pathway regulates adult subventricular zone neurogenesis in an age-dependent manner. *Mol. Cell. Neurosci.* 38, 526–536. doi: 10.1016/j.mcn.2008.05.001

Gong, J.-P., Onaivi, E. S., Ishiguro, H., Liu, Q.-R., Tagliaferro, P. A., Brusco, A., et al. (2006). Cannabinoid CB2 receptors: immunohistochemical localization in rat brain. *Brain Res.* 1071, 10–23. doi: 10.1016/j.brainres.2005.11.035

Green, S. T., Nathwani, D., Goldberg, D. J., and Kennedy, D. H. (1989). Nabilone as effective therapy for intractable nausea and vomiting in AIDS. *Br. J. Clin. Pharmacol.* 28, 494–495. doi: 10.1111/j.1365-2125.1989.tb03533.x

Guo, J., Pavlopoulos, S., Tian, X., Lu, D., Nikas, S. P., Yang, D., et al. (2003). Conformational study of lipophilic ligands in phospholipid model membrane systems by solution NMR. *J. Med. Chem.* 46, 4838–4846. doi: 10.1021/jm020385r

Guo, K., Mou, X., Huang, J., Xiong, N., and Li, H. (2014). Trans-caryophyllene suppresses hypoxia-induced neuroinflammatory responses by inhibiting NF-κB activation in microglia. *J. Mol. Neurosci.* 54, 41–48. doi: 10.1007/s12031-014-0243-5

Han, S., Chen, J. J., and Chen, J.-Z. (2014). Latest progress in the identification of novel synthetic ligands for the cannabinoid CB2 receptor. *Mini Rev. Med. Chem.* 14, 426–443. doi: 10.2174/1389557514666140428105753

Han, S., Zhang, F.-F., Qian, H.-Y., Chen, L.-L., Pu, J.-B., Xie, X., et al. (2015). Development of quinoline-2,4(1 H,3 H)-diones as potent and selective ligands of the cannabinoid type 2 receptor. *J. Med. Chem.* 58, 5751–5769. doi: 10.1021/acs.jmedchem.5b00227

Hortala, L., Arnaud, J., Roux, P., Oustric, D., Boulu, L., Oury-Donat, F., et al. (2014). Synthesis and preliminary evaluation of a new fluorine-18 labelled triazine derivative for PET imaging of cannabinoid CB2 receptor. *Bioorganic Med. Chem. Lett.* 24, 283–287. doi: 10.1016/j.bmcl.2013.11.023

Hu, B., Doods, H., Treede, R.-D., and Ceci, A. (2009). Depression-like behaviour in rats with mononeuropathy is reduced by the CB2-selective agonist GW405833. *Pain* 143, 206–212. doi: 10.1016/j.pain.2009.02.018

Hu, S. S.-J., and Mackie, K. (2015). Distribution of the endocannabinoid system in the central nervous system. *Handb. Exp. Pharmacol.* 231, 59–93. doi: 10.1007/978-3-319-20825-1_3

Hurst, D. P., Grossfield, A., Lynch, D. L., Feller, S., Romo, T. D., Gawrisch, K., et al. (2010). A lipid pathway for ligand binding is necessary for a cannabinoid G protein-coupled receptor. *J. Biol. Chem.* 285, 17954–17964. doi: 10.1074/jbc.M109.041590

Ishiguro, H., Carpio, O., Horiuchi, Y., Shu, A., Higuchi, S., Schanz, N., et al. (2010a). A nonsynonymous polymorphism in cannabinoid CB2 receptor gene is associated with eating disorders in humans and food intake is modified in mice by its ligands. *Synapse* 64, 92–96. doi: 10.1002/syn.20714

Ishiguro, H., Horiuchi, Y., Ishikawa, M., Koga, M., Imai, K., Suzuki, Y., et al. (2010b). Brain cannabinoid CB2 receptor in schizophrenia. *Biol. Psychiatry* 67, 974–982. doi: 10.1016/j.biopsych.2009.09.024

Jhaveri, M. D., Sagar, D. R., Elmes, S. J. R., Kendall, D. A., and Chapman, V. (2007). Cannabinoid CB2 receptor-mediated anti-nociception in models of acute and chronic pain. *Mol. Neurobiol.* 36, 26–35. doi: 10.1007/s12035-007-8007-7

Jia, J., Peng, J., Li, Z., Wu, Y., Wu, Q., Tu, W., et al. (2016). Cannabinoid CB2 receptor mediates nicotine-induced anti-inflammation in n9 microglial cells exposed to β amyloid via protein kinase C. *Mediat. Inflamm.* 2016:4854378. doi: 10.1155/2016/4854378

Khajehali, E., Malone, D. T., Glass, M., Sexton, P. M., Christopoulos, A., and Leach, K. (2015). Biased agonism and biased allosteric modulation at the CB1 cannabinoid receptors. *Mol. Pharmacol.* 88, 368–379. doi: 10.1124/mol.115.099192

Köfalvi, A., Lemos, C., Martín-Moreno, A. M., Pinheiro, B. S., García-García, L., Pozo, M. A., et al. (2016). Stimulation of brain glucose uptake by cannabinoid CB2 receptors and its therapeutic potential in Alzheimer's disease. *Neuropharmacology*. doi: 10.1016/j.neuropharm.2016.03.015. [Epub ahead of print].

Lanciego, J. L., Barroso-Chinea, P., Rico, A. J., Conte-Perales, L., Callén, L., Roda, E., et al. (2011). Expression of the mRNA coding the cannabinoid receptor 2 in the pallidal complex of *Macaca fascicularis*. *J. Psychopharmacol.* 25, 97–104. doi: 10.1177/0269881110367732

Makriyannis, A., Tian, X., and Guo, J. (2005). How lipophilic cannabinergic ligands reach their receptor sites. *Neurobiol. Dis.* 77, 210–218. doi: 10.1016/j.prostaglandins.2004.01.010

Malek, N., Popiolek-Barczyk, K., Mika, J., Przewlocka, B., and Starowicz, K. (2015). Anandamide, acting via CB2 receptors, alleviates LPS-induced neuroinflammation in rat primary microglial cultures. *Neural Plast.* 2015:130639. doi: 10.1155/2015/130639

Mecha, M., Feliú, A., Iñigo, P. M., Mestre, L., and Guaza, C. (2013). Cannabidiol provides long-lasting protection against the deleterious effects of inflammation in a viral model of multiple sclerosis: a role for A2A receptors. *Neurobiol. Dis.* 59, 141–150. doi: 10.1016/j.nbd.2013.06.016

Micale, V., Mazzola, C., and Drago, F. (2007). Endocannabinoids and neurodegenerative diseases. *Pharmacol. Res.* 56, 382–392. doi: 10.1016/j.phrs.2007.09.008

Molina-Holgado, E., Vela, J. M., Arévalo-Martín, A., Almazán, G., Molina-Holgado, F., Borrell, J., et al. (2002). Cannabinoids promote oligodendrocyte progenitor survival: involvement of cannabinoid receptors and phosphatidylinositol-3 kinase/Akt signaling. *J. Neurosci.* 22, 9742–9753.

Molina-Holgado, F., Pinteaux, E., Moore, J. D., Molina-Holgado, E., Guaza, C., Gibson, R. M., et al. (2003). Endogenous interleukin-1 receptor antagonist mediates anti-inflammatory and neuroprotective actions of cannabinoids in neurons and glia. *J. Neurosci.* 23, 6470–6474.

Morales, P., Goya, P., Jagerovic, N., and Hernandez-Folgado, L. (2016). Allosteric modulators of the CB 1 cannabinoid receptor : a structural update review. *Cannabis Cannabinoid Res.* 1, 22–30. doi: 10.1089/can.2015.0005

Mu, L., Bieri, D., Slavik, R., Drandarov, K., Muller, A., Cermak, S., et al. (2013). Radiolabeling and *in vitro* /*in vivo* evaluation of N-(1-adamantyl)-8-methoxy-4-oxo-1-phenyl-1,4-dihydroquinoline-3-carboxamide as a PET probe for imaging cannabinoid type 2 receptor. *J. Neurochem.* 126, 616–624. doi: 10.1111/jnc.12354

Navarrete, F., Pérez-Ortiz, J. M., and Manzanares, J. (2012). Cannabinoid CB2 receptor-mediated regulation of impulsive-like behaviour in DBA/2 mice. *Br. J. Pharmacol.* 165, 260–273. doi: 10.1111/j.1476-5381.2011.01542.x

Navarrete, F., Rodríguez-Arias, M., Martín-García, E., Navarro, D., García-Gutiérrez, M. S., Aguilar, M. A., et al. (2013). Role of CB2 cannabinoid receptors in the rewarding, reinforcing, and physical effects of nicotine. *Neuropsychopharmacology* 38, 2515–2524. doi: 10.1038/npp.2013.157

Nimczick, M., and Decker, M. (2015). New approaches in the design and development of cannabinoid receptor ligands: multifunctional and bivalent compounds. *ChemMedChem* 10, 773–786. doi: 10.1002/cmdc.201500041

Nimczick, M., Pemp, D., Darras, F. H., Chen, X., Heilmann, J., and Decker, M. (2014). Synthesis and biological evaluation of bivalent cannabinoid receptor ligands based on hCB2 R selective benzimidazoles reveal unexpected intrinsic properties. *Bioorg. Med. Chem.* 22, 3938–3946. doi: 10.1016/j.bmc.2014.06.008

Núñez, E., Benito, C., Pazos, M. R., Barbachano, A., Fajardo, O., González, S., et al. (2004). Cannabinoid CB2 receptors are expressed by perivascular microglial cells in the human brain: an immunohistochemical study. *Synapse* 53, 208–213. doi: 10.1002/syn.20050

Onaivi, E. S., Carpio, O., Ishiguro, H., Schanz, N., Uhl, G. R., and Benno, R. (2008a). Behavioral effects of CB2 cannabinoid receptor activation and its influence on food and alcohol consumption. *Ann. N.Y. Acad. Sci.* 1139, 426–433. doi: 10.1196/annals.1432.035

Onaivi, E. S., Chaudhuri, G., Abaci, A. S., Parker, M., Manier, D. H., Martin, P. R., et al. (1999). Expression of cannabinoid receptors and their gene transcripts in human blood cells. *Prog. Neuropsychopharmacol. Biol. Psychiatry* 23, 1063–1077.

Onaivi, E. S., Ishiguro, H., Gong, J.-P., Patel, S., Meozzi, P. A., Myers, L., et al. (2008b). Brain neuronal CB2 cannabinoid receptors in drug abuse and depression: from mice to human subjects. *PLoS ONE* 3:e1640. doi: 10.1371/journal.pone.0001640

Onaivi, E. S., Ishiguro, H., Gong, J.-P., Patel, S., Meozzi, P. A., Myers, L., et al. (2008c). Functional expression of brain neuronal CB2 cannabinoid receptors are involved in the effects of drugs of abuse and in depression. *Ann. N.Y. Acad. Sci.* 1139, 434–449. doi: 10.1196/annals.1432.036

Ortega-Alvaro, A., Aracil-Fernández, A., García-Gutiérrez, M. S., Navarrete, F., and Manzanares, J. (2011). Deletion of CB2 cannabinoid receptor induces schizophrenia-related behaviors in mice. *Neuropsychopharmacology* 36, 1489–1504. doi: 10.1038/npp.2011.34

Ortega-Álvaro, A., Ternianov, A., Aracil-Fernández, A., Navarrete, F., García-Gutiérrez, M. S., and Manzanares, J. (2015). Role of cannabinoid CB2 receptor in the reinforcing actions of ethanol. *Addict. Biol.* 20, 43–55. doi: 10.1111/adb.12076

Palazuelos, J., Aguado, T., Egia, A., Mechoulam, R., Guzmán, M., and Galve-Roperh, I. (2006). Non-psychoactive CB2 cannabinoid agonists stimulate neural progenitor proliferation. *FASEB J.* 20, 2405–2407. doi: 10.1096/fj.06-6164fje

Palazuelos, J., Aguado, T., Pazos, M. R., Julien, B., Carrasco, C., Resel, E., et al. (2009). Microglial CB2 cannabinoid receptors are neuroprotective in Huntington's disease excitotoxicity. *Brain* 132, 3152–3164. doi: 10.1093/brain/awp239

Palazuelos, J., Ortega, Z., Díaz-Alonso, J., Guzmán, M., and Galve-Roperh, I. (2012). CB2 cannabinoid receptors promote neural progenitor cell proliferation via mTORC1 signaling. *J. Biol. Chem.* 287, 1198–1209. doi: 10.1074/jbc.M111.291294

Presley, C. S., Mustafa, S. M., Abidi, A. H., and Moore, B. M. (2015). Synthesis and biological evaluation of (3′,5′-dichloro-2,6-dihydroxy-biphenyl-4-yl)-aryl/alkyl-methanone selective CB2 inverse agonist. *Bioorg. Med. Chem.* 23, 5390–5401. doi: 10.1016/j.bmc.2015.07.057

Price, D. A., Martinez, A. A., Seillier, A., Koek, W., Acosta, Y., Fernandez, E., et al. (2009). WIN55,212-2, a cannabinoid receptor agonist, protects against nigrostriatal cell loss in the 1-methyl-4-phenyl-1,2,3,6-tetrahydropyridine mouse model of Parkinson's disease. *Eur. J. Neurosci.* 29, 2177–2186. doi: 10.1111/j.1460-9568.2009.06764.x

Reiner, A., Heldt, S. A., Presley, C. S., Guley, N. H., Elberger, A. J., Deng, Y., et al. (2015). Motor, visual and emotional deficits in mice after closed-head mild traumatic brain injury are alleviated by the novel CB2 inverse agonist SMM-189. *Int. J. Mol. Sci.* 16, 758–787. doi: 10.3390/ijms16010758

Ribeiro, R., Wen, J., Li, S., and Zhang, Y. (2013). Involvement of ERK1/2, cPLA2 and NF-κB in microglia suppression by cannabinoid receptor agonists and antagonists. *Prostaglandins Other Lipid Mediat.* 100–101, 1–14. doi: 10.1016/j.prostaglandins.2012.11.003

Rodríguez-Arias, M., Navarrete, F., Blanco-Gandia, M. C., Arenas, M. C., Aguilar, M. A., Bartoll-Andrés, A., et al. (2015). Role of CB2 receptors in social and aggressive behavior in male mice. *Psychopharmacology* 232, 3019–3031. doi: 10.1007/s00213-015-3939-5

Rodríguez-Cueto, C., Benito, C., Fernández-Ruiz, J., Romero, J., Hernández-Gálvez, M., and Gómez-Ruiz, M. (2014). Changes in CB(1) and CB(2) receptors in the post-mortem cerebellum of humans affected by spinocerebellar ataxias. *Br. J. Pharmacol.* 171, 1472–1489. doi: 10.1111/bph.12283

Sagredo, O., González, S., Aroyo, I., Pazos, M. R., Benito, C., Lastres-Becker, I., et al. (2009). Cannabinoid CB2 receptor agonists protect the striatum against malonate toxicity: relevance for Huntington's disease. *Glia* 57, 1154–1167. doi: 10.1002/glia.20838

Sam, A. H., Salem, V., and Ghatei, M. A. (2011). Rimonabant: from RIO to Ban. *J. Obes.* 2011:432607. doi: 10.1155/2011/432607

Savonenko, A. V., Melnikova, T., Wang, Y., Ravert, H., Gao, Y., Koppel, J., et al. (2015). Cannabinoid CB2 receptors in a mouse model of Aβ amyloidosis: immunohistochemical analysis and suitability as a PET biomarker of neuroinflammation. *PLoS ONE* 10:e0129618. doi: 10.1371/journal.pone.0129618

Sheng, W. S., Hu, S., Ni, H. T., Rock, R. B., and Peterson, P. K. (2009). WIN55,212-2 Inhibits production of CX3CL1 by human astrocytes: involvement of p38 MAP Kinase. *J. Neuroimmune Pharmacol.* 4, 244–248. doi: 10.1007/s11481-009-9147-5

Shoemaker, J. L., Seely, K. A., Reed, R. L., Crow, J. P., and Prather, P. L. (2007). The CB2 cannabinoid agonist AM-1241 prolongs survival in a transgenic mouse model of amyotrophic lateral sclerosis when initiated at symptom onset. *J. Neurochem.* 101, 87–98. doi: 10.1111/j.1471-4159.2006.04346.x

Sierra, S., Luquin, N., Rico, A. J., Gómez-Bautista, V., Roda, E., Dopeso-Reyes, I. G., et al. (2015). Detection of cannabinoid receptors CB1 and CB2 within basal ganglia output neurons in macaques: changes following experimental parkinsonism. *Brain Struct. Funct.* 220, 2721–2738. doi: 10.1007/s00429-014-0823-8

Skaper, S. D., Buriani, A., Dal Toso, R., Petrelli, L., Romanello, S., Facci, L., et al. (1996). The ALIAmide palmitoylethanolamide and cannabinoids, but not anandamide, are protective in a delayed postglutamate paradigm of excitotoxic death in cerebellar granule neurons. *Proc. Natl. Acad. Sci. U.S.A.* 93, 3984–3989. doi: 10.1073/pnas.93.9.3984

Slavik, R., Grether, U., Müller Herde, A., Gobbi, L., Fingerle, J., Ullmer, C., et al. (2015a). Discovery of a high affinity and selective pyridine analog as a potential positron emission tomography imaging agent for cannabinoid type 2 receptor. *J. Med. Chem.* 58, 4266–4277. doi: 10.1021/acs.jmedchem.5b00283

Slavik, R., Herde, A. M., Bieri, D., Weber, M., Schibli, R., Krämer, S. D., et al. (2015b). Synthesis, radiolabeling and evaluation of novel 4-oxo-quinoline derivatives as PET tracers for imaging cannabinoid type 2 receptor. *Eur. J. Med. Chem.* 92, 554–564. doi: 10.1016/j.ejmech.2015.01.028

Smith, S. R., Terminelli, C., and Denhardt, G. (2000). Effects of cannabinoid receptor agonist and antagonist ligands on production of inflammatory cytokines and anti-inflammatory interleukin-10 in endotoxemic mice. *J. Pharmacol. Exp. Ther.* 293, 136–50.

Stella, N. (2010). Cannabinoid and cannabinoid-like receptors in microglia, astrocytes, and astrocytomas. *Glia* 58, 1017–1030. doi: 10.1002/glia.20983

Tao, Q., McAllister, S. D., Andreassi, J., Nowell, K. W., Cabral, G. A., Hurst, D. P., et al. (1999). Role of a conserved lysine residue in the peripheral cannabinoid receptor (CB2): evidence for subtype specificity. *Mol. Pharmacol.* 55, 605–613.

Van Sickle, M. D., Duncan, M., Kingsley, P. J., Mouihate, A., Urbani, P., Mackie, K., et al. (2005). Identification and functional characterization of brainstem cannabinoid CB2 receptors. *Science* 310, 329–332. doi: 10.1126/science.1115740

Vendel, E., and de Lange, E. C. M. (2014). Functions of the CB1 and CB 2 receptors in neuroprotection at the level of the blood-brain barrier. *Neuromolecular Med.* 16, 620–642. doi: 10.1007/s12017-014-8314-x

Walter, L., Franklin, A., Witting, A., Wade, C., Xie, Y., Kunos, G., et al. (2003). Nonpsychotropic cannabinoid receptors regulate microglial cell migration. *J. Neurosci.* 23, 1398–1405.

Yiangou, Y., Facer, P., Durrenberger, P., Chessell, I. P., Naylor, A., Bountra, C., et al. (2006). COX-2, CB2 and P2X7-immunoreactivities are increased in activated microglial cells/macrophages of multiple sclerosis and amyotrophic lateral sclerosis spinal cord. *BMC Neurol.* 6:12. doi: 10.1186/1471-2377-6-12

Zarruk, J. G., Fernandez-Lopez, D., Garcia-Yebenes, I., Garcia-Gutierrez, M. S., Vivancos, J., Nombela, F., et al. (2012). Cannabinoid type 2 receptor activation downregulates stroke-induced classic and alternative brain macrophage/microglial activation concomitant to neuroprotection. *Stroke* 49, 211–219. doi: 10.1161/STROKEAHA.111.631044

Zhang, L., Kline, R. H., McNearney, T. A., Johnson, M. P., and Westlund, K. N. (2014). Cannabinoid receptor 2 agonist attenuates pain related behavior in rats with chronic alcohol/high fat diet induced pancreatitis. *Mol. Pain* 10:66. doi: 10.1186/1744-8069-10-66

Conflict of Interest Statement: The authors declare that the research was conducted in the absence of any commercial or financial relationships that could be construed as a potential conflict of interest.

Copyright © 2016 Navarro, Morales, Rodríguez-Cueto, Fernández-Ruiz, Jagerovic and Franco. This is an open-access article distributed under the terms of the Creative Commons Attribution License (CC BY). The use, distribution or reproduction in other forums is permitted, provided the original author(s) or licensor are credited and that the original publication in this journal is cited, in accordance with accepted academic practice. No use, distribution or reproduction is permitted which does not comply with these terms.

frontiers in Neuroscience

ORIGINAL RESEARCH
published: 27 July 2016
doi: 10.3389/fnins.2016.00350

Synthesis and Biological Evaluation of Thiophene-Based Cannabinoid Receptor Type 2 Radiotracers for PET Imaging

Achi Haider [1], Adrienne Müller Herde [1], Roger Slavik [2], Markus Weber [3], Claudia Mugnaini [4], Alessia Ligresti [5], Roger Schibli [1], Linjing Mu [6] and Simon Mensah Ametamey [1]**

[1] Department of Chemistry and Applied Biology, Institute of Pharmaceutical Sciences, Swiss Federal Institute of Technology, Zurich, Switzerland, [2] Department of Molecular and Medical Pharmacology, University of California, Los Angeles, Los Angeles, CA, USA, [3] Neuromuscular Diseases Unit/ALS Clinic, Kantonsspital St. Gallen, St. Gallen, Switzerland, [4] Department of Biotechnology Chemistry and Pharmacy, University of Siena, Siena, Italy, [5] Institute of Biomolecular Chemistry, National Research Counsil of Italy, Naples, Italy, [6] Department of Nuclear Medicine, University Hospital Zurich, Zurich, Switzerland

OPEN ACCESS

Edited by:
Elena Capparelli,
University of Bari, Italy

Reviewed by:
Adriaan Anthonius Lammertsma,
VU University Medical Center, Netherlands
Alexander Neumeister,
Mitsubishi Tanabe Pharma Development America, USA

***Correspondence:**
Linjing Mu
linjing.mu@pharma.ethz.ch
Simon Mensah Ametamey
simon.ametamey@pharma.ethz.ch

Specialty section:
This article was submitted to Neurodegeneration, a section of the journal Frontiers in Neuroscience

Received: 15 April 2016
Accepted: 12 July 2016
Published: 27 July 2016

Citation:
Haider A, Müller Herde A, Slavik R, Weber M, Mugnaini C, Ligresti A, Schibli R, Mu L and Mensah Ametamey S (2016) Synthesis and Biological Evaluation of Thiophene-Based Cannabinoid Receptor Type 2 Radiotracers for PET Imaging. Front. Neurosci. 10:350. doi: 10.3389/fnins.2016.00350

Over the past two decades, our understanding of the endocannabinoid system has greatly improved due to the wealth of results obtained from exploratory studies. Currently, two cannabinoid receptor subtypes have been well-characterized. The cannabinoid receptor type 1 (CB_1) is widely expressed in the central nervous system, while the levels of the cannabinoid receptor type 2 (CB_2) in the brain and spinal cord of healthy individuals are relatively low. However, recent studies demonstrated a CB_2 upregulation on activated microglia upon neuroinflammation, an indicator of neurodegeneration. Our research group aims to develop a suitable positron emission tomography (PET) tracer to visualize the CB_2 receptor in patients suffering from neurodegenerative diseases. Herein we report two novel thiophene-based ^{11}C-labeled PET ligands designated [^{11}C]AAT-015 and [^{11}C]AAT-778. The reference compounds were synthesized using Gewald reaction conditions to obtain the aminothiophene intermediates, followed by amide formation. Saponification of the esters provided their corresponding precursors. Binding affinity studies revealed K_i-values of 3.3 ± 0.5 nM (CB_2) and 1.0 ± 0.2 μM (CB_1) for AAT-015. AAT-778 showed similar K_i-values of 4.3 ± 0.7 nM (CB_2) and 1.1 ± 0.1 μM (CB_1). Radiosynthesis was carried out under basic conditions using [^{11}C]iodomethane as methylating agent. After semi-preparative HPLC purification both radiolabeled compounds were obtained in 99% radiochemical purity and the radiochemical yields ranged from 12 to 37%. Specific activity was between 96 and 449 GBq/μmol for both tracers. In order to demonstrate CB_2 specificity of [^{11}C]AAT-015 and [^{11}C]AAT-778, we carried out autoradiography studies using CB_2-positive mouse/rat spleen tissues. The obtained results revealed unspecific binding in spleen tissue that was not blocked by an excess of CB_2-specific ligand GW402833. For *in vivo*

analysis, [^{11}C]AAT-015 was administered to healthy rats via tail-vein injection. Evaluation of the CB_2-positive spleen, however, showed no accumulation of the radiotracer. Despite the promising *in vitro* binding affinities, specific binding of [^{11}C]AAT-015, and [^{11}C]AAT-778 could not be demonstrated.

Keywords: cannabinoid receptor type 2, neuroinflammation, positron emission tomography, neurodegenerative disorders, thiophene-based structures

INTRODUCTION

Cannabinoid receptors belong to the large family of G protein-coupled receptors (GPCRs) exhibiting the characteristics of a glycosylated extracellular N-terminus, seven transmembrane α-helixes, and an intracellular C-terminus (Mackie, 2008; Rom and Persidsky, 2013). They are key players in a series of physiological processes resulting in an overall auto-protective effect in mammalians (Pertwee, 2005). Currently, there are two well-characterized subtypes of the cannabinoid receptor (CB_1 and CB_2) that share 44% sequence similarity and differ substantially in their expression profiles (Pertwee, 1997). The CB_1 receptor is mainly expressed in the central nervous system (CNS), CB_2 is predominantly found in peripheral immune cells (Matsuda et al., 1990; Herkenham et al., 1991; Maresz et al., 2005; Chin et al., 2008). Under physiological conditions, the CB_2 receptor expression in the brain and the spinal cord is barely detectable (Van Sickle et al., 2005). However, there are several studies demonstrating an upregulation of CB_2 on activated microglial cells (macrophages of the CNS), rendering the receptor a promising target to exploit neuroinflammatory changes involved in neurodegenerative disorders such as multiple sclerosis, amyotrophic lateral sclerosis (ALS), Parkinson's or Alzheimer's disease (Benito et al., 2008; Onaivi, 2009).

The various implications of the CB_2 receptor as well as the fact that it is only marginally expressed in the CNS of healthy subjects make it a promising target for diagnostic and clinical applications. The development of a successful CB_2 PET ligand might improve our understanding of the mechanisms underlying disease pathogenesis as well as provide a tool for therapy monitoring and development of novel therapeutic drug candidates. In particular, this would be beneficial for patients suffering from rare diseases with no current effective drug treatment like ALS (Zinman and Cudkowicz, 2011). Several CB_2 radioligands have been published by various research groups but till now, none of these radioligands has been found to be useful in the clinics. Their limitations included lack of selectivity over CB_1, high lipophilicity, low brain uptake due to P-glycoprotein efflux, brain penetrating radiometabolites, and trapped radiometabolites (Evens et al., 2008; Horti et al., 2010; Vandeputte et al., 2011; Hortala et al., 2014). Our research group is interested in evaluating different structural scaffolds in order to determine potential candidate compounds as CB_2-specific radioligands. In our previous work, we reported the development of oxoquinoline- as well as pyridine-based CB_2 radiotracers (Mu et al., 2013, 2014; Slavik et al., 2015a,b). Recently, a new class of thiophene amide derivatives emerged as potent and selective CB_2 agonists (Nelson et al., 2012). Several studies have been conducted to show the therapeutic applicability of thiophene-based derivatives in pain management, but this class of compounds has not yet been tested within the context of neurodegeneration. Herein we report the development of two novel thiophene-based PET radioligands designated [^{11}C]AAT-015 and [^{11}C]AAT-778 for a diagnostic approach toward CB_2 receptor imaging.

MATERIALS AND METHODS

All animal experiments were carried out in accordance with the Swiss Animal Welfare legislation and approved by the Veterinary Office of the Canton Zurich. Male Wistar rats and male CD1 mice were purchased from Charles River Laboratories (Sulzfeld, DE) and kept under standard conditions.

All chemicals, unless otherwise stated, were purchased from Sigma Aldrich GmbH (Taufkirchen, DE), ABCR GmbH (Karlsruhe, DE), Merck (Darmstadt, DE), or Fluka (Buchs, CH) and were used without further purification. Solvents for thin layer chromatography (TLC), column chromatography and extractions were purchased as commercial grade. Organic chemistry reactions were monitored by TLC using Sigma-Aldrich silica gel 60 plates under UV light at 254 nm. Nuclear magnetic resonance (NMR) spectra (^{1}H and ^{13}C NMR) were obtained on a Bruker Avance FT-NMR spectrometer (400 MHz). Chemical shifts are given in delta (δ) units, in ppm relative to tetramethylsilane (TMS, 0 ppm). Multiplicities in the ^{1}H NMR spectra are described as: s = singlet, d = doublet, t = triplet, m = multiplet and br = broad peak. Coupling constants (J) are reported in Hz. High resolution mass spectrometry (HRMS) was performed on a Bruker's maXis (ESI-Qq-TOF-MS) spectrometer (Bruker Daltonik GmbH, DE) and are given in m/z.

High-performance liquid chromatography (HPLC) analysis were performed using a reversed phase column (ACE column, C18, 3 μm) with a gradient system of acetonitrile and 0.1% trifluoroacetic acid in water. Analytical radio-HPLC was performed with a flow rate of 1 mL/min on an Agilent 1100 series system equipped with a Raytest Gabi Star radiodetector (Agilent Technologies, Morges, CH). Semi-preparative HPLC purifications were carried out using a reversed phase column (ACE column, Symmetry C8 5 μm; 7.8 × 50 mm) under the following conditions: 0.1% H_3PO_4 in H_2O (solvent A), MeCN (solvent B); 0.0–8.0 min, 20% B; 8.1–30.0 min, 20–90% B; 30.1–32.0 min, 90% B; 32.1–34.0 min, 90–20% B; 34.1–40.0 min, 20% B; flow rate: 4 mL/min. Specific activity was calculated by comparing ultraviolet peak intensity of the final formulated products with calibration curves of corresponding non-radioactive standards of known concentrations.

Chemistry

Methyl 2-amino-5-methyl-4-propylthiophene-3-carboxylate (1)

Morpholine (0.87 mL, 10 mmol) was added to a mixture of 3-hexanone (1.0 g, 10 mmol), methyl cyanoacetate (0.88 mL, 10 mmol) and sulfur (0.32 g, 10 mmol) in MeOH (5 mL). The mixture was refluxed overnight, then cooled to room temperature and poured into ice water. The resulting precipitate was filtered and the solid was then dissolved in dichloromethane. The solution was dried over anhydrous sodium sulfate and evaporated to dryness. The residue was purified by flash column chromatography on silica gel using petroleum ether/ethyl acetate (9:1) as eluent to give the title compound (230 mg, 11%) as a white solid. ^{1}H NMR (400 MHz, DMSO-d_6): δ 7.14 (s, 2H), 3.68 (s, 3H), 3.32 (s, 3H), 2.54 (t, J = 7.4 Hz, 2H), 1.38 (m, 2H), 0.85 (t, J = 7.4 Hz, 3H). ^{13}C NMR (100 MHz, DMSO-d_6): δ 165.0, 162.4, 136.2, 112.5, 103.0, 50.3, 29.6, 23.2, 13.9, 12.0. HRMS calculated for $C_{10}H_{16}NO_2S$ (M+H) 214.0896, found 214.0897.

Methyl 2-(adamantane-1-carboxamido)-5-methyl-4-propylthiophene-3-carboxylate (AAT-778)

A solution of 1-adamantane-carbonyl chloride (240 mg, 1.22 mmol) in dry 1,4-dioxane (3 mL) was added dropwise to a solution of compound **1** (200 mg, 0.94 mmol) in 10 mL of the same solvent while maintaining the reaction temperature at 70°C. After the addition was completed, the solution was stirred at 100°C for 2 h and then concentrated under reduced pressure. The residue was dissolved in dichloromethane, washed with aq. HCl (1M) and $NaHCO_3$ (saturated solution), dried over anhydrous sodium sulfate and evaporated to dryness. The crude product was purified by flash column chromatography on silica gel and eluted with petroleum ether/ethyl acetate (9:1). Subsequent recrystallization from MeOH gave the title compound (166 mg, 47%). ^{1}H NMR (400 MHz, $CDCl_3$): δ 11.6 (s, 1H), 3.9 (s, 3H), 2.7 (t, J = 6.7 Hz, 2H), 2.2 (s, 3H), 2.1 (m, 3H), 2.0 (m, 7H), 1.8 (m, 7H), 1.5 (m, 2H), 0.9 (t, J = 6.7 Hz, 2H). ^{13}C NMR (100 MHz, $CDCl_3$): δ 175.3, 167.1, 148.0, 133.7, 123.6, 111.6, 51.4, 39.0, 36.4, 29.8, 28.0, 23.8, 14.0, 12.3. HRMS calculated for $C_{21}H_{30}NO_4S$ (M+H) 392.1890, found 392.1888.

2-(adamantane-1-carboxamido)-5-methyl-4-propylthiophene-3-carboxylic acid (2)

A solution of NaOH (140 mg, 3.5 mmol) in water (2 mL) was added to a solution of **AAT-778** (100 mg, 0.26 mmol) in MeOH (2 mL) and the mixture was stirred at 80°C for 3 h. After cooling, aq. HCl (1 M) was added until a pH of 2 was reached. The resulting precipitate was filtered and dried to afford the pure acid (71 mg, 75%) as a white solid. ^{1}H NMR (400 MHz, DMSO-d_6): δ 13.2 (s, 1H), 11.7 (s, 1H), 2.7 (t, J = 5.7 Hz, 2H), 2.2 (s, 3H), 2.0 (m, 3H), 1.9 (m, 7H), 1.7 (m, 7H), 1.4 (m, 2H), 0.9 (t, J = 6.7 Hz, 2H). ^{13}C NMR (100 MHz, DMSO-d_6): δ 174.5, 167.8 146.7, 134.3, 123.2, 112.7, 38.9, 36.3, 29.4, 27.9, 23.8, 14.3, 12.4. HRMS calculated for $C_{20}H_{27}NO_3S$ (M+H) 362.1784, found 362.1781.

Methyl 2-amino-4,5,6,7-tetrahydrobenzo[b]thiophene-3-carboxylate (3)

To a suspension of sulfur in MeOH (10 mL) was added methyl 2-cyanoacetate (0.93 mL, 10.54 mmol) and cyclohexanone (0.993 mL, 9.58 mmol). Subsequent addition of diethylamine (0.49 mL, 4.69 mmol) gave a clear solution which was stirred at 50°C for 12 h. After cooling to room temperature, the reaction mixture was poured into ice-water and the resulting precipitate was filtered. The crude product was purified by flash column chromatography on silica gel using hexane/ethyl acetate (8:2) as eluent to obtain compound **3** (1.570 g, 78%). ^{1}H NMR (400 MHz, DMSO-d_6): δ 7.20 (s, 2H), 3.66 (s, 3H), 2.57 (t, J = 6.0 Hz, 2H), 2.41 (t, J = 6.0 Hz, 2H), 1.66 (m, 4H). ^{13}C NMR (100 MHz, DMSO-d_6): δ 165.5, 163.1, 131.5, 115.6, 102.6, 50.4, 26.6, 24.1, 23.0, 22.5. HRMS calculated for $C_{10}H_{13}NO_2S$ (M+H) 212.0740, found 212.743.

Methyl 2-3-hydroxyadamantane-1-carboxamido)-4,5,6,7-tetrahydroben-zo[b]thiophene-3-carboxylate (AAT-015)

To a solution of 3-hydroxyadamantane-1-carbonyl chloride (108 mg, 0.503 mmol) in dry DCM (2 mL) was added dropwise a mixture of compound **3** (213 mg, 1.006 mmol) and triethylamine (70.1 μL, 0.503 mmol) in 0.8 mL of the same solvent. The reaction mixture was stirred at room temperature for 3 h, diluted with DCM and extracted with aq. $NaHCO_3$ (saturated solution), aq. HCl (0.2 M) and brine. The organic layer was dried over magnesium sulfate and evaporated under reduced pressure. The crude product was purified by flash column chromatography on silica gel using hexane/ethyl acetate (6:4) as eluent to yield the title compound as a white solid (27 mg, 14%). ^{1}H NMR (400 MHz, $CDCl_3$): δ 11.6 (s, 1H), 3.9 (s, 3H), 2.7 (t, J = 5.6 Hz, 2H), 2.6 (t, J = 5.6 Hz, 2H), 2.4 (br. m, 2H), 1.9 (m, 6H), 1.8 (m, 8H), 1.6 (m, 2H). ^{13}C NMR (100 MHz, $CDCl_3$): δ 173.8, 167.4, 148.1, 130.7, 126.8, 111.4, 68.4, 51.5, 46.6, 44.2, 37.9, 34.9, 30.4, 26.3, 24.4, 23.0, 22.8. HRMS calculated for $C_{21}H_{27}NO_4S$ (M+H) 390.1734, found 390.1729.

2-3-(hydroxyadamantane-1-carboxamido)-4,5,6,7-tetrahydrobenzo[b]thio-phene-3-carboxylic acid (4)

To a solution of **AAT-015** (50 mg, 0.128 mmol) in MeOH (5 mL) was added dropwise NaOH (0.385 mL, 0.385 mmol) and the reaction mixture was refluxed for 3 h. The reaction mixture was diluted with water and aq. HCl (1 M) was added until a pH of 2 was reached. The resulting precipitate was filtered and washed with ice water to give compound **4** (33 mg, 69%). ^{1}H NMR (400 MHz, aceton-d_6): δ 11.7 (s, 1H), 2.8 (t, J = 5.7 Hz, 2H), 2.6 (t, J = 5.7 Hz, 2H), 2.3 (br. m, 2H), 2.1 (s, 1H), 1.9 (m, 6H), 1.7 (m, 8H), 1.6 (m, 2H). ^{13}C NMR (100 MHz, aceton-d_6): δ 174.3, 168.2, 149.3, 131.8, 126.8, 112.1, 67.7, 47.4, 45.1, 38.7, 35.8, 31.2, 26.9, 24.8, 23.8, 23.5. HRMS calculated for $C_{20}H_{25}NO_4S$ (M+H) 376.1577, found 376.1573.

In vitro Binding Assay

Membrane preparations originating from CHO-K1 cells stably transfected with either hCB_1 or hCB_2 (0.5 mg/tube, PerkinElmer, Massachusetts, US) and tritiated cannabinoid receptor agonist

CP-55,940 (1.4 nM, CB_2 agonist, Perkin Elmer, Boston, US) were used to determine inhibition constants of AAT-015 and AAT-778 in a competitive *in vitro* binding assay. A dilution series ranging from 1 pM to 1 mM in assay buffer (50 mM TRIS, 1 mM EDTA, 3 mM $MgCl_2$ and 0.05% bovine serum albumin, pH adjusted to 7.4) was prepared for each ligand to be tested. Nonspecific binding was determined in the presence of AM251 (5 μM, CB_1 inverse agonist, BIOTREND AG, Zürich, CH) and GW405833 (5 μM, CB_2 partial agonist, Sigma Aldrich GmbH, Taufkirchen, DE), respectively. The samples were incubated at 30°C for 90 min and subsequently diluted with ice cold assay buffer (3 mL) in order to be vacuum-filtered through Whatman GF/C filters (pre-treated with aq. polyethylenimine, 0.05%). Each sample was washed twice with ice cold assay buffer (3 mL) and filtered again. After addition of scintillation cocktail (Ultima Gold, Perkin Elmer), radioactivity was measured using a Beckman LS 6500 Liquid Scintillation Counter. IC_{50} mean values were calculated after performing three independent experiments, each as triplicate. The Cheng-Prusoff equation (Cheng and Prusoff, 1973) was used to calculate the inhibition constants.

Radiochemistry

Radiosynthesis of [^{11}c]AAT-015

[^{11}C]CO_2 was produced by proton bombardment of nitrogen gas fortified with 0.5% oxygen in a Cyclone 18/9 cyclotron (18-MeV; IBA, Ottignies-Louvain-la-Neuve, Belgium) via the $^{14}N(p,a)^{11}C$ nuclear reaction. In a first step, nickel-based catalytic reduction of [^{11}C]CO_2 yielded [^{11}C]methane which was subsequently iodinated to give [^{11}C]MeI. In order to prepare [^{11}C]AAT-015, the methylating agent was bubbled into a reaction mixture containing precursor **4** (1 mg) and cesium carbonate (5 mg) in DMF (0.6 mL) and stirred at 90°C for 3 min. After dilution of the crude product with water (1.4 mL), purification was performed by semi-preparative HPLC. The collected radiotracer was diluted with water (10 mL) and passed through a C18 cartridge (Waters, pre-conditioned with 5 mL EtOH and 5 mL water). After washing of the cartridge with water (5 mL), the product was eluted with EtOH (0.5 mL) into a sterile vial and diluted with water for injection (9.5 mL) to give a final formulation containing 5% of ethanol. The formulation was used for all *in vitro/in vivo* studies. For the purpose of quality control, an aliquot of the final formulation was injected into the analytical HPLC system. Identity of the product was confirmed by co-injection and comparison with the retention time of the standard reference. The specific activity was calculated by linear regression using a UV-intensity based calibration curve of standard reference AAT-015.

Radiosynthesis of [^{11}C]AAT-778

[^{11}C]AAT-778 was prepared according to the radiosynthetic procedure described in Section Radiosynthesis of [11 C]AAT-015, starting from precursor **2**.

In vitro Autoradiography

Autoradiography was performed on rat/mouse spleen tissue. Sections were prepared in 20 μm thickness using a cryostat (Cryo-Star NX 50; Thermo Scientific). The tissue slices were adsorbed to SuperFrost Plus (Menzel) slides and stored at −20°C until use. After thawing on ice for 10 min, sections were pre-incubated in the assay buffer containing 50 mM TRIS, 5 mM $MgCl_2$, 2.5 mM EDTA, and 0.5% BSA (pH 7.4). Slices were dried and incubated in a humidified chamber with [^{11}C]AAT-015 (5 nM) or [^{11}C]AAT-778 (5 nM) in assay buffer for 15 min at room temperature. In order to test for specificity toward CB_2, a solution containing both radiotracer and an excess of CB_2 specific partial agonist GW405833 (10 μM) was prepared and added to the tissue. The tissue slices were washed twice with assay buffer (each 2 min) and twice with distilled water (each 5 s) on ice, air dried, and exposed to a phosphor imager plate for a period of 25 min. The plate was scanned using a BAS5000 reader (Fujifilm, Dielsdorf, CH).

In vivo PET

PET and CT scans were obtained with a Super Argus PET/CT tomograph (Sedecal, Madrid, Spain) after injection of [^{11}C]AAT-015 (10–15 MBq, 0.02–0.10 nmol) into the tail of male Wistar rats (416 ± 32 g, $n = 4$) immobilized by isoflurane. Under baseline conditions, radiotracer accumulation was recorded in the region of the spleen in dynamic PET acquisition mode over 60 min ($n = 2$). During this whole time period rats were kept under anesthesia, body temperature and respiratory rate were constantly monitored. Under blockade conditions, 1.5 mg/kg GW405833 was injected shortly before radiotracer application in two of the four rats. Acquired PET data were reconstructed as user-defined time frames with a voxel size of 0.3875 × 0.3875 × 0.775 mm. For anatomical orientation, CT scans were acquired after each PET scan. Images were evaluated with PMOD v3.4 (PMOD Technologies Inc., Zurich, CH) software. Regions of interest (spleen, liver, and muscle) were drawn manually using the PMOD fusion tool. Time activity curves (TACs) for spleen, liver and muscle were expressed as standardized uptake values (SUV) which are the decay-corrected radioactivity per cm^3 divided by the injected radioactivity dose per gram of body weight.

RESULTS

Chemistry and Radiochemistry

Thiophene-based reference compounds AAT-778 and AAT-015 were synthesized starting from commercially available methyl cyanoacetate and the appropriate ketones as depicted in **Scheme 1**. The thiophene amine compounds **1** and **3** were obtained in 11 and 78%, respectively under the Gewald reaction conditions (Puterová et al., 2010). Subsequent coupling of **1** and **3** with 1-adamantanecarbonyl chloride and 3-hydroxyadamantane-1-carbonyl chloride, respectively, yielded the reference compounds AAT-778 and AAT-015. Saponification of the ester moiety of AAT-778 afforded precursor **2** for radiolabeling in 75% yield. Similarly, compound **4** was obtained from AAT-015 in 69% yield.

The radiosynthesis of [^{11}C]AAT-778 and [^{11}C]AAT-015 was accomplished by methyl ester formation from their corresponding carboxylic acids with [^{11}C]MeI (**Scheme 2**). The

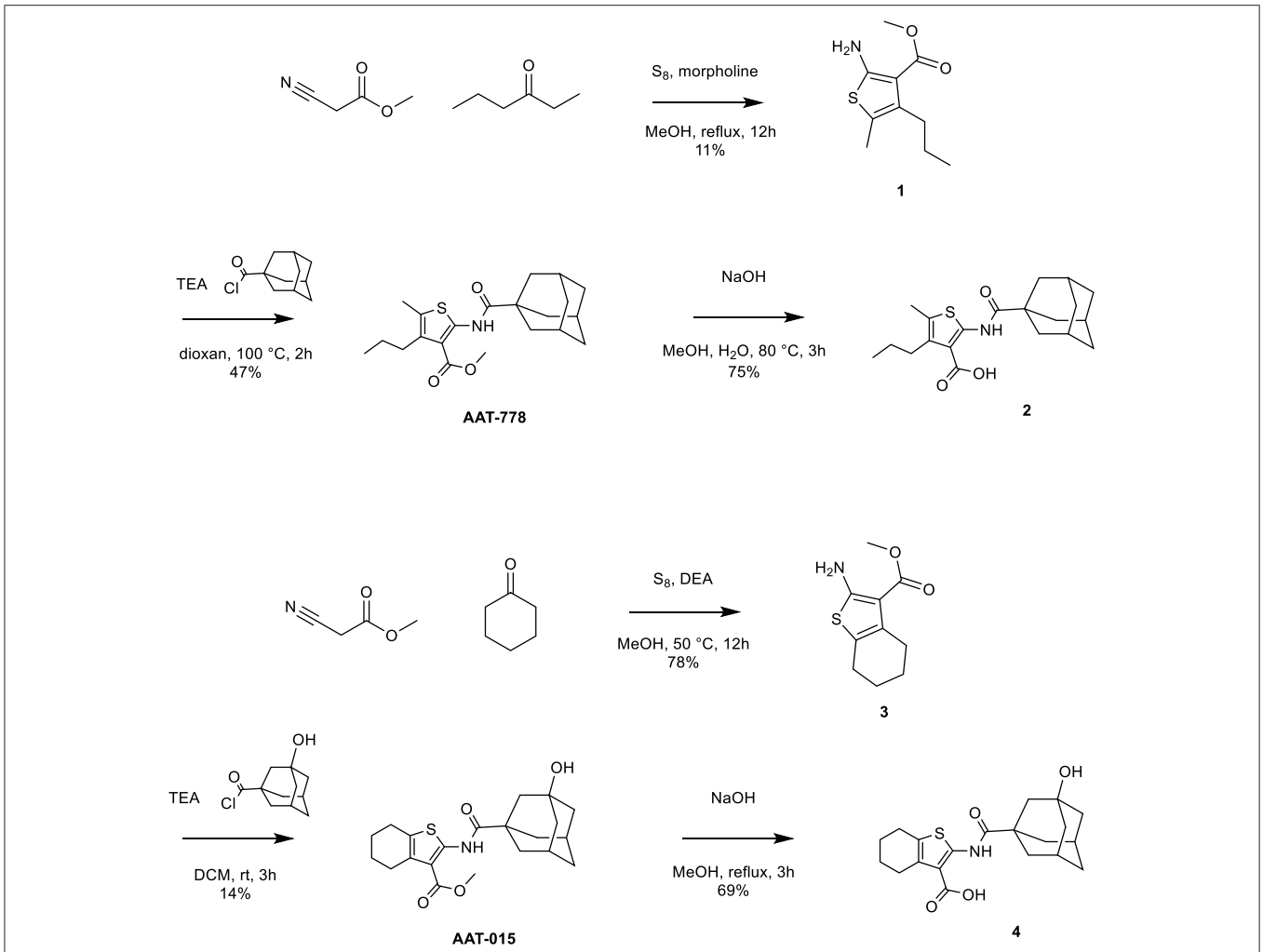

SCHEME 1 | Synthesis of thiophene-based CB_2 ligands AAT-778 and AAT-015 and their respective precursors for C-11 radiolabeling.

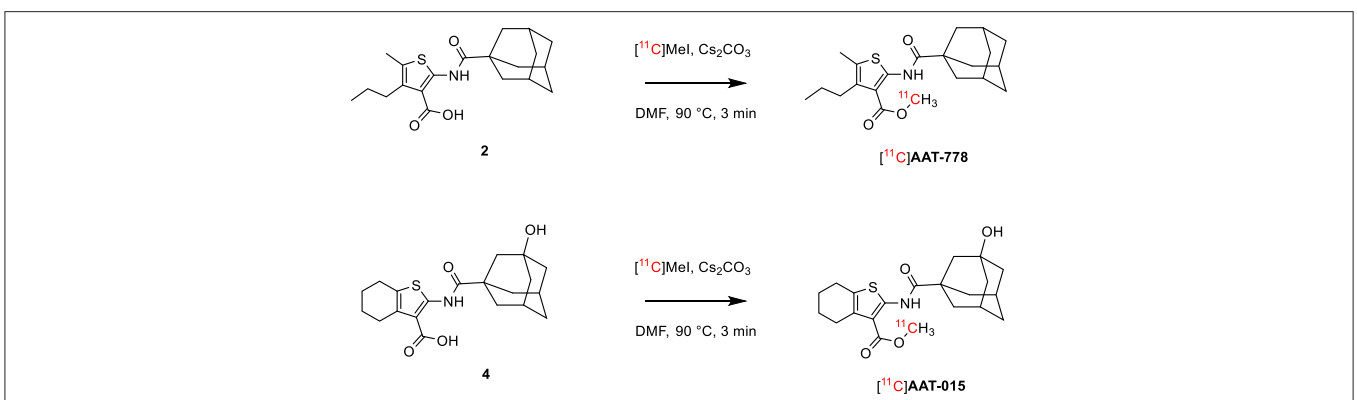

SCHEME 2 | Radiosynthesis of [^{11}C]AAT-778 and [^{11}C]AAT-015.

obtained radiochemical yields ranged from 12 to 37% (decay corrected) with specific activities between 96 and 449 GBq/μmol at the end of synthesis. In all cases, a radiochemical purity of 99% was attained after semi-preparative HPLC purification (**Figures 1**, **2**). The total radiosynthesis time from end of bombardment to the end of synthesis was 40 min.

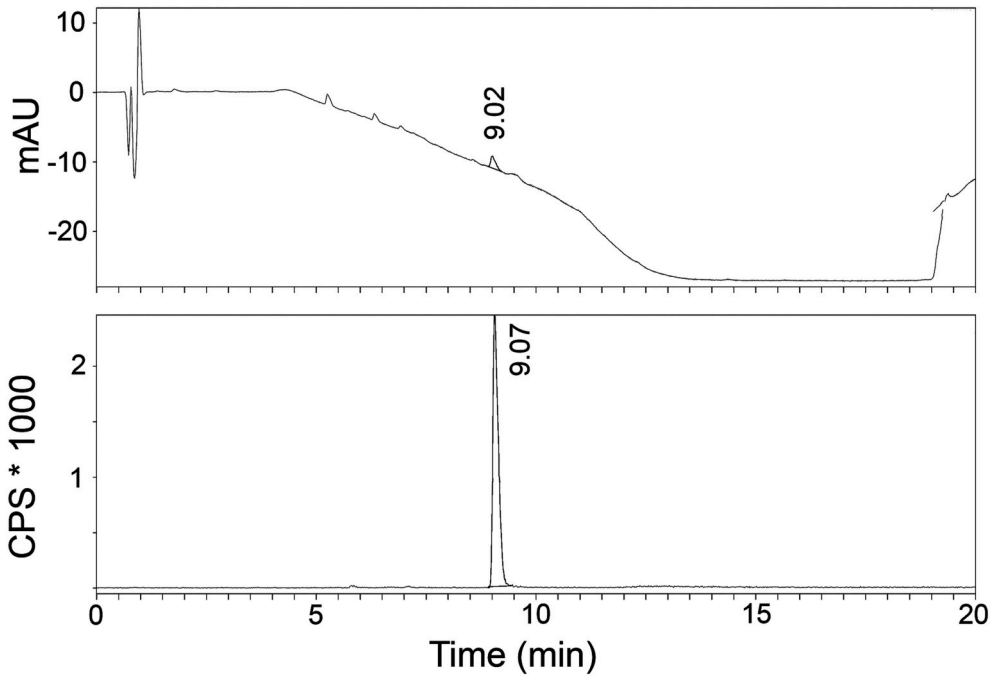

FIGURE 1 | A typical analytical HPLC profile of [^{11}C]AAT-015 [UV-trace (top) and radio-trace (bottom)].

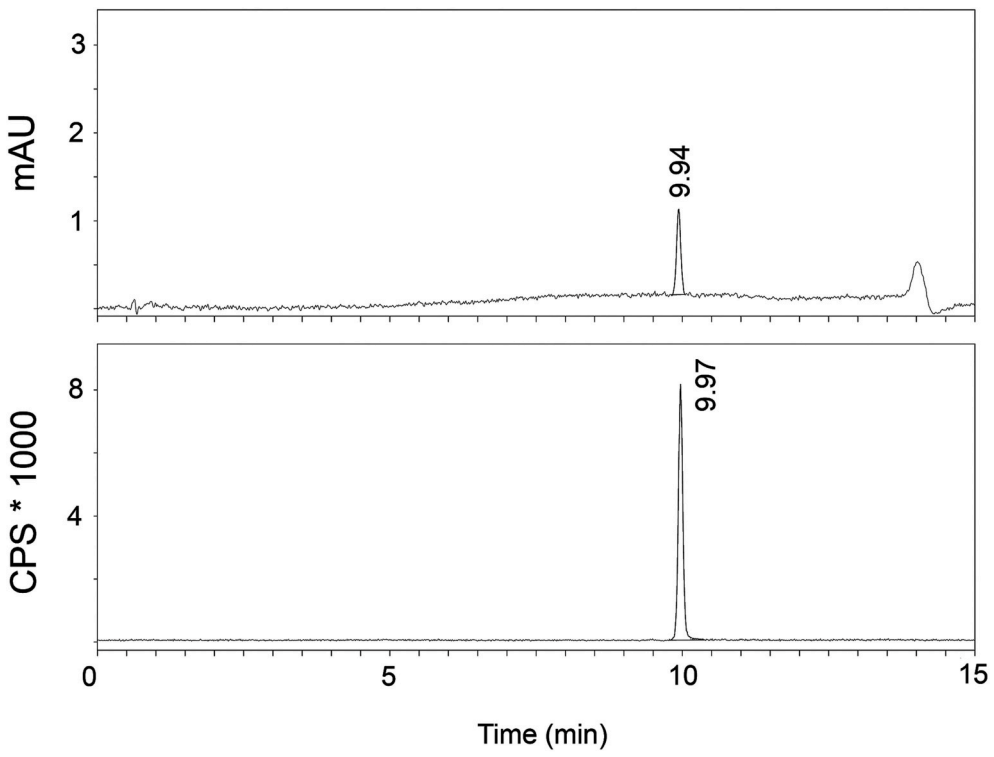

FIGURE 2 | A typical analytical HPLC profile of [^{11}C]AAT-778 [UV-trace (top) and radio-trace (bottom)].

In vitro Characterization

Binding affinity studies were performed using membranes stably transfected with human CB_1 and CB_2, respectively. A K_i-value of 4.3 ± 0.7 nM toward CB_2 and a 250-fold selectivity over CB_1 (**Table 1**) was obtained for compound AAT-778. We found that introduction of a polar hydroxyl on the adamantane moiety and ring closure to form the rather rigid cyclohexene did not impact the binding affinity and selectivity toward CB_2 as shown by the K_i-value of 3.3 ± 0.5 nM (toward CB_2) and 300-fold selectivity over CB_1 for AAT-015. One limitation of our *in vitro* work is that besides CB_1 we did not investigate the binding affinity of our ligands to other targets. Furthermore, clogP values depicted in **Table 1** indicate a significant reduction of lipophilicity after introduction of the hydroxyl group on the adamantane moiety in AAT-015.

Autoradiography with CD1 mouse and Wistar rat spleen tissue revealed binding of [^{11}C]AAT-778 to the spleen tissue in both species under baseline conditions (**Figures 3A,C**). No blocking effect was observed using an excess of CB_2-specific ligand GW405833, suggesting that the binding was unspecific (**Figures 3B,D**). Similar results were obtained with the less lipophilic [^{11}C]AAT-015 (**Figure 4**).

In vivo Characterization

For *in vivo* evaluation, [^{11}C]AAT-015 was selected due to the favored lipophilicity profile. Coronal and axial PET/CT slices of the abdominal region of a representative Wistar rat which was administered with [^{11}C]AAT-015 are shown in **Figure 5**. The spleen is encircled in all the images depicted in **Figure 5** and shows only low uptake of [^{11}C]AAT-015.

Time activity curves (TACs) are depicted in **Figure 6** for the liver, spleen and muscle under baseline (**Figure 6A**) and blockade (**Figure 6B**) conditions. There was no difference in the spleen uptake of [^{11}C]AAT-015 when comparing the TACs under baseline and blockade conditions. Radioactivity washout from the spleen was rather rapid, suggesting a perfusion-like profile rather than specific accumulation in the target organ. Thus, the uptake in the spleen was not specific.

DISCUSSION

Thiophene-based structures with high affinity toward CB_2 have been previously reported by Nelson et al. (2012). A series of derivatives were screened within the context of pain therapy. We developed two novel thiophene-based compounds, with an ester functionality which allows generating the precursors for C-11 radiolabeling. The designated compounds were obtained in a two-step synthetic approach involving Gewald reaction to form the thiophene amine. In the Gewald reaction, methyl cyanoacetate was treated with the corresponding ketones, followed by reaction with sulfur to afford thiophene amine derivatives **1** and **3**. In the case of the linear 3-hexanone, two different regioisomers were obtained which were not separable by column chromatography. Therefore, an additional recrystallization step was necessary in order to obtain pure compound **1** which may partly explain the lower yield when compared to the synthesis of 2-aminothiophene **3**. Coupling of the amine building blocks to adamantanecarboxylic acid using HBTU as the coupling reagent did not give the desired amides. However, amides AAT-015 and AAT-778 could be obtained by the reaction of the acid chloride with the corresponding thiophene amines. Subsequently, saponification of the ester intermediates gave the acid precursors in good chemical yields.

TABLE 1 | K_i-values of known CB_1/CB_2 ligands (entry 1–3; Showalter et al., 1996; Lan et al., 1999; Valenzano et al., 2005) and newly synthesized compounds (entry 4, 5).

	K_i (hCB_2) [nM]	K_i (hCB_1) [nM]	clogP
1. CP-55940	0.7 ± 0.02	0.6 ± 0.1	5.82
2. AM251	2290 ± 900	7.5 ± 1.1	5.62
3. GW405833	3.9 ± 1.6	4772 ± 1676	6.90
4. AAT-778	4.3 ± 0.7	1100 ± 100	6.00
5. AAT-015	3.3 ± 0.5	1000 ± 200	4.11

Binding affinity studies revealed that the introduction of the hydrophilic OH-group at the adamantane moiety did not have any influence on the affinity toward the CB_2 receptor since similar K_i-values were obtained for both AAT-015 and AAT-0778. Furthermore, the introduction of rigidity by ring-closure did not affect the binding affinity, which enlarges the compound selection and simplifies compound synthesis. As expected, the lipophilicity of AAT-015 was significantly reduced to 4.11 compared to 6.00 for AAT-778, which is highly desired. Carbon-11 radiolabelings of the acid precursors were carried out under similar conditions for both tracers and yielded comparable results in terms of radiochemical yield and purity as well as specific activity. In autoradiography studies with rodent spleen tissue [^{11}C]AAT-778 exhibited high unspecific binding. We speculate that this high unspecific binding is related to the high lipophilicity of the molecule. In order to reduce this unspecific binding, we modified AAT-778 by introducing a hydroxyl moiety on the adamantine ring to deliver AAT-015. However, despite the significant reduction of clogP, [^{11}C]AAT-015 still revealed a high unspecific binding in mouse and rat spleen tissues. PET studies of [^{11}C]AAT-015 confirmed the lack of specificity toward CB_2-positive spleen tissue *in vivo*. Possible reasons for the described *in vivo* results might include high plasma protein binding and rapid metabolism. The ester functionality can be cleaved by the action of carboxylesterases which are present in the plasma. This would, however, lead to a loss of the radiolabel from the core structure.

In conclusion, the novel thiophene-based radiotracers [^{11}C]AAT-778 and [^{11}C]AAT-015 are not suitable CB_2 PET tracers due to the lack of specificity for CB_2-positive spleen tissue and therefore were not further evaluated in neuroinflammatory animal models. Nonetheless, the high *in vitro* binding affinity toward CB_2 as well as the high selectivity over CB_1 makes this class of compounds interesting for further structural optimization toward improved physicochemical and pharmacological properties.

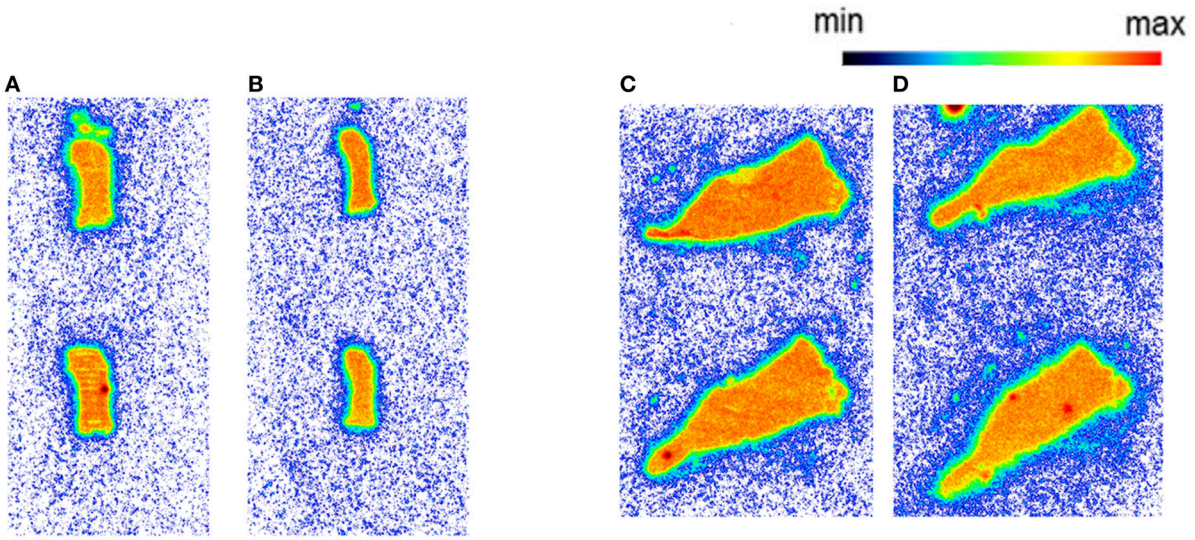

FIGURE 3 | The autoradiography results obtained with 5 nM [^{11}C]AAT-778 using spleen tissue sections. (A) Mouse spleen under baseline condition; **(B)** Mouse spleen under blockade conditions (10 μM GW405833); **(C)** Rat spleen under baseline conditions; **(D)** Rat spleen under blockade conditions (10 μM GW405833); $n = 2$.

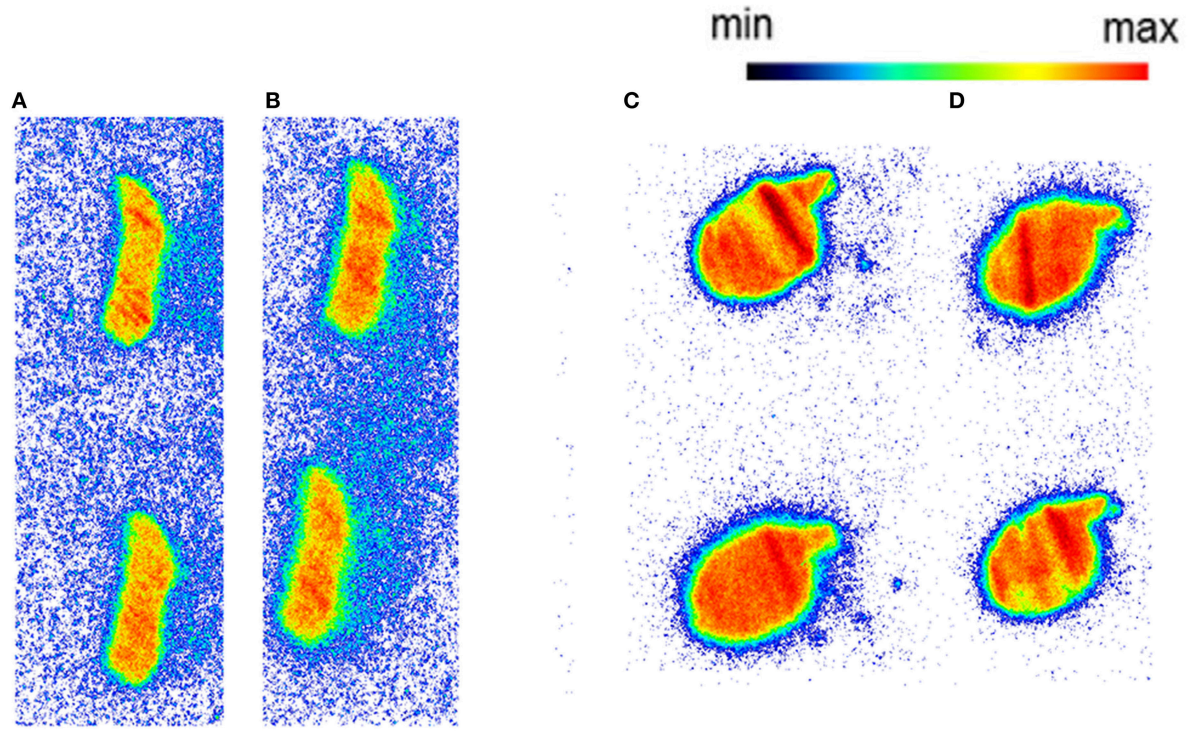

FIGURE 4 | The autoradiography results obtained with 5 nM [^{11}C]AAT-015 using spleen tissue sections. (A) Mouse spleen under baseline condition; **(B)** Mouse spleen under blockade conditions (10 μM GW405833); **(C)** Rat spleen under baseline conditions; **(D)** Rat spleen under blockade conditions (10 μM GW405833); $n = 2$.

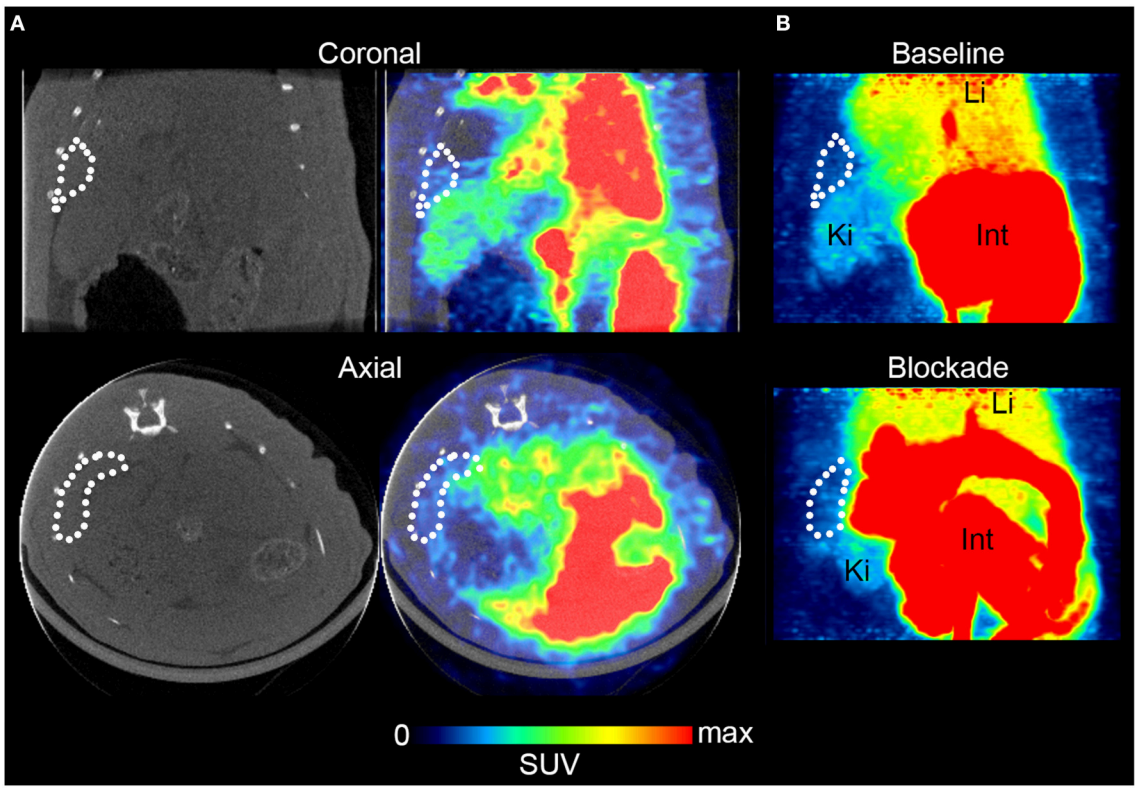

FIGURE 5 | Rat spleen PET/CT images after injection of [^{11}C]AAT-015 (averaged 0–60 min post injection). (A) Coronal and axial slices of the abdominal region. Spleen is encircled in the CT and PET/CT images, demonstrating low uptake of [^{11}C]AAT-015. SUV max = 4. **(B)** Maximal intensity projection (MIP) images of the abdominal region under baseline (same rat as in **A**) and blockade conditions (injection of 1.5 mg/kg GW405833 shortly before radiotracer). Spleen is encircled. Li, liver; Ki, kidney; Int, intestine. SUV max = 6.

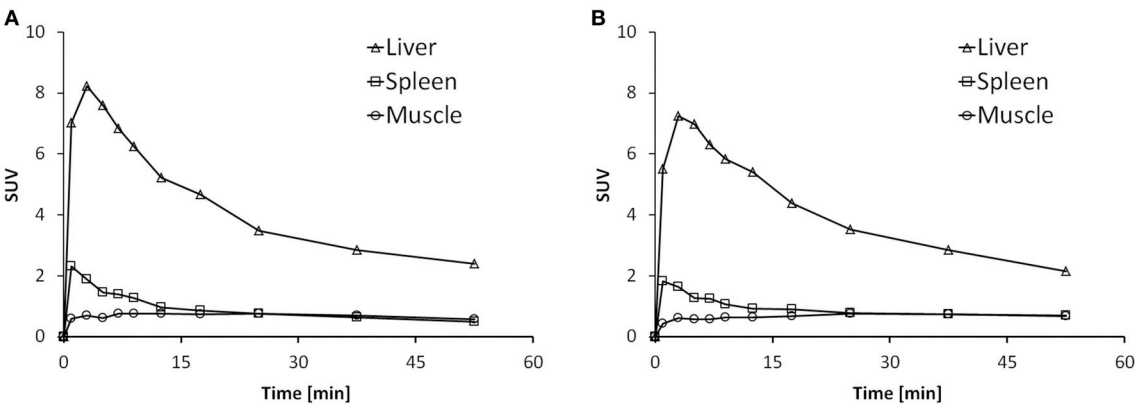

FIGURE 6 | Representative time activity curves (TACs) showing the standardized uptake values (SUV) of spleen, liver, and muscle in the time course of 60 min after injection of [^{11}C]AAT-015 into Wistar rats. (A) Injection of tracer only; **(B)** Injection of tracer and 1.5 mg/kg GW405833 (shortly before tracer).

AUTHOR CONTRIBUTIONS

AH performed the organic synthesis of precursor **4** and reference compound AAT-015 and conducted the IC_{50} studies with AAT-015. He further performed the radiosynthesis and autoradiography studies with [^{11}C]AAT-015 and wrote the manuscript. AM planned and evaluated the *in vivo* experiments and helped writing the manuscript. RS performed the radiosynthesis and autoradiography with [^{11}C]AAT-778. MW was involved in result discussions and revised the manuscript. CM and AL synthesized precursor **2** and reference compound AAT-778 and determined the Ki-value of AAT-778.

RS revised and approved the manuscript. LM and SM planned and organized the whole project and approved the manuscript.

ACKNOWLEDGMENTS

We would like to express our gratitude to Bruno Mancosu for his technical support with the carbon-11 module and to Claudia Keller for performing the PET/CT scans. Furthermore, we thank Hazem Ahmed for the support on the manuscript, Anna Katherina Boninsegni and Melinda Glier for the assistance in IC_{50} and autoradiography studies. The authors also thank the Swiss ALS Association and the Vontobel Foundation for the financial support.

REFERENCES

Benito, C., Tolón, R. M., Pazos, M. R., Núñez, E., Castillo, A. I., and Romero, J. (2008). Cannabinoid CB2 receptors in human brain inflammation. *J. Pharmacol.* 153, 277–285. doi: 10.1038/sj.bjp.0707505

Cheng, Y., and Prusoff, W. H. (1973). Relationship between the inhibition constant (K_1) and the concentration of inhibitor which causes 50 per cent inhibition (I50) of an enzymatic reaction. *Biochem. Pharmacol.* 22, 3099–3108. doi: 10.1016/0006-2952(73)90196-2

Chin, C. L., Tovcimak, A. E., Hradil, V. P., Seifert, T. R., Hollingsworth, P. R., Chandran, P., et al. (2008). Differential effects of cannabinoid receptor agonists on regional brain activity using pharmacological MRI. *Br. J. Pharmacol.* 153, 367–379. doi: 10.1038/sj.bjp.0707506

Evens, N., Bosier, B., Lavey, B. J., Kozlowski, J. A., Vermaelen, P., and Baudemprez, L. (2008). Labelling and biological evaluation of [^{11}C]methoxy-Sch225336: a radioligand for the cannabinoid-type 2 receptor. *Nucl. Med. Biol.* 5, 793–800, doi: 10.1016/j.nucmedbio.2008.07.004

Herkenham, M., Lynn, A. B., Johnson, M. R., Melvin, L. S., de Costa, B. R., and Rice, K. C. (1991). Characterization and localization of cannabinoid receptors in rat brain: a quantitative *in vitro* autoradiographic study. *J. Neurosci.* 11, 563–583.

Hortala, L., Arnaud, J., Roux, P., Oustric, D., Boulu, L., and Oury-Donat, F. (2014). Synthesis and preliminary evaluation of a new fluorine-18 labelled triazine derivative for PET imaging of cannabinoid CB2 receptor. *Bioorg. Med. Chem. Lett.* 24, 283–287. doi: 10.1016/j.bmcl.2013.11.023

Horti, A. G., Gao, Y., Ravert, H. T., Finley, P., Valentine, H., and Wong, D. F. (2010). Synthesis and biodistribution of [^{11}C]A-836339, a new potential radioligand for PET imaging of cannabinoid type 2 receptors (CB2). *Bioorg. Med. Chem.* 18, 5202–5207. doi: 10.1016/j.bmc.2010.05.058

Lan, R., Liu, Q., Fan, P., Lin, S., Fernando, S. R., and McCallion, D. (1999). Structure-activity relationships of pyrazole derivatives as cannabinoid receptor antagonists. *J. Med. Chem.* 42, 769–776. doi: 10.1021/jm980363y

Mackie, K. (2008). Cannabinoid receptors: where they are and what they do. *J. Neuroendocrinol.* 20, 1365–2826. doi: 10.1111/j.1365-2826.2008.01671.x

Maresz, K., Carrier, E. J., Ponomarev, E. D., Hillard, C. J., and Dittel, B. N. (2005). Modulation of the cannabinoid CB2 receptor in microglial cells in response to inflammatory stimuli. *J. Neurochem.* 95, 437–445. doi: 10.1111/j.1471-4159.2005.03380.x

Matsuda, L. A., Lolait, S. J., Brownstein, M. J., Young, A. C., and Bonner, T. I. (1990). Structure of a cannabinoid receptor and functional expression of the cloned cDNA. *Nature* 346, 561–564.

Mu, L., Bieri, D., Slavik, R., Drandarov, K., Müller, A., Cermak, S., et al. (2013). Radiolabeling and *in vitro/in vivo* evaluation of N-(1-adamantyl)-8-methoxy-4-oxo-1-phenyl- 1,4-dihydroquinoline-3-carboxamide as a PET probe for imaging cannabinoid type 2 receptor. *J. Neurochem.* 126, 616–624. doi: 10.1111/jnc.12354

Mu, L., Slavik, R., Müller, A., Popaj, K., Cermak, S., and Weber, M. (2014). Synthesis and preliminary evaluation of a 2-oxoquinoline carboxylic acid derivative for pet imaging the cannabinoid type 2 receptor. *Pharmaceuticals (Basel)* 7, 339–352. doi: 10.3390/ph7030339

Nelson, D. W., Frost, J. M., Tietje, K. R., Florjancic, A. S., Ryther, K., and Carroll, W. A. (2012). Synthesis and evaluation of 2-amido-3-carboxamide thiophene CB_2 receptor agonists for pain management. *Bioorg. Med. Chem. Lett.* 22, 2604–2608. doi: 10.1016/j.bmcl.2012.01.121

Onaivi, E. S. (2009). Cannabinoid receptors in brain: pharmacogenetics, neuropharmacology, neurotoxicology, and potential therapeutic applications. *Int. Rev. Neurobiol.* 88, 335–369. doi: 10.1016/s0074-7742(09)88012-4

Pertwee, R. G. (1997). Pharmacology of cannabinoid CB1 and CB2 receptors. *Pharmacol. Ther.* 74, 129–180. doi: 10.1016/S0163-7258(97)82001-3

Pertwee, R. G. (2005). The therapeutic potential of drugs that target cannabinoid receptors or modulate the tissue levels or actions of endocannabinoids. *AAPS J.* 7, 625–654. doi: 10.1208/aapsj070364

Puterová, Z., Krutošíková, A., and Véghc, D. (2010). Gewald reaction: synthesis, properties and applications of substituted 2-aminothiophenes. *Arch. Organ. Chem.* 2010, 209–246. doi: 10.3998/ark.5550190.0011.105

Rom, S., and Persidsky, Y. (2013). Cannabinoid receptors: where they are and what they do. *J. Neuroimmun. Pharmacol.* 8, 608–620. doi: 10.1007/s11481-013-9445-9

Showalter, V. M., Compton, D. R., Martin, B. R., and Abood, M. E. (1996). Evaluation of binding in a transfected cell line expressing a peripheral cannabinoid receptor (CB2): identification of cannabinoid receptor subtype selective ligands. *J. Pharmacol. Exp. Ther.* 278, 989–999.

Slavik, R., Grether, U., Müller Herde, A., Gobbi, L., Fingerle, J., Ullmer, C., et al. (2015b). Discovery of a high affinity and selective pyridine analog as a potential positron emission tomography imaging agent for cannabinoid type 2 receptor. *J. Med. Chem.* 58, 4266−4277. doi: 10.1021/acs.jmedchem.5b00283

Slavik, R., Herde, A. M., Bieri, D., Weber, M., Schibli, R., Krämer, S. D., et al. (2015a). Synthesis, radiolabeling and evaluation of novel 4-oxo-quinoline derivatives as PET tracers for imaging cannabinoid type 2 receptor. *Eur. J. Med. Chem.* 92, 554–564. doi: 10.1016/j.ejmech.2015.01.028

Valenzano, K. J., Tafesse, L., Lee, G., Harrison, J. E., Boulet, J. M., Gottshall, S. L., Mark, L., et al. (2005). Pharmacological and pharmacokinetic characterization of the cannabinoid receptor 2 agonist, GW405833, utilizing rodent models of acute and chronic pain, anxiety, ataxia and catalepsy. *Neuropharmacology* 48, 658–672. doi: 10.1016/j.neuropharm.2004.12.008

Vandeputte, C., Evens, N., Toelen, J., Deroose, C. M., Bosier, B., and Ibrahimi, A. (2011). A PET brain reporter gene system based on type 2 cannabinoid receptors. *J. Nucl. Med.* 2, 1102–1109. doi: 10.2967/jnumed.110.084426

Van Sickle, M. D., Duncan, M., Kingsley, P. J., Mouihate, A., Urbani, P., Mackie, K., et al. (2005). Identification and functional characterization of brainstem cannabinoid CB2 receptors. *Science* 310, 329–332. doi: 10.1126/science.1115740

Zinman, L., and Cudkowicz, M. (2011). Emerging targets and treatments in amyotrophic lateral sclerosis. *Lancet Neurol.* 10, 481–490. doi: 10.1016/S1474-4422(11)70024-2

Conflict of Interest Statement: The authors declare that the research was conducted in the absence of any commercial or financial relationships that could be construed as a potential conflict of interest.

Copyright © 2016 Haider, Müller Herde, Slavik, Weber, Mugnaini, Ligresti, Schibli, Mu and Mensah Ametamey. This is an open-access article distributed under the terms of the Creative Commons Attribution License (CC BY). The use, distribution or reproduction in other forums is permitted, provided the original author(s) or licensor are credited and that the original publication in this journal is cited, in accordance with accepted academic practice. No use, distribution or reproduction is permitted which does not comply with these terms.

frontiers in Neuroscience

ORIGINAL RESEARCH
published: 22 September 2016
doi: 10.3389/fnins.2016.00431

Synthesis, Biodistribution and *In vitro* Evaluation of Brain Permeable High Affinity Type 2 Cannabinoid Receptor Agonists [^{11}C]MA2 and [^{18}F]MA3

*Muneer Ahamed[1], Daisy van Veghel[1], Christoph Ullmer[2], Koen Van Laere[3], Alfons Verbruggen[1] and Guy M. Bormans[1]**

[1] *Laboratory for Radiopharmacy, KU Leuven, Leuven, Belgium,* [2] *Roche Pharma Research and Early Development, Roche Innovation Center Basel, F. Hoffmann-La Roche Ltd, Basel, Switzerland,* [3] *Division of Nuclear Medicine, University Hospital and KU Leuven, Leuven, Belgium*

The type 2 cannabinoid receptor (CB2) is a member of the endocannabinoid system and is known for its important role in (neuro)inflammation. A PET-imaging agent that allows *in vivo* visualization of CB2 expression may thus allow quantification of neuroinflammation. In this paper, we report the synthesis, radiosynthesis, biodistribution and *in vitro* evaluation of a carbon-11 ([^{11}C]MA2) and a fluorine-18 ([^{18}F]MA3) labeled analog of a highly potent *N*-arylamide oxadiazole CB2 agonist (EC_{50} = 0.015 nM). MA2 and MA3 behaved as potent CB2 agonist (EC_{50}: 3 nM and 0.1 nM, respectively) and their *in vitro* binding affinity for *h*CB2 was found to be 87 nM and 0.8 nM, respectively. Also MA3 (substituted with a fluoro ethyl group) was found to have higher binding affinity and EC_{50} values when compared to the originally reported trifluoromethyl analog **12**. [^{11}C]MA2 and [^{18}F]MA3 were successfully synthesized with good radiochemical yield, high radiochemical purity and high specific activity. In mice, both tracers were efficiently cleared from blood and all major organs by the hepatobiliary pathway and importantly these compounds showed high brain uptake. In conclusion, [^{11}C]MA2 and [^{18}F]MA3 are shown to be high potent CB2 agonists with good brain uptake, these favorable characteristics makes them potential PET probes for *in vivo* imaging of brain CB2 receptors. However, in view of its higher affinity and selectivity, further detailed evaluation of MA3 as a PET tracer for CB2 is warranted.

Keywords: Type 2 cannabinoid receptor, CB2 agonists, Positron emission tomography, Radiosynthesis

OPEN ACCESS

Edited by:
Marialessandra Contino, University of Bari Aldo Moro, Italy

Reviewed by:
Luigi Bubacco, University of Padua, Italy
Ildikó Rácz, University of Bonn, Germany

****Correspondence:***
Guy M. Bormans
guy.bormans@pharm.kuleuven.be

Specialty section:
This article was submitted to Neurodegeneration, a section of the journal Frontiers in Neuroscience

Received: *04 July 2016*
Accepted: *06 September 2016*
Published: *22 September 2016*

Citation:
Ahamed M, van Veghel D, Ullmer C, Van Laere K, Verbruggen A and Bormans GM (2016) Synthesis, Biodistribution and In vitro Evaluation of Brain Permeable High Affinity Type 2 Cannabinoid Receptor Agonists [^{11}C]MA2 and [^{18}F]MA3 Front. Neurosci. 10:431. doi: 10.3389/fnins.2016.00431

INTRODUCTION

The two types of cannabinoid receptors, CB1 and CB2, together with their endogenous lipid ligands (endocannabinoids) and all proteins responsible for synthesis, transport and degradation of these endocannabinoids represent the endocannabinoid system (ECS) (Rodríguez de Fonseca et al., 2005; Mackie, 2008). CB1 and CB2 are both G-protein coupled receptors, but exhibit different expression patterns and signaling profiles. CB1 receptors are mainly located in brain and are responsible for the psychoactive effects of cannabinoids (Piomelli, 2003), whereas cannabinoid's immunomodulatory activity is assigned to CB2 receptors, which are predominantly expressed on β-lymphocytes and

organs and tissues related to the immune system such as the spleen and lymph nodes (Lynn and Herkenham, 1994; Galiegue et al., 1995).

In addition, low levels of CB2 mRNA and protein have been detected in healthy brain in Purkinje cells of the cerebellum, hippocampal neurons, and various nuclei of the brain stem (Atwood and Mackie, 2010). This may indicate that the physiological role of CB2 in the central nervous system (CNS) has been underestimated and that both CB1 and CB2 may control central functions. CB2 is, however, up-regulated in the CNS under neuroinflammation. This CB2 overexpression has been predominantly assigned to microglia, the resident immune cells of the brain, and alters depending on their activation state(Cabral and Griffin-Thomas, 2009; Atwood and Mackie, 2010). CB2-positive microglia have been detected in β-amyloid plaques of Alzheimer's disease patients (Ramirez et al., 2005), in spinal cords of an amyotrophic lateral sclerosis (ALS) mouse model (Shoemaker et al., 2006), in active plaques of patients with multiple sclerosis (MS) (Benito et al., 2007) and in striatal lesions of Huntington's disease (HD) transgenic mouse models and patients (Palazuelos et al., 2009). Moreover, selective CB2 activation results in a decrease of microglial activation in HD and ALS transgenic mouse models and appears to be effective in reducing neurodegeneration (Shoemaker et al., 2006; Palazuelos et al., 2009; Sagredo et al., 2009). These observations suggest that therapeutic modulation of CB2 may be a new promising treatment for neuropathogenic disorders characterized by a neuroinflammatory component.

Various CB2-selective drugs and companion PET-imaging agents have been developed over the past years (Evens et al., 2008, 2009, 2011; Horti et al., 2010; Turkman et al., 2012; Slavik et al., 2015, 2016; Moldovan et al., 2016). Horti and co-workers demonstrated binding of [^{11}C]A-836339 to CB2 in lipopolysaccharide (LPS)-induced neuroinflammation and AD mouse models (Horti et al., 2010). Our group previously showed [^{11}C]NE40 had CB2-specific retention in the spleen of mice (Evens et al., 2009) and in a rat model with local overexpression of a human inactive CB2 variant (Evens et al., 2012). Rühl et al. reported the synthesis of a ^{18}F-labeled *N*-aryl-oxadiazolyl-propionamide derivative with low nanomolar binding affinity for hCB2 (Rühl et al., 2012). The non-radioactive compound was shown to bind CB2 in mouse spleen in an autoradiographic study using [^{3}H]CP55940 as radioligand.

There is still a need for CB2 PET-tracers with improved imaging profiles and high affinity and selectivity for CB2. Such high affinity PET-radioligands may allow *in vivo* visualization of the low density brain CB2 receptors. Moreover, agonists preferentially bind to cannabinoid receptors in their (functionally) activated conformation (Gullapalli et al., 2010). Therefore, agonist CB2 PET-radioligands may allow visualization of the activated fraction of the receptor which may correlate better with CB2 related pathology of the receptor system. Here we report the synthesis, radiosynthesis, and biological evaluation of potent carbon-11 and a fluorine-18 labeled CB2 agonists as potential PET tracers for *in vivo* imaging of brain CB2 receptors.

RESULTS

Synthesis and Radiolabelling

Compound **1** was synthesized using a previously reported procedure where nitromethane ($MeNO_2$) was treated with 10 M sodium hydroxide (NaOH) to form potentially explosive methazoic acid **1**. (Cheng et al., 2008; DiMauro et al., 2008) Condensation of **1** with *in situ* generated *ortho*-aminoaldehyde (**3**) formed 3-nitro-6-hydroxyquinoline **4**, in 19% overall yield starting from compound **2**. Compound **4** was methylated using methyl iodide (MeI) in the presence of potassium carbonate (K_2CO_3) under reflux to give 3-nitro-6-methoxyquinoline **5a** in 61% yield. Also compound **4** was converted into **5b** in 67% yield, using 1-Bromo-2-fluoroethane (FEtBr) and K_2CO_3 in DMF. Finally, **6**, **6a**, and **6b** were synthesized (36, 45, and 60% yields respectively) by reducing the corresponding nitro compounds **4**, **5a**, and **5b** respectively, *via* a standard reduction using iron (Fe) powder/acetic acid (**Figure 1**).

The oxadiazole fragment (**11**) was synthesized as shown in **Figure 2**. Commercially available 2-chloro-4-fluoro-benzonitrile (**7**) was converted into an oxime (**8**) in 97% yield when treated with hydroxylamine hydrochloride ($NH_2OH{\cdot}HCl$). The oxadiazole core was formed by condensing **8** with succinic anhydride and obtained in 28% yield after column purification. The carboxylic acid (**9**) then underwent a Steglich esterification (Neises and Steglich, 1978) with *N,N′*-dicyclohexylcarbodiimide (DCC)/4-dimethylaminopyridine (DMAP) to form the desired methyl ester (**10**) in 63% yield. The ester group of compound **10** was then subjected to diisobutylaluminium hydride (DIBAL-H) reduction at −80°C to form the corresponding aldehyde (**11**) in 45% yield. Longer reaction times and increasing DIBAL-H loading led to the formation of a side product, presumably the corresponding alcohol.

The final reductive amination of **11** with **6a-c** was performed using an excess of titanium isopropoxide ($Ti(O\text{-}iPr)_4$), followed by reduction with sodium borohydride ($NaBH_4$) to form respectively, the desired precursor 3-(3-(3-(2-chloro-4-fluorophenyl)-1,2,4-oxadiazol-5-yl)propylamino) quinolin-6-ol (MA1, 57% yield) and reference compounds *N*-(3-(3-(2-chloro-4-fluorophenyl)-1,2,4-oxadiazol-5-yl) propyl)-6-methoxyquinolin-3-amine (MA2, 49% yield), 6-(2-Fluoroethoxy)-*N*-(3-(3-(2-chloro-4-fluorophenyl)-1,2,4-oxadiazol-5-yl)propyl)quinolin-3-amine (MA3, 51% yield) as shown in **Figure 3**. Compound **12** was synthesized using a literature procedure and NMR and MS data matched reported data (Cheng et al., 2008).

[^{11}C]MA2 and [^{18}F]MA3 were successfully produced *via* a nucleophilic substitution reaction on the phenol moiety of precursor MA1 using, respectively, [^{11}C]MeI or 1-bromo-2-[^{18}F] fluoroethane ([^{18}F]FEtBr) as presented in **Figure 4**. Carbon-11 methylation yields ranged from 34 to 47% of HPLC-recovered radioactivity relative to [^{11}C]MeI, with corresponding isolated amounts of 1628–3145 MBq. Fluorine-18 alkylations yielded isolated amounts of 617–706 MBq (24–68% of HPLC-recovered radioactivity relative to [^{18}F]FEtBr). The desired radiolabeled compounds were separated from the precursor, unreacted [^{11}C]MeI or [^{18}F]FEtBr, and side products by high-performance

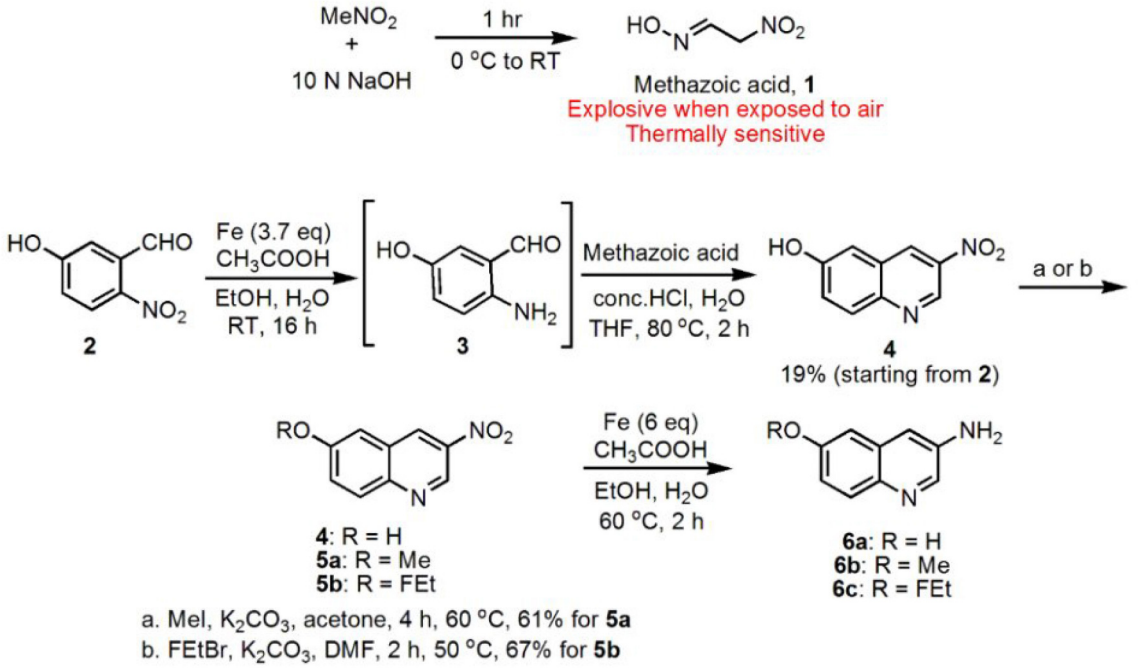

FIGURE 1 | Synthesis of substituted 3-amino quinolines (6a-c).

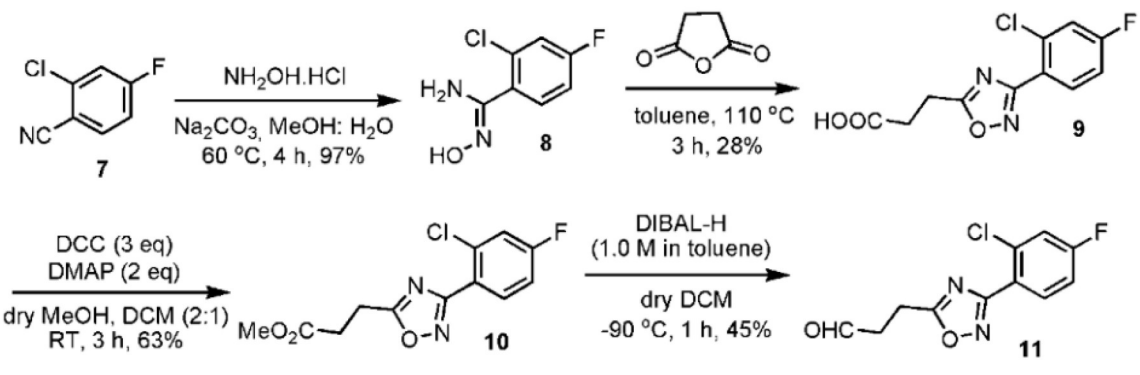

FIGURE 2 | Synthesis of the oxadiazole fragment 11.

liquid chromatography (HPLC) yielding over 98% pure [^{11}C]MA2 and over 99% pure [^{18}F]MA3 with a specific activity of 518 ± 284 GBq/μmol (n = 5) and 560 GBq/μmol (n = 2), respectively. Non-radioactive MA2 or MA3 were co-injected on the analytical HPLC system to confirm the identity of, respectively, [^{11}C]MA2 and [^{18}F]MA3.

Biodistribution Studies

The tissue distribution and kinetics of [^{11}C]MA2 and [^{18}F]MA3 were studied in male NMRI mice at 2, 10, 30, and 60 min post injection of the tracer. The results of the biodistribution studies are presented in **Table 1** ([^{11}C]MA2) and **Table 2** ([^{18}F]MA3) as percentage of injected dose (% ID) and standard uptake value (SUV).

[^{11}C]MA2 and [^{18}F]MA3 were efficiently cleared from blood (% ID 2 min/60 min ratio = 8.6 and 5.2, respectively) and all major organs. Elimination of the tracers occurred predominantly *via* the hepatobiliary pathway with excretion of radioactivity (*via* liver) into the intestines ([^{11}C]MA2: 63.8% ID and [^{18}F]MA3: 64.4% ID at 60 min post injection) and to a lesser extent *via* renal pathway, as urinary excretion was minimal with only 4.5% ID ([^{11}C]MA2) and 1.6% ID ([^{18}F]MA3) at 60 min after injection of the tracers. This is expected, as usually compounds with higher lipophilicity are expected to be excreted *via* hepatobiliary pathway. The calculated logD and polar surface area (PSA) values for [^{11}C]MA2 [logD = 4.7; PSA = 73 Å (Mackie, 2008)] and [^{18}F]MA3 [clogD = 4.9; PSA = 73 Å (Mackie, 2008)]suggest that the tracers may cross the blood-brain barrier (BBB) through

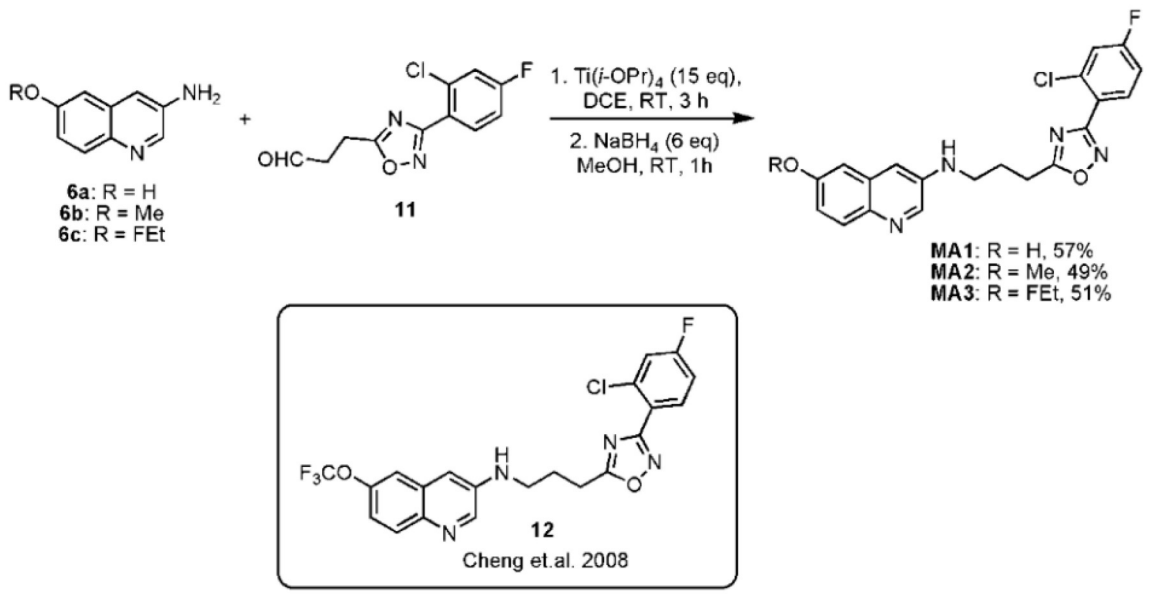

FIGURE 3 | Final step to synthesize precursor MA1 and reference compounds MA2 and MA3 with structure of compound 12.

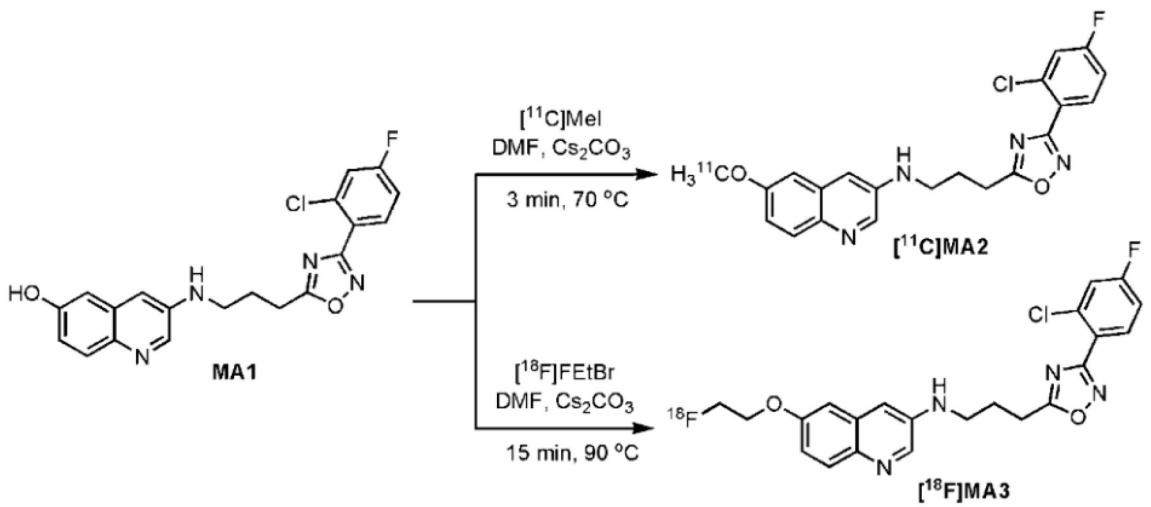

FIGURE 4 | Radiosynthesis of [^{11}C]MA2 and [^{18}F]MA3.

passive diffusion. In accordance, brain uptake of [^{11}C]MA2 (1.6% ID at 2 min post injection) was higher than brain uptake of [^{18}F]MA3 (1.2% ID at 2 min post injection) although the difference was not statistically significant ($p = 0.7$), but was followed by a rapid wash-out from brain (% ID 2 min/60 min ratio = 18.4 and 9.2, respectively). None of the studied organs, except the liver (SUV = 2.0 and 2.1, respectively, at 60 min post injection), retained [^{11}C]MA2 or [^{18}F]MA3.

Radiometabolites

The fraction of radiometabolites in mouse plasma at 2 and 30 min after injection of the tracer was determined by RP-HPLC analysis to investigate the *in vivo* stability of [^{11}C]MA2. The obtained data show that [^{11}C]MA2 is rapidly metabolized *in vivo*. At 2 min post injection of [^{11}C]MA2, 88% ($n = 2$) of the recovered radioactivity was assigned to the intact parent tracer. The percentage of intact [^{11}C]MA2 decreased to 34% at 30 min post injection of the tracer. All detected radiometabolites were more polar than the intact tracer.

Binding Profile

The results from the binding and functional assays are presented in **Table 3**. MA2, MA3, and **12** behaved as agonists with an EC_{50} of, respectively, 3, 0.13, and 0.15 nM for human CB2 (hCB2)

and an efficacy of 101, 102, and 100% in the cAMP assays. Among the tested compounds MA3 exhibited the highest binding affinity (K_i) for hCB2 (K_i = 0.8 nM) and had about 4 times higher affinity compared to **12,** about 100 times higher affinity compared to MA2 and 5 times higher affinity compared to NE40. MA2 showed a lower selectivity toward the CB1 receptor (K_i ratio hCB1/hCB2 = 19) compared with MA3 (K_i ratio hCB1/hCB2 = 127), NE40 (K_i ratio hCB1/hCB2 = 241), and 12 (K_i ratio hCB1/hCB2 = 202). NE40 behaved as an inverse agonist in the cAMP assay displaying an EC_{50} of 8 nM for hCB2 and a negative efficacy (−178%). With NE40 no species difference in binding affinity was observed.

TABLE 1 | Tissue distribution of [^{11}C]MA2 in control mice at 2 and 60 min post injection (n = 4 per time point).

[^{11}C]MA2	% ID[a]		SUV[b]	
	2 min	60 min	2 min	60 min
Bladder + urine	0.2 ± 0.1	4.5 ± 1.0	–	–
Kidneys	8.3 ± 1.6	1.0 ± 0.3	5.1 ± 0.7	0.6 ± 0.1
Liver	28.3 ± 2.9	9.1 ± 3.0	6.0 ± 0.1	2.0 ± 0.5
Spleen	0.5 ± 0.2	0.03 ± 0.01	2.0 ± 0.2	0.2 ± 0.0
Pancreas	1.6 ± 0.8	0.2 ± 0.1	2.2 ± 1.0	0.3 ± 0.0
Lungs	1.4 ± 0.3	0.1 ± 0.0	2.3 ± 0.4	0.2 ± 0.0
Heart	1.4 ± 0.4	0.1 ± 0.0	3.3 ± 0.6	0.1 ± 0.0
Intestines	9.7 ± 0.4	63.8 ± 2.9	–	–
Stomach	1.3 ± 0.3	4.2 ± 3.9	–	–
Brain	1.6 ± 0.5	0.1 ± 0.0	1.8 ± 0.2	0.1 ± 0.0
Blood	5.8 ± 0.4	0.7 ± 0.1	0.8 ± 0.1	0.1 ± 0.0

Mice were anesthetized with isoflurane (2% in oxygen) and injected i.v. with ∼9.25 MBq. Data are expressed as mean ± standard deviation; [a]Percentage of injected dose calculated as counts per minute in organ/total counts per minute recovered; [b]Standard uptake value calculated as (radioactivity as counts per minute in organ/weight of the organ in grams)/(total counts recovered / body weight in grams).

DISCUSSION

The aim of this study was to synthesize new high-affinity CB2 agonists, evaluate their brain uptake and potential for *in vivo* visualization of peripheral and brain CB2 receptors. A highly potent *N*-arylamide oxadiazole CB2 agonist was selected from literature as lead compound for the development of our radiolabeled analog 25. However, it should be noted that in the paper of Cheng et al. (2008) the position of the nitrogen atom in the biaryl moiety of the lead compound's structure is incorrectly indicated. A CB2 agonist PET-radioligand would allow to study the functional state of the CB2 receptor system under (patho)physiological conditions. The tracers were obtained in favorable yields, with a high radiochemical purity and high specific activity.

Though there may be some exceptions, the optimal logD value for molecules to cross the BBB *via* passive diffusion is assumed to be between 2.0 and 3.5 (Pike, 2009) and the PSA value is ideally less than 90 Å (van de Waterbeemd et al., 1998). As shown in **Table 4**, replacement of trifluoromethyl group (**12**) with fluoroethyl group (MA3) leads to higher Ki and EC_{50} values among the tested compounds both in mouse and human varients whereas substitution of the trifluoromethyl with a methyl group (MA2) decreases affinity. Despite slightly higher lipophilicity for MA2 compared to MA3 (clogD = 4.7 and 4.9 respectively), [^{11}C]MA2 have crossed the BBB efficiently (1.6 and 1.2% of ID at 2 min post injection respectively) and wash-out from brain was rapid for both the tracers. The brain uptake of [^{11}C]MA2 was found to be similar to that of [^{11}C]NE40 (% ID = 1.7 in mouse brain at 2 min post injection) (Evens et al., 2012) and in comparision to that of [^{11}C]A-836339 (SUV ∼ 0.5

TABLE 2 | Tissue distribution of [^{18}F]MA3 in control mice at 2, 10, 30, and 60 min post injection (n = 3 or 4 per time point).

[^{18}F]MA3	% ID[a]				SUV[b]			
	2 min	10 min	30 min	60 min	2 min	10 min	30 min	60 min
Bladder + urine	0.2 ± 0.2	0.4 ± 0.0	1.7 ± 0.3	1.6 ± 1.4	–	–	–	–
Kidneys	9.0 ± 1.2	1.6 ± 0.2	1.0 ± 0.2	0.7 ± 0.3	5.4 ± 0.4	1.1 ± 0.1	0.6 ± 0.1	0.5 ± 0.1
Liver	31.4 ± 8.4	26.1 ± 3.4	17.3 ± 6.7	10.2 ± 5.2	7.2 ± 2.0	4.7 ± 0.7	3.7 ± 1.4	2.1 ± 1.1
Spleen	0.4 ± 0.1	0.3 ± 0.1	0.1 ± 0.0	0.03 ± 0.01	5.1 ± 0.6	0.5 ± 0.0	0.5 ± 0.3	0.5 ± 0.1
Pancreas	1.4 ± 0.3	0.4 ± 0.1	0.2 ± 0.1	0.1 ± 0.0	3.0 ± 0.5	0.8 ± 0.0	0.4 ± 0.1	0.3 ± 0.1
Lungs	1.2 ± 0.3	0.5 ± 0.0	0.2 ± 0.0	0.1 ± 0.0	2.8 ± 0.7	0.7 ± 0.1	0.4 ± 0.1	0.3 ± 0.1
Heart	1.2 ± 0.1	0.3 ± 0.0	0.1 ± 0.0	0.1 ± 0.0	3.4 ± 0.3	0.6 ± 0.0	0.4 ± 0.1	0.3 ± 0.0
Intestines	9.4 ± 3.9	30.8 ± 6.1	56.2 ± 5.4	64.4 ± 2.6	–	–	–	–
Stomach	1.4 ± 0.2	0.5 ± 0.0	0.8 ± 1.0	4.4 ± 5.1	–	–	–	–
Brain	1.2 ± 0.2	1.0 ± 0.1	0.3 ± 0.1	0.1 ± 0.0	1.1 ± 0.1	0.5 ± 0.0	0.2 ± 0.0	0.1 ± 0.0
Blood	5.4 ± 0.4	2.2 ± 0.3	1.2 ± 0.1	1.0 ± 0.3	0.8 ± 0.1	0.3 ± 0.0	0.2 ± 0.0	0.1 ± 0.0
Bone	5.3 ± 1.2	3.5 ± 0.2	1.6 ± 0.5	2.2 ± 0.3	0.4 ± 0.1	0.3 ± 0.0	0.1 ± 0.0	0.2 ± 0.0

Mice were anesthetized with isoflurane (2% in oxygen) and injected i.v. with ∼0.92 MBq. Data are expressed as mean ± standard deviation; [a]Percentage of injected dose calculated as counts per minute in organ/total counts per minute recovered; [b]Standard uptake value calculated as (radioactivity as counts per minute in organ/weight of the organ in grams)/(total counts recovered/body weight in grams).

TABLE 3 | Radiometabolite analysis in blood plasma.

% of intact tracer in blood plasma (average of 2 assays)	2 min	30 min
[^{11}C]MA2	88	34

TABLE 4 | Characterization of MA2, MA3, 12, and NE40 in functional cAMP assays and radioligand binding assays with [^{3}H]CP55940.

	NE40	MA2	MA3	12
*h*CB2 cAMP EC_{50} [nM] (% eff)	8 (−178)	3 (101)	0.13 (102)	0.15 (100)
*m*CB2 cAMP EC_{50} [nM] (% eff)	11 (−128)	2 (100)	0.09 (101)	0.18 (100)
EC_{50} ratio *h*CB1/*h*CB2	> 1250	430	563	1300
*h*CB2 K_i [nM]	4	87	0.8	2.8
*h*CB1 K_i [nM]	1037	1611	102	568
K_i ratio *h*CB1/*h*CB2	241	19	127	202
*m*CB2 K_i [nM]	2	241	2.6	4.6

in rat brain at 2 min post injection) (Horti et al., 2010). The biodistribution studies also showed that [^{11}C]MA2 and [^{18}F]MA3 were cleared from blood *via* the hepatobiliary system, as could be expected for compounds with lipophilic properties. [^{11}C]MA2 was substantially metabolized as a significant fraction (> 60%) of unidentified polar radiometabolites was found in plasma of mice at 30 min after injection of the tracer. Besides the activity in the liver, due to metabolism and/or excretion of the tracers, radioactivity in other major organs was negligible at 60 min after injection of [^{11}C]MA2 or [^{18}F]MA3. Retention of the tracers in the spleen was anticipated, as this organ is known to express high levels of CB2 (Lynn and Herkenham, 1994; Galiegue et al., 1995). Surprisingly no accumulation of [^{11}C]MA2 or [^{18}F]MA3 was observed in the spleen and tracer washout from the spleen was comparable to that from other organs such as the pancreas and lungs. Previously, a lack of retention in the spleen of mice and rats was also observed for other specific CB2 PET-tracers including [^{11}C]GW405833 (Evens et al., 2011), [^{18}F]FE-GW405833 (Evens et al., 2011), and a ^{18}F-labeled 2-oxoquinoline derivative (Turkman et al., 2012). The low spleen uptake could also due to the lower binding affinity of [^{11}C]GW405833 (35 nM) and [^{18}F]FE-GW405833 (27 nM) for CB2 or in the case of the ^{18}F-labeled 2-oxoquinoline derivative a low specific activity (44.4 GBq/μmol) (Turkman et al., 2012). Also recently, a 1,3,5-triazine based CB2 agonist labeled with fluorine-18 was reported to have a low spleen uptake (0.39% ID/g, at 15 min) (Yrjölä et al., 2015). In general agonists bind to activated receptor sites, which only represent a fraction of total binding sites, and this may explain the low spleen uptake. However, the specific *in vivo* binding of these tracers to CB2 receptors has to be established, experiments with these two tracers on local overexpression of *h*CB2 in rats (as previously shown) (Evens et al., 2011; Turkman et al., 2012) are currently underway.

CONCLUSIONS

We successfully synthesized MA2 and MA3 and their *in vitro* binding affinity for *h*CB2 was found to be 87 nM and 0.8 nM, respectively. Radiolabeled [^{11}C]MA2 and [^{18}F]MA3 was obtained in relatively high yields, high radiochemical purity, and high specific activity. Preliminary biodistribution studies indicate favorable brain uptake and clearance from blood and major organs. These preliminary results indicate [^{11}C]MA2 and [^{18}F]MA3 can be potential tracers for imaging brain CB2 receptors, in the view of their higher CB2 affinity and good brain uptake. It has to be noted that, not many CB2 agonists are available for pharmacologic studies that have both high affinity and excellent brain uptake and the compounds described here are suited to perform pharmacological experiments studying the role of CB2 in CNS.

MATERIALS AND METHODS

General

2-Chloro-4-fluorobenzonitrile was purchased from TCI Europe (Zwijndrecht, Belgium). All other chemicals and solvents were obtained from Acros Organics (Geel, Belgium), Sigma-Aldrich (Bornem, Belgium), or VWR International (Leuven, Belgium). For ascending thin layer chromatography (TLC), pre-coated aluminum backed plates (Silica gel 60 with fluorescent indicator UV 254 nm, 0.2 mm thickness; Macherey-Nagel, Düren, Germany) were used. Molecular mass measurements were performed on a time-of-flight mass spectrometer (LCT, Micromass, Manchester, UK) equipped with an orthogonal electrospray ionization (ESI) interface. Acquisition and processing of data was done using MassLynx software (version 3.5, Micromass). Mass data were rounded to the whole number. ^{1}H nuclear magnetic resonance (NMR) spectra were acquired with a Bruker Avance II spectrometer (400 MHz, 5 mm probe, Fällanden, Switzerland). Chemical shifts are reported in parts per million relative to tetramethylsilane ($\delta = 0$). Coupling constants are reported in hertz (Hz). Splitting patterns are defined by s (singlet), d (doublet), t (triplet), or m (multiplet). The clogD and PSA values were calculated using, respectively, Marvinsketch 5.7.0 software and the calculator from Daylight (http://www.daylight.com/meetings/emug00/Ertl/tpsa.html).
HPLC analysis was performed on an L2130 LaChrom Elite pump (Hitachi, Tokyo, Japan) connected to a UV L2400 LaChrom Elite spectrometer (Hitachi). Radiolabeled compounds were analyzed by passage of the HPLC eluate (after passing through the UV detector) over a 3-inch NaI(Tl) scintillation detector connected to a single channel analyzer (GABI box; Raytest, Straubenhardt, Germany). Data were acquired and analyzed using a RaChel (Lablogic, Sheffield, UK) or GINA Star (Raytest) data acquisition system. Quantification of radioactivity during biodistribution and metabolite studies was performed using an automated gamma counter equipped with a 3-inch NaI(Tl) well crystal coupled to a multichannel analyzer, mounted in a sample changer [2480 Wizard (Mackie, 2008), Perkin Elmer, Massachusetts, USA]. The values are corrected for background radiation, physical decay and counter dead time.

Animals were housed in individually ventilated cages in a thermo-regulated (22°C), humidity-controlled facility under a 12 h light/12 h dark cycle, with free access to food and water. All animal experiments were performed in compliance with the

principles set by the Belgian law relating to the conduct of animal experimentation, after approval from the university (KU Leuven) animal ethics committee.

Organic Synthesis

Methazoic Acid (1)

Caution:

Methazoic acid is a potential explosive, heat, and shock sensitive compound. To a solution of 10 M NaOH (3 mL) at 0°C was added dropwise $MeNO_2$ (0.5 mL) and the resulting mixture was stirred for 15 min. The reaction mixture was allowed to warm to room temperature, stirred for 15 min and a second amount of $MeNO_2$ (0.5 mL) was added. After stirring until a clear brown solution was formed (∼30 min), ice-cold water (50 mL), and concentrated hydrochloric acid (∼11.6 M HCl, 3 mL) were slowly added to the mixture. The resultant solution was extracted with diethyl ether (Et_2O; 2 × 100 mL) and the organic layers were collected and dried over magnesium sulfate ($MgSO_4$). The solvent was carefully removed under reduced pressure without heating to yield compound **1** (∼1 g) as an orange-yellow viscous oil, which was used in the synthesis of **4**, without any further purification.

3-Nitro-6-Hydroxyquinoline (4)

Step A:

To a solution of 2-nitro-5-hydroxybenzaldehyde (**2**; 1.20 g, 7.18 mmol, 1.0 eq) in ethanol (EtOH; 30 mL) was added Fe powder (1.48 g, 26.57 mmol, 3.7 eq), followed by acetic acid (2.4 mL) and H_2O (0.8 mL). After stirring at room temperature for 16 h, the dark brown reaction mixture was diluted with EtOH (30 mL), filtered through a sintered funnel, and concentrated *in vacuo*. The crude mixture was extracted with dichloromethane (DCM; 2 × 200 mL), the combined organic layers were dried over $MgSO_4$ and concentrated *in vacuo*. Compound **3** was obtained as a crude yellow powder, which was used in step B without any further purification.

Step B:

To a stirred solution of **3** in either tetrahydrofuran (THF) or EtOH (10 mL) was added a solution of compound **1** (∼1 g) in a mixture of H_2O (5 mL) and 5 M HCl (5 mL). The dark brown mixture was heated to 80°C and stirred for 2 h. The solvent was evaporated under reduced pressure, the crude material was extracted with DCM (3 × 100 mL) and the solution was again concentrated under reduced pressure and purified over silica column to give **4** as a pale brown solid. ^{1}H NMR ($CDCl_3$): δ 7.10–7.17 (m, 1H, Ar), 7.41–7.45 (m, 1H, Ar), 8.11 (s, 1H, Ar), 8.67 (s, 1H, Ar), 9.24 (s, 1H, Ar). MS (ESI) m/z: 191.2 [$(M+H)^+$, 100%].

3-Nitro-6-Methoxyquinoline (5a)

To a solution of compound **4** (260 mg, 1.37 mmol, 1 eq) in acetone (15 mL), K_2CO_3 (283 mg, 2.05 mmol, 1.5 eq) and MeI (5 eq) were added and the reaction mixture was stirred at 60 °C for 4 h. Completion of reaction was confirmed by TLC (EtOAc/heptane 1:1). Acetone was removed under reduced pressure and the crude residue was diluted with DCM (100 mL) and washed with H_2O (3 × 25 mL). The organic layer was dried over $MgSO_4$ and the solvent was removed under reduced pressure. Silica gel column purification yielded **5** (171 mg) as pale yellow crystalline needles. Yield: 61%. TLC (EtOAc/heptane 1:1): $R_f = 0.55$. ^{1}H NMR ($CDCl_3$): δ 3.94 (s, 3H, OMe), 7.19–7.23 (m, 1H, Ar), 7.50–7.55 (m, 1H, Ar), 8.05 (s, 1H, Ar), 8.86 (s, 1H, Ar), 9.44 (s, 1H, Ar). MS (ESI) m/z: 205.2 [$(M+H)^+$, 100%].

6-(2-Fluoroethoxy)-3-Nitroquinoline (5b)

To a solution of compound **4** (260 mg, 1.37 mmol, 1 eq) in DMF (15 mL), K_2CO_3 (283 mg, 2.05 mmol, 1.5 eq) and FEtBr (5 eq) were added and the reaction mixture was stirred at 50°C for 2 h. Completion of reaction was confirmed by TLC (EtOAc/heptane 1:1). The crude residue was diluted with DCM (100 mL) and washed with H_2O (3 × 25 mL). The organic layer was dried over $MgSO_4$ and the solvent was removed under reduced pressure. Silica gel column purification yielded **5b** (230 mg) as pale yellow crystalline needles. Yield: 67%. TLC (EtOAc/heptane 1:1): $R_f = 0.60$. ^{1}H NMR ($CDCl_3$): δ 4.36 (dt, 2H, *J* 2.4 & 19.4), 4.84 (dt, 2H, *J* 2.4 & 39.2), 7.22 (s, 1H, Ar), 7.59 (d, 1H, *J* 9.2, Ar), 8.10 (d, 1H, *J* 9.2, Ar), 8.87 (s, 1H, Ar), 9.47 (s, 1H, Ar). MS (ESI) m/z: 236.8 [$(M+H)^+$, 100%].

3-Amino-6-Quinolinols (6a-c)

*3-Aminoquinolin-6-ol (**6a**)* To a solution of compound **4** (330 mg, 1.74 mmol, 1 eq) in EtOH (10 mL), Fe powder (485 mg, 8.68 mmol, 5 eq) was added and the mixture was stirred. After adding acetic acid (1 mL) and H_2O (0.2 mL), the reaction mixture was heated to 60°C and stirred for 3 h. The Fe powder was removed by filtering the reaction mixture over a sintered funnel. The filtrate was collected, dried over $MgSO_4$ and concentrated to yield **6a** (100 mg) as a pale yellow powder. Yield: 36%. TLC (DCM/MeOH, 95:5): $R_f = 0.21$. MS (ESI) m/z: 161.0 [$(M+H)^+$, 100%].

*6-Methoxyquinolin-3-amine (**6b**)* Compound **6b** was synthesized starting from compound **5a** in accordance with the procedure described for compound **6a**. Yellow solid was obtained in 45% yield. TLC (DCM/MeOH 95:5): $R_f = 0.25$. MS (ESI) m/z: 174.7 [$(M+H)^+$, 100%].

*6-(2-Fluoroethoxy)quinolin-3-amine (**6c**)* Compound **6c** was also synthesized starting from compound **5b** as described for compound **6a**. Colorless powder was obtained in 60% yield (175 mg). R_F 0.25 (9.5:0.5 DCM:MeOH). ^{1}H NMR (MeOD): δ 4.55 (dt, 2H, *J* 3.5 & 28.8), 5.01 (dt, 2H, *J* 3.4 & 47.8), 7.35 (d, 1H, *J* 9.2, Ar), 7.25 (s, 1H, Ar), 7.51 (s, 1H, Ar), 7.98 (d, 1H, *J* 9.2, Ar) 8.54 (s, 1H, Ar). MS (ESI) m/z: 206.9 [$(M+H)^+$, 100%].

2-Chloro-4-Fluoro-N′-Hydroxybenzamidine (8)

To a solution of 2-chloro-4-fluoro-benzonitrile (**7**; 1.0 g, 6.45 mmol, 1.0 eq) in MeOH was added $NH_2OH{\cdot}HCl$ (0.58 g, 8.36 mmol, 1.3 eq), Na_2CO_3 (1.0 g, 9.64 mmol, 1.5 eq) and H_2O (4 mL), and the reaction mixture was stirred for 4 h at 60°C. The solvent was evaporated under reduced pressure and the crude residue was extracted with DCM (2 × 500 mL). The combined organic layers were dried over $MgSO_4$ and the solvent was removed under reduced pressure. The crude compound **8** (1.18 g, 97%) was used as such in the next step without any further

purification. R_F 0.41 (1:1 hexane:EtOH). MS (ESI) *m/z*: 189.0 [$(M+H)^+$, 100%].

3-(3-(2-Chloro-4-Fluorophenyl)-1,2,4-Oxadiazol-5-yl) Propanoic Acid (9)

A solution of compound **8** (1.0 g, 5.32 mmol, 1.0 eq) and succinic anhydride (0.53 g, 5.32 mmol, 1.0 eq) in toluene (15 mL) was stirred for 3 h at 110°C. Toluene was evaporated under reduced pressure, the crude residue was extracted with DCM (3 × 250 mL), the combined organic extracts were dried over $MgSO_4$ and concentrated under reduced pressure. The crude residue was purified using silica gel column chromatography (EtOAc/heptane gradient 10–30% EtOAc) and compound **9** was obtained as a white solid (425 mg). Yield: 28%. R_F 0.25 (1:1 hexane:EtOH). ^{1}H NMR (DMSO-d_6): δ 2.56 (t, 2H, *J* 6.7, CH2), 2.94 (t, 2H, *J* 6.9, CH2), 7.11–7.18 (m, 1H, Ar), 7.39–7.44 (m, 1H, Ar), 7.65–7.71 (m, 1H, Ar). MS (ESI) *m/z*: 269.29 [(MH^-), 100%].

Methyl-3-(3-(2-Chloro-4-Fluorophenyl)-1,2,4-Oxadiazol-5-yl)Propanoate (10)

Compound **9** (100 mg, 0.370 mmol, 1 eq) was dissolved in dry DCM (4 mL) followed by the addition of DCC (229 mg, 1.11 mmol, 3 eq), DMAP (90 mg, 0.740 mmol, 2 eq), and dry MeOH (0.5 mL). The reaction mixture was stirred for 16 h at room temperature. The reaction mixture was concentrated under reduced pressure, DCM (50 mL) was added and the solution was washed with H_2O (2 × 20 mL). After drying the organic layer over $MgSO_4$, the solvent was removed and the crude product purified through silica gel column chromatography (EtOAc/heptane gradient 0–10% EtOAc) yielded pure compound **10**. *Colorless oil (63% yield, 66 mg)*. R_F 0.55 (1:1 hexane:EtOH). ^{1}H NMR ($CDCl_3$): δ 2.54 (t, 2H, *J* 7.3, CH2), 2.89 (t, 2H, *J* 7.3, CH2), 3.33 (s, 3H, CH3), 6.66–6.72 (m, 1H, Ar), 6.85–6.89 (m, 1H, Ar), 7.50–7.55 (m, 1H, Ar). MS (ESI) *m/z*: 285.1 [(MH^+), 100%].

3-(3-(2-Chloro-4-Fluorophenyl)-1,2,4-Oxadiazol-5-yl)Propanal (11)

To a solution of compound **10** (100 mg, 0.352 mmol, 1 eq) in dry DCM (5 mL) cooled to −80°C was added drop-wise over 5 min DIBAL-H 1.5 M in toluene (0.107 mL, 0.528 mmol, 1.5 eq) and the reaction mixture was stirred at the same temperature for 1 h. The reaction was quenched with a few drops of H_2O, DCM (50 mL) was added and the mixture was washed with H_2O (2 × 20 mL). The organic layer was dried over $MgSO_4$ and the solvent was removed under reduced pressure. The crude residue was purified through silica gel flash chromatography using a mixture of heptane/EtOAc (2:1) to yield the desired aldehyde **11** (40 mg). *Colorless powder* (40 mg, 45%). R_F 0.40 (1:1 hexane:EtOH). ^{1}H NMR ($CDCl_3$): δ 2.72 (t, 2H, *J* 6.8, CH2), 2.87 (t, 2H, *J* 6.9, CH2), 6.67–6.70 (m, 1H, Ar), 6.85–6.89 (m, 1H, Ar), 7.54–7.56 (m, 1H, Ar), 9.49 (s. 1H, CHO). MS (ESI) *m/z*: 255.1 [(MH^+), 100%].

N-(3-(3-(2-Chloro-4-Fluorophenyl)-1,2,4-Oxadiazol-5-yl)Propyl)-6-Methoxyquinolin-3-Amine (MA2)

Compound **11** (87.0 mg, 0.343 mmol, 1 eq) and amine **6b** (60.0 mg, 0.343 mmol, 1 eq) were dissolved in dichloroethane (DCE; 3 mL), followed by the addition of Ti(O-*i*Pr)$_4$ (1.68 mL, 5.142 mmol, 15 eq) at room temperature. After stirring for 1 h, the reaction mixture was added dropwise to a stirred solution of $NaBH_4$ (77.8 mg, 2.057 mmol, 6 eq) in dry MeOH (6 mL) at 0^{o}C. After the addition was complete the mixture was brought to room temperature and stirred for 2 h. The reaction was quenched with a few drops of 1 M HCl and solvents were evaporated under reduced pressure. The residue was dissolved in DCM (100 mL), the solution was washed with H_2O (2 × 15 mL) and the organic layer was dried and concentrated by vacuum evaporation. The crude product was purified over silica gel chromatography using mixtures of DCM/MeOH as eluent. Pale yellow oil (70 mg), yield: 49%. TLC (hexane/EtOH 1:1): R_f = 0.21. ^{1}H NMR ($CDCl_3$): δ 2.25–2.30 (m, 2H, H^{3b}), 3.10–3.16 (m, 2H, H^{3c}), 3.40 (t, 2H, *J* 6.7, H^{3a}), 3.87 (s, 3H, OMe), 6.86–6.88 (m, 1H, Ar), 6.94–6.97 (m, 1H, Ar), 7.02–7.11 (m, 2H, Ar), 7.21–7.27 (m, 2H, Ar), 7.78–7.83 (m, 1H, Ar), 7.85–7.91 (m, 1H, Ar), 8.25 (br s, 1H, NH). MS (ESI) *m/z*: 412 [$(M+H)^+$, 100%].

3-(3-(3-(2-Chloro-4-Fluorophenyl)-1,2,4-Oxadiazol-5-yl)Propylamino)Quinolin-6-ol (MA1)

MA1 was synthesized starting from compound **6a** in accordance with the procedure described for **MA2**. Pale yellow solid (90 mg), yield: 57%. TLC (hexane/EtOH 1:1): R_f = 0.20. MS (ESI) *m/z*: 398 [$(M+H)^+$, 100%]. ^{1}H NMR ($CDCl_3$): δ 2.50–2.56 (m, 2H, H^{3b}), 3.40–3.46 (m, 2H, H^{3c}), 3.60–3.65 (m, 2H, H^{3a}), 7.16–7.26 (m, 4H, Ar), 7.42–7.48 (m, 1H, Ar), 7.65–7.70 (m, 1H, Ar), 8.09–8.13 (m, 1H, Ar), 8.24–8.28 (m, 1H, Ar), 8.45 (s, 1H, NH). HRMS (ESI) Calcd. for $C_{20}H_{17}ClFN_4O_2$ $[M+H]^+$: 399.1018. Found: 399.1058.

6-(2-Fluoroethoxy)-N-(3-(3-(2-Chloro-4-Fluorophenyl) -1,2,4-Oxadiazol-5-yl)Propyl)Quinolin-3-amine (MA3)

Yellow crystalline solid (55 mg, 51%). R_F 0.25 (1:1 hexane:EtOH). ^{1}H NMR ($CDCl_3$): δ 2.20–2.30 (m, 2H), 3.11 (t, 2H, *J* 7.2), 3.37 (t, 2H, *J* 6.8), 4.25 (dt, 2H, *J* 4.2 & 27.7), 4.77 (dt, 2H, *J* 4.1 & 47.4), 6.86 (d, 1H, *J* 2.7, Ar), 6.92 (d, 1H, *J* 2.6, Ar), 7.03–7.11 (m, 2H, Ar), 7.23–7.28 (m, 1H, Ar), 7.78–7.89 (m, 2H, Ar), 8.25 (d, 1H, *J* 2.7, Ar). HRMS (ESI) Calcd. for $C_{22}H_{20}ClF_2N_4O_2$ (MH^+): 445.1237. Found: 445.1276.

Radiosynthesis

[^{11}C]CH_3I and [^{18}F]FEtBr were produced according to methods described by Evens et al. (2008) and Chitneni et al. (2008), respectively. [^{11}C]CH_3I was bubbled with a stream of helium through a solution of the precursor MA1 (100 μg) and cesium carbonate (Cs_2CO_3; 1–2 mg) in dimethylformamide (DMF, 100 μL) until the radioactivity in the reaction vial was stabilized. The reaction mixture was heated for 3 min at 70°C, diluted with 1 mL of water for injection and applied onto an HPLC column (Waters XBridge RP-C18, 5 μm, 4.6 × 150 mm) that was eluted with a mixture of EtOH/sodium acetate (NaOAc) buffer 0.05 M pH 5.5 (53:47 V/V) as mobile phase at a flow rate of 1 mL/min. The

desired product [^{11}C]MA2 eluted after 11 min. [^{18}F]FEtBr was distilled with a stream of helium and passed through an ascarite column (6 × 150 mm) in a reaction vial containing MA1 (100 μg) and Cs_2CO_3 (1–2 mg) in DMF (100 μL). After heating for 15 min at 90°C, the reaction mixture was diluted with 1 mL of water for injection and injected on an XBridge column (5 μm, 4.6 × 150 mm) which was eluted with a mixture of EtOH/NaOAc 0.05 M pH 5.5 (45:55 V/V) at a flow rate of 1 mL/min. The desired product [^{18}F]MA3 was collected after 20 min. Quality control of [^{11}C]MA2 and [^{18}F]MA3 was performed on an analytical HPLC system consisting of an XBridge column (RP-C18, 3.5 μm, 3.0 × 100 mm; Waters) eluted with a mixture of CH_3CN/NaOAc buffer 0.05 M pH 5.5 ([^{11}C]MA2: 45:55 V/V and [^{18}F]MA3: 40:60 V/V) at a flow rate of 0.8 mL/min. UV detection was performed at 254 nm.

Biodistribution Studies

The biodistribution of [^{11}C]MA2 and [^{18}F]MA3 was studied in normal male Naval Medical Research Institute (NMRI) mice. A solution of HPLC-purified [^{11}C]MA2 or [^{18}F]MA3 was diluted with saline to obtain an ethanol concentration < 10%. Mice were anesthetized with isoflurane (2% in oxygen) and injected intravenously (i.v.) with [^{11}C]MA2 (∼ 9.25 MBq) or [^{18}F]MA3 (∼ 0.92 MBq) via a lateral tail vein. The mice were sacrificed by decapitation at 2, and 60 min post injection (for [^{11}C]MA2, $n = 4$) and at 2, 10, 30, or 60 min post injection (for [^{18}F]MA3, $n = 3$ or 4 per time point) and dissected. Blood, organs, and other body parts were collected in tared tubes and the radioactivity in each tube was measured using an automated gamma counter. The tubes containing selected organs and blood were weighed. For calculation of total radioactivity in blood, blood mass was assumed to be 7% of the body mass (Fritzberg et al., 1982). Quantitative data are expressed as mean ± standard deviation (SD). Means were compared using an unpaired two-tailed student *t*-test. Values were considered statistically significant for $P \leq 0.05$.

Plasma Radiometabolite Analysis

After i.v. administration of [^{11}C]MA2 (∼ 9.25 MBq) via a lateral tail vein to anesthetized NMRI mice (isoflurane 2% in oxygen), the mice were decapitated at 2 or 30 min post injection ($n = 2$ per time point). Blood was collected into lithium heparin-containing tubes (4.5-mL lithium heparin PST tubes, BD Vacutainer; BD, Franklin Lakes, New Jersey) and stored on ice. The blood samples were centrifuged for 10 min at 3000 rpm to separate the plasma. The isolated plasma was spiked with authentic non-radioactive MA2 (15 μL of 1 mg/mL solution in CH_3CN) and analyzed by RP-HPLC on a Chromolith RP C_{18} column (3 mm x 100 mm; Merck) eluted with gradient mixtures of CH_3CN (A) and 0.05 M NaOAc pH 5.5 (B) (0–5 min: Isocratic 100% B, flow rate of 0.5 mL/min; 5–10 min: Linear gradient 100 B to 10% B, flow rate of 1 mL/min; 10–13 min: Isocratic 10% B, flow rate of 1 mL/min; 13–13.1 min: Linear gradient 10 B to 100% B, flow rate of 0.5 mL/min; 13.1–15 min: Isocratic 100% B, flow rate of 0.5 mL/min). After passing through a UV detector (254 nm) and an in-line 3-inch NaI(Tl) scintillation detector, the HPLC eluate was collected as 0.5- or 1-mL fractions (model 2110 fraction collector, Biorad, Hercules, CA). The radioactivity in all fractions was measured using an automated gamma counter. The recovery of the injected radioactivity from the HPLC apparatus and Chromolith column was 94.9 ± 0.9 % ($n = 4$).

Functional and Binding Experiments

The competition binding experiments and functional assays were performed by Roche Healthcare.

Cell Culture

CHO-K1 beta-arrestin cells (DiscoveRx, Fremont, CA) expressing hCB2, mouse CB2 (mCB2), and human CB1 (hCB1) were cultured in F-12 Nutrient Mixture (HAM) supplemented with 10% fetal bovine serum (FBS), 300 μg/mL hygromycin and 800 μg/mL geneticin (G418). Cells were incubated in a humidified atmosphere at 37°C with 5% CO_2.

cAMP Assay

cAMP was measured using cAMP-Nano-TRF detection kit (Roche Diagnostics, Penzberg, Germany). Cells were seeded 17–24 h prior to the experiment 3 × 10^4 cells per well in a black 96-well plate with flat clear bottom (Corning, Wiesbaden, Germany) in growth medium and incubated in 5% CO_2 at 37°C in a humidified incubator. The growth medium was exchanged with Krebs Ringer bicarbonate buffer with 1 mmol/L 3-isobutyl-1-methylxanthine (IBMX), 0.1% fatty acid-free bovine serum albumin (BSA) and incubated at 30°C for 60 min. Agonist was added to a final assay volume of 100 μL and the mixture was incubated for 30 min at 30°C. The assay was stopped by the addition of 50 μL 3x lysis reagent and shaken for 2 h at room temperature. The time-resolved energy transfer was measured using an LF502 Nanoscan FLT (IOM, Berlin, Germany), equipped with a laser as excitation source. cAMP content was determined from the function of a standard curve spanning from 10 to 0.13 nmol/L cAMP.

Radioligand Binding Assay

Stably transfected cells were treated for 24 h with 5 mM butyrate in growth medium before harvesting, followed by homogenization in 15 mmol/L Hepes, 0.3 mmol/L EDTA, 1 mmol/L EGTA, 2 mmol/L $MgCl_2$, complete EDTA-free protease inhibitor (Roche Applied Science, Rotkreuz, Switzerland), pH 7.4 using a glass potter and centrifugation at 47,800 g at 4°C for 30 min. The pellet was then rehomogenized twice in the same buffer and centrifuged (47,800 g, 4°C, 30 min). The final pellet was then resuspended in 75 mmol/L Tris, 0.3 mmol/L EDTA, 1 mmol/L EGTA, 12.5 mmol/L $MgCl_2$, 250 mmol/L sucrose, pH 7.4 at a protein concentration of 1 to 3 mg/mL, aliquoted, frozen on dry ice and stored at −80°C. Saturation binding was performed with 0.05 to 2.6 nM [^{3}H]CP55940 (Perkin Elmer) and 1.0 μg of membrane protein. CP55940 (10 μM) was used to define non-specific binding. More than 95% of the total binding signal was specific. Assay buffer consisted of 50 mmol/L Tris-HCl, 5 mmol/L $MgCl_2$, 2.5 mmol/L EGTA, and 0.1% fatty acid-free BSA, pH 7.4. Assays were initiated by addition of membranes in a final

volume of 250 μL/well. Mixtures were incubated for 3 h at room temperature and then vacuum filtered and rinsed with wash buffer (50 mmol/L Tris-HCl, 5 mmol/L $MgCl_2$, 2.5 mmol/L EGTA, and 0.5% fatty acid-free BSA, pH 7.4) on a Filtermate cell harvester through Packard GF/B filters presoaked in 0.3% polyethylenimine.

For competition binding, membrane preparations were incubated with 0.3 nM [^{3}H]CP55940 in the presence or absence of increasing concentrations of ligands for 60 min at 30°C in a final volume of 0.2 mL of 50 mmol/L Tris-HCl, 5 mmol/L $MgCl_2$, 2.5 mmol/L EGTA, 0.1% fatty acid-free BSA, and 1% DMSO, pH 7.4, buffer, gently shaking. Non-specific binding was defined with 10 μM CP55940. All binding reactions were terminated by vacuum filtration onto 0.5% polyethylenimine presoaked GF/B filter plates (Packard) followed by seven brief washes with 2 mL of ice-cold binding buffer containing 0.5% fatty acid-free BSA. Plates were dried at 50°C for 1 h and liquid scintillation counting was used to determine bound radiolabel. IC_{50} values and Hill slopes were determined by a four parameter logistic model using ActivityBase (ID Business Solution, Guilford, UK). pK_i values were determined by the generalized Cheng-Prusoff equation (Yung-Chi and Prusoff, 1973).

AUTHOR CONTRIBUTIONS

DV and MA performed experiments. CU contributed to binding assay experiments. DV, MA, GB analyzed the data. All the authors contributed toward designing the experiments and writing the manuscript.

ACKNOWLEDGMENTS

We thank Ann Van Santvoort (Department of Nuclear Medicine, KU Leuven) for her assistance in the small-animal PET scans and Julie Cornelis (Laboratory for Radiopharmacy, KU Leuven) for her skillful help with the animal experiments. We also would like to thank Dr. Sofie Celen for useful discussions. This research was funded by a Ph.D. grant of the Institute for the Promotion of Innovation through Science and Technology in Flanders (IWT) and in part by *in-vivo* molecular imaging research (IMIR grant PF/10/017).

REFERENCES

Atwood, B. K., and Mackie, K. (2010). CB2: a cannabinoid receptor with an identity crisis. *Br. J. Pharmacol.* 160, 467–479. doi: 10.1111/j.1476-5381.2010.00729.x

Benito, C., Romero, J. P., Tolon, R. M., Clemente, D., Docagne, F., Hillard, C. J., et al. (2007). Cannabinoid CB1 and CB2 receptors and fatty acid amide hydrolase are specific markers of plaque cell subtypes in human multiple sclerosis. *J. Neurosci.* 27, 2396–2402. doi: 10.1523/JNEUROSCI.4814-06.2007

Cabral, G. A., and Griffin-Thomas, L. (2009). Emerging role of the cannabinoid receptor CB2 in immune regulation: therapeutic prospects for neuroinflammation. *Expert Rev. Mol. Med.* 11, e3. doi: 10.1017/S1462399409000957

Cheng, Y., Albrecht, B. K., Brown, J., Buchanan, J. L., Buckner, W. H., DiMauro, E. F., et al. (2008). Discovery and optimization of a novel series of *N* -arylamide oxadiazoles as potent, highly selective and orally bioavailable cannabinoid receptor 2 (CB_2) agonists. *J. Med. Chem.* 51, 5019–5034. doi: 10.1021/jm800463f

Chitneni, S. K., Garreau, L., Cleynhens, B., Evens, N., Bex, M., Vermaelen, P., et al. (2008). Improved synthesis and metabolic stability analysis of the dopamine transporter ligand [18F]FECT. *Nucl. Med. Biol.* 35, 75–82. doi: 10.1016/j.nucmedbio.2007.09.001

DiMauro, E. F., Buchanan, J. L., Cheng, A., Emkey, R., Hitchcock, S. A., Huang, L., et al. (2008). Structural modifications of *N*-arylamide oxadiazoles: Identification of *N*-arylpiperidine oxadiazoles as potent and selective agonists of CB_2. *Bioorg. Med. Chem. Lett.* 18, 4267–4274. doi: 10.1016/j.bmcl.2008.06.096

Evens, N., Bosier, B., Lavey, B. J., Kozlowski, J. A., Vermaelen, P., Baudemprez, L., et al. (2008). Labelling and biological evaluation of [11C]methoxy-Sch225336: a radioligand for the cannabinoid-type 2 receptor. *Nucl. Med. Biol.* 35, 793–800. doi: 10.1016/j.nucmedbio.2008.07.004

Evens, N., Muccioli, G. G., Houbrechts, N., Lambert, D. M., Verbruggen, A. M., Van Laere, K., et al. (2009). Synthesis and biological evaluation of carbon-11- and fluorine-18-labeled 2-oxoquinoline derivatives for type 2 cannabinoid receptor positron emission tomography imaging. *Nucl. Med. Biol.* 36, 455–465. doi: 10.1016/j.nucmedbio.2009.01.009

Evens, N., Vandeputte, C., Coolen, C., Janssen, P., Sciot, R., Baekelandt, V., et al. (2012). Preclinical evaluation of [11C]NE40, a type 2 cannabinoid receptor PET tracer. *Nucl. Med. Biol.* 39, 389–399. doi: 10.1016/j.nucmedbio.2011.09.005

Evens, N., Vandeputte, C., Muccioli, G. G., Lambert, D. M., Baekelandt, V., Verbruggen, A. M., et al. (2011). Synthesis, *in vitro* and *in vivo* evaluation of fluorine-18 labelled FE-GW405833 as a PET tracer for type 2 cannabinoid receptor imaging. *Bioorg. Med. Chem.* 19, 4499–4505. doi: 10.1016/j.bmc.2011.06.033

Fritzberg, A. R., Whitney, W. P., Kuni, C. C., and Klingensmith, W. (1982). Biodistribution and renal excretion of 99mTc-N,N′-bis-(mercaptoacetamido) ethylenediamine. Effect of renal tubular transport inhibitors. *Int. J. Nucl. Med. Biol.* 9, 79–82. doi: 10.1016/0047-0740(82)90081-X

Galiegue, S., Mary, S., Marchand, J., Dussossoy, D., Carriere, D., Carayon, P., et al. (1995). Expression of central and peripheral cannabinoid receptors in human immune tissues and leukocyte subpopulations. *Eur. J. Biochem.* 232, 54–61. doi: 10.1111/j.1432-1033.1995.tb20780.x

Gullapalli, S., Amrutkar, D., Gupta, S., Kandadi, M. R., Kumar, H., Gandhi, M., et al. (2010). Characterization of active and inactive states of CB1 receptor and the differential binding state modulation by cannabinoid agonists, antagonists and inverse agonists. *Neuropharmacology* 58, 1215–1219. doi: 10.1016/j.neuropharm.2010.03.001

Horti, A. G., Gao, Y., Ravert, H. T., Finley, P., Valentine, H., Wong, D. F., et al. (2010). Synthesis and biodistribution of [11C]A-836339, a new potential radioligand for PET imaging of cannabinoid type 2 receptors (CB2). *Bioorg. Med. Chem.* 18, 5202–5207. doi: 10.1016/j.bmc.2010.05.058

Lynn, A. B., and Herkenham, M. (1994). Localization of cannabinoid receptors and nonsaturable high-density cannabinoid binding sites in peripheral tissues of the rat: implications for receptor-mediated immune modulation by cannabinoids. *J. Pharmacol. Exp. Ther.* 268, 1612–1623.

Mackie, K. (2008). Cannabinoid receptors: where they are and what they do. *J. Neuroendocrinol.* 20(Suppl. 1), 10–14. doi: 10.1111/j.1365-2826.2008.01671.x

Moldovan, R.-P., Teodoro, R., Gao, Y., Deuther-Conrad, W., Kranz, M., Wang, Y., et al. (2016). Development of a high-affinity PET radioligand for imaging cannabinoid subtype 2 receptor. *J. Med. Chem.* 59, 7840–7855. doi: 10.1021/acs.jmedchem.6b00554

Neises, B., and Steglich, W. (1978). Simple method for the esterification of carboxylic acids. *Angew. Chemie Int. Ed.* 17, 522–524. doi: 10.1002/anie.197805221

Palazuelos, J., Aguado, T., Pazos, M. R., Julien, B., Carrasco, C., Resel, E., et al. (2009). Microglial CB2 cannabinoid receptors are neuroprotective in Huntington's disease excitotoxicity. *Brain* 132, 3152–3164. doi: 10.1093/brain/awp239

Pike, V. W. (2009). PET radiotracers: crossing the blood–brain barrier and surviving metabolism. *Trends Pharmacol. Sci.* 30, 431–440. doi: 10.1016/j.tips.2009.05.005

Piomelli, D. (2003). The molecular logic of endocannabinoid signalling. *Nat. Rev. Neurosci.* 4, 873–884. doi: 10.1038/nrn1247

Ramirez, B. G., Blázquez, C., Gómez del Pulgar T., Guzmán, M., and de Ceballos, M. L. (2005). Prevention of Alzheimer's Disease pathology by cannabinoids: neuroprotection mediated by blockade of microglial activation. *J. Neurosci.* 25, 1904–1913. doi: 10.1523/JNEUROSCI.4540-04.2005

Rodríguez de Fonseca, F., Del Arco, I., Bermudez-Silva, F. J., Bilbao, A., Cippitelli, A., and Navarro, M. (2005). The endocannabinoid system: physiology and pharmacology. *Alcohol Alcohol* 40, 2–14. doi: 10.1093/alcalc/agh110

Rühl, T., Deuther-Conrad, W., Fischer, S., Günther, R., Hennig, L., Krautscheid, H., et al. (2012). Cannabinoid receptor type 2 (CB2)-selective N-aryl-oxadiazolyl-propionamides: synthesis, radiolabelling, molecular modelling and biological evaluation. *Org. Med. Chem. Lett.* 2:32. doi: 10.1186/2191-2858-2-32

Sagredo, O., González, S., Aroyo, I., Pazos, M. R., Benito, C., Lastres-Becker, I., et al. (2009). Cannabinoid CB2 receptor agonists protect the striatum against malonate toxicity: relevance for Huntington's disease. *Glia* 57, 1154–1167. doi: 10.1002/glia.20838

Shoemaker, J. L., Seely, K. A., Reed, R. L., Crow, J. P., and Prather, P. L. (2006). The CB2 cannabinoid agonist AM-1241 prolongs survival in a transgenic mouse model of amyotrophic lateral sclerosis when initiated at symptom onset. *J. Neurochem.* 101, 87–98. doi: 10.1111/j.1471-4159.2006.04346.x

Slavik, R., Herde, A. M., Bieri, D., Weber, M., Schibli, R., Krämer, S. D., et al. (2015). Synthesis, radiolabeling and evaluation of novel 4-oxo-quinoline derivatives as PET tracers for imaging cannabinoid type 2 receptor. *Eur. J. Med. Chem.* 92, 554–564. doi: 10.1016/j.ejmech.2015.01.028

Slavik, R., Müller Herde, A., Haider, A., Krämer, S. D., Weber, M., Schibli, R., et al. (2016). Discovery of a fluorinated 4-oxo-quinoline derivative as a potential positron emission tomography radiotracer for imaging cannabinoid receptor type 2. *J. Neurochem.* 138, 874–886. doi: 10.1111/jnc.13716

Turkman, N., Shavrin, A., Paolillo, V., Yeh, H. H., Flores, L., Soghomonian, S., et al. (2012). Synthesis and preliminary evaluation of [18F]-labeled 2-oxoquinoline derivatives for PET imaging of cannabinoid CB2 receptor. *Nucl. Med. Biol.* 39, 593–600. doi: 10.1016/j.nucmedbio.2011.10.019

van de Waterbeemd, H., Camenisch, G., Folkers, G., Chretien, J. R., and Raevsky, O. A. (1998). Estimation of blood-brain barrier crossing of drugs using molecular size and shape, and H-bonding descriptors. *J. Drug Target.* 6, 151–165. doi: 10.3109/10611869808997889

Yrjölä, S., Sarparanta, M., Airaksinen, A. J., Hytti, M., Kauppinen, A., Pasonen-Seppänen, S., et al. (2015). Synthesis, *in vitro* and *in vivo* evaluation of 1,3,5-triazines as cannabinoid CB2 receptor agonists. *Eur. J. Pharm. Sci.* 67, 85–96. doi: 10.1016/j.ejps.2014.11.003

Yung-Chi, C., and Prusoff, W. H. (1973). Relationship between the inhibition constant (KI) and the concentration of inhibitor which causes 50 per cent inhibition (I50) of an enzymatic reaction. *Biochem. Pharmacol.* 22, 3099–3108. doi: 10.1016/0006-2952(73)90196-2

Conflict of Interest Statement: The authors declare that the research was conducted in the absence of any commercial or financial relationships that could be construed as a potential conflict of interest.

Copyright © 2016 Ahamed, van Veghel, Ullmer, Van Laere, Verbruggen and Bormans. This is an open-access article distributed under the terms of the Creative Commons Attribution License (CC BY). The use, distribution or reproduction in other forums is permitted, provided the original author(s) or licensor are credited and that the original publication in this journal is cited, in accordance with accepted academic practice. No use, distribution or reproduction is permitted which does not comply with these terms.

Advantages of publishing in Frontiers

OPEN ACCESS
Articles are free to read, for greatest visibility

COLLABORATIVE PEER-REVIEW
Designed to be rigorous – yet also collaborative, fair and constructive

FAST PUBLICATION
Average 85 days from submission to publication (across all journals)

COPYRIGHT TO AUTHORS
No limit to article distribution and re-use

TRANSPARENT
Editors and reviewers acknowledged by name on published articles

SUPPORT
By our Swiss-based editorial team

IMPACT METRICS
Advanced metrics track your article's impact

GLOBAL SPREAD
5'100'000+ monthly article views and downloads

LOOP RESEARCH NETWORK
Our network increases readership for your article

Frontiers
EPFL Innovation Park, Building I • 1015 Lausanne • Switzerland
Tel +41 21 510 17 00 • Fax +41 21 510 17 01 • info@frontiersin.org
www.frontiersin.org

Find us on